MACROPHYTE-FLOW INTERACTIONS IN AQUATIC PLANTS

By

Julianne Trelenberg

B.Sc., University of Northern British Columbia, 2001

THESIS SUBMITTED IN PARTIAL FULFILLMENT OF THE REQUIREMENTS

FOR THE DEGREE OF

MASTER OF SCIENCE

in

NATURAL RESOURCES AND ENVIRONMENTAL STUDIES

ENVIRONMENTAL SCIENCE

THE UNIVERSITY OF NORTHERN BRITISH COLUMBIA

October 8, 2004

Your file Votre référence
ISBN: 0-494-04651-1
Our file Notre référence
ISBN: 0-494-04651-1

Abstract
Macrophyte-Flow Interactions

Linear-bladed (*Vallisneria americana*), whorled (*Elodea canadensis*), and dissected (*Ceratophyllum demersum*) leaf morphologies occur convergently in aquatic plants. It is likely that fluid dynamics have had an effect on plant morphology, by acting on exchange processes at low flows and drag forces at higher flows. These species were examined using flow visualization and digital imagery at five velocities (1 – 11 cms^{-1}) in a flume. Results indicated that in terms of fluid retention, *Elodea* and *Vallisneria* acted like a cylinder, whereas *Ceratophyllum* acted like a mesh. Transitional flows occurred at lower velocities than the cylinder, indicating an increase in local mixing. However, this was reversed when the internodal spacing was increased experimentally for *Elodea* and *Ceratophyllum*. This reduction in plant-flow interaction would allow these plants to remain erect in a relatively low energy environment. These results suggest that the flow environment has influenced the plasticity of leaf types and the evolution of macrophyte form in general.

TABLE OF CONTENTS

List of Tables

Chapter 3: The Effect of Macrophyte Morphology (Linear-bladed, Whorled, and Dissected) on Fluid Dynamics

Chapter 4: The Effect of Internodal Spacing on Downstream Flow Patterns and Compliance in *Elodea canadensis* and *Ceratophyllum demersum.*

List of Figures

Chapter 2: Literature Review: Fluid Dynamics and Macrophytes

Chapter 3: The Effect of Macrophyte Morphology (Linear-bladed, Whorled, and Dissected) on Fluid Dynamics

Chapter 1: Introduction to Thesis

The natural flow regime of rivers is dynamic, and influences the population and community structure of aquatic organisms, with abiotic processes dominating at higher velocities (i.e., flow regime: Poff et al., 1997; Bernez et al., 2004), and biotic processes dominating at slower velocities (i.e., grazing and competition: Abrams, 1980; Poff and Ward, 1989). Among these organisms, freshwater macrophytes have the ability to modify the physiochemical aspects of their microenvironment by slowing water flow, which, in turn, leads to the trapping of sediments and increase in organic content, and a change in the water chemistry profiles (i.e., due to photosynthesis and nutrient uptake; Chambers et al., 1999). Consequently, freshwater macrophytes can be considered ecosystem engineers in that they create and alter habitats for other organisms by affecting physical resources such as light, sediments, and water flow (Posey et al., 1993; Alper, 1998; Crooks, 2002; Wright et al., 2004). At the larger scale, macrophytes can alter the geomorphology of an area by affecting erosion and sedimentation rates thus affecting the geometry of water channels, and the hydrology of an area by affecting the surface flow patterns (Gordon, 1998).

As indicated above, macrophytes affect their environment but, the environment also affects them. As a result, many aquatic plants are highly plastic morphologically, and similar morphological patterns occur in unrelated species. With the exception of fenestration (a morphology found in the tropics in a select number of species (i.e., *Aponogeton*; Sculthorpe, 1967), three main morphological patterns occur in freshwater macrophytes: linear-bladed (e.g., *Vallisneria americana*); simple whorled (e.g., *Elodea canadensis*); and dissected (e.g., *Ceratophyllum demersum*). Variations in these patterns

occur when plants of the same species (or even the same plant) exposed to different environmental conditions exhibit heterophylly or foliar plasticity. For example, submerged leaves tend to be highly dissected, whereas aerial leaves tend to be much thicker with smoother margins (Sculthorpe, 1967; Wells and Pigliucci, 2000). Additionally, the length of the internodal space in whorled species can change depending on environmental conditions, with the space being longer for plants in sheltered sites (Idestam-Almquist and Kautsky, 1995), or in areas of low light (Cronin and Lodge, 2003).

In terms of flow environment, plants are exposed to diffusional stresses at slower velocities (Hurd et al., 1997) and to mechanical stresses at higher velocities (Schutten and Davy, 2000). Diffusional stresses occur because at slower velocities there is a thick diffusional boundary layer, that limits the supply of nutrients to the leaf surface layer (Cheer and Koehl, 1987; Koehl, 1996; Hurd et al., 1997). In order overcome these limitations, some macrophytes have small roughness elements on their leaves (Abelson et al., 1993; Hurd, 2000) that change the conditions in the boundary layer from laminar to turbulent, thus increasing the amount of local mixing, and consequently nutrient uptake by the plants. At faster velocities, productivity can be limited by tissue damage and dislodgment (Koch, 1993; Stewart and Carpenter, 2003), self-shading (Koehl and Alberte, 1988; Niinemets and Fleck, 2002), and the inhibition of enzymes (Koch, 1994). However, the central issue to living in high flow conditions is the reduction of drag, which is accomplished by the plant becoming smaller in stature and/or compliant with the flow (Ennos, 1999; Sand-Jensen, 2003), through a change in shape and orientation (Schutten and Davy, 2000).

Given the common morphological patterns found in macrophytes and the importance of fluid flow to productivity and ecology it would be appropriate to examine whether plants with different leaf types (linear-bladed, whorled and dissected) interact with the flow in the same manner. Furthermore, it is important to examine whether the internodal spacing effects the flow patterns due to flow separation (Coutanceau and Defaye, 1991) and their compliance under different velocities. This examination should also include a comparison to a physical model of a circular cylinder, which is often used as an approximation for aquatic plants (e.g. Nepf, 1999). Specifically, the major features of the plants (e.g., entire leaves, dissected leaves, and rigidity) can be contrasted with the model.

The question of the macrophyte-flow interaction is addressed in Chapter 2 through a literature review of: (1) basic fluid dynamic concepts; (2) the architecture of aquatic plants and how they differ from those in terrestrial systems; (3) adaptation of plants to a flow environment at both the individual and canopy scale, and the implications on distribution, photosynthesis, nutrient uptake, and grazing, predation, and competition; and (4) some of the methodologies used the characterize flow conditions. This background leads to the examination of the null hypothesis that plants with different leaf types (linear-bladed, whorled and dissected) affect the downstream fluid in the same manner in Chapter 3. This is done by taking short video sequences of Fluoroscein dye moving past the different plant morphologies, and conducting image analysis to determine the area of dye coverage and the concentration of dye in specified areas around the three different plant morphologies and a physical model. Similar techniques are used in Chapter 4 to examine the null hypothesis that internodal spacing has no effect on the

flow patterns generated by the plants and their compliance under different velocities. Together, these chapters combine to address the issue of whether the morphological patterns seen in freshwater macrophytes have been influenced by fluid dynamics factors.

Literature Cited

Abelson, A., T. Miloh, and Y. Loya. 1993. Flow patterns induced by substrata and body morphologies of benthic organisms, and their roles in determining availability of food particles. *Limnology and Oceanography.* 38(6):1116-1124.

Abrams, P. 1980. Some comments on measuring niche overlap. *Ecology.* 61(1):44-49.

Alper, J. 1998. Ecosystem 'engineers' shape habitats for other species. *Science.* 280(5367):1195-1196.

Bernez, I., H. Daniel, J. Haury, and M.T. Ferreira. 2004. Combined effects of environmental factors and regulation on macrophyte vegetation along three rivers in western France. *River Research and Applications.* 20:43-59.

Chambers, P.A., R.E. DeWreede, E.A. Irlandi, and H. Vandermeulen. 1999. Management issues in aquatic macrophyte ecology: a Canadian perspective. *Canadian Journal of Botany.* 77:471-487.

Cheer, A.Y.L, and M.A.R. Koehl. 1987. Paddles and rakes: fluid flow through bristled appendages of small organisms. *Journal of Theoretical Biology.* 129:17-39

Coutanceau, M., and J. Defaye. 1991. Circular cylinder wake configurations: A flow visulization survey. *Applied Mechanics Reviews.* 44(6):255-305.

Crooks, J.A. 2002. Characterizing ecosystem-level consequences of biological invasions: the role of ecosystem engineers. *Oikos.* 97:153-166.

Cronin, G., and D.M. Lodge. 2003. Effects of light and nutrient availability on the growth, allocation, carbon/nitrogen balance, phenolic chemistry, and resistance to herbivory of two freshwater macrophytes. *Oecologia.* 137:32-41.

Gordon, D.R. 1998. Effects of invasive, non-indigenous plant species on ecosystem processes: Lesson from Florida. *Ecological Applications.* 8(4):975-989.

Ennos, A.R. 1999. The aerodynamics and hydrodynamics of plants. *The Journal of Experimental Biology.* 202:3281-3284.

Hurd, C.L. 2000. Water motion, marine macroalgal physiology, and production. *Journal of Phycology.* 36:453-472.

Hurd, C.L, C.L Stevens, B.E. Laval, G.A. Lawrence, and P.J. Harrison. 1997. Visualization of seawater flow around morphologically distinct forms of the giant kelp *Macrocystis integrifolia* from wave-sheltered and exposed sites. *Limnology and Oceanography.* 42(1):156-163.

Idestam-Almquist, J., and L. Kautsky. 1995. Plastic responses in morphology of *Potamogeton pectinatus* L. to sediment and above-sediment conditions at two sites in the northern Baltic proper. *Aquatic Botany.* 52:205-216.

Koch, E.W. 1993. The effect of water flow on photosynthetic processes of the alga *Ulva lactuca* L. *Hydrobiologia.* 260/261:457-462.

Koch, E.W. 1994. Hydrodynamics, diffusion-boundary layers and photosynthesis of the seagrass *Thalassia testudinum* and *Cymodocea nodosa. Marine Biology.* 119:767-776.

Koehl, M.A.R. 1996. When does morphology matter? *Annual Review of Ecological Systems.* 27:501-542.

Koehl, M.A.R., and R.S. Alberte. 1988. Flow, flapping, and photosynthesis of Nereocystis luetkeana: a functional comparison of undulate and flat blade morphologies. *Marine Biology.* 99: 435-444.

Nepf, H.M. 1999. Drag, turbulence, and diffusion in flow through emergent vegetation. *Water Resources Research.* 35(2): 479-489.

Niinemets, U., and S. Fleck. 2002. Petiole mechanics, leaf inclination, morphology, and investment in support in relation to light availability in the canopy of *Liriodendron tulipifera. Oecologia.* 132:21-33.

Poff, N.L., J.D. Allan, M.B. Bain, J.R. Kar, K.L. Prestgaard, B.D. Ritcher, R.E. Sparks, and J.C. Stromberg. 1997. The natural flow regime. *Bioscience.* 47(11): 769-782.

Poff, N.L., and J.V. Ward. 1989. Implications of streamflow variability and predictability for lotic community structure: A regional analysis of streamflow patterns. *Canadian Journal of Fisheries and Aquatic Sciences.* 46:1805-1817.

Posey, M.H., C. Wigand, and J.C. Stevenson. 1993. Effects of an introduced aquatic plant, *Hydrilla verticillata,* on benthic communities in the upper Chesapeake Bay. *Estuarine, Coastal and Shelf Science.* 37:539-555.

Sand-Jensen, K. 2003. Drag and reconfiguration of freshwater macrophytes. *Freshwater Biology.* 48:271-283.

Schutten, J., and A.J. Davy. 2000. Predicting the hydraulic forces on submerged macrophytes from current velocity, biomass and morphology. *Oecologia.* 123:445-452.

Sculthorpe, C.D. 1967. *The Biology of Aquatic Vascular Plants.* Edward Arnold, London (Reprinted 1985 Koeltz Scientific, Konigstein), 610 pp.

Stewart, H.L., and R.C. Carpenter. 2003. The effects of morphology and water flow on photosynthesis of marine macroalgae. *Ecology.* 84(11):2999-3012.

Wells, C.L., and M. Pigliucci. 2000. Adaptive phenotypic plasticity: the case of heterophylly in aquatic plants. *Perspectives in Plant Ecology, Evolution and Systematics.* 3(1):1-18.

Wright, J.P., W.S.C. Gurney, and C.G. Jones. 2004. Patch dynamics in a landscape modifies by ecosystem engineers. *Oikos.* 105:336-348.

Fluid Dynamics and Macrophytes

Introduction

Freshwater aquatic plants (macrophytes) are important components of lake and river ecosystems (Biggs, 1996). They are considered ecosystem engineers because they create, and alter habitat for aquatic organisms by: (1) slowing or modifying water velocities; (2) altering oxygen regimes; (3) blocking light; (4) trapping detritus; (5) providing refuges from predators and disturbance; (6) providing oviposition sites; and (7) increasing the amount of attachment surface (Biggs, 1996; Wright et al., 2004). In addition, emergent vegetation around the edges of rivers and lakes help to reduce shoreline erosion by dampening the effect of wave energy (Kalff, 2002). Conversely, dense beds of submerged macrophytes in riverine systems can impair discharge, thus increasing the potential for flooding, as well as interfering with the use of water craft (Kalff, 2002). Macrophyte communities also have important ecological effects whereby they may increase the pH of poorly buffered waters, reduce dissolved oxygen levels, alter stream courses and bed roughness, shift invertebrate communities from free stone dwelling taxa to small burrowing taxa, and degrade the appearance of the stream (Biggs, 1996). These positive and negative aspects of freshwater macrophytes speak to the importance of understanding vegetated hydraulic systems; especially since macrophytes increase the complexity of underwater landscapes (Chambers et al., 1999).

There are several critical components of the flow regime that regulate ecological processes in river ecosystems including: the magnitude; frequency; duration; timing; rate of change of hydraulic conditions in a set location; and development of the mainstream flow (Poff et al., 1997). There are also factors that affect the smaller scale velocities

within macrophyte beds, which include: velocity over unvegetated substrate; biomass of macrophytes at a specific location; biomass of macrophytes immediately upstream of the location; and the depth of the water at that site (Gregg and Rose, 1982). At the river and the macrophyte scale, the physical structure of the riverine environment can be defined largely by physical processes, especially those related to the movement of water and sediment (Poff et al., 1997). The following chapter will examine fluid dynamic issues on the smaller scale, specifically, the flow patterns around individual macrophytes and through canopies. These smaller scale fluid dynamics are important because they speak directly to plant productivity through nutrient uptake (Borchardt, 1994), photosynthesis (Dennison, 1987), and sediment capture (Gregg and Rose, 1982). In addition, a basic understanding of fluid dynamics must be presented before one can examine how flow influences freshwater plant communities, and how flow is in turn influenced by individual plants. Patterns of water movement can be examined both qualitatively and quantitatively in order to characterize the macrophyte-flow interaction. It will become evident that the macrophyte-flow interaction is important for the autoecology of plants and the ecology of aquatic systems.

Fluid Dynamics and Macrophytes

Types of Flow

The most logical place to begin a discussion of macrophyte-flow interaction is to look at the flow conditions, specifically, laminar, transitional, and turbulent (Figure 2.1). In laminar flow, it is assumed that all fluid particles move nearly parallel to each other in a smooth path. The large- and small-scale movements of the fluid are the same, at least down to the level at which molecular diffusion becomes the dominant mode of transport

(Vogel, 1994). Transition flow, where the particle paths begin to deviate from a parallel path, occurs between laminar and turbulent flow, with the transition often occurring quickly (Vogel, 1994). Finally, turbulent flow occurs when individual fluid particles move in a chaotic fashion, even if the fluid as a whole appears to be traveling uniformly in one direction. In other words, intense small-scale motion in all directions is superimposed on the mean velocity (Vogel, 1994). Virtually all flows of aquatic interest are turbulent at large spatial scales (Nowell and Jumars, 1984), and as such, laminar and transitional flows are generally not applicable to natural systems except on very small scales (e.g., around individual leaves and within canopies; Ackerman and Okubo, 1993; Ackerman, 2002).

Reynolds Number

Reynolds number ($Re = \frac{ul}{\upsilon}$; where u = velocity, l = characteristic length, and ν = the kinematic viscosity [the ratio of dynamic viscosity to density]) provides an indication of the flow conditions (Figure 2.1, 2.2), as it is a ratio of inertial to viscous forces (Vogel, 1994). The situation where viscous flow dominates (e.g., $Re << 1$; creeping flow) is not dealt with in much detail here, rather the more typically flow conditions where inertia is relevant (e.g., $Re > 1$) are presented. If the Reynolds number is low (e.g. small, slowly moving structures), the situation is relatively viscous, and the flow is smooth and orderly (e.g., Figure 2.2a). At high Reynolds numbers (e.g. large, rapidly moving structures), inertial forces dominate, and the flow is turbulent (Koehl, 1996). In natural rivers the transition to turbulent flow often occurs around $Re = 10^3 - 10^4$ using the hydraulic diameter of the channel, but the actual value is dependent on the roughness of the bed relative to the water depth (Carling, 1992).

Boundary Layers

Velocity gradients occur near boundaries when the fluid comes in contact with a solid object due to the 'no-slip' condition at the boundary (Figure 2.3). This causes the velocity of the flow to decline toward the boundary (Thompson and Trioan, 1997) because the velocity of a fluid at the surface of a solid is actually zero. In general, a higher Re implies a thinner boundary layer but a higher shear rate (as will be defined in the next section). Similarly, the lower the Re, the thicker the boundary layer and the lower the shear rate in the boundary layer (Cheer and Koehl, 1987). The thickness of the boundary layer (δ) around a cylinder shaped object under laminar flow conditions can be approximated by the formula: $\delta \approx 5x/\sqrt{Re_x}$, where 5 is a constant (which may range from 4.65-5.84), x is the downstream distance, and Re_x is the local Reynolds number taken x distance from the leading edge (Vogel, 1994; Zhang and Malmqvist, 1997). Additionally, shear is a consequence of the dissipation of momentum and energy, so another way of viewing the boundary layer is as the region near a surface where the action of viscosity produces a large loss of total pressure head (Vogel, 1994).

Drag is another important concept related to boundary layers. Drag is the hydrodynamic force that pulls a body in the direction opposite to fluid movement and in the case of boundary layers, the force that slows the flow (Koehl, 1996). At low Re, drag is due to skin friction, which is the viscous resistance of the fluid in the boundary layer around the body being sheared as the fluid moves past the body, so a greater wetted area leads to higher skin friction. At high Re drag is also due to skin friction but is dominated by pressure drag, which is the pressure difference across the body due to the fluid dynamic separation or the formation of a wake on the downstream side of the body

(Vogel, 1987; Koehl, 1996). These concepts are important when considering boundary layers because differences in velocity can control the thickness of the boundary layer close to the plant surface and as both velocity and plant size increase so does the skin friction and drag, which effects the plant community (Biggs, 1996).

An example of the importance of boundary layers in macrophyte ecology can be seen in plants with an undulate or bullate blade morphology where the boundary layer thickness along the curved body changes due to changing pressure gradients. Hurd et al. (1997) demonstrated that when water moves up the rising portion of an undulation of a macrophyte blade, the velocity increases and the boundary layer thickness decreases. Conversely, as water moves down the descending portion of an undulation, the velocity decreases and the thickness of the boundary layer increases rapidly. Macroalgae in wave-exposed versus sheltered sites have different morphologies (smooth vs. undulate) because of contrasting demands of diffusional and mechanical stress. At low flows characteristic of sheltered environment, seaweed productivity may be limited by diffusion due to the development of a thick boundary layer that reduces the transport of essential inorganic nutrients to the blade surface (Hurd et al., 1996). Undulations are interpreted to be the plant's response to water motion that increase local mixing. Conversely at high flows characteristic of wave-exposed environments, drag can damage or detach seaweeds from the bottom (Hurd et al., 1997). Smooth blades cause little water motion, specifically separation, allowing for less drag, which is an advantage in highly energetic environments because it prevents the plants from being broken, damaged, or uprooted. Undulate blades cause an increase in the water motion around them thus increasing the

drag, which is advantageous in low energy environments because this added movement limits self-shading and increases mixing.

Changes in boundary layers are important to the productivity of aquatic plants for a number of reasons. First, turbulence caused by the interaction of flow with leaves greatly decreases the time that nutrients are exchanged relative to molecular diffusion alone. Second, where flow is laminar, as in lentic systems and at very small scales in other systems, boundary layer thickness depends on the velocity, and the size and orientation of the macrophyte blade (Losee and Wetzel, 1993; Crossley et al., 2002). Within dense macrophyte beds, thick boundary layers are the result of reduced turbulence caused by the hydroelastic response of plants (Ackerman and Okubo, 1993). In other words, viscous forces dominate over turbulent forces at a small distance from the plant or sediment surface. Conceptually, a layer of water sticks to plant and sediment surfaces and does not partake in the watver circulation (Kalff, 2002).

The concept of the roughness Reynolds number ($Re_* = u_*k/\nu$ where u_* = shear velocity $=\sqrt{\tau/\rho}$, τ = shear stress, ρ = density, k = height of roughness elements, and ν = kinematic viscosity), provides a better description of the flow situation close to the bottom, than the Re of the mean flow (Davis and Barmuta, 1989). This is because, the height of the roughness elements relative to the thickness of the viscous sublayer of the boundary layer (see below) determines the flow conditions near the bed (Davis and Barmuta, 1989). When the height of the roughness element is smaller than the thickness of the viscous sublayer, flow conditions are considered to be smooth turbulent, whereas if the height of the roughness is greater than the thickness of the viscous sublayer, the flow conditions are considered rough turbulent (Davis and Barmuta, 1989). Smooth turbulent

flows can only occur in smooth flow conditions, such that occurs over fine sediments, or adjacent to streamlined submerged macrophytes (Davis and Barmuta, 1989).

Shear Stress

Turbulent shear stress (τ), which is the resistive force caused by the no-slip condition, can be determined from a log-linear regression of the logarithmic portions of velocity profiles (or viscous sublayer; Figure 2.3; Ackerman, 1997; Ackerman and Hoover, 2001), providing enough measurements are taken to achieve reasonable confidence limits (Nowell and Jumars, 1984). However, it must be mentioned that non-logarithmic layers may occur in strongly accelerating or decelerating flow such as in river reaches which narrow or widen rapidly (Hoover and Ackerman, in Press). The logarithmic profile may also be deformed by spatial variation in the mixture of the bottom roughness, which would include the presence of large rocks (Carling, 1992). Shear stress is perhaps the most meaningful measure of flow as far as benthic organisms are concerned because it is the shearing force of water rather than velocity that is likely to erode or dislodge organisms (Lancaster and Hildrew, 1993). Shear forces are also important because they set a limit to the size of fine particles that can settle to the sediment surface. For example, at faster flows fine particles will not settle, creating a coarse substrata (Sand-Jensen, 1998). As such, the evaluation of the bed shear stress is important, because it is necessary not only for normalizing turbulence characteristics but also for assessing issues regarding sediments (Nezu and Onitsuka, 2001).

Laminar shear stress ($\tau = \mu \frac{du}{dz}$, where μ is the dynamic viscosity, z is the height (or depth) and du/dz is the local velocity gradient) is important in momentum transfer to the leaf surface. Since the viscosity of the fluid is directly related to the

thickness of the boundary layer (i.e., how rapidly layers of fluid move with respect to each other), the presence of the no-slip condition denotes an area where shear stress exists (Vogel, 1988). Hence, the more viscous a fluid the larger the velocity gradient of the boundary layer and, the less viscous a fluid the steeper the velocity gradient of the boundary layer (Vogel, 1988). This is important because the process of nutrient exchange to a plant's surface is enhanced by steeper boundary layers, which increase the rate of momentum transfer and thus the replenishment of the site of exchange.

Drag

Drag is a property of fluid dynamics that is of interest when considering the productivity of macrophytes. As indicated above there are two types of drag, skin friction and pressure drag (Vogel, 1988; 1994). In other words, the drag force on an object in a moving fluid depends on the velocity of the fluid, the size, and roughness of the object. Additionally, for a non-spherical object, the shape and orientation in relation to the flow are also important (Schutten and Davy, 2000). The drag on small organisms is mainly due to skin friction, whereas, for larger (and more upright) organisms pressure drag tends to be much greater (Biggs and Thomsen, 1995). An example of this occurs when plant stems bend downstream in response to faster flow, so that the frontal area is reduced, lowering pressure drag, whereas long ribbon-shaped leafs can fold against the stem, reducing skin friction (Ennos, 1999). Consequently, pressure drag will be high on dense plant communities because of the pressure drop from upstream to downstream. This occurs because there is an area of slow flow at the end of the canopy due to the flow separation around the canopy (Vogel, 1994). Conversely, pressure drag will be lower in open plant stands due to the additional drag exerted by the plants that reduce the mean

flow within vegetated regions relative to unvegetated ones, thus making the energy distribution even throughout the flow (Ackerman and Okubo, 1993; Vogel, 1994; Nepf, 1999). A consequence of this velocity/pressure range is that more individual plants will have access to nutrients in open vs. dense canopies, whereas plants in dense canopies will have more protection from drag. For example, drag and acceleration forces may limit productivity by dislodging macrophytes from the substratum (Hurd et al., 1996).

At some point the momentum acquired by a macrophyte must be stopped because the plant is anchored to the substratum. A large, flexible structure can move with the flow for a time, thereby reducing drag and lift (a force perpendicular to the direction of flow), but this can only occur while acquiring momentum (Denny et al., 1997). Accelerating a body in a fluid involves a force with three additive components: (1) drag; (2) the force needed to accelerate the mass of the body forward; and (3) the force needed to accelerate the displaced mass of fluid backward. The additive forces, which depend upon the shape of the object, the volume of the body, and the density of the surrounding fluid, is commonly called the acceleration reaction. In other words, if an object is accelerated in one direction, an equal volume of fluid must be accelerated in the other direction. As such, to accelerate an object, a force proportional to the object's volume and to the density of the medium must be applied (Vogel, 1994). This concept is relevant to aquatic systems because when a current flows past a plant, the plant resists acceleration thus causing a displacement of the fluid. For example, if the plant is large enough, it can simply comply as water passes by reducing the relative velocity and acceleration between the plant and the surrounding water and, thereby, reducing the

hydrodynamic forces (Denny et al., 1997). These concepts are especially important in intertidal systems involving kelps (Dawes, 1981).

Froude number

The Froude number, ($Fr = \frac{\overline{u}}{\sqrt{gD}}$ where $\overline{u}$ = mean velocity, g = acceleration due to gravity, and D = water depth), is the ratio of inertial to gravitational forces that describes the surface condition in a flowing system (i.e., the ratio of the inertia of the flow to the speed of a wave). The inertial force causes plant movement (i.e., compliance with the flow) or divert it from a straight course at constant speed (i.e., oscillations; Vogel, 1988). For conditions where $Fr < 1$ the flow is designated as sub-critical or tranquil flow, when $Fr = 1$ flow is critical, and for $Fr > 1$ flow is super-critical. Super-critical flow is characterized by broken, white water and is described as shooting or streaming flow (Davis and Barmuta, 1989). Nezu and Onitsuka (2001) showed that in biological systems, the maximum value of vorticity increases with an increase in Froude number. They also noted that the strength of the secondary currents increased with an increase of the Froude number. Secondary currents vary in flow direction from the mean flow, leading to what one might consider very large scale turbulence intensity. In other words, Froude number is relevant to macrophytes because it also characterizes the mean flow (Davis and Barmuta, 1989), and it describes the distribution of momentum in the main-stream velocity (Kundu, 1990). Correspondingly, drag increases more quickly with velocity at the surface than in the water column (Vogel, 1994). Consequently, floating and emergent leaved plants exist in still or very slow moving water, whereas submerged plants, which are more adapted to comply to drag conditions exist in faster moving environments (Dawson, 1988).

Turbulence Intensity

Mean velocity gives a measure of the average unidirectional flux of water past macrophyte blades, whereas turbulence intensity (i.e., $u_{rms} / \overline{u} * 100$, where u_{rms} is the root mean square of the velocity) provides an indication of the velocity fluctuations that may lead to local mixing (Koehl and Alberte, 1988). Vegetation not only affects the mean velocity, but also affects the turbulence intensity and the resultant transport of nutrients. The conversion of mean flow to turbulent flow within stem wakes increases the turbulence intensity, and because wake turbulence is generated at the stem scale, the dominant turbulent length scale is reduced, relative to unvegetated, open-channel conditions (Ackerman and Okubo, 1993; Nepf, 1999). The combination of reduced velocity and reduced eddy-scale should reduce the in-canopy turbulent diffusion relative to unvegetated regions (Ackerman and Okubo, 1993; Nepf, 1999).

The eddy viscosity (the turbulent transfer of momentum that characterizes the transport and dissipation of energy in the smaller-scale flow), which is determined by the properties of the turbulence, characterizes mean momentum transfer by turbulence fluctuations (Mathieu and Scott, 2000). As such, it is an essential property of mass transfer to aquatic plants, since eddy viscosity is not constant within the boundary layer (Hinze, 1987) or the plant canopy (Ackerman and Okubo, 1993). For example, it has been shown that turbulence intensity is enhanced by the presence of a mesh, yet the diffusivity is diminished because the eddy scale is reduced (Nepf, 1999). That being said, it is clear that turbulent flows modify the rate at which materials and energy are exchanged between a macrophyte and its immediate environment (Hart et al., 1996).

The random motion of eddies is an efficient way of transferring mass and momentum, because each eddy carries with it the properties of the fluid contained within it (Hurd, 2000). Mass transfer is an important concept in aquatic systems, whereby nutrients and wastes are transported towards and away from organisms. Any nutrient uptake by the macrophyte blade generates a nutrient depleted region adjacent the blade surface, called the concentration boundary-layer (Stevens and Hurd, 1997). If the timescale for significant changes in the viscous sublayer is much less than the timescale for molecular transport, then it is possible for there to be reduced net advection (Stevens and Hurd, 1997) that can be related to a thick diffusive boundary layer and ultimately to diffusional stress. In turbulent flow, mass shifts around in directions other than that of the overall flow (Vogel, 1994). For this reason, the thinner the diffusive boundary layer in the water flowing along a blade, the greater the rate of mass transfer to the blade surface (Koehl and Alberte, 1988). Thus, fluid dynamics can define the environment where freshwater macrophytes are productive.

Freshwater Macrophytes

Architecture

The term freshwater macrophyte is broad, and used to encompass emergent, floating, floating-leaved and submerged plants that include representatives of Angiosperms, Pteridophytes, Bryophytes and large algae (Dawson, 1988). Plant architecture is also a broad term, but it is defined here to include only the photosynthetically active part of the plant. It is important to understand the function of plant architecture, and to determine whether it is a result of common ancestry, or whether it is due to similar environmental pressures. The uncertainty of the origin of plant

architecture arises from the observation that freshwater macrophytes in different families have similar morphologies, whereas species in the same family can have different architectures. This may be because plants generally acclimate to changing environmental conditions through morphological rather than physiological means (Wells and Pigliucci, 2000; Santamaria, 2002). Heterophylly (foliage plasticity) occurs in some species of freshwater macrophytes whereby the plant has more than one kind of leaf structure depending on whether they are under, on, or above the water surface. Heteroblastic development is a form of heterophylly whereby juvenile leaves have a different morphology than the adult leaves regardless of the environment (Sculthorpe, 1967).

The classification of organisms and the evolutionary relationships among them (systematics) is determined using comparisons of the evolved similarities (e.g., synapomorphies) in plant characteristics such as genetics and morphology (Raven et al., 1999). However, this is sometimes difficult in aquatic plants, because they exhibit a wide range of phenotypic plasticity (the ability of an individual organism to alter its morphology and physiology in response to environmental conditions; Idestam-Almquist and Kautsky, 1995; Wells and Pigluicci, 2000; Santamaria, 2002) as well as similarity of form (Sculthorpe, 1967). Phylogeny is also a difficult concept to apply to aquatic plants because they represent a functional group. For instance, it is known that aquatic Pteridophytes (i.e., ferns) and Angiosperms (i.e., herbs) evolved from terrestrial ancestors polyphyletically (Sculthorpe, 1967), thus providing examples of convergent evolution. However, heterophylly occurs across distant taxa, which suggests that unrelated plants have adapted in a similar fashion to the aquatic environment (Wells and Pigliucci, 2000);

adding to the argument that structural similarities occur due to adaptation to a common environment.

Freshwater macrophytes vary in morphology at different scales, ranging from leaf shape to growth form. There are four basic growth forms of vascular macrophytes: (1) emergent; (2) floating-leaved; (3) submerged; and (4) free-floating (Figure 2.5). Emergent plants (e.g., *Sparganium*) tend to be mainly rhizomatous (having a horizontal, usually underground stem that often sends out roots and shoots from its nodes) or cormous (having a short thick solid food-storing underground stem) and are perennial. Heterophylly can be experienced in emergent plants due to the submerged or floating leaves preceding the aerial leaves in development (Sculthorpe, 1967). In addition, emergent macrophytes have aerial reproductive structures. Floating-leaved plants (e.g., *Nuphar* and *Nympheae*) can either have leaves attached to long flexible petioles that are rhizomatous or cormous or they can have compliant stems that rise through the water and produce floating leaves on relatively short petioles and be stoloniferous (stems growing horizontally above the ground and producing roots and shoots at the nodes). The reproductive structures are either floating or aerial, and consequently, heterophylly can be experienced since the submerged leaves precede the floating leaves in development (Schulthrope, 1967). Submerged macrophytes can be divided into three main types: (1) caulescent; (2) rosette; and (3) thalloid (Figure 2.6). Caulescent plants (ones with a well-developed aboveground stem), can be with or without rhizomes, and consist of long flexible stems that root from the nodes (e.g., *Elodea* and *Myriophyllum*). Rosette types (e.g., *Isoetes* and *Vallisneria*) are often stoloniferous, and have radical leaves arising from a condensed, often tuberous rhizome. Lastly, plants where the body is reduced to a

cylindrical or flattened form, often bearing secondary branches (e.g., *Podostemaceae*) are of the thalloid type (Sculthorpe, 1967). Submerged leaves tend to be filiform, ribbon-shaped, fenestrated, or finely divided (Sculthorpe, 1967). Finally, free-floating plants include small surface floating plants (e.g., *Lemma* and *Wolffia*), as well as plants that are submerged with few or no roots (e.g., *Ceratophyllum*; Sculthorpe, 1967). Considering these different growth forms, submerged plants generally occur in deeper water, floating leaved communities occur closer to the shore, and emergent plants occur in reed-swamp communities, although this zonation can, and does overlap (Schulthorpe, 1967).

In freshwater macrophytes, there are two main patterns of growth, the first being an abbreviated axis producing a rosette of radical leaves (e.g., *Isoetes spp.*), the second being an elongated flexuous stem which is covered in leaves and rooted from its nodes (e.g., *Myriophyllum;* Sculthrope, 1967). There are several ways that leaves can be arranged around the stems of these macrophytes. For example, the leaves of caulescent macrophytes may be: (1) alternate (e.g., *Potamogeton*); (2) paired and opposite (e.g., *Cabomba*); whorled (e.g., *Hippuris* and most species of *Elodea* and *Myriophyllum*; Figure 2.7); or (3) pseudo-whorled whereby the leaves actually occur alternately, but several condensed internodes occur between two successive long internodes (e.g., *Myriophyllum heterophyllum*) (Sculthorpe, 1967).

There are three main leaf forms in freshwater macrophytes, these being entire, fenestrated, and dissected. Entire leaves are generally thin and translucent, the shape varying from awl-like and linear to ovate and sagittate (or cordate; Figure 2.8). Entire leaves can also be petiole-like with sheathing at the base and upper limb with the leaf being either wide or narrow where it attaches to the petiole (Figure 2.9). Within the

entire morphology, many of the broad leaf types either have undulate margins (Figure 2.10) or bullate surfaces (Sculthorpe, 1967). Undulate margins along with fenestration occur in the leaves of the genus *Aponogeton,* which are entire and narrowly lanceoate. In this case, the margin is slightly undulate to tightly crinkled, and the leaf is generally twisted because the marginal regions grow faster than then median regions. The fenestration in *Aponogeton madagascariensis* is observed by the small areas of interstitial tissue that are lacking at maturity, sometimes to the extent that the lamina is thoroughly perforated leaving a skeleton like structure of veins (Figure 2.11; Sculthorpe, 1967). Thirdly, dissected leaves (e.g., *Ceratophyllum*) occur when the leaf is split into many free segments radiating from the petiole. The leaves of *Ceratophyllum* are quite rigid, 1-4 times forked, and have two rows of teeth along the segments at the tip of the leaf (Figure 2.12; Sculthorpe, 1967). Alternatively, the leaves of *Myriophyllum spicatum* are also dissected, but instead of being radial in structure, the segments grow alternately from a central vein, giving a feathery appearance.

As mentioned previously, leaf variations can be found: (1) across species; (2) among the population of the same species; and (3) between the leaves of a single plant (heterophylly; Wells and Pigliucci, 2000). For example, heterophylly occurs in *Prosperpinaca palustris* as a response to light quantity (Figure 2.13). When the leaves are submerged, or experience only eight hours of light a day, the leaves are highly dissected. Whereas the aerial leaves, or the leaves that experience sixteen hours of light a day are entire lanceolate leaves with serrated margins (Wells and Pigliucci, 2000). Heterophylly can also be induced by light quality as in *Hippuris vulgaris* whereby

changes in red:far red signal the transition from submerged to aerial leaf morphology (Wells and Pigliucci, 2000).

Hormones also play a role in changes to plant morphology. It has been shown that plants exposed to abscisic acid produce aerial leaf morphology while still submerged. Abscisic acid is the drought stress hormone in terrestrial plants that regulates plants to changes in water availability. Gibberellic acid encourages the production of leaves characteristic of submerged plants while still in an aerial environment, but it is considered to be a response to photoperiod rather than water availability (Wells and Pigliucci, 2000).

Freshwater macrophytes have different morphological features depending on their environment. For example, lake sites with high wind exposure are usually dominated by small compact (rosette-like) species with stiff leaves arising from the base of the stem, and a strong root system. In contrast, species with long, slender highly flexible stems usually dominate shallow river channels or shorelines of low turbulence, which allow rooting and prevent damage to the stems. Macrophytes with floating leaves, such as *Nuphar*, are restricted to areas of little or no flow (Dawson, 1988; Kalff, 2002). Erect and canopy-forming species with apical growth, commonly dominate in deeper waters under relatively sheltered conditions (Figure 2.14; Kalff, 2002). To expand upon this concept, it has been shown that plant species occurring in highly energetic and disturbed environments are predicted to be more robust; i.e., shorter in height (Stewart and Carpenter, 2003), limited in lateral spread, shorter lived, have a larger proportion of annual production devoted to seeds, as well as having fewer storage structures (Barrat-Segretain, 2001). Conversely, competitive species that occur in more predictable habitats are predicted to be more delicate (i.e., taller in height; Stewart and Carpenter, 2003),

extensive in lateral spread, longer lived, have a smaller proportion of production for annual reproduction, as well as having important vegetative storage structures (Barrat-Segretain, 2001). To further contrast the difference between low and fast flow, it has been observed that plants from fast-moving streams tend to have leaves with low branching angles (i.e., present a smooth surface to the flow), whereas, plants from slow-moving streams tend to have higher branching angles, and the leaves stick out more into the flow (i.e., present a rough surface to the flow; Ennos, 1999). This increase in angle also increases the drag, but results in the production of small vortices behind the leaves that would increase the supply of carbon dioxide and other nutrients (Ennos, 1999).

It is reasonable to suggest that the physical interaction of plants with the water flowing past them governs and selects for suitable plant forms and species. Thus the plants' size, form and stand structure, together with the strength of its stems and the security of its method of anchoring to the substratum, are major factors in plant survival (Dawson, 1988). Another factor that may be useful in the description of architecture is the leaf-area index, which provides an estimate of the photosynthetically active surface in the macrophyte community, as well as the amount of substrate available that specific community (Den Hartog, 1982).

Several factors influence near-bed velocity and sediment composition within macrophyte beds in lowland streams, which are also closely related to differences in macrophyte morphology (Barrat-Segretain, 2001). Anderson and Charters (1982) suggested that water motion affects marine macroalgae through the transport of mass, momentum, and energy from the main body of the fluid through the boundary layer to the plant's surface. The transport rates depend strongly on whether the flow in the boundary

layer is laminar or turbulent, because the transfer rates in turbulent flow with turbulent diffusion are orders of magnitudes greater than those in laminar flow with rates determined by molecular diffusion alone. Plants occurring within or near the boundary layer or those that create their own unstirred layer through dense canopies tolerate the least hydrodynamic stress, whereas plants that are less densely branched and stronger are predicted to break at higher velocities than highly branched filaments and tufts (Sheath and Hambrook, 1988), thus demonstrating that where aquatic plants of different morphologies grow is dependent mainly on the fluid dynamics in that area.

Aquatic versus Terrestrial Plants

There are several important environmental (i.e., chemical and physical) factors that affect plants in aquatic systems. The first of these comparisons is of a mechanical and structural nature, which examines how plants support themselves in air compared to water. Secondly, the physiology of gas exchange is important when dealing with the transport of important nutrients given the different diffusivities of oxygen (O_2) and carbon dioxide (CO_2) in air versus water. Another factor to consider is photon capture (discussed in a later section) which, relates directly to the productivity of plants and how light is attenuated in aquatic versus terrestrial environments. There is also the issue of mechanical damage caused by hydraulic stress, which will differ between aquatic and terrestrial systems. Finally, ecological factors such as pollination and diaspore dispersal differ given the lack of animal agents in aquatic systems.

One of the main differences between living in water versus air is the density of the medium. For example, the density of air varies directly with temperature, pressure, and altitude, with a variation of about 13%. Conversely, changes in the density of water

are small (0.8%) over the biologically relevant range of temperatures (Denny, 1993). However, since water weighs much more then air, a small difference in density can have large implications for aquatic organisms (Denny, 1993). Another major difference between the density of air and water is that water density does not respond in a linear fashion to temperature; rather, water goes through a transition phase whereby ice is less dense than water, and so it floats (Denny, 1993). Similarly, if the density of any object is greater than the surrounding fluid, the object experiences a downward force proportional to its volume (negatively buoyant). Conversely, if the density of an object is less than the surrounding fluid, there is a net upward force (positively buoyant). Consequently, since the density of water is so close to the body density of plants, the effective or excess density ($\rho_d - \rho_f$ where ρ_d = density of the body, and ρ_f = density of the fluid) is very sensitive to small changes in the density of the fluid. Comparatively, because the density of air is so small, it has little effect on the effective density of terrestrial plants (Denny, 1993).

One consequence of the differences in density discussed above, is that terrestrial and aquatic plants have different means of supporting themselves. Specifically, terrestrial plants are rigid with a dominant axis, whereas aquatic plants do not possess a dominant axis because they are partially supported by the water itself. The support given to submerged macrophytes is also provided by the buoyancy provided by lancunate tissues (air filled spaces that run along the leaf in the mesophyll), which reduces the need for mechanical strength and rigidity (Sculthorpe, 1967). For this reason, aquatic stems do not need to support the weight of leaves, as is the case in terrestrial environments. Additionally, given the differences in density discussed above, and the fact that aquatic

plants have low bulk densities, aquatic plants tend to be neutrally or positively (due to lacunae) buoyant. In contrast, terrestrial plants are roughly a thousand times denser than air and experience the compressing effects of gravity (Niklas, 1997).

The density differences between air and water translate to differences in kinematic viscosity, which is the ratio of the molecular or dynamic viscosity to density. In addition, there are differences in the molecular diffusivity of gases related to photosynthesis. For example, even though the concentration of carbon dioxide (CO_2) is the same in water and air between of 10°C and 20°C, a terrestrial leaf receives CO_2 at a higher rate than that of an aquatic leaf due to greater diffusivity in air. Thus, aquatic plants must overcome diffusional stresses by living in areas of mixing (i.e., moving water), or they must have smaller or more dissected leaves (i.e., to increase surface area: volume) than terrestrial plants to maintain an adequate delivery rate of CO_2. There is also a possibility that leaf edges influence the fluid and thus induce turbulence (Coutanceau and Defaye, 1991). Another difference between aquatic and terrestrial environments is related to the dissociation of CO_2 in water (Denny, 1993). An equilibrium is reached in aquatic systems whereby when CO_2 dissolves in water, much of it combines chemically with its surroundings to produce carbonic acid (H_2CO_3), which then dissociated into a hydrogen ion and a bicarbonate ion (HCO_3^-), which is often used by aquatic plants as their carbon source for photosynthesis. The final ion in the equilibrium, carbonate (CO_3^{2-}), is not used by plants. Carbon dioxide has a lower molecular diffusivity in freshwater than in air, consequently as indicated above, plants living in air can acquire CO_2 more efficiently than their aquatic counterparts (Niklas, 1997). That being said, land plants and

aquatic mosses are only able to use carbon dioxide (CO_2), but many aquatic seed plants and algae are also able to use HCO_3^- (Sculthorpe, 1967).

The differences in the diffusivity of oxygen and carbon dioxide in air and water, may relate to the morphological differences between submerged macrophytes and the aerial form of the same species. This heterophylly is the presence on a single individual of two or more distinct types of leaf. For example, *Proserpinaca palustris* in the aerial form, has leaves with toothed margins that are smaller, broader, thicker, and fewer in number than those on submerged stems, which are highly dissected (Figure 2.13; Schulthorpe, 1967). In extreme examples of heterophylly, the leaf types are different in three aspects, habit, shape and anatomy, and a single plant may bear submerged, floating, and aerial leaves (Sculthorpe, 1967). There are many aquatic plants (e.g. *Cabomba, Ceratophyllum, Potamogeton,* and *Sparganium*) that change the morphology of their leaves when the shoot apex reaches the water surface and emerges into the aerial environment. This change usually consists of the submerged form being either linear or highly dissected, to an aerial form that is lanceolate or a more entire leaf form respectively (Figure 2.15; Sculthorpe, 1967).

On a smaller scale, the terrestrial plants have an external layer of waxy material (cuticle) that reduces the rate of water loss, the internalization of exchange surfaces such as superficial pores or stomata, and the development of conducting tissues (Niklas, 1992). These adaptations exist because terrestrial plants are exposed to the drier atmosphere, whereas aquatic plants are continuously covered in water (Niklas, 1997). It is important to note that aquatic plants do not possess stomata and as such nutrient exchange can occur over the entire surface (Sculthorpe, 1967). Consequently, the limiting state for

uptake in aquatic plants is diffusional stress, rather than stomatal resistance in terrestrial plants (Eugster and Hesterberg, 1996; Vesala, 1998).

Terrestrial and aquatic plants also experience different mechanical stresses. One way that mechanical stresses are increased in both environments is through an increase in height, which is a strategy used by plants to maximize light capture for photosynthesis (Ennos, 1999; Strand and Weisner, 2001). As such, at increasing velocities, a strategy of minimizing mechanical stress in aerial environments is for leaves to reconfigure into a conical or cylindrical shape, and become more tightly rolled as wind speed increases. A similar phenomenon occurs with clusters of leaves, which form bundles that become tighter as wind speed increases (Vogel, 1994). In aquatic systems ribbon-shaped plants (e.g. *Vallisneria spp.*) become more compliant with the flow (streamlined) due to their lack of strengthening tissue, which reduces the hydrodynamic drag (at higher flows) and thus the mechanical damage (Sculthorpe, 1967). However, in order to colonize faster moving environments, the length of the leaf must be small since drag is a function of surface area (Vogel, 1994; Wilson et al., 2003). Highly dissected leaves are also able to reduce mechanical stresses by the segments grouping together thereby reducing the surface area exposed to the approaching flow (Vogel, 1994). Hence, in order to reduce drag, plants must either become compliant with the flow, or reduce the size of the individual surfaces facing the flow. Thus, it is clear that aquatic plants have adapted to these hydrodynamic constraints, however, the mechanisms are as yet not understood.

There are limitations to pollination in submerged aquatic plants due to a number of factors including the lack of animal agents in aquatic environments. Although the vegetative features of aquatic plants show modifications of morphology and anatomy in

response to the aquatic environment, the reproductive structures are generally similar to those of related terrestrial plants in both general organization and microscopic structure (Sculthorpe, 1967; Ackerman, 1995). The flowers of the majority of aquatic angiosperms are adapted to aerial life, with either insects or wind as pollinating agents (Ackerman 1995, 2000). Pollen can also be dispersed by water with the pollen being carried by wind, water currents, or surface tension (Ackerman, 2000). Truly submerged pollination also occurs whereby the drifting pollen, which are individually filiform or adherent in long chains, become entangled in the typically filiform, feathery, or peltate stigmas (Sculthorpe, 1967). Since there are no known aquatic organisms that transfer pollen among aquatically pollinated plants, pollen is transferred on or in the water by wind, gravity, and water currents (Ackerman, 2000).

There are several dispersal mechanisms for macrophytes. One of these is by animals and water birds, which are the main agents in the short and potentially long range dispersal of aquatic plants. Additionally, many submerged species spread by runners or by vigorous growth in their rhizomes (Philbrick and Les, 1996). Another means of dispersing, as with *Isoetes spp.*, is to produce plantlets (young plant with a developing rhizome, adventitious roots, and two leaves) instead of sporangia (Sculthorpe, 1967). However, floods and normal river currents are probably the most powerful agents in distributing vegetative propagules. Whole plants of all life forms, rooted rhizomes and tubers, vegetative fragments, and turions (small specialized shoots), are often torn away and carried for kilometers (Sculthorpe, 1967); thus demonstrating how aquatic plants may be dispersed over large distances.

Adaptations to Flow

Macrophytes must be able to support themselves in a variety of freshwater environments. It has been noted by Stevens and Hurd (1997) that under almost any field conditions the pressure gradients at leading edges of macrophyte leaves will be sufficient to cause separation in the flow. Separation points occur when the flow stops moving up the surface of the plant, and starts moving in the downstream direction (Vogel, 1994), where vortices are shed. Thus, with vorticity being generated in the wakes of the leaf edges, the vortex streets from the leaf wakes combine to produce the turbulence in the flow within and downstream of the plant body (Anderson and Charters, 1982). Accordingly, one of the consequences of increased branching angle is to increase vorticity, and with it the amount of nutrient and light getting to the plant (Denny and Robertson, 2002), whereas the function of decreased branching angle is to increase the amount of compliance and thus lower the drag that the plant experiences (Ennos, 1999; Speck, 2003).

Macrophytes have various strategies to overcome high fluid forces including: greater structural strength; greater flexibility; growth in thin layers; and by the restriction of their growth to non-critical seasons of water flow (Dawson, 1988). The more compliant plants adopt a more streamlined and compact form with increasing velocity (until the velocity is so high that they become damaged or dislodged). Less compliant plants have a low initial resistance and can tolerate small increases in velocity by having leaves at the water surface, but hydraulic resistance increases rapidly as leaves bend into the water and become submerged (Dawson, 1988). However, most aquatic plant species have flexible stems allowing them to bend into the flow, thus reducing the surface area

directly exposed to the approaching flow (Sand-Jensen, 2003). Fortunately, compliance can occur without reducing the plant's capacity for photosynthesis or nutrient uptake, and without negatively affecting productivity (Gerard, 1987), as will be discussed in the photosynthesis section. Flexibility also determines which sort of flow habitat is most mechanically stressful; for rigid organisms, waves produce larger forces than do unidirectional currents of the same peak velocity, whereas the opposite is true for flexible organisms (Koehl, 1996). Plants that grow in energetic environments tend to be small in stature and limited in lateral spread, whereas plants that grow in predictable habitats tend to be higher in stature and extensive in lateral spread (Barrat-Segretain, 2001). However, most giant kelps are both long and flexible while living in an energetic environment, and this morphology may be able to reduce the drag experienced by these plants (Denny et al., 1997). It has also been found that species with fewer branches break at higher current velocities as compared to highly branched species (Sheath and Hambrook, 1988). Plant architecture is clearly important as the shoot area defines the domain of the interaction with the water current, and the ability of the plant to uptake nutrients (Schutten and Davy, 2000). The relative magnitudes of the stem's compliance and the anchorage strength determine whether an individual plant remains in position, breaks, or is uprooted. More specifically, compliance is the ability of the shoot structure to deform with increasing current velocity, thus reducing its roughness and frontal area (Schutten and Davy, 2000), and increasing the likelihood of the plant remaining anchored.

Distribution of Macrophytes

The vegetation of freshwater environments is defined by the effect and interactions of a single physical factor, water flow, which determines plant-form, growth-

controlling factors, and habitat (Dawson, 1988). Dawson (1988) reported that at high flows, aquatic vegetation may be confined to the margins of the channel and to islands where emergent vegetation can be in direct competition with terrestrial vegetation. Very low flows allow the development of a vegetation characteristic of still water (e.g. emergent and floating plants; Dawson, 1988). Other factors to consider in regards to macrophyte distribution are that low flows may be accompanied by reduced oxygen concentrations, increased temperature, and desiccation (i.e., small ponds and streams can dry up due to extreme climatic variations; Lancaster and Hildrew, 1993), all of which can influence stream communities. Conversely, unusually high flows are often accompanied by increased velocity and hydraulic forces (i.e., drag and shear stress) on the stream bed (Lancaster and Hildrew, 1993). At intermediate flow regimes, the physical and chemical factors can control growth, interact with aquatic plants to regulate seasonal biomass (Dawson, 1988). For this reason, the plant community at a site reflects the balance achieved between the physiochemical environment and the plant's tolerance, adaptation to, or the modification of these conditions by the plants' presence (Dawson, 1988). Other factors influencing the distribution and growth of freshwater macrophytes are known to include turbulence, seasonal temperature patterns, surface and interstitial water chemistry, sediment composition, light, and other biota (White and Hendricks, 2000). Establishment of well-developed macrophyte patches, however, appear to be related primarily to constant or predictable discharge, turbidity, and canopy cover. Additionally, most macrophytes will grow where favorable combinations of substrate type, water depth, surface velocity, nutrient availability, and other environmental factors, occur (White and Hendricks, 2000).

Flow Around Individual Plants

Photosynthesis

Flow around individual plants directly influences the productivity of the plant as well as the plant canopy. For example, macroalgae rely on the movement of water for the delivery of nutrients to their surface, as such, an increase in velocity increases photosynthesis and thus, productivity (Stewart and Carpenter, 2003). However, many abiotic and biotic factors control net macrophyte productivity including: photon flux density and spectral composition (Dennison, 1987; Falkowski and Raven, 1997); nutrient availability (Borchardt, 1994); temperature (Davison, 1991); water motion (Wheeler, 1988); inter- and intra-specific competition for space and resources (Creed et al., 1996); and rates of herbivory (Leonard et al., 1998; reviewed in Hurd, 2000). Although, it is generally agreed that light intensity is the limiting factor in determining the maximum depth at which plants will occur in a given body of water. The depth where respiration equals photosynthesis for a particular plant is known as the compensation depth; plants cannot exist below this depth (Riemer, 1993). Due to the limitations surrounding photon capture in aquatic systems, freshwater macrophytes must maximize photosynthesis. As indicated by Hurd and Stevens (1997) flapping is a technique used by marine algae in order to enhance photon capture by reducing self-shading. Schutten and Davy (2000) also noted that at low current velocities, the spreading of leaves increases the area for light interception. However, when exposed to faster currents, the plant receives less efficient light interceptions due to the resulting compliance, which reduces resistance and minimizes mechanical damage (Koehl and Alberte, 1988). Another strategy used by plants to maximize photon capture under poor light conditions is to have longer branches

and taller plants (associated with a decreased number of branches and below-ground biomass); this is also a physical response to flow (Strand and Weisner, 2001). The most basic morphological response however, is to increase the size of the leaf surface and the number of photosynthetic cells on that surface (Rascio, 2002).

Gas exchange and light capture are essential to the productivity of plants, making heterophylly a prime example of the functional explanation for plant morphology. Accordingly, an increase in surface area:volume is a technique used to maximize light capture (Gerard and Mann, 1979; Gutschick, 1999), and to increase the flux of nutrients available to the plant (Wheeler, 1988; reviewed in Hurd, 2000). Fine-scale morphological features might act as roughness elements generating transitional or turbulent flow at the plant surface at low mainstream velocities (Koch, 1994; reviewed in Hurd, 2000). Additionally, the hairs of some macroalgae may increase the deposition of particulate material and create a still region at the thallus surface in which extracelluar enzymes can act (Koch, 1993).

Photon capture differs between aquatic and terrestrial environments due to the different spectral characteristics of light in these two systems. This is related to the fact that water attenuates the intensity of sunlight and preferentially absorbs the red wavelengths of light. In contrast, air neither attenuates nor alters the spectral properties of light (Niklas, 1997), although forest canopies have been found to reduce the red to far-red ratio (the ratio between transmitted light in the red band (655-665 nm) to far-red light (725-735 nm; Lieffers et al., 1999). Light can penetrate only a relatively small distance (as compared to the atmosphere) into an aqueous medium because water absorbs light more strongly than air. For example, light traveling through 50 m of air, will lose almost

none of its intensity, but only 78% of incident blue light will still present, and virtually none of the incident red light when light travels through 50 m of water (Denny, 1993). In addition to this, turbidity decreases water transparency and thus increases light attenuation (James et al., 2004), which leads to a decrease in plant biomass (Christian and Sheng, 2003). For this reason, aquatic plants living a few centimeters below the water surface can experience significantly lower light intensities shifted in favour of blue wavelengths than plants living in air (Niklas, 1997). In addition to the problem of the reception of necessary intensities of appropriate wavelengths of light, a photosynthetic organism under water must also acquire dissolved carbon (Sculthorpe, 1967). Structural modifications of submerged leaves to increase their photosynthetic efficiency include: an extremely thin cuticle; thin leaves; and the presence of chloroplasts in the epidermis (as opposed to being found only in the mesophyll as with land plants; Sculthorpe, 1967). Leaf shape, the length of internodes, and the pattern of leaf arrangement are all important in defining the total amount of direct light a shoot can receive (Niklas, 1992). For example, it has been documented that in terrestrial plants, leaves that are more erect tend to have better light-use efficiency (Gutschick, 1999). However, in aquatic systems, a canopy with horizontal leaves is more successful in low light conditions, where leaf angles become more erect with increasing irradiance (Niinemets and Fleck, 2002). In terms of the length of the internodes, low light levels increase this length as a way to extend leaves higher in the water column (Cronin and Lodge, 2003). Moreover, because chlorophyll *a* (the most common photosynthetic pigment) absorbs strongly at a wavelength of 680-710 nm (red light; Kirk, 1994), it is a relatively ineffective means for

gathering light at depth (Denny, 1993). Interestingly, the diversity of accessory pigments found in the algae, are not seen in freshwater macrophytes (Dawes, 1981).

Nuritents

Barrat-Segretain (2001) has shown that one modification to poor nutrient conditions is for the shoot to root ratio to increase with decreasing sediment fertility in turbulent flow. The shoot to root ratio varies greatly among species and growth forms with bottom dwelling angiosperms having the lowest ratio, and taller erect and canopy-producing angiosperm species generating the highest ratios. Angiosperms growing in nutrient-poor environments have disproportionately large root systems and a reduced shoot to root ratio (Kalff, 2002) to aid in nutrient uptake as well as with anchorage. Additionally, plants at sheltered sites with thick diffusive boundary layers, increase their below-ground biomass, compared to plants at wave-exposed sites, probably in order to supply the plant with nutrients through root uptake (Strand and Weisner, 2001). It is known that rooted submerged macrophytes can take up inorganic nutrients from both the sediments and from the water column, but the rooted macrophytes generally obtain most of their phosphorus and nitrogen from the sediments (White and Hendricks, 2000; Kalff, 2002). This is important because nutrients, especially nitrogen and phosphorus, usually control the rates of growth after disturbance (Biggs, 1996). Consequently, the maximum biomass that macrophytes achieve at a particular site, is the result of a balance between the conditions available for growth and the plants' physiological responses at its current phase of growth (Hurd et al., 1996). In macrophytes lacking roots, nutrient uptake generally occurs across the blade surface, making surface area the measure that best reflects the rate at which nutrients are taken up across the cell membrane (Hurd et al.,

1996). Advection ensures a near continual supply and availability of nutrients to macrophytes directly through the replenishment of water, and indirectly through the supply to the sediments (Dawson, 1988).

Phosphorous is a nutrient that is mainly associated with organic matter and fine mineral particles of aluminum, calcium, and iron compounds. As a result, coarse-textured sediments contain much lower concentrations of nitrogen and phosphorous than fine-textured sediments (Sand-Jensen, 1998). Temporary sediment retention during summer exerts a strong influence on sediment processes and reduces the transport of nitrogen and phosphorous to downstream lakes and estuaries (Sand-Jensen, 1998). Phosphorous and nitrogen are generally considered the most critical nutrients for autotrophic production, although other elements (e.g., iron, potassium, and silica) can limit growth under certain circumstances. In nutrient-poor freshwaters, phosphorous is usually the principal nutrient limiting autotrophic production, whereas is in temperate marine waters, nitrogen is the more common limiting nutrient (Chambers et al., 1999). The relatively large and slow-growing macrophytes also have a much lower nitrogen and phosphorus requirement per unit carbon (biomass) than the much smaller phytoplankton (Kalff, 2002). When phosphorous is not limiting, temperature exerts the dominant control over algal growth rates (Bothwell, 1988).

Grazing, Predation, and Competition

It is also possible for grazers and predators to have an effect on macrophyte productivity. Although, direct grazing is generally not a controlling factor in the overall distribution and biomass of freshwater plants (Chambers et al., 1999). The higher structural carbon content appears to be responsible for making macrophytes as a group less desirable to herbivores than phytoplankton or periphyton (Kalff, 2002).

Additionally, if resources are plentiful, there is no competition, regardless of the amount of niche (not canopy) overlap between individual plants as well as different macrophyte species (Abrams, 1980). Alternatively, if there is territoriality or if species actively alter their resource utilization to avoid a competitor, competition may occur in spite of the fact that there is little or no niche overlap (Abrams, 1980). Furthermore, it has been said that abiotic processes dominate lotic processes when flows are highly energetic, whereas biotic interactions such as competition or predation tend to occur in more predictable flow environments (Poff and Ward, 1989). Competition can be defined as a contest between plants for environmental resource, when that resource is limiting, and can be identified by growth inhibitions in one species that are caused by another (Agami and Waisel, 2002). For example, floating macrophytes (e.g., *Azolla*) can block light from submerged species (e.g., *Elodea*) thus decreasing its productivity (Forchhammer, 1999). Allelopathy is another form of competition whereby one organism produces a chemical substance that inhibits the growth of another organism, giving the first species the competitive advantage (Gopal and Goel, 1993). For example in *Ceratophyllum demersum* emits a chemical which limit the growth of cyanobacteria (Gross et al., 2003). Thus, competition is a complicated phenomena which is highly dependent on nutrient acquisition; generally a function of flow.

Flow in Macrophyte Canopies

Effect of Macrophytes on Flow

Changes in water flow or velocity can alter the biomass and species composition of submerged plant communities, however, aquatic plants can also alter flow patterns. Marine and freshwater macrophytes can modify their physiochemical environment by

slowing water flow, trapping sediments, and altering temperature and water chemistry profiles (Ackerman and Okubo, 1993; Chambers et al., 1999). These modifications occur because the nature of flow is changed as it enters and passes through plant canopies. Ackerman and Okubo (1993) have shown that upon entering the canopy, the velocity of the ambient current is considerably reduced. They also demonstrated that flow within the mid-portion of the canopy is consistent in terms of average velocity, with a slight increase in speed below the region of maximum leaf area. Accordingly, turbulence in the flow entering the canopy is suppressed by the consumption of energy by the hydrodynamic drag forces of large, divided fronds (Anderson and Charters, 1982). The drag is also reduced in canopies due to the protection of neighbouring plants (Sand-Jensen, 2003). In short, because turbulence in the incoming flow is damped, the net effect is a smooth internal and exiting flow at velocities below a critical value (6-12 cms^{-1} depending on the spacing of the branches), and an abrupt transition to turbulent flow at velocities above (Anderson and Charters, 1982). Anderson and Charters (1982) also demonstrated that the decrease in transition velocity from single plants to groups of plants suggests that the transition depends on the density of branches in the flow path, not only on a single dimension characteristic of the plant's morphology. This is evident in the modification of turbulence in the flow passing though an algae with bushy morphology. If the flow entering the plant mass is turbulent, the turbulence will be damped as the water flows through the plant. This occurs because the dense morphology of the plant reduces the velocity within the plant structure. Conversely, turbulence is generated in the flow within the plant canopy because small branches act a roughness elements that trip the boundary layer creating an area of turbulence close to the plant

surface (Anderson and Charters, 1982). Additionally, it has been shown that different macrophyte morphologies affect the flow within the canopy differently due to their differences in stem flexibility (Shi and Hughes, 2002).

The plastic morphological response of macrophytes to water motion has prompted the suggestion that by changing their morphology, submerged plants are able to modify their hydrodynamic environment and thereby reduce drag or diffusional stresses (Hurd et al., 1997). In a plant canopy, most of the flow enters through the upstream margin, whereas the deflected flow moves above and along the sides of the plant canopy. The high macrophyte density at the surface of the canopy develops in the unidirectional flow of the shallow streams because the shoots and leaves bend over becoming very dense at the canopy surface (Sand-Jensen and Pedersen, 1999). Sand-Jensen and Mebus (1996) demonstrated that as water velocity is reduced within these macrophyte patches, the velocity is accelerated around the patches to maintain the downstream discharge (i.e., continuity) of water, resulting in steeper vertical velocity gradients at the patch surface than those encountered above the sediment surface upstream of the patch. Hurd and Stevens (1997) showed that since small, finely branched plants slow down and dampen turbulence, conditions within the plant body at low mainstream flows could be ideal for the formation of thick diffusion boundary layers. Thus, for small, branched plants, the potential for diffusion-limited productivity is much greater than that for larger, broadly branched macrophytes.

Due to the fact that plants are flexible and interact with the flow, branching patterns, leaf/stem length and stiffness will influence the effective plant surface area exposed perpendicularly to the flow, and, thereby, the effective pressure drag. However,

due to the uncertainty of estimates of typical plant parameters, transition from turbulent to laminar flow, and the flexibility of the plant canopies, it is very difficult to predict or model turbulence since flow rates and boundary layer thickness change temporally (Sand-Jensen and Pedersen, 1999). Sand-Jensen and Pedersen (1999) indicate that these scaling parameters are important because the flow patterns generated or modified by the presence of the plants have strong implications for: (1) plant metabolism, physical resistance and canopy development; (2) sedimentation and resuspension of sediment particles; and (3) the growth and survival of micro-organisms and invertebrates on plant surfaces or on sediments shielded by the canopies.

Disturbance

Flow may be disrupted in streams due to unpredictable peak flows, which may move the substratum, wash away individual organisms, and cause high mortality to biota (Winterbottom et al., 1997). Hydraulic disturbance by sudden increases in flow may be the major mechanism controlling differences in biomass and structure between streams. The type and duration of disturbance may be more important to stream ecosystems than factors such as nutrient levels or plant/animal interactions due to biomass removal (Biggs and Thomsen, 1995). Extreme hydraulic forces accompanying spates (i.e., sudden floods) can erode organisms from the stream bed, particularly where the substrate is moved. Consequently, flow structures in the water column determine the likelihood that entrained particles and benthic organisms will be transported out of the reach (Lancaster and Hildrew, 1993). The degree of disturbance of the plant communities for a given peak flow depends on the properties of both the plants and the habitat. At the plant level, the physical structure of the organism (which determines the drag properties), the strength of

the root systems, intercellular connections, and how flexible the organism is, are important factors determining the impact of disturbance. At the habitat level, the age of the community and the shear stress to which it is already acclimatized contribute to the biotic resistance of the community (Biggs, 1996). Along these lines, the degree of habitat resistance is primarily a function of bed sediment stability or, more specifically, the ability of given sediments to resist being carried along in the current (Biggs, 1996).

Velocity Profiles

The complex spatial distribution of roughness elements among plant stands, stream bed and banks, and the differences in flow velocity outside and inside plant canopies, may result in variable velocity profiles and the distortion of logarithmic profiles (Sand-Jensen and Pedersen, 1999). This variability is representative of higher slopes and higher hydraulic roughness leading to a more turbulent flow for the same mean velocity. The vertical hydraulic gradients and deviations from the mean current flow created by streambed features such as riffles and bars may play a strong role in the distribution and nutrition of lotic macrophytes (White and Hendricks, 2000). Another factor influencing velocity profiles is seasonal variability in the rate of discharge, however, the seasonal growth of plants can in turn modify the speed or velocity of this flow. Major changes in flow may eliminate or strongly suppress the growth of a plant population. Plants adjust to increased flow conditions by shedding their above-substratum parts or by rapid reinvasion from less vulnerable areas through the production of numerous propogules or seeds (Dawson, 1988).

Sediments

The creation of a low energy environment above the sediments within macrophyte patches leads to the retention of fine mineral and organic particles (Petticrew and Kalff, 1992; Sand-Jensen, 1998). This trapping of particles by macrophytes also produces sediments with a higher organic content and smaller grain size within the bed than in nearby uncolonized areas (Chambers et al., 1999). Increased current velocity, however, results in river beds with larger sediment particles that are usually less nutrient rich, and less densely packed than river beds that experience slower current velocity. For this reason, aquatic macrophytes tend to grow better in low flows, either because of increased sediment nutrient concentrations or due to the increased sediment stability (Chambers et al., 1991). Consequently, both macrophyte diversity and the distribution of macrophytes is positively correlated to the substratum type (Baattrup-Pedersen and Riis, 1999) demonstrating the importance of having fine sediments settle out of the water column (French and Chambers, 1996).

Baattrup-Pedersen and Riis (1999) showed that emergent macrophyte species are primarily associated with finer-textured substrata (e.g. mud, peat and fine sand), whereas submerged macrophyte species are primarily associated with the coarser-textured substrata (e.g. coarse sand, stone, and gravel). For macrophytes, substrate type and cohesiveness also affect the strength of below-ground anchorage. In sediments that are not yet compact, the long-rooting plants (e.g. *Sparganium erectum*) are best adapted to resist spates. On coarser gravels the plants usually have a dense interweaving of shallow, often horizontal, roots (e.g. *Rannunculus* spp.), which curl around particles. These

different methods of anchoring can stabilize the habitat and increase the overall resistance of a site to flow changes (Biggs, 1996).

Methodologies

Given the importance of fluid dynamics to aquatic plants, it is important to characterize and measure the fluid dynamic conditions in and around macrophyte canopies. A variety of flow visualization techniques exist that allow the observer to see the flow patterns, and depending on the complexity of the technique, measurement velocity and turbulence. Additionally, there are several methods of measuring velocity from which other quantities such as shear stress can be derived. It is important to have an accurate representation of flow conditions since they are one of the main factors regulating freshwater macrophyte productivity.

Flow Visualization

One of the most effective ways of assessing fluid flow is by observing streaklines of dye. Dye is injected into the flow upstream of the working section through an L-shaped hypodermic tube. The tube has to be so thin that its wake is smooth and laminar (Anderson and Charters, 1982). This method was used by Sand-Jensen and Pedersen (1999), whereby dye was injected into the flow upstream and along the sides of macrophyte stands, as well as in the interior, and the movements of the dye were observed to aid in the interpretation of the flow patterns. Nepf (1999) used a similar dye plume technique to measure diffusivity in the field within an emergent stand of *Spartina alterniflora*. When using dye tracking as a method of quantifying flow patterns, it is important to record the water depth, canopy height, percentage of the water column occupied by vegetation, vegetation density, size and patchiness of the plant bed, wind

intensity and direction, and waves if possible and applicable (Koch and Verduin, 2001). The disadvantage of flow visualization with dye is it only allows for an estimation of average flows over relatively broad spatial scales when used in the field. Thus, when smaller scale questions are asked, more sophisticated techniques (such as PIV as is discussed in a later section) need to be employed (e.g., Koch and Verduin, 2001).

Alternatively, according to Hurd et al. (1997) another way to visualize the flow is by using time-lapse photography of two tracers, whereby a thin mixture of reflective resin is added to the tank and used to create particle streaks. Using this technique, Hurd et al. (1997) were able to see that the gradient region of the velocity profile becomes thinner with increasing free-stream velocity. It is possible to compare these observations with predicted values from the flat-plate boundary layer theory (Hurd et al., 1997). Neutrally buoyant particles can also be added to the water, and be illuminated by a laser light sheet. Images of the illuminated particles are taken using a high-resolution video camera equipped with a macro lens, mounted perpendicular to the light sheet (Stamhuis and Videler, 1998). Mica Pearlescence flakes acting as tracers are another way to assess flow patterns. These particles are generally too fine to be used in velocity analysis but have the advantage that their plate-like nature aligns with velocity gradients so that regions of velocity variation, including turbulence, are visually represented (Hurd and Stevens, 1997). For example, in steep velocity gradients, the mica particles minimize drag by aligning with the shear. There is little reflection of light off of the aligned particles, and the viewer sees a dark patch of fluid; the black regions in the photographs therefore indicate shear. In regions where velocity gradients are weak, the mica particles are

aligned randomly and scatter light in all directions, appearing silvery white (Hurd and Stevens, 1997).

Velocimetry

Particle-image velocimetry (PIV) is a powerful method to measure turbulence as well as coherent vortices in shallow water flows. This method offers spatial information related to the velocity field (Nezu and Onitsuka, 2001). A laser beam is expanded with a cylindrical lens system to form the plane light sheet whose thickness can be made less than 1 mm. Tracer particles are illuminated only when moving through this light sheet, and their images are recorded by a camera whose direction of observation is usually facing the sheet (Khalili et al., 2001). In the most frequently used PIV technique, two short exposures are taken, separated by a short time interval. The velocity measurement is thereby reduced to a recording of the displacement of individual particles during that time interval (Khalili et al., 2001).

An acoustic Doppler velicometer (ADV) can be used to measure velocity, turbulence, Reynolds stress and turbulence intensity for a given volume adjacent to or above the substratum (Bouckaert and Davis, 1998), as well as around macrophyte blades (Rybicki et al., 1997; reviewed in Hurd, 2000). The probe emits a series of acoustic pulses and records the reflection of these pulses from particles suspended in water (Khalili et al., 2001). The acoustic sensor consists of a transmitting transducer surrounded by two (2D) or three (3D) receiving transducers, usually mounted on short arms. The transmitted beams are typically orientated so that the sampling volume is located below the probe. This volume has a cylindrical shape, with a diameter of approximately 0.5 cm and a height of about 1 cm (Khalili et al., 2001).

Velocity can also be measured with cylindrical hot-wire anemometers, to help with the interpretations of flow visualization around and within macrophyte stands (Sand-Jensen and Pedersen, 1999). The working principle of the thermal anemometer is based on heat transfer from an immersed, electrically heated sensor to a fluid. In homogeneous fluids with constant temperature and pressure, the velocity of the fluid passing the sensor determines the rate of heat loss from the heated element; that is, more heat is released to the fluid at higher velocities (Khalili et al., 2001).

Approximations and Derived Measurements

To determine values for mean shear stress, velocity profiles are measured, from which velocity is regressed against the logged depth values from the log-linear part of the velocity profile (Biggs and Thomsen, 1995; reviewed in Ackerman and Hoover, 2001). However, non-logarithmic layers may occur in strongly accelerating or decelerating flow like those found in river reaches which narrow or widen rapidly. The logarithmic profile may also be distorted by spatial variation in the mixture of roughness types on the bed, or by the extreme bed roughness that occur over dunes and large rocks (Carling, 1992; Hoover and Ackerman, in Press). In these circumstances it is often possible to obtain near log-normal distributions of velocity from close to the bed, which can be used to estimate the local bed shear stress (Carling, 1992). The velocity of the fluid is zero at the surface of any solid object and a velocity gradient (du/dz) must form perpendicular to the solid surface. This gradient (as extrapolated from the velocity profile) is the change in velocity with the change in distance perpendicular to the solid surface. The shear stress in laminar flow is thus expressed as: $\tau = \mu$ (du/dz); where μ is the viscosity (Vogel, 1994; Ackerman, 1997; reviewed in Hurd, 2000). However, things are complicated in turbulent

flow because flow moves in both the horizontal and the vertical direction. To account for this the equation becomes $\tau = \rho\varepsilon\frac{du}{dz}$ where $\varepsilon = 1_m^2\frac{du}{dz}$ is the kinematic eddy viscosity (Kundu, 1990). This is simplified into the law of the wall $u = \frac{u_*}{\kappa}\ln\left(\frac{z}{z_o}\right)$, where u_* is the friction velocity and $\tau = \rho u_*^2$.

A Preston-static tube can be used to measure shear stress in laboratory as well as field settings (Ackerman and Hoover, 2001). This technique involves the use of a surface mounted Pitot tube to measure the total pressure at the boundary and a static pressure tap. The Preston tube must be small enough to be within the wall layer, pressure differences must be large, and the static pressure must be constant and measured close to the dynamic pressure tap (Ackerman and Hoover, 2001). This technique is however limited in that the flow needs to be as unidirectional as possible, and the water needs to be fast flowing since this method depends on measuring the dynamic pressure of the flow (Ackerman and Hoover, 2001).

Other Measurements

Drag, according to Schutten and Davy (2000), can be measured by attaching each individual shoot to a spring balance using a clamp of neutral buoyancy, with known and very small resistance, before submerging the blade into the flume current. The resulting tension is then read from the spring balance and corrected for the resistance arising from the clamp. Forces measured with the spring balance could potentially have a vertical component included because of the angle between the current and the plane of measurement; however, any such component would have been transferred to the tension only as the sine of that small angle.

The dispersion of particles released and captured in a macrophyte canopy were used to measure the eddy diffusivity (Ackerman, 2002). This method can also be used with plastic models of plants as the capturing surface in order to examine the eddy diffusivity around different shapes, and at different heights in the water column (Harvey et al., 1995). A similar technique is to inject microparticles over a set period of time, after which those attached to glass rods (covered in vacuum grease) are counted under a black light. Once again, this is a technique used to determine the particle distribution and thus, the eddy viscosity, across the flume section (Harvey et al., 1995).

A technique that provides a relative estimate of water motion between and within sites is to measure the dissolution of a substance such as plaster, sugar, or benzoic acid from a module attached to the macrophyte surface (Angradi and Hood, 1998; Koehl and Alberte, 1988; reviewed in Hurd, 2000). Rough estimates of average shear velocities along surfaces of blades of different morphologies exposed to the same field conditions were made by measuring the weight loss during a 10 min interval of candy (e.g., Life Savers) sewn to blades (Koehl and Alberte, 1988). This method requires that a calibration model be developed in a flume to relate mass loss of plaster, sugar or benzoic acid standards to water velocity and temperature. This model can then be used to calculate water velocity based on *in situ* loss of these substance standards (Angradi and Hood, 1998). This method is, however, very limited because the flow variables addressed using dissolution are diverse and are often nonspecific. For example, one cannot discern between the measurement of current velocity, flow intensity, turbulence intensity, or water motion (Porter et al., 2000).

Conclusion

The vegetation of aquatic systems is defined by the movement of water, which influences plant form, dominates the growth-controlling factors (e.g. nutrients and light), and defines the canopy structure. Thus, different flows will directly determine the presence (or absence), and location of instream vegetation (Dawson, 1988). On a smaller scale, it can be seen that water motion affects an aquatic plant through the transport of mass, momentum, and energy from the flowing water through the boundary layer to the plant's surface. The transport rates depend strongly on whether the flow in the boundary layer is laminar or turbulent. This is because the transport rates in turbulent flow with eddy diffusion are much larger than those in laminar flow with molecular diffusion (Anderson and Charters, 1982). Consequently, it is important for macrophytes to be able to alter morphologically to flow conditions because, different morphologies (i.e., bladed, whorled, and dissected leaves) potentially have different implications on the flow. This is relevant since it has been documented that there is a close relationship between environment and leaf structure and function (Rascio, 2002). Additionally, since plant form is important in creating and defining habitat in aquatic systems, it is important to examine the fluid dynamics surrounding macrophytes at a small scale using flow visualization techniques in order to determine what is happening around individual macrophytes to make implications to an ecological scale. The ecological scale provides an integrated response to a broad range of disturbances (Bunn et al., 1999). Intact ecosystems are required as references to compare the effectiveness of restoration programs, and as sources of natural genetic material for local stream reaches in need of restoration (Kauffman et al., 1997). Unfortunately, undisturbed ecosystems are becoming

rare, and for many rivers it is due to anthropogenic processes (e.g. timber harvest, livestock grazing, agriculture, and urbanization; Poff et al., 1997) which alter flow regimes.

Literature Cited

Abrams, P. 1980. Some comments on niche overlap. *Ecology* 61(1):44-49.

Ackerman, J.D. 1995. Convergence of filiform pollen morphologies in seagrasses: functional mechanisms. *Evolutionary Ecology.* 9:139-153.

Ackerman, J.D. 1997. Submarine pollination in the marine angiosperm *Zostera marina* (Zosteraceae). I. The influence of floral morphology on fluid flow. *Journal of Botany* 84(8):1099-1109.

Ackerman, J.D. 2000. Abiotic pollen and pollination: ecological, functional, and evolutionary perspectives. *Plant Systematics and Evolution* 222:167-185.

Ackerman, J.D. 2002. Diffusivity in a marine macrophyte canopy: Implications for submarine pollination and dispersal. *American Journal of Botany* 89(7):1119-1127.

Ackerman, J.D. and T.M. Hoover. 2001. Measurement of local bed shear stress in streams using a Preson-static tube. *Limnology and Oceanography* 46(8):2080-2087.

Ackerman, J.D., and A. Okubo. 1993. Reduced mixing in a marine macrophyte canopy. *Functional Ecology* 7:305-309.

Agami, M., and Y. Waisel. 2002. Competitive relationships between two water plant species: *Najas marina* L. and *Myriophyllum spicatum* L. *Hydrobiologia.* 482:197-200.

Anderson, S.M., and A.C. Charters. 1982. A fluid dynamics study of seawater flow though *Gelidium nudifrons. Limnology and Oceanography* 27(3):399-412.

Angradi, T., and R. Hood. 1998. An application of the plaster dissolution method for quantifying water velocity in the shallow hyporheic zone of an Appalachian stream system. *Freshwater Biology* 39:301-315.

Baattrup-Pedersen, A. and T. Riis. 1999. Macrophyte diversity and composition in relation to substratum characteristics in regulated and unregulated Danish streams. *Freshwater Biology* 42:375-385.

Barrat-Segretain, M-H. 2001. Biomass allocation in three macrophyte species in relation to the disturbance level of their habitat. *Freshwater Biology* 46:935-945.

Biggs, B.J.F. 1996. Hydraulic habitat of plants in streams. *Regulated Rivers: Research and Management* 12:131-144.

Biggs, B.J.F., and H.A. Thomsen. 1995. Disturbance of stream periphyton by perturbations in shear stress: time to structural failure and differences in community resistance. *Journal of Phycology* 31:233-241.

Borchardt, M.A. 1994. Effects of flowing water on nitrogen- and phosphorous-limited photosynthesis and optimum N:P ratios by *Spirogyra Fluviatilis* (Charophyceae). *Journal of Phycology* 30:418-430.

Bothwell, M.L. 1988. Growth rate responses of lotic periphytic diatoms to experimental phosphorous enrichment: The influence of temperature and light. *Canadian Journal of Fisheries and Aquatic Sciences* 45:261-270.

Bouckaert, F.W. and J. Davis. 1998. Microflow regimes and the distribution of macroinvertebrates around stream boulders. *Freshwater Biology* 40:77-86.

Bunn, S.E., P.M. Davis, and T.D. Mosisch. 1999. Ecosystems measures of river health and their response to riparian and catchment degradation. *Freshwater Biology* 41:333-345.

Carling, P.A. 1992. The nature of the fluid boundary layer and the selection of parameters for benthic ecology. *Freshwater Biology* 28:273-284.

Chambers, P.A., R.E. DeWreede, E.A. Irlandi, and H. Vandermeulen. 1999. Management issues in aquatic macrophyte ecology: a Canadian perspective. *Canadian Journal of Botany* 77:471-487.

Chambers, P.A., E.E. Prepas, H.R. Hamilton, and M.L. Bothwell. 1991. Current velocity and its effect on aquatic macrophytes in flowing waters. *Ecological Applications* 1(3):249-257.

Cheer, A.Y.L., and M.A.R. Koehl. 1987. Paddles and rakes: Fluid flow through bristled appendages of small organisms. *Journal of Theoretical Biology* 129:17-39.

Christian, D., and Y.P. Sheng. 2003. Relative influence of various water quality parameters on light attenuation in Indian River Lagoon. *Estuarine, Coastal and Shelf Science.* 57:961-971.

Coutanceau, M., and J. Defaye. 1991. Circular cylinder wake configurations: A flow visulization survey. *Applied Mechanics Reviews.* 44(6):255-305.

Creed, J.C., T.A. Norton, and J.M. Kain. 1996. Are neighbours harmful of helpful in *Fucus vesicolosus* populations? *Marine Ecology Progress Series* 133:191-201.

Cronin, G., and D.M. Lodge. 2003. Effects of light and nutrient availability on the growth, allocation, carbon/nitrogen balance, phenolic chemistry, was resistance to herbivory to two freshwater macrophytes. *Oecologia* 137:32-41.

Crossley, M.N., W.C. Dennison, R.R. Williams, and A.H. Wearing. 2002. The interaction of water flow and nutrients on aquatic plant growth. *Hydrobiologia* 489:63-70.

Davis, J.A., and L.A. Barmuta. 1989. An ecologically useful classification of mean and near-bed flows in streams and rivers. *Freshwater Biology* 21:271-282.

Davison, I.R. 1991. Environmental effects on algal photosynthesis: temperature. *Journal of Phycology* 27:2-8.

Dawes, C.J. 1981. *Marine Botany.* John Wiley and Sons, Inc. U.S.A. 628 pp.

Dawson, F.H. 1988. J.J. Symoens (ed.), *Vegetation of Inland Waters.* Kluwer Academic Publishers, Dordrecht. Netherlands. Pp. 283-309.

Den Hartog, C. 1982. Architecture of macrophyte-dominated aquatic communities. *Studies on Aquatic Vascular Plants.* ed. Symoens, J.J., S.S. Hooper and P. Compere. Royal Botanical Society of Belgium, Brussels. Pp. 222-234.

Dennison, W.C. 1987. Effects of light on seagrass photosynthesis, growth and depth distribution. *Aquatic Botany* 27:15-26.

Denny, M.W. 1993. *Air and Water: The Biology and Physics of Life's Media.* Princeton University Press, U.S.A. 341 pp.

Denny, M.W., B.P Gaylord, and E.A. Cowen. 1997. Flow and flexibility II. The roles of size and shape in determining wave forces on the bull kelp *Nereocystis luetkeana. Journal of Experimental Biology* 200:3165-3183.

Denny, M., B. Gaylord, B. Helmuth, and T. Daniel. 1998. The menace of momentum: dynamic forces on flexible orgamisms. *Limnology and Oceanography* 43(5):955-968.

Denny, M., and L. Robertson. 2002. Blade motion and nutrient flux to the kelp, *Eisenia arborea. Biological Bulletin* 203:1-13.

Ennos, A.R. 1999. The aerodynamics and hydrodynamics of plants. *Journal of Experimental Biology* 202:3281-3284.

Eugster, W., and R. Hesterberg. 1996. Transfer resistances of NO2 determined form eddy correlation flux measurements over a litter meadow at a rural side on the Swiss Plateau. *Atmospheric Environment.* 30(8):1247-1254.

Falkowski, P., and J.A. Raven. 1997. *Aquatic Photosynthesis.* Blackwell, Oxford, 375pp.

French, T.D., and P.A. Chambers, 1996. Habitat partitioning in riverine macrophyte communities. *Freshwater Biology* 36:509-520.

Forchhammer, N.C. 1999. Production potential of aquatic plants in systems mixing floating and submerged macrophytes. *Freshwater Biology.* 41:183-191.

Gerard, V.A. 1987. Hydrodynamic streamlining of *Laminaria saccharina* Lamour. in response to mechanical stress. *Journal of Experimental Marine Biology and Ecology* 107:237-244.

Gerard, V.A., and K.H. Mann. 1979. Growth and production of *Laminaria longicruris* (Phaeophyta) populations exposed to different intensities of water movement. *Journal of Phycology* 15:33-41.

Gopal, B., and U. Goel. 1993. Competition and allelopathy in aquatic plant communities. *The Botanical Review* 59(3):155-210.

Gregg, W.W., and F.L. Rose. 1983. The effects of aquatic macrophytes on the stream micro-environment. *Aquatic Botany* 14:309-324.

Gross, E.M., D. Erhard, and E. Ivanyi. 2003. Allelopathic activity of *Ceratophyllum demersum* L. and *Najas marina* ssp. *intermedia* (Wolfgang) Casper. *Hydrobiologia.* 506-509:583-589.

Gutschick, V.P. 1999. Research reviews: biotic and abiotic consequences of differences in leaf structure. *New Phytologist* 143(1):3-18.

Hart, D.D., B.D. Clark, and A. Jasentuliyana. 1996. Fine-scale field measurement of benthic flow environments inhabited by stream invertebrates. *Limnology and Oceanography* 41(2):297-308.

Harvey, M., E. Bourget, and R.G. Ingram. 1995. Experimental evidence of passive accumulation of marine bivalve larvae on filamentous epibenthic structures. *Limnology and Oceanography* 40(1):94-104).

Hinze, J.O. 1987. *Turbulence 2nd ed.* McGraw-Hill, Inc.

Hoover, T.M., and J.D. Ackerman. In Press. Near-bed hydrodynamics measurements above bolders in shallow torrential streams: Implications for stream biota. *Journal of Environmental Engineering and Science.*

Hurd, C.L. 2000. Water motion, marine macroalgal physiology, and production. *Journal of Phycology* 36:453-472.

Hurd, C.L., P.J. Harrison, and L.D. Druehl. 1996. Effect of seawater velocity on inorganic nitrogen uptake by morphologically distinct forms of *Macrocystic integrifolia* from wave-sheltered and exposed sites. *Marine Biology* 126:205-214.

Hurd, C.L., C.L. Stevens, E.L. Bernard, G.A. Lawrence, and P.J. Harrison. 1997. Visualization of seawater flow around morphologically distinct forms of the giant kelp *Macrocystis integrifolia* from wave-sheltered and exposed sites. *Limnology and Oceanography* 42(1):156-163.

Hurd, C.L., and C.L. Stevens. 1997. Flow visualization around single- and multiple-bladed seaweeds with various morphologies. *Journal of Phycology* 33:360-367.

Idestam-Almquist, J., and L. Kautsky. 1995. Plastic responses in morphology of *Potamogeton pectinatus* L. to sediment and above-sediment conditions at two sites in the northern Baltic proper. *Aquatic Botany* 52:205-216.

James, W.F., E.P. Best, and J.W. Barko. 2004. Sediment resuspension and light attenuation in Peoria Lake: can macrophytes improve water quality in this shallow system? *Hydrobiologia.* 515:193-201.

Kalff, J. 2002. *Limnology: Inland Water Ecosystems.* Prentice Hall, Upper Saddle River, New Jersey.

Kauffman, J.B., R.L. Beschta, N. Otting, and D. Lytjen. 1997. An ecological perspective of riparian and stream restoration in the western United States, *Watershed Restoration* 22(5):12-24.

Khalili, A., M. Huettel, and W. Merzkirch. 2001. Fine-scale flow measurements in the benthic boundary layer. Pp. 44-77 In *The Benthic Boundary Layer Transport Processes and Biogeochemistry.* ed. Boudreau, B.P. and B.B. Jorgensen. Oxford University Press.

Kirk, J.T.O. 1994. *Light and Photosynthesis in Aquatic Systems.* Cambridge University Press, Cambridge. 509 pp.

Koch, E.W. 1993. The effect of water flow on photosynthetic processes of the alga *Ulva lactuca* L. *Hydrobiologia* 260/261:457-462.

Koch, E.W. 1994. Hydrodynamics, diffusion-boundary layers and photosynthesis of the seagrasses *Thalassia testudinum* and *Cymodocea nodosa. Marine Biology* 118:767-776.

Koch, E.W. and J.J. Verduin. 2001. Measurements of physical parameters in seagrasss habitats. Pp. 325-344 In *Global Seagrass Research Methods.* ed. Short, F.T., R.G. Coles, and C.A. Short. Elsevier Science B.V.

Koehl, M.A.R. 1996. When does morphology matter? *Annual Review of Ecology and Systematics* 27:501-542.

Koehl, M.A.R., and R.S. Alberte. 1988. Flow, flapping, and photosynthesis of *Nereocystis luetkeana:* a functional comparison of undulate and flat blade morphologies. *Marine Biology* 99:435-444.

Kundu, P.K. 1990. *Fluid Mechanics.* Academic Press, Inc. pp. 638.

Lancaster, J., and A.G. Hildrew. 1993. Characterizing in-stream flow refugia. *Canadian Journal of Fisheries and Aquatic Sciences* 50:1663-1675.

Lieffers, V.J., C. Messier, K.J. Stadt, F. Gendron and P.G. Comeau. 1999. Predicting and managing light in the understory of boreal forests. *Canadian Journal of Forest Research* 29:796-811.

Leonard, G.H., J.M. Levine, P.R. Schmidt, and M.D. Bertness. 1998. Flow-driven variation in intertidal community structure in a Maine estuary. *Ecology* 79:1395-1411.

Losee, R.F., and R.G. Wetzel. 1993. Littoral flow rates within and around submersed macrophyte communities. *Freshwater Biology* 29:7-17.

Mathieu, J., and J. Scott. 2000. *An Introduction to Turbulent Flow.* Cambridge University Press.

Nepf, H.M. 1999. Drag, turbulence, and diffusion in flow through emergent vegetation. *Water Resources Research* 35(2):479-489.

Nezu, I., and K. Onitsuka. 2001. Turbulent structures in partly vegetated open-channel flows with LDA and PIV measurements. *Journal of Hydraulic Research* 39(6):629-642.

Niinemets, U., and S. Fleck. 2002. Petiole mechanics, leaf inclination, morphology, and investment in support in relation to light availability in the canopy of *Liriodendron tulipifera. Oecologia* 132:21-33.

Niklas, K.J. 1992. *Plant Biomechanics: An Engineering Approach to Plant Form and Function.* The University of Chicago Press, Chicago. 607 pp.

Niklas, K.J. 1997. *The Evolutionary Biology of Plants.* The University of Chicago Press, Chicago. 449 pp.

Nowell, A.R.M., and P.A. Jumars. 1984. Flow environments of aquatic benthos. *Annual Review of Ecology and Systematics* 15:303-328.

Petticrew, E.L., and J. Kalff. 1992. Water flow and clay retention in submerged macrophyte bed. *Canadian Journal of Fisheries and Aquatic Science.* 49(12):2483-2489.

Philbrick, C.T., and D.H. Les. 1996. Evolution of aquatic angiosperm reproductive systems. *Bioscience.* 46(11):813-826.

Poff, N.L., and J.V. Ward. 1989. Implications of streamflow variability and predictability for lotic community structure: a regional analysis of streamflow patterns. *Canadian Journal of Fisheries and Aquatic Sciences* 46:1805-1817.

Poff, N.L., J.D. Allan, M.B. Bain, J.R. Karr, K.L. Prestegaard, B.D. Richter, R.E. Sparks, and J.C. Stromberg. 1997. The natural flow regime a paradigm for river conservation and restoration. *Bioscience* 47(11):769-782.

Porter, E.T., L.P. Sanford, and S.E. Suttles. 2000. Gypsum dissolution is not a universal integrator of 'water motion'. *Limnology and Oceanography* 45(1):145-158.

Rascio, N. 2002. The underwater life of secondarily aquatic plants: some problems and solutions. *Critical Reviews in Plant Science* 21(4):401-427.

Raven, P.H., R.F. Evert, and S.E. Eichhorn. 1999. *Biology of Plants.* 6th ed. W.H. Freeman and Company, New York. 944 Pp.

Reimer, D.N. 1993. *Introduction to Freshwater Vegetation.* Krieger publishing company, Malabar, Florida. Pp. 205.

Rybicki, N.B., H.L. Jenter, V. Carter, R.A. Baltzer, and M. Turtora. 1997. Observations of tidal flux between a submersed aquatic plant stand and the adjacent channel in the Potomac River near Washington, D.C. *Limnology and Oceanography* 42:307-317.

Sand-Jensen, K. 1998. Influence of submerged macrophytes on sediment composition and near-bed flow in lowland streams. *Freshwater Biology* 39:663-679.

Sand-Jensen, K. 2003. Drag and reconfiguration of freshwater macrophytes. *Freshwater Biology* 48:271-283.

Sand-Jensen, K., and J.R. Mebus. 1996. Fine-scale patterns of water velocity within macrophyte patches in streams. *Oikos* 76:169-180.

Sand-Jensen, K., and O. Pedersen. 1999. Velocity gradients and turbulence around macrophyte stands in streams. *Freshwater Biology* 42:315-328.

Santamaria, L. 2002. Why are most aquatic plants widely distributed? Dispersal, clonal growth and small-scale heterogeneity in a stressful environment. *Acta Oecologica* 23:137-154.

Schutten, J., and A.J. Davy. 2000. Predicting the hydraulic forces on submerged macrophytes from current velocity, biomass and morphology. *Oecologia* 123:445-452.

Sculthorpe, C.D. 1967. *The Biology of Aquatic Vascular Plants.* Edward Arnold, London (Reprinted 1985 Koeltz Scientific, Konigstein), 610 pp.

Sheath, R.G., and J.A. Hambrook. 1988. Mechanical adaptations to flow in freshwater red algae. *Journal of Phycology* 24:107-111.

Shi, Z., and J.M.R. Hughes. 2002. Laboratory flume studies of microflow environments of aquatic plants. *Hydrological Processes* 16:3279-3289.

Speck, O. 2003. Field measurements of wind speed and reconfiguration in *Arundo donax* (Poaceae) with estimates of drag force. *American Journal of Botany* 90(8):1253-1256.

Stamhuis, E.J., and J.J. Videler. 1998. Burrow ventilation in the tube-dwelling shrimp *Callianassa subterranean* (Decopoda: Thalassinidea). *Journal of Experimental Biology* 201:2159-2170.

Stevens, C.L., and C.L. Hurd. 1997. Boundary-layers around bladed aquatic macrophytes. *Hydrobiologia* 346:119-128.

Stewart, H.L., and R.C. Carpenter. 2003. The effects of morphology and water flow on photosynthesis of marine macroalgae. *Ecology* (84)11:2999-3012.

Strand, J.A., and S.E.B. Weisner. 2001. Morphological plastic responses to water depth and wave exposure in and aquatic plant (*Myriophyllum spicatum). Journal of Ecology* 89:166-175.

Thompson, P.A., and S.M. Troian. 1997. A general boundary condition for liquid flow at solid surfaces. *Nature* 389:369-362.

Vesala, T. 1998. On the concept of leaf boundary layer resistance for forced convection. *Journal of Theoretical Biology.* 194:91-100.

Vogel, S. 1987. Flow-assisted mantle cavity refilling in jetting squid. *Biological Bulletin* 172:61-68.

Vogel, S. 1988. *Life's Devices The Physical World of Animals and Plants.* Princeton University Press. Princeton, N.J.

Vogel, S. 1994. *Life in Moving Fluids The Physical Biology of Flow.* 2nd ed. Princeton University Press, Princeton, N.J.

Watson, L., and M.J. Dalhoitz. 1992 (onwards). The families of flowering plants: descriptions, illustrations, identification, and information retrival. Version: 6th August 2003. http://delta-intkey.com.

Wells, C.L., and M. Pigliucci. 2000. Adaptive phenotypic plasticity: the case of heterophylly in aquatic plants. *Perspectives in Plant Ecology, Evolution and Systematics* 3(1):1-18.

Wheeler, W.N. 1988. Algal productivity and hydrodynamics - a synthesis. *Progress in Phycological Research* 6:23-58.

White, D.S., and S.P. Hendricks. 2000. J.B. Jones and P.J. Mulholland (eds.) Lotic macrophytes and surface-subsurface exchange processes Pp. 363-379 In *Streams and Ground Waters.* ed. Jones, J.B., and P.J. Mulholland. Academic Press.

Wilson, C.A.M.E., T. Stoesser, P.D. Bates, and A. Batemann Pinzen. 2003. Open channel flow through different forms of submerged flexible vegetation. *Journal of Hydraulic Engineering* 129(11):847-853.

Winterbottom, J.H., S.E. Orton, A.G. Hildrew, and J. Lancaster. 1997. Field experiments on flow refugia in stream. *Freshwater Biology* 37:569-580.

Wright, J.P., W.S.C. Gurney, and C.G. Jones. 2004. Patch dynamics in a landscape modifies by ecosystem engineers. *Oikos* 105:336-348.

Zhang, Y., and B. Malmqvist. 1997. Phenotypic plasticity in a suspension-feeding insect, *Simulium lundstromi* (Diptera: Simuliidae), in response to current velocity. *Oikos* 78:503-510.

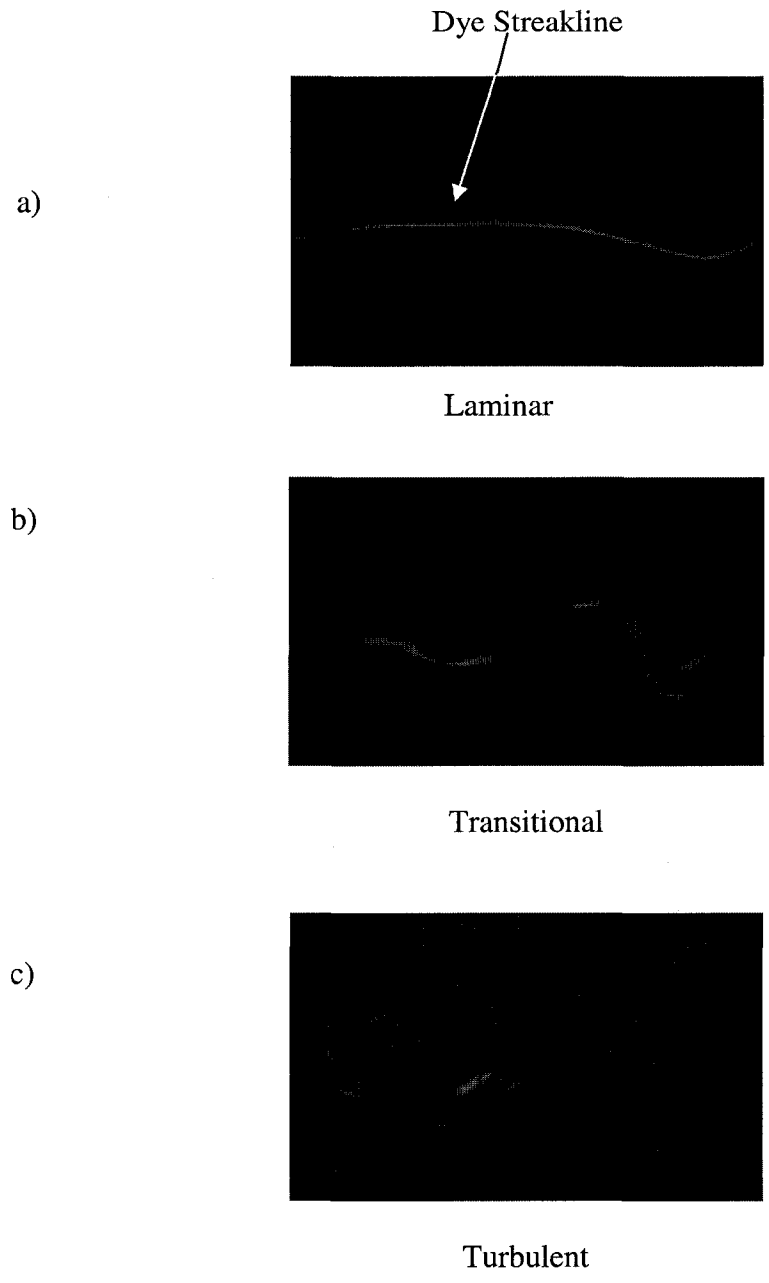

Figure 2.1: a) Laminar flow as seen by the smooth dye streakline, b) transitional flow as seen by the increasing waviness of the streakline, and c) turbulent flow as seen by the choatic nature of the streakline.

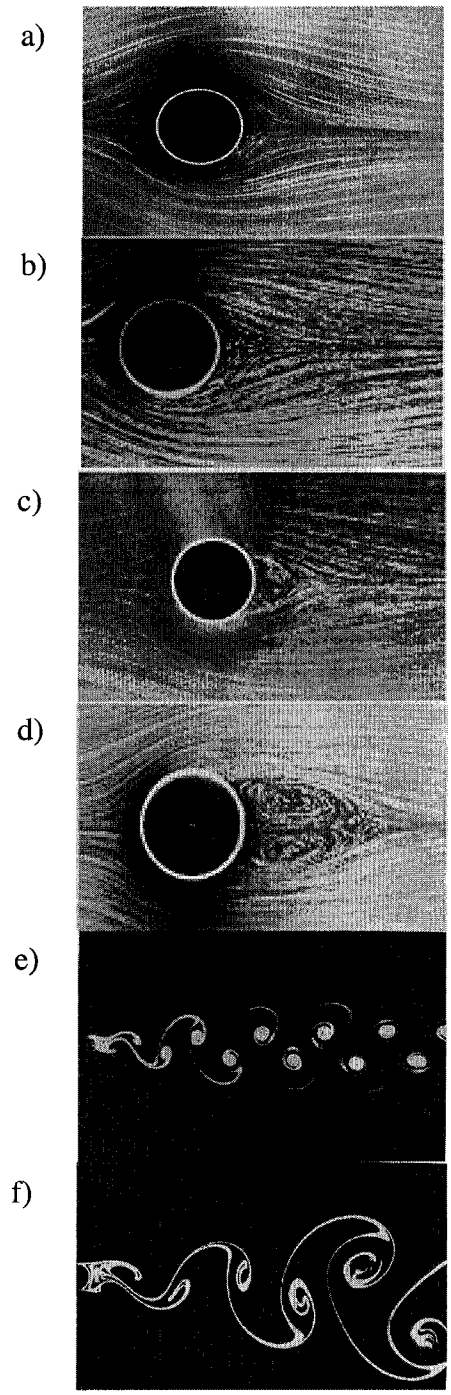

Figure 2.2: The transition to turbulent flow of a fluid as it passes a circular cylinder seen in cross section at different Reynolds numbers: (a) 1, (b) 10, (c) 13, (d) 26, (e)105, and (f) 150.
(From: http://nmm.media.mit.edu/student/95/aries/mas864/obstacles.html)

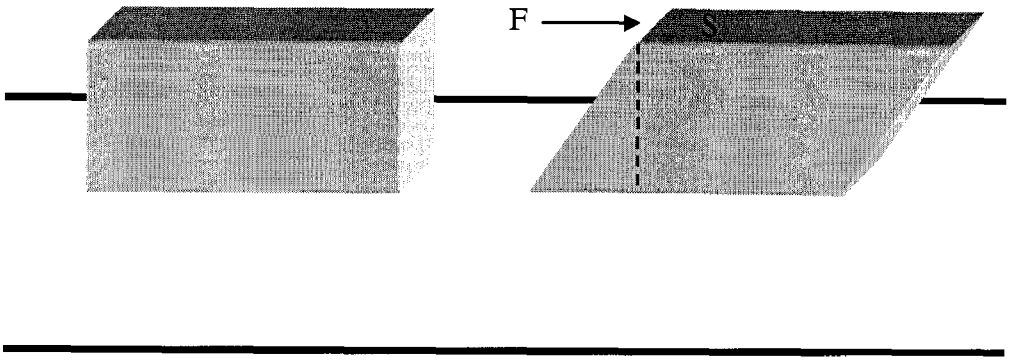

Figure 2.3: A rectangular block of fluid is deformed by shear stress, so two faces become parallelograms (after Vogel, 1994).

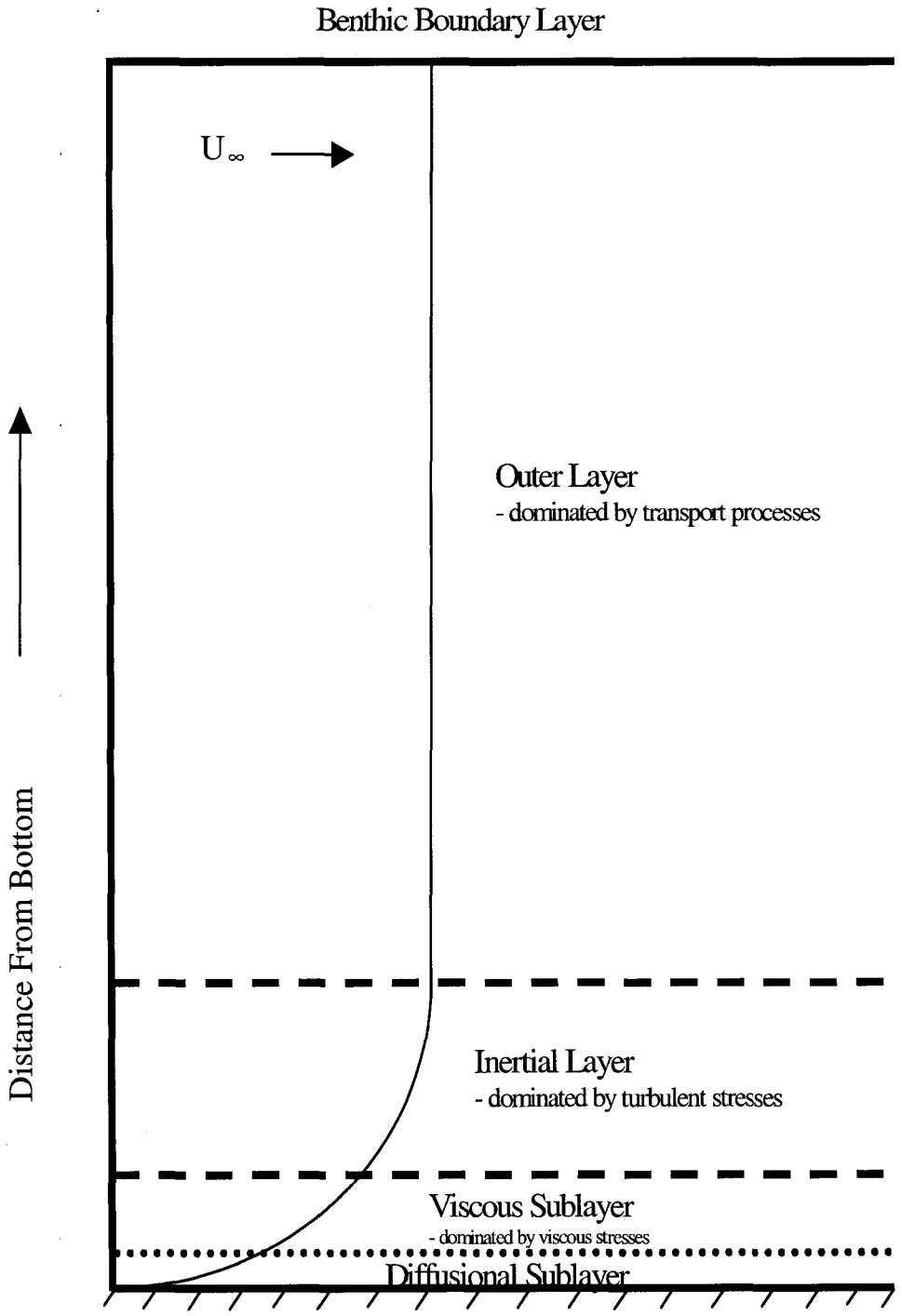

Figure 2.4: The benthic boundary layer concept. A velocity profile is presented from the surface (U = 0) to the free stream (U = U_∞; after Ackerman, 1989).

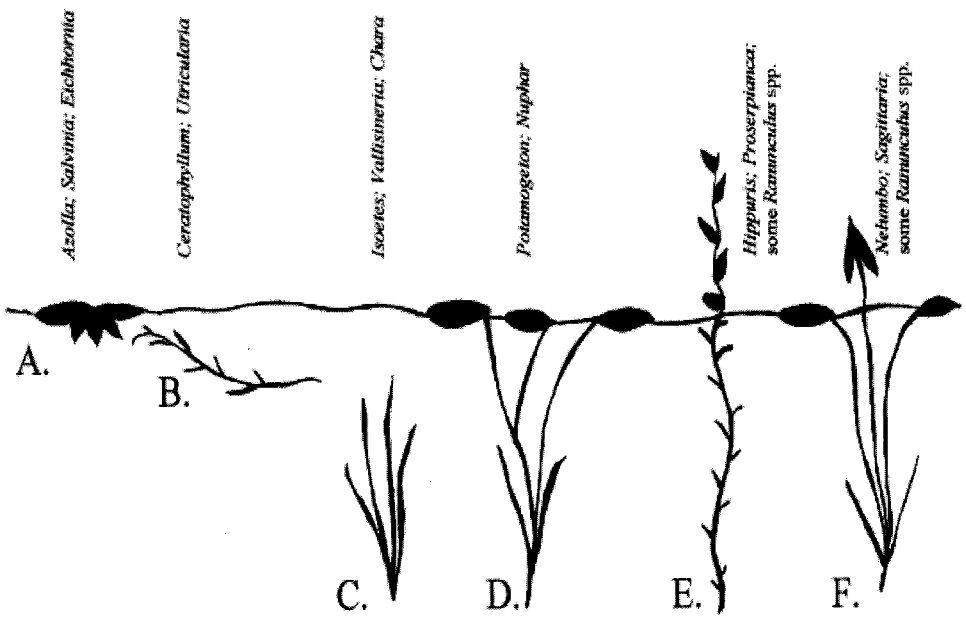

Figure 2.5: The four basic habitats of freshwater macrophytes: (A, B) free-floating; (C) submerged; (D, F) floating-leaved; and (E, F) emergent (Wells and Pigliucci, 2000).

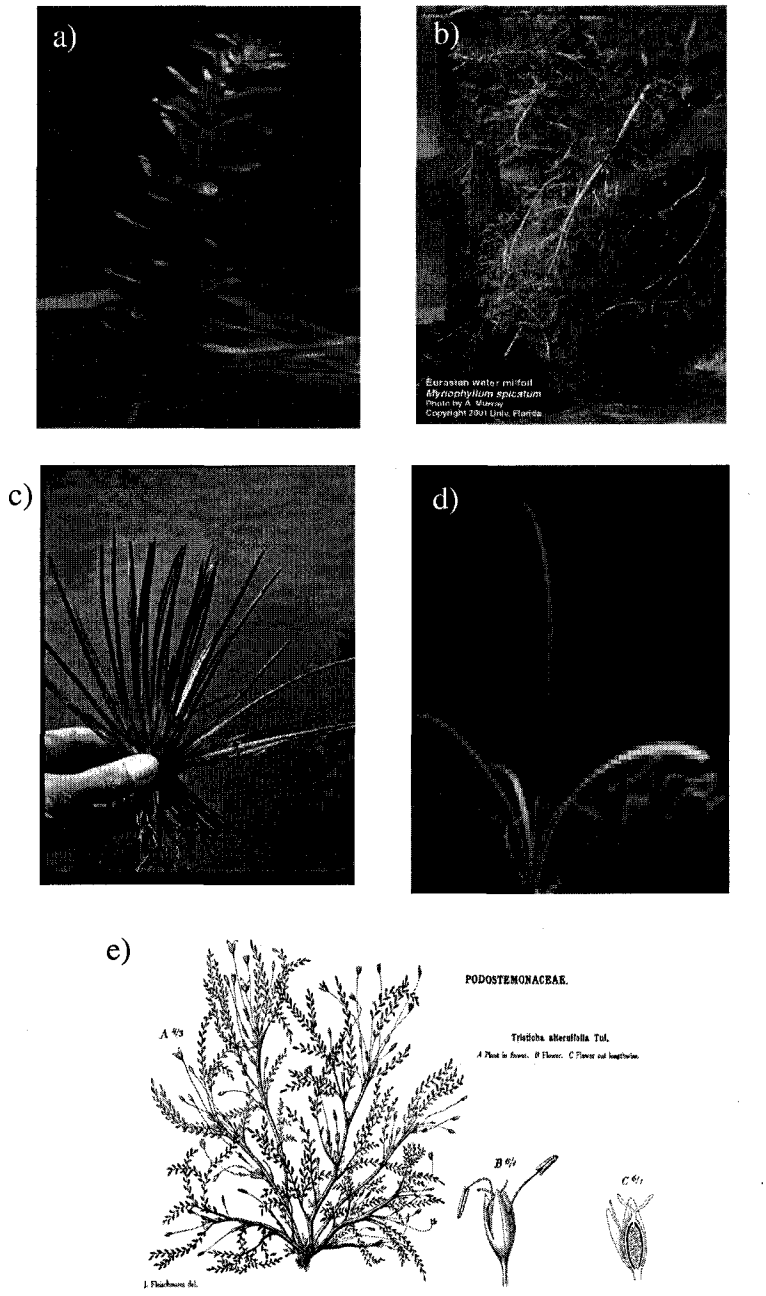

Figure 2.6: Examples of caulescent macrophytes a) *Elodea canadensis* and b) *Myriophyllum spicatum* (from: http://plants.ifas.ufl.edu/myrspi8.jpg; Vic Ramey, University of Florida) ; rosette macrophytes c) *Isoetes* spp. (from: http://www.anbg.gov.au/images/photo_cd/9J18G146043/006; Murray Fag, Australian National Botanic Gardens) and d) *Vallisneria americana*; and a thalloid macrophyte e) *Tristicha alternifolia* (From: http://biodiversity.uno.edu/delta/angio/www/podostem.htm; Watson and Dalhoitz, 1992 onwards).

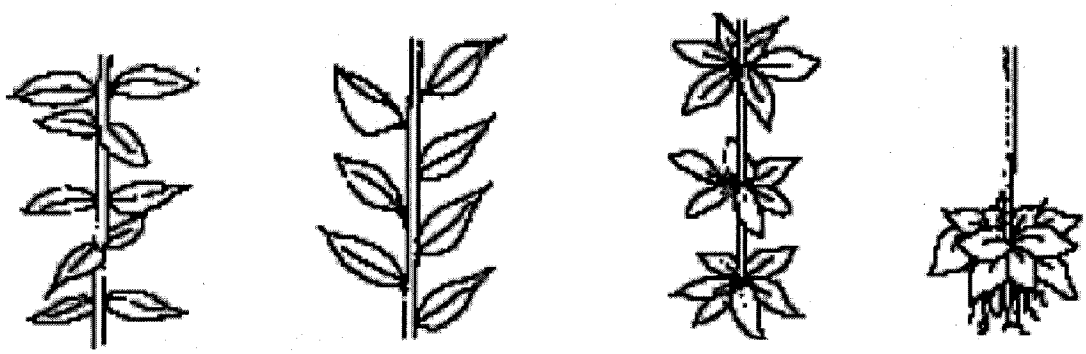

Figure 2.7: Different arrangements of leaves around plant stems: a) opposite, b) alternate, c) whorled, and d) rosulate. (From: http://extension.oregonstate.edu/mg/botany/leaves3.html; 2004 Oregon Sate University)

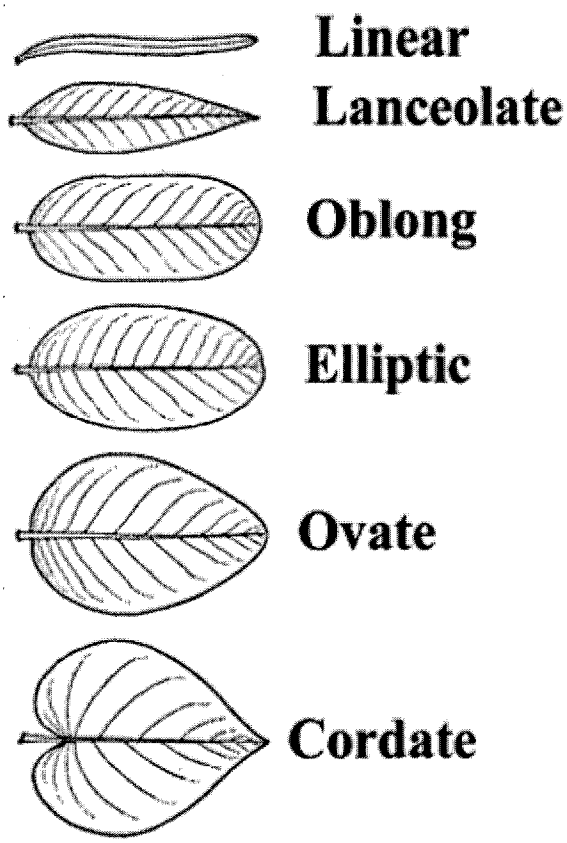

Figure 2.8: Morphologies of entire leaves ranging from linear to sagittate (cordate). (From: http://www.csdl.tamu.edu/FLORA/Wilson/tfp/veg/shapes3.gif)

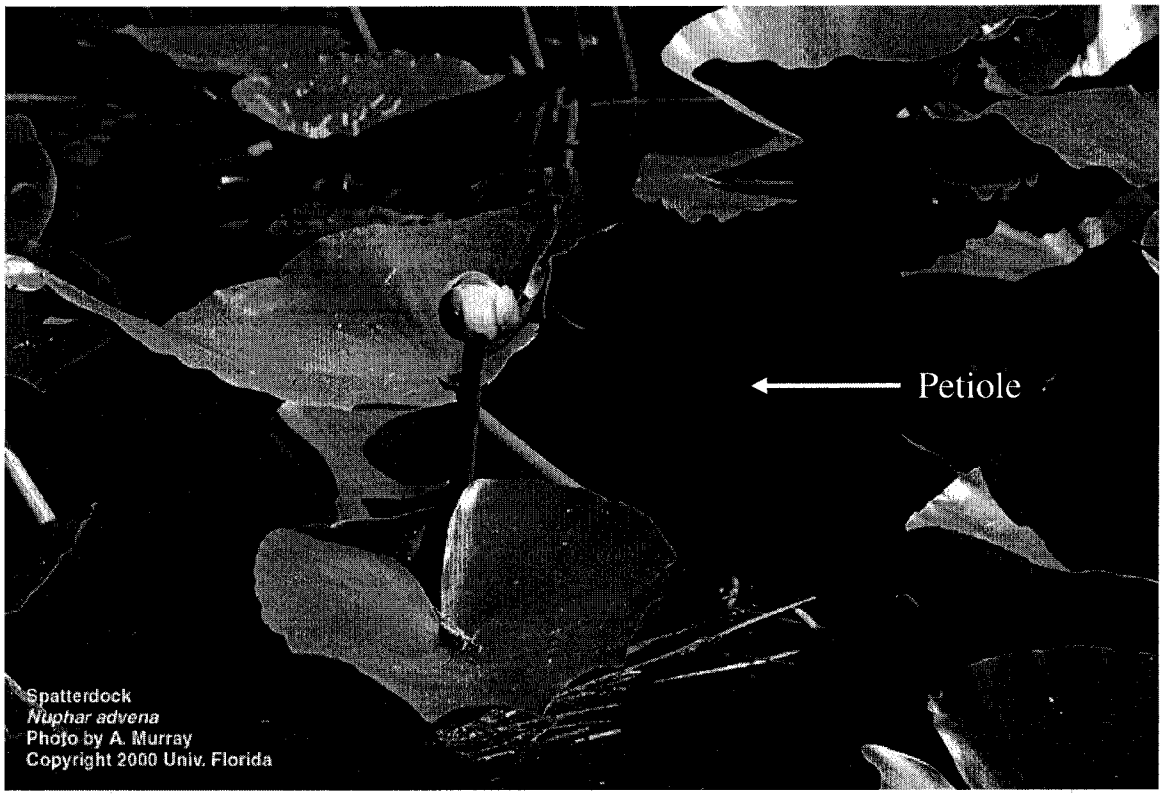

Figure 2.9: An example of a petiole-like freshwater macrophyte, *Nuphar advena* (from: http://plants.ifas.ufl.edu/nupadv7.jpg; Vic Ramey, University of Florida)

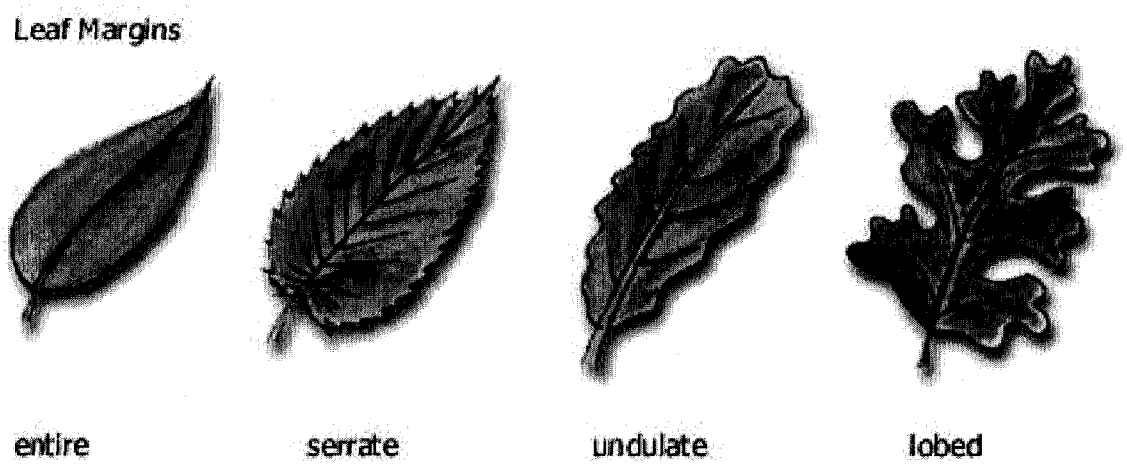

Figure 2.10: Different leaf margins that occur within entire leaf morphologies (From: http://collections.ic.gc.ca/gardens/Horticulture/The%20Structure%20of%20Plants.htm).

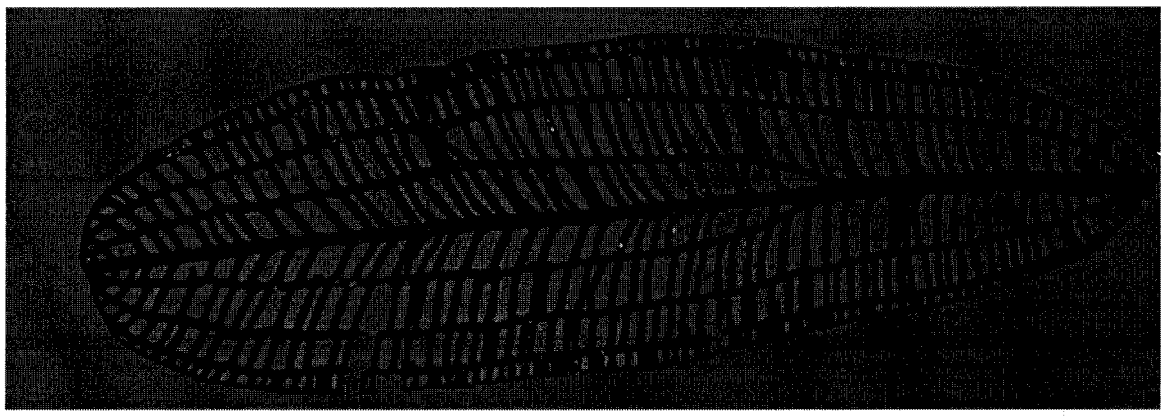

Figure 2.11: Fenestration occurs when small areas of interstitial tissue are lacking at maturity as demonstrated in this leaf of *Aponogeton madagascariensis* (Photo by Patrick Ragaz).

Figure 2.12: Dissected leaves (e.g. *Ceratophyllum*) occur when the leaf is subdivided.

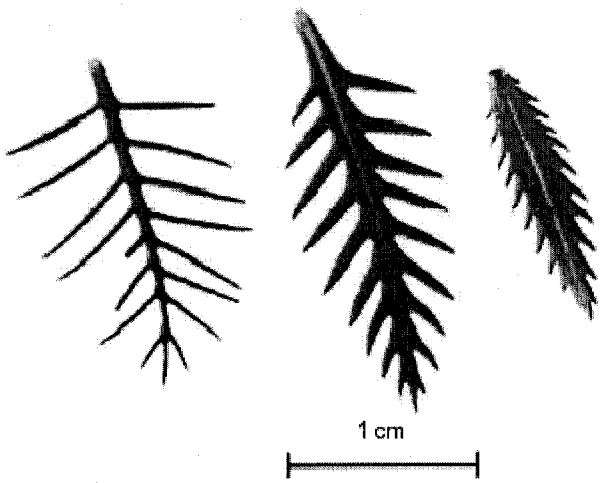

Figure 2.13: From left to right, the leaves represent the transition from submerged to aerial leaf morphology observed in the vertically ascending stems of *Proserpinaca palustris*. (Wells and Pigliucci, 2000).

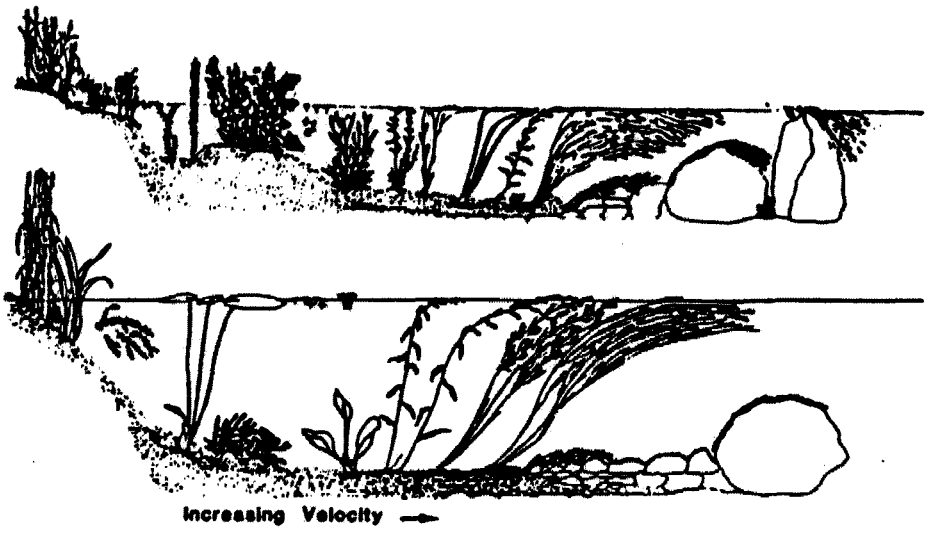

Figure 2.14: Typical growth forms of freshwater macrophytes in slow to very fast flows in shallow an deeper flowing waters (Dawson, 1988).

a)

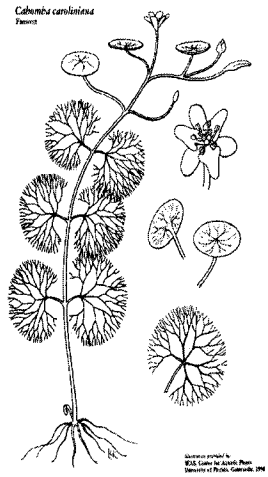

b)

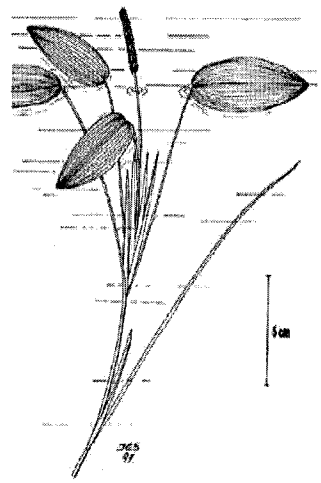

Figure 2.15: Two examples of heterophylly: (a) *Cabomba caroliniana* has dissected submerged leaves and entire floating leaves, and (b) *Potamogeton natans* has linear submerged leaves and ovate floating leaves. (From: http://plants.ifas.ufl.edu/cabaqu2.jpg; Vic Ramey, University of Florida, and http://www.miljolare.no/bilder/planter/ferskvann/makro/potamogeton_natans.jpg)

The Effect of Macrophyte Morphology (Linear-bladed, Whorled, and Dissected) on Fluid Dynamics

Abstract:

Fluid dynamic factors are important in defining the environments in which macrophytes live, and have likely played a role in their evolution. For example, freshwater macrophytes with different leaf morphologies (i.e., linear-bladed, whorled and dissected) are common, but it is not known how these morphologies affect the flow around them. An examination of the manner by which macrophytes affect their flow environment was undertaken using flow visualization and image analysis of three macrophyte species, *Vallisneria americana* (linear linear-bladed or ribbon-shaped), *Elodea canadensis* (whorled), and *Ceratophyllum demersum* (dissected), and a circular cylinder (physical model). The study was undertaken at five velocities ranging from ~1 – 11 cms^{-1}, using fluoroscein dye to visualize the flow patterns and digital recording to capture the information. The flow patterns showed that at slower velocities the flow was laminar as indicated by smooth dye streams, and stickiness as indicated by the loops of dye attached to the leaf of *Vallisneria*, to the individual leaf whorls of *Elodea,* and to the individual leaf segments of *Ceratophyllum.* At faster velocities, turbulence in the flow was indicated by the generation of eddies, which were widely spaced downstream of the cylinder, *Vallisneria,* and *Elodea*, and closely spaced downstream of *Ceratophyllum.* The transition from laminar to turbulent flow occurred at lower velocities for the plants than for a circular cylinder, with the exception of *Ceratophyllum*, thus indicating an increase in local mixing. In addition, both the area of dye coverage and the concentration of dye decreased at slower rates for the plants than for the cylinder, suggesting that plants retain more fluid relative to the physical model. The consequence of these results

indicated that there is both an increase in local flow around the plants and a retention of fluid near the plants which provides more opportunity for nutrient exchange in the boundary layers surrounding freshwater macrophytes. Therefore, it appears that aquatic plants alter the flow in ways that maximize flow across leaves, which would enhance nutrient exchange and thus macrophyte productivity.

Introduction:

Aquatic plants are important primary producers in aquatic ecosystems (Dodds and Biggs, 2002), and are also ecosystem engineers in that they can (1) promote water quality by providing physical protection for algal grazers; (2) compete with the algae for nutrients; and (3) reduce water currents and allow suspended material to settle (Schutten and Davy, 2000; Palmer et al., 2004; Wright et al., 2004). Interestingly, there are freshwater macrophytes from different families that share common architecture and habitat, and plants from the same families that differ in architecture suggesting that genetics is probably not the only factor influencing plant morphology (Sculthorpe, 1967; Schlichting, 1986; Ackerly et al., 2000; Givnish, 2002; Santamaria, 2002; Santamaria et al., 2003; Dorken and Barrett, 2004). For example, *Vallisneria* and *Elodea* are in the same family (Hydrocharitaceae monocotyledons) yet have very different architectures; *Vallisneria* has long ribbon-shaped leaves, and *Elodea* has shorter whorled leaves. *Ceratophyllum* (Ceratophylleaceae) and the submerged foliage of *Cabomba* (Nymphaeaceae) in the dicotyledons have highly dissected whorled morphologies and are in different families. Moreover, heterophylly (foliage plasticity) occurs in some species of freshwater macrophytes whereby a plant may have different leaf shapes depending on whether they are under, on, or above the water surface. Heterophylly occurs across

distant taxa, which suggests that unrelated plants have adapted in a similar fashion to the aquatic environment (Sculthorpe, 1967; Goliber and Feldman, 1990; Wells and Pigliucci, 2000); adding to the argument that structural similarities occur due to adaptation to a common fluid environment. The three common patterns of macrophyte morphology (i.e., linear-bladed, whorled, and dissected leaves) exist in different flow habitats ranging from stagnant ponds to flowing streams (Dawson, 1988). Specifically, *Vallisneria, Elodea* and *Ceratophyllum* all live in both still and flowing water (Cook et al., 1974). As such, it would be appropriate to examine the nature of the factors that have potentially influenced these morphologies, including fluid dynamic factors.

Fluid dynamics may play a large role in influencing macrophyte structure as fluid dynamic factors are important in defining the microenvironments in which plants live (Dawson, 1988). For example, plants living in energetic environments are exposed to high drag forces that may cause damage to their leaves or blades, whereas in low energy environments productivity may be limited by a thick boundary layer over which nutrients are absorbed (Hurd et al., 1997; Schutten and Davy, 2000). Regardless of the environmental conditions, a boundary layer begins at the surface of a boundary, where the velocity is zero, and grows until the velocity of the boundary equals that of the mainstream velocity (Vogel, 1994). Boundary layers are influenced largely by Reynolds number (Re), which is the ratio of inertial to viscous forces (Vogel, 1994). The higher the Re, the thinner the boundary layer, and the higher the shear rate (i.e., the faster the fluid moves past a solid surface); and the lower the Re the thicker the boundary layer and the lower the shear rate (Cheer and Koehl, 1987). If the Re is low (e.g., small, slowly moving objects or low flow velocities), the flow is dominated by viscous forces, and is

consequently smooth and orderly, encouraging the growth of a thick boundary layer (Koehl, 1996). This thick boundary layer may lead to diffusional stresses (i.e., limited mass transfer) due to the low flux of nutrients through the boundary layer to the leaf surface compared to the rate at which the plants can utilize these nutrients.

Drag is also an important concept related to plants as it is the hydrodynamic force that pulls a body in the direction opposite to fluid movement and in the case of boundary layers, the force that slows the flow (Koehl, 1996). At low Re, drag is due to skin friction, which is the viscous resistance of the fluid in the boundary layer around the body being sheared as the fluid moves past the body. Consequently, the greater the surface area, the greater the skin friction. At high Re, drag includes skin friction but is dominated by pressure drag, which is the pressure difference across the body due to the fluid dynamic separation or the formation of a wake on the downstream side of the body (Vogel, 1987; Koehl, 1996). The drag force depends on the velocity of the fluid, the frontal area and roughness of the object. Additionally, for a non-spherical object, the shape and orientation of the object in relation to the flow are also important (Schutten and Davy, 2000). For example, when plant stems bend downstream in response to faster flow, their frontal area is reduced, lowering pressure drag. Long ribbon shaped leaves can fold against the stem or each other, reducing skin friction (Ennos, 1999). It is thus important to consider how fluid dynamic factors at low and high velocity effect the morphological patterns observed in macrophytes.

This study will focus on the null hypothesis that plants with different leaf types (linear-bladed, whorled and dissected) effect the downstream flow patterns in the same manner. It is expected that *Vallisneria* (linear-bladed) will act in a manner similar to a

physical model provided by a circular cylinder despite its flexibility, because of its smooth-linear-bladed morphology. It is expected that *Elodea* (whorled) will also act similar to the cylinder because of its rigid structure, and because the whorls of entire leaves are likely spaced far enough apart to not have a significant effect on flow separation. It is, however, expected that *Ceratophyllum* (dissected) will act more as a mesh because of the high level of dissection in its leaves.

Materials and Methods:

The data were obtained from photographs and short videos of Fluorescein dye moving past (1) the empty test section of the flume, (2) a circular cylinder (0.7 cm diameter), (3) *Vallisneria americana,* (4) *Elodea canadensis,* and (5) *Ceratophyllum demersum* (5 cm long sections). The empty flume was used to establish that the observed patterns in the study were due to the subject-flow interaction. The circular cylinder was used as a physical model for comparison as it is a well characterized fluid dynamic system and a first approximation to an aquatic plant (Kundu, 1990; Coutanceau and Defaye, 1991; Williamson, 1996; Palmer et al., 2004); *E. canadensis* was acquired from Tabor Lake, Prince George, B.C., whereas *V. americana* and *C. demersum* were purchased from Ward Scientific Supply (Rochester, NY, USA). Plants were maintained in aquaria at ~20 °C under natural light conditions, with potting soil (vermiculite removed) as the substrate. Water velocities over the range of 1-11 cms^{-1} were used in this study, which are similar to velocities used by Nepf and Koch (1999) and Leonard and Luther (1995). These velocities are at the lower end of the range where the macrophytes occur in the field (Wiegleb, 1984; French and Chambers, 1996; Elliot, 2000; Shi and

Hughes, 2002; Wuest and Lorke, 2003), but are consistent with within-canopy flows (Sand-Jensen and Mebus, 1996).

Flume

A recirculating flume of dimensions 19.2 cm (width) x 24.7 cm (height) x 170 cm (length) was used for this study, with the test section being 120 cm downstream of the flow straighteners (Figure 3.1). Velocity profiles were obtained using a 3-dimensional Acoustic Doppler Velocimeter (ADV; SonTek; sampling at 25 Hz) for each mainstream velocity examined during the experiments. These profiles show the logarithmic boundary layer development, except at the faster velocities, where not enough data points were collected in the logarithmic layer close to the bottom of the flume. The log portion of these profiles was used to calculate the shear velocity (u_* from $u = \frac{u_*}{\kappa} \ln \frac{z}{z_0}$: where u is the velocity in the downstream direction, κ is the von Karman constant (= 0.40), z is the distance from the boundary, and z_0 is the roughness length (height): Table 3.1; Hoover and Ackerman, 2001; Figure 3.2 a-e).

Photographs

Photographs or short videos (duration 40 seconds) were taken from both a top and side perspective with a Nikon CoolPix995 (Melville, NY, USA) digital camera placed approximately 60 cm directly across from the subject. The camera was set with the ISO (sensitivity setting) at 400; the image adjustment at lighten image; the shutter speed at 1/30; and the overall camera setting was at shutter priority auto. All photographs were taken with a black cloth surrounding the working section of the flume and the camera so that no external light could enter the system.

Dye (3 g/L sodium fluoroscein in distilled water) was released 3 cm upstream of the subject and 3 cm vertically up from the base of the stem using a peristaltic pump (mini-pump variable flow; slow flow, VWR, Canada; see Figure 3.1). Dye was released isokinetically, i.e., to match the mainstream velocity as close as possible (Table 3.2). Dye was used to provide an indication of the pattern of water flow around the subjects (i.e., physical model, and three plant species).

Top perspective

A positioning device consisting of a modified syringe attached perpendicularly to a Plexiglas plate was mounted to the side of the flume. The subject (i.e., model or plant species) was placed in the top of the syringe and held in place with mounting putty (Lepage, FUN-TAK) the putty was covered in black tape in order to reduce reflectance (Figure 3.3). The subject was positioned so that the dye would intercept in the centre, 3 cm up from the false bottom of the flume. The lighting consisted of: (1) a 15 W florescent black light (41 cm long, 2.5 cm diameter; General Electric; Burnsville, MN, USA) attached approximately 15 cm above the flume, 15 cm downstream of the plant; and (2) a 6V 15W white halogen microscope light (set at intensity #6; VWR; Mississauga, ON, Canada) that was placed on the stand directly over top of the subject (Figure 3.1). A corrugated plastic sheet with a 1 cm wide and 17 cm long slit was placed on the top of the flume to illuminate the flow behind the subject. It was assumed that surface waves and buoyancy effect (i.e., gravity) were not likely significant based on the depth of the positioning device below the surface (~ 6-8 cm below

the surface depending on the velocity) and on the relatively short distance (~ 10 cm) that the dye travels horizontally. Based on these assumptions, the fluid patterns in the empty test section were set as the base to which comparisons were made (i.e., they were set as the control).

Side perspective

A similar set up was used for photographs in the side perspective. In this case, the subject was placed in the hole drilled in a false bottom placed in the flume and held in place with putty, such that the putty was flush with the false bottom. The lighting scheme was the same as for the top view except that the corrugated plastic sheet with the slit was not used (Figure 3.1).

Concentration Curve

A concentration curve was generated in order to convert from pixel value in the photographs to the concentration of dye in the flow. This process was undertaken separately for side and top perspectives because of the different lighting schemes. The 100% dye concentration was set at 3g (sodium fluorescein) /L (distilled water), and serial dilutions were made (i.e., 100-0.01% [= 100, 10, 1, 0.1, 0.01%], 200-0.02%, 300-0.03% and 50-5%) omitting the values above 100% in the analyses. The dye of a given concentration was placed in a cuvette with black tape on the upstream and downstream sides and around the cap to minimize leakage. The cuvette was placed upside down in the test section of the flume and a cuvette containing 100% dye was placed 0.5 cm upstream, and a cuvette containing 0% dye was placed 0.5 cm downstream of the cuvette under investigation (Figure 3.4). Photographs of the cuvettes were made using the same lighting scheme as was used to take the photos. The photos were

imported into MATLAB version 6.5 (Mathworks, Natick, Massachusetts) for conversion to gray scale and the background dye, determined as 69 in the side perspective and 19 in the top perspective, was subtracted (see below). Since the flume water was changed frequently (i.e., after every trial) the background dye never exceeded the aforementioned pixel values. Five pixels were sampled from each cuvette directly below the top of the cuvette, where the reflectance of the plastic no longer influenced the dye. This technique was verified by sampling pixels in the dye stream immediately downstream of the dye injector, where the concentration of dye should be 100%. The results from both locations were similar in side (186 ± 0 [mean ± standard error], n = 10 where a pixel value of 186 = 100% concentration) and top perspectives (89 ± 3, n = 10 where a pixel value of 88 = 100% concentration). Lastly, the positions of the 100% and 0% dye cuvettes were changed to determine whether the lighting varied across the test section, but no differences (186 ± 0, n = 10 for 100% concentration, and 0 ± 0, n = 10 for 0% concentration) were detected.

The concentration curve (Figure 3.5) was non linear and was, therefore, divided into two portions: (1) an exponential portion for 0.01-5% dye plotted using a log-log transform; and (2) a linear portion from 10-100% dye data (Figure 3.6 a-d). The 10% dye concentration was used as the demarcation between the two portions of the curve because that is where the curve changed in the original plot (Figure 3.5).

Pixel values were grouped into fourteen bins of non-uniform size based on the following equation, (((actual $_{\text{pixel value}}$ – estimated $_{\text{pixel value}}$)/ actual $_{\text{pixel value}}$)

x 100%), where actual pixel is the value from the cuvette photographs, and estimated pixel is the pixel value determined from the concentration curve. The bin sizes are as follows: 0, 0.001-0.050, 0.051-0.150, 0.151-0.250, 0.251-0.500, 0.501-1.000, 1.001-2.000, 2.001-5.000, 5.001-10.000, 10.001- 20.000, 20.001-40.000, 40.001-60.000, 60.001-80.000, and 80.001-100. The reason for non-uniformity in bin size was to minimize the error in estimation. In this case the degree of error accepted was set differently for the non-linear (< 10% dye concentration) and linear (> 10% dye concentration) portions of the concentration curve. The errors were 27% and 12 % for non-linear and linear portions, respectively for the side perspective and 25% and 13% for the top perspective. A mock photograph of known area was examined to test this binning method (Figure 3.7). The distribution of colour within the photograph was set as white = 23.6%; gray = 27.7 %; black = 48.7 %. The distribution determined using the MATLAB based system was white = 24.3 %; gray = 27.0 %; black = 48.7%. These results indicate that the binning method appears to work well and would be appropriate to apply to the dye patterns in the photographs and videos. Since it is known that 100% dye concentration is 3g/L, the actual dye concentration was calculated through cross multiplication and used in further analysis.

Image Analysis

A MATLAB program (Image Analysis Toolkit – version 6.5.0 Release 13.0.1) was used to edit the photos and to extract the digital information in the flow around the subject of interest (e.g. cylinder or plant) (Box 3.1). Before the

photos were processed in MATLAB, the subject was removed from the picture in Adobe PhotoShop (Version 5.0 limited edition; Adobe system, San Jose, California) so that it would not be included in the analysis. The photos were converted to gray scale so that the output was a two dimensional array corresponding to the spatial location and pixel intensity (0 – 255). The brightness and intensity of the image was then adjusted using MATLAB routines to maximize visibility and any background level of dye (i.e., the dye in the flow from an earlier trial) was subtracted from the image (see box 3.1). Four domains of interest were identified: (1) upstream of the subject in the side perspective (6 cm high x 2 cm wide), (2) downstream of the subject in the side perspective (6 cm high x 7 cm wide), (3) upstream of the subject in the top perspective (4 cm wide x 2 cm long) and, (4) downstream of the subject in the top perspective (4 cm wide x 7 cm long). These domains were compared in the statistical analyses, which will be discussed in a later section.

The area of dye coverage was defined as any area in the domain (i.e., upstream vs. downstream in top and side perspectives) containing dye (i.e., a non-zero pixel after background correction). The concentration of dye in the domain was determined from these same data by converting the pixel intensities to dye concentration using the relationship described above (see Concentration Curve). This procedure used the frequency distribution of the pixel intensities, which were multiplied by the concentration at the midpoint of each frequency bin (recall that 100% dye concentration is 3g/L). This analysis was repeated for

each of the three photographs taken at a given velocity. The average and standard deviation of the three observations are reported.

Acoustic Doppler Velocimeter (ADV; SonTek) Measurements

Velocity measurements in three dimensions were taken on a horizontal plane (i.e., top perspective) 3 cm above the bottom of the flume using an ADV to examine the flow around: (1) the empty test section; (2) a circular cylinder; (3) *Vallisneria americana;* (4) *Elodea canadensis;* and (5) *Ceratophyllum demersum.* Each set of measurements was taken at a frequency of 25 Hz for 120 s in a 2 cm x 2 cm grid that was 8 cm wide and 16 cm long. The exception occurred in the vicinity of the subject where measurements were taken at a 3 cm distance due to interference of the acoustic signal with the subject (Figure 3.8). These measurements were made at the same five flume velocities as the photos in order to have quantitative verification of any patterns that may occur. The ADV also gives the root mean square of the velocity, which can be divided by the average velocity to give turbulence intensity. This data was not included in this thesis because the trend was similar to that seen in the velocity contour plots, where there was an increase in turbulence intensity directly behind the plant. In all cases (cylinder and plants) the turbulence intensity was approximately 60% upstream and beside the subject, and approximately 100% behind the test subject at the lowest velocity (1.3 cms^{-1}). At the fastest velocity (11.0 cms^{-1}), the turbulence intensity ranged from 20% upstream and around the cyinder to 40% behind the cylinder, in *Vallisneria* the range was from 20-25%, in *Elodea* from 30-50%, and in *Ceratophyllum* from 25-30%.

Plant Angles and Oscillations

The downstream deflection and rate of oscillation of the plants in the flow were examined using the 40 s video recordings. The angle of deflection (angle from the

vertical) of the subject was measured for the cylinder and the three plant morphologies. Since the plants did not remain stationary (i.e., they oscillated), the angle of deflection was measured at the mean position taken at the location where the moving plant tips were most frequently (Stephan and Gutknecht, 2002), under the assumption that the plant stem is a straight line as in most cases there was a slight curve in the stem. The oscillations were counted as the number of times the plant rose and fell during the 40 s recording. With *Vallisneria*, only one blade was examined; the one that was parallel to the flow in the downstream position. Additionally, the angle of the leaf from the stem was measured for *Ceratophyllum* for the leaves in both the upstream and downstream position, from the base of the plant to the apex.

Statistical Analysis

Effect of Velocity on Dye Coverage and Concentration

To determine whether increasing velocity affected the area of dye coverage and/or the concentration of dye in that area, the average and standard deviation in each domain were determined for three images taken at each velocity. The resultant values (area or concentration) were then regressed on the test velocity and stem Reynolds number based on the diameter of the subject (i.e., $\mathrm{Re} = \frac{ul}{\upsilon}$, where u is the velocity, l is the diameter of the plant stem and whorl, and υ is the kinematic velocity; Vogel, 1994). The null hypothesis examined was that the slope of the regression would equal zero. In other words there is no relationship in area of dye coverage or concentration of dye with increasing velocity.

Effect of Location and Perspective on the Dye Coverage and Concentration

An analysis of covariance (ANCOVA) was used to test the null hypothesis that there is no difference in the upstream and downstream flow patterns in both the side and top perspectives for the different subjects. Area was normalized by using the relative frequency (# pixels of dye/ total # pixels x 100%) of dye in the calculation of the area of dye coverage. In this case, the area of dye coverage was used as the dependent variable, the domains (i.e., side or top perspective, upstream or downstream) were the categorical factors, and velocity was the continuous predictor (the covariate). Comparisons between side and top views were make within the same test section. A Fisher least significant difference (LSD) test was used for Post Hoc pair wise comparisons. The same analysis was used to examine the concentration of dye in the specified area.

Effect of Morphology on the Rate of Oscillation

ANCOVAs were conducted to test the null hypothesis that the rate of stem oscillation did not differ among plant morphologies. The oscillation rate was used as the dependent variable, the different subjects were the categorical factors, and velocity was the continuous predictor. A Fisher LSD test was used for Post Hoc comparisons.

Effect of Velocity and Node Position on the Leaf Angles of *Ceratophyllum*

ANCOVAs were used to test the null hypothesis that the position of the leaf on the stem (i.e., from base to apex) had no effect on the angle of the leaf. The angle of the *Ceratophyllum* leaf from the stem was used as the dependent variable, the node position on the stem was the categorical factor, and velocity was the continuous predictor. A Fisher LSD test was used for Post Hoc comparisons.

Effect of Location on Velocity

ANCOVAs were used to test the null hypothesis that the pattern of velocity upstream of the subject is the same as the pattern of velocity downstream of the subject. This was done by grouping together the upstream ADV velocity measurements (14 points) and the downstream ADV velocity measurements (30 points). The average measured velocity (of each point) was used as the dependent variable, the position (upstream or downstream) of the measurements was the categorical factor, and test velocity was the continuous predictor (the covariate). A Fisher LSD test was used for Post Hoc pairwise comparisons. Since the area where the ADV velocity measurements were taken was larger then the area used in the image analysis, only the measures of velocity that were in the same area used in photos from the top perspective were used (i.e., 4 cm wide and 2 cm long upstream, and 4 cm wide by 7 cm long downstream.

Results:

Empty flume

The flow, as indicated by the dye streaklines was similar in both side and top perspectives (i.e., left and right panels, respectively (Figure 3.9a-j). The dye streaks were approximately linear at the two lowest velocities (1.3 and 2.0 cms^{-1}; Figure 3.9a-d), but became "wavy" at the higher velocities (5.0, 8.4, and 11.0 cms^{-1}; Figure 3.9e-j). In addition the dye streaks were wider (had less contrast) at the higher velocities indicating relatively fast flows (e.g. Figure 3.9i-j). In terms of the area of dye coverage, there was little evidence of an effect of velocity in the "upstream" or "downstream" (defined arbitrarily here as there was no subject placed in the flow) domains (Figure 3.10a-d). The concentration of dye imaged in the domains tended to decrease with increasing velocity, and this was significant in three of the four domains and was on the order of $-0.1 gL^{-1}/cms^{-1}$ (Figure 3.10f-h).

In terms of the area of dye coverage in a specified domain, the ANCOVA showed that there was a significant difference between the flow upstream and downstream of the empty test section ($p < 0.001$), but not between the side and top perspectives ($p = 0.082$; Table 3.3a), suggesting that surface waves and buoyancy do not have a significant effect on the side vs. top fluid patterns. A significant interaction ($p = 0.047$) was found for the side versus top perspectives by the upstream and downstream position. The post hoc comparisons for the empty test section support this, showing that significant differences occurred between all domains ($p < 0.003$), with the exception of the side and top perspectives upstream of the test section ($p = 0.81$: Table 3.4a).

In terms of the concentration of dye in a specified domain, the ANCOVA showed that there was a significant difference between the upstream and downstream positions ($p = 0.017$), but not between side and top views ($p = 0.95$; Table 3.3a), supporting the assumption that surface waves and buoyancy do not have a significant effect on the side vs. top fluid patterns. Post hoc comparisons agreed, whereby significant differences occurred between the upstream and downstream position in the side perspective ($p = 0.011$), between the side perspective upstream and the top perspective downstream ($p = 0.034$) and between the top perspective upstream and the side perspective downstream ($p = 0.042$; Table 3.5a).

Cylinder

The dye streakline upstream of the circular cylinder did not appear to change with increasing velocity, in that it remained in a straight stream in both side and top perspective (Figure 3.11). However, downstream of the cylinder, there was laminar flow, with loops of dye that indicate "stickiness", and a large area of recirculation at the slower velocities. The transition between laminar and turbulent flow as indicated by the onset of

eddies occurred between 5.0 cms^{-1} and 8.4 cms^{-1} (Re ~ 350-590). At the faster velocities, the flow was turbulent, and as such less sticky, and the recirculation zone was smaller. The dye streaklines downstream in the top perspective revealed a classic attached eddy at 1.3 cms^{-1} (Re ~ 90; Figure 3.11b), a von Karman vortex street at 2 cms^{-1} (Re ~ 140; Figure 3.11d), and more turbulent structures at higher velocities (Figure 3.11f,h,j).

The image analysis indicated that there was no relationship between the area of dye coverage and velocity in the upstream flow ($p = 0.19$ and 0.28; Figure 3.12a,b). However, there was a significant increase, on the order of 0.5 cm^2/cms^{-1}, in the dye coverage downstream in the side perspective with velocity ($p = 0.018$; Figure 3.12c), and a tendency for increase in the top perspective ($p = 0.41$; Figure 3.12d). Additionally, there was a tendency for the dye concentration to decrease with velocity in the upstream and downstream domains (e.g., ~ -0.05 gL^{-1}/cms^{-1}), and this was significant in the case of the downstream side perspective ($p = 0.014$; Figure 3.12g).

In terms of the area of dye coverage in a specified domain, the ANCOVA indicated that there were significant differences upstream and downstream of the cylinder ($p < 0.001$), but no differences occurred between the side and top perspectives ($p = 0.52$; Table 3.3b). The post hoc comparisons concurred in that there were significant differences ($p < 0.001$) between the upstream and dowstream domains, but no significant difference between side and top perspectives upstream of the cylinder ($p = 0.94$: Table 3.4b). Furthermore, there was no significant difference between the side and top perspective downstream of the clinder ($p = 0.28$).

The ANCOVA of the concentration of dye indicated that there was no significant difference between side and top perspectives ($p = 0.39$), nor between the upstream and

downstream position of the cylinder ($p = 0.22$: Table 3.3b). Post hoc comparisons also showed that domain had no significant effect on the concentration of dye (Table 3.5b).

Vallisneria americana

The dye streakline upstream of *Vallisneria* remained in a relatively straight stream in both side and top perspective (Figure 3.13). The dye streaklines downstream showed a large amount of recirculation under the leaf, and a high amount of stickiness on the leaf. The flow was laminar at 1.3 cms^{-1} (Re ~ 25) as indicated by the smooth dye streakline (Figure 3.13a,b); the transition from laminar to turbulent occurred at about 2.0 cms^{-1} (Re ~ 40) when eddies began to detach (Figure 3.13c,d); von Karman vortices were shed at 5.0 cms^{-1} (Re ~ 100; Figure 3.13f); and more widely spaced eddies with less stickiness and recirculation were observed at the higher velocities (Figure 3.13g-j).

The image analysis indicated that there was no relationship between the area of dye coverage and velocity in both the upstream ($p = 0.072$) and downstream ($p = 0.69$) flow in the top perspective (Figure 3.14b,d). However, there were significant increases in the area of dye coverage with velocity in both the upstream ($p = 0.034$) and downstream ($p = 0.014$) flow in the side perspective, with slopes of 0.03 cm^2/cms^{-1} and 0.2 cm^2/cms^{-1}, respectively (Figure 3.14a,c). In addition, there was a significant decrease of –0.05 gL^{-1}/cms^{-1} in the dye concentration with velocity in the side perspective upstream ($p = 0.042$), although a non-significant increase in the top perspective upstream ($p = 0.64$; Figure 3.14e,f). There was also a tendency for the dye concentration to decrease with velocity in the up and downstream domains (Figure 3.14g,h).

The ANCOVA of the area of dye coverage in a specified domain, revealed that there was a significant difference in the flow upstream and downstream of *Vallisneria* ($p < 0.001$), but not between the side and top perspectives ($p = 0.37$; Table 3.3c). The post

hoc comparisons indicated the same whereby, there were significant differences between the upstream and dowstream domains in the top and side perspectives ($p < 0.001$), and no significant difference in the side and top perspectives upstream ($p = 0.95$) or downstream of *Vallisneria* ($p = 0.26$; Table 3.4c).

The ANCOVA of the concentration of dye showed that there was no significant difference between side and top view ($p = 0.84$), nor between the up and downstream position of *Vallisneria* ($p = 0.64$: Table 3.3b). Post hoc comparisons showed that no significant effect occurred between any of the domains (Table 3.5c).

Elodea canadensis

The dye streakline upstream of *Elodea* was reasonably straight up to a velocity of 8.4 cms^{-1} (Re ~ 840) when some waviness was noted (Figure 3.15). The dye streaklines downstream were attached to the individual whorls of leaves (i.e., "sticky"), were in filamentous loops at the lower velocities and recirculation was present (Figure 3.14a-d). The transition from laminar to turbulent occurred at ~ 5.0 cms^{-1} (Re ~ 500) when the dye streak was no longer smooth and eddies began to form (Figure 3.15e,f); von Karman vortices were shed at 8.4 cms^{-1} (Re ~ 840; Figure 3.15h); and turbulent structures occurred at 11.0 cms^{-1} (Re ~ 1100) as indicated by the widely spaced eddies, less stickiness on leaves and lower recirculation (Figure 3.15i-j).

The image analysis indicated that there was no relationship between the area of dye coverage and velocity in the upstream flow in both the side and top perspective (Figure 3.16a,b), nor in the side perspective downstream (Figure 3.16c). However, there was a significant increase in the area of dye coverage with velocity downstream in the top perspective ($p = 0.026$) of ~ 0.10 cm^2/cms^{-1} (Figure 3.16d). There was also a tendency for the dye concentration to decrease with velocity in the up and downstream domains,

and this was significant in the case of the downstream side ($p = 0.049$) and top perspectives ($p = 0.046$; Figure 3.16g,h).

The ANCOVA of the area of dye coverage showed that there was a significant difference between the flow upstream and downstream of *Elodea* ($p < 0.001$), but no significant difference between the side and top perspectives ($p = 0.26$; Table 3.3d). The post hoc comparisons showed that there were significant differences between the upstream and dowstream domains in the side and top perspective ($p < 0.001$). No significant differences were detected in the side and top perspectives upstream ($p = 0.58$), or downstream of *Elodea* ($p = 0.26$; Table 3.4d), but a significant interaction ($p = 0.043$) was found between the side versus top perspective by upstream versus downstream comparisons (Table 3.3d).

The results of the ANCOVA of the concentration of dye showed that there was no significant difference between side and top view ($p = 0.29$), or between the up and downstream position ($p = 0.30$: Table 3.3d). Post hoc comparisons showed that domain had no significant effect on the concentration of dye (Table 3.5d).

Ceratophyllum demersum

The dye streakline upstream of *Ceratophyllum* was relatively straight although some waviness was noted at 5 cms^{-1} (Figure 3.17). The dye streaklines downstream of *Ceratophyllum* showed a high amount of "stickiness" to the individual leaf segments due to laminar flow at 1.3 cms^{-1} (Re ~ 300), along with a large amount of recirculation (Figure 3.17a,b). The flow became transitional between 5.0 and 8.4 cms^{-1} (Re ~ 1200-2000) where the loops of dye could no longer be detected (Figure 3.17c-f). Turbulent structures were evident at the higher velocities as indicated by closely spaced eddies, and a reduced amount of stickiness and recirculation (Figure 3.17g-j).

There was no relationship between the area of dye coverage and velocity in the upstream flow in the side and top perspectives (Figure 3.18a,b). However, there was a significant decrease in the area of dye coverage with velocity downstream in the top perspective ($p = 0.028$) on the order of -0.12 cm^2/cms^{-1}, and a similar trend in side perspective ($p = 0.31$; Figure 3.18d). The dye concentration tended to decrease with velocity in all perspectives, but these were not significant (Figure 3.18e-h).

Results of the ANCOVA of the area of dye coverage indicated that there was a significant difference between the flow upstream and downstream of *Ceratophyllum* ($p < 0.001$), and only marginal significance between the side and top perspectives ($p = 0.057$; Table 3.3e). A significant interaction ($p = 0.047$) was found in the side versus top perspective by upstream versus downstream position. The pairwise comparisons revealed signficant differences between all combinations of perspectives with the exception of top versus side upstream (Table 3.4e).

The ANCOVA of the concentration of dye showed that there was no significant difference between side and top perspective ($p = 0.25$), nor in the up and downstream position ($p = 0.83$: Table 3.3e). Post hoc comparisons showed that domain had no significant effect on the concentration of dye (Table 3.5e).

Comparison of the Three Plant Morphologies and the Theoretical Model

A direct comparison of the results should reveal whether there are differences among the three plant morphologies and the physical model. Firstly, the velocity at which the transition from laminar (smooth streakline) to turbulent (eddies) flow occurs was lower for the plants, with the exception of *Ceratophyllum,* than for the cylinder (Figure 3.19a). The transition occurred in *Vallisneria* (linear-bladed) at ~2 cms^{-1}, in

Elodea (whorled) between ~2-5 cms^{-1}, and in *Ceratophyllum* (dissected) between ~5-8.4 cms^{-1}. It should be noted that the use of Re does not change the pattern of observation reported here. Specifically the Re for the cylinder ranged from 90-770, *Vallisneria* from 25-220, *Elodea* from 130-110, and *Ceratophyllum* from 300-2600. Secondly, in all cases, the rate of change in the area of dye coverage with velocity was lower for the plants than for the cylinder (Figure 3.19b). More specifically, the rate of change increased significantly for the cylinder at a rate of ~0.5 cm^2/cms^{-1}, as it did for *Vallisneria* at ~0.2 cm^2/cms^{-1}. There was no significant trend for *Elodea* (~ -0.0004 cm^2/cms^{-1}), and the rate for *Ceratophyllum* decreased non-significantly at ~ -0.2 cm^2/cms^{-1}. Thirdly, the rate of change in the concentration of dye with velocity also decreased at a slower rate for the plants then for the physical model (Figure 3.19c). The concentration of dye downstream of the circular cylinder decreased significantly at a rate of ~ -0.05 gL^{-1}/cms^{-1}. For *Vallisneria,* the trend was non-significant with the decrease being on the order of ~ -0.07 gL^{-1}/cms^{-1}. The rate for *Elodea* decreased significantly on the order of ~ -0.06 gL^{-1}/cms^{-1}. Although the rate was similar for *Ceratophyllum* (~ -0.06 gL^{-1}/cms^{-1}), it was non-significant. The non-significant trends are likely due to a higher degree of variance.

ANCOVA's were used to determine if there were differences among the cylinder and the linear-bladed, whorled, and dissected leaf morphologies, when adjusted for a common mean velocity and a common regression line. Plant morphology ($p < 0.001$: Table 3.6a), side versus top perspective ($p = 0.044$), and upstream versus downstream position ($p < 0.001$) were found to have a significant effect on the area of the domain covered in dye, whereas there was no significant effect of velocity ($p = 0.083$). More

specifically, post hoc comparisons revealed that there were no significant differences between subjects in the upstream direction from both the side and top perspectives (Table 3.7a,b). This indicates that the upstream flow was similar in all cases. There were significant differences in the side perspective, downstream of the subjects between: (1) the cylinder and the empty test section ($p = 0.007$: Table 3.7c); (2) *Elodea* and *Vallisneria* ($p = 0.043$); (3) the empty test section and *Elodea* ($p = 0.002$); and (4) a marginally significant difference ($p = 0.059$) between *Ceratophyllum* and the empty test section. There were also significant differences in the top perspective, downstream of the subjects between: (1) all subjects and the empty test section ($p < 0.009$: Table 3.7d); (2) the cylinder and *Ceratophyllum* ($p = 0.036$); and (3) *Vallisneria* and *Ceratophyllum* ($p = 0.010$). There were also significant interactions between the plant and the upstream and downstream position ($p = 0.003$), and between the side and top perspectives and the upstream and downstream positions ($p = 0.014$; Table 3.6).

The concentration of dye was affected significantly by velocity ($p < 0.001$: Table 3.6b). However, neither plant morphology ($p = 0.13$), side versus top perspective ($p = 0.17$), nor upstream versus downstream position ($p = 0.17$) had a significant effect on the concentration of dye. Post hoc comparisons revealed that there was no significant difference upstream of the subjects in the side and top perspectives (Table 3.8a,b). The only significant differences that occurred in the downstream position was in the side perspective between the empty test section and the cylinder ($p = 0.005$), *Elodea* ($p = 0.025$), and *Ceratophyllum* ($p = 0.038$; Table 3.8c). Marginally significant differences were observed in the top downstream perspective for the circular cylinder and *Ceratophyllum* ($p = 0.055$) and the empty test section ($p = 0.052$).

Velocity Measurements

ADV measurements were taken in a horizontal slice and velocities were recorded in u (streamwise), v (cross-stream), and w (vertical) components, though statistics were only performed for the u and w velocity components. The contour plots of the u velocity component showed a pattern of decreasing velocity behind the subject (Figures 3.20-3.24a,c). The patterns in both the streamwise (u) and vertical (w) velocity components in the empty test section showed a relatively uniform pattern, although there was more variance with increasing velocity (Figure 3.20a-d). The velocity pattern downstream of the circular cylinder showed that there was an area of reduced velocity which, diminished in size with increasing velocity (Figure 3.21a,c). In the vertical component, there was downward velocity (i.e., negative velocity) directly downstream of the cylinder at the slower velocity (Figure 3.21b), and this region moved ~ 5 cm downstream of the cylinder at the faster velocity (Figure 3.21d). The velocity patterns in the streamwise component (u) of *Vallisneria* showed a small area of reduced flow downstream of the plant at the slower velocity (Figure 3.22a), but this pattern disappeared as velocity increased (Figure 3.22c). Similarly, in the vertical component (w), the flow moved upwards directly downstream of the plant at the slower velocity (Figure 3.22b), with no obvious pattern occurring at the fastest velocity (Figure 3.22d). *Elodea* showed a pattern of reduced flow in the streamwise component (u), though this area of reduced flow was much larger (~10 cm vs. 5 cm) at the faster velocities (Figure 3.23a,c). In terms of w, the flow moved upwards downstream of the plant at the slow velocity (Figure 3.23b), but no obvious trend was noted as velocity increased (Figure 3.23d). Finally, *Ceratophyllum* showed an area of reduced flow directly downstream the plant at the slower velocity in the

streamwise component (u) (Figure 3.24a), but the flow remained fairly uniform as velocity increased (Figure 3.24c). In the vertical velocity component (w), the flow was fairly uniform at the slower velocity (Figure 3.24b), but began to move upwards directly downstream the plant as velocity increased (Figure 3.24d).

An ANCOVA of the velocity data showed that there was a significant effect of test subject on the streamwise velocity (u) at the different test velocities ($p < 0.001$; Table 3.9a), as well as on the upstream and downstream position ($p = 0.023$), however, there was no effect between plant morphologies ($p = 0.47$). In the vertical velocity (w), there was also a significant effect on the velocity contours at the different test velocities ($p = 0.014$: Table 3.9b). Additionally, there was a significant difference in velocity between the different plant morphologies ($p < 0.001$), and between the upstream and downstream positions ($p < 0.001$). Post hoc comparisons of the streamwise component (u) showed that there were significant differences between downstream of the cylinder and of the empty test section ($p = 0.044$: Table 3.10a), between the upstream and downstream position of *Elodea* ($p = 0.034$), between upstream of *Elodea* and downstream of *Vallisneria* ($p = 0.010$), between downstream of *Elodea* and the empty test section ($p = 0.014$), between up and downstream position of *Vallisneria* ($p = 0.034$), between downstream of *Vallisneria* and upstream of the empty test section ($p = 0.046$), and between downstream of *Vallisneria* and the empty test section ($p = 0.0021$). An evaluation of the vertical velocity component (w), indicated that there were significant differences between upstream and downstream position of the cylinder ($p < 0.001$: Table 3.10b). Downstream of the cylinder was significantly different than all other plant and position combinations ($p < 0.002$), as was upstream of *Elodea* ($p < 0.008$).

Plant Response to Flow

The angle of deflection remained stationary at 0° for the circular cylinder (Figure 3.25a), however it increased with velocity for the plants. The deflection from the vertical increased significantly for *Elodea* ($p < 0.001$: Figure 3.25c) and *Ceratophyllum* ($p = 0.003$; Figure 3.23d). The results for *Vallisneria* ($p = 0.30$; Figure 3.25b) were not significant. An ANCOVA of these results indicated that velocity had a significant effect on the angle of deflection ($p < 0.001$), as did the plant morphology ($p < 0.001$; Table 3.11a). Significant pairwise differences ($p < 0.008$: Table 3.11b) were found between all combinations of subjects. To summarize, the rate of change in the angle of deflection remained at zero for the cylinder due to its rigid architecture. For *Vallisneria* there was a slight though non-significant increase, a larger and significant increase for *Elodea,* and a larger and also significant increase for *Ceratophyllum,* thus demonstrating that the more complex the plant architecture, the greater the rate of change in the angle of deflection with increasing velocity (Figure 3.26a).

Oscillations were not observed for the circular cylinder (Figure 3.25e). Significant or near significant increases in oscillation were observed for *Ceratophyllum* ($p = 0.018$; Figure 3.25h), *Vallisneria* ($p = 0.087$; Figure 3.25f), and *Elodea* ($p = 0.083$; Figure 3.25g) and the rate was on the order of 0.05 Hz/cms^{-1}. The ANCOVA revealed significant effects of velocity ($p < 0.001$: Table 3.12a) and plant morphology ($p < 0.001$). Pairwise comparisons however, showed that all differences occurred between the cylinder and the plants ($p < 0.001$: Table 3.12b), with no significant differences in oscillation rate occurring between the different plant morphologies. As an overview, the cylinder did not oscillate because of its rigid structure, the three plant morphologies

however, showed a similar trend of an increasing rate of oscillation with increasing velocity, which was significant only for *Ceratophyllum* (Figure 3.26b).

Discussion:

Macrophyte-Flow Interaction

The transition from laminar to turbulent flow (smooth dye streaks to eddies) occurred at lower velocities for the plants, with the exception of *Ceratophyllum,* than for the cylinder. This is interesting because Hurd and Stevens (1997) documented that the blades of marine algae induce the transition to turbulence at lower velocities than a flat plate, which was their physical model. Additionally, the transition for *Ceratophyllum* occurred at approximately the same velocity (> 5 cms^{-1}) as for the coarsely branched algae *Gelidium coulteri* (Hurd and Stevens, 1997). The transition to turbulent flow is important because it lead to a reduction in the thickness of the diffusional sublayer on the leaf surface, thus enhancing local mixing and nutrient delivery (Anderson and Charters, 1982; Borchardt, 1994; Hurd et al., 1996; Nepf, 1999). Additionally, both the area of dye coverage and the concentration of dye decreased at slower rates for the plants than for the circular cylinder, which demonstrates that plants retain more fluid, thus increasing the opportunity for exchange between the water column and the leaf surface. This would indicate that both fluid retention and mixing occur around the plants. This would provide the opportunity for nutrient uptake by the plants and replenishment of nutrients from the surrounding fluid. In other words, the recirculation on the downstream side of the plant increases the opportunity for the well mixed fluid to come in contact with the plant surface. Therefore it appears that aquatic plants alter the flow in ways that maximize flow across leaves, which would enhance nutrient exchange.

In this study, a circular cylinder was used as a physical model because it is a simple form, and the downstream flow patterns have been well documented (e.g., Kundu, 1990). The similarities among the plants (with the exception of *Ceratophyllum*) likely occurred because the Reynolds numbers examined here (cylinder (Re = 90-770), *Vallisneria* (Re = 25-220), *Elodea* (Re = 130-1100), and *Ceratophyllum* (300-2600)) were above the point (with the exception of *Vallisneria*) where attached vortices are shed (Re > 80; Kundu, 1990), and below the point where the wake is completely turbulent (Re < 5000; Kundu, 1990). The wake remained laminar for all Re examined here, however, changes occurred in the downstream eddies which began as small recirculating vortices, and grew with increasing Re and eventually became unstable and detached (von Karman vortex street; Figure 3.27). As such, the experimental results coincided with the theoretical expectations in most cases. Specifically, it was expected that *Vallisneria* would act like a cylinder because of its uniform structure (i.e., no branches). This was generally the case except that it retained more fluid than the cylinder, perhaps due to the inclined orientation. It was expected that *Elodea* would act similar to the cylinder because of its rigid cylinder-like structure. This was however, not the case as the leaf whorls trapped the dye and the regression analysis indicated that *Elodea* was more similar to *Ceratophyllum*. *Ceratophyllum* was expected to act more as a mesh, because of its high level of dissection which was predicted to break up the vertical circulation behind the plant, similar to a mesh (Nowell and Jumars, 1984). This is an important distinction because turbulence is dissipated by the resistance of the mesh, and as such is straightened, as has been demonstrated with the red alga *Gelidium nudifrons* (Anderson and Charters, 1982), and with *Gelidium coulteri* (Hurd and Stevens, 1997). Additionally,

as Re increases, vortices form closer to the branch (Kundu, 1990), leading to less entrainment of the dye because the recirculation zone is smaller. Hence, if features on the plant generate small scale turbulence it could enhance mass and momentum transfer, and thus productivity. However, it has also been suggested that that since mesh-like structures slow fluid down and dampen turbulence, there could be the potential for diffusion-limited productivity to be greater in branched rather than linear-bladed morphologies (Hurd and Stevens, 1997). This is, however unlikely considering that it has been shown that the critical velocity where limitations change from diffusional to mechanical stress is between 2 and 6 cms^{-1} (Jumars et al., 2001; Hurd et al., 1996; Koch, 1993; Koch, 1994). This is consistent with this study as the transition from laminar to turbulent flow occurred at approximately 5 cms^{-1}.

It was reasonable to expect differences in area of dye coverage among plant morphologies (*Vallisneria* > *Elodea* > *Ceratophyllum*) because leaves can act as edges to which dye can attach, and flow separation occurs (Coutanceau and Defaye, 1991); separation would increase the dispersion of the dye. Separation points occur when the flow stops moving up the surface of the plant, and starts moving in the downstream direction (Vogel, 1994). Stevens and Hurd (1997) noted that under almost any field conditions in the marine environment, the pressure gradients at leading edges of macrophyte leaves will be sufficient to cause separation in the flow. This process of separation, whereby the separated shear layer attaches on the solid boundary, forms a closed recirculating zone (Kiya et al., 2000), has been shown to enhance mass-transfer (Schwinge et al., 2002). This area of recirculation would be much larger for *Vallisneria* than for *Elodea* and *Ceratophyllum* because the size and shape of recirculation is

dependent on how the leaves are arranged, their diameter and length (Schwinge et al., 2002), and the boundary layer thickness (Lozee and Wetzel, 1993). This is demonstrated by flow through a mesh, which reduces highly turbulent flow structures to smaller eddies (Nowell and Jumars, 1984; Sand-Jensen and Pedersen, 1999) because of the thinness of the structure and the small size of the openings.

The rate of change in the concentration of dye with change in velocity decreased in all cases, but less so for the plants than for the cylinder, which indicates that more fluid is being retained by the plants. It is interesting that the area of dye coverage is affected by the different plant morphologies, but that the concentration of dye downstream of the plant is not. In other words, the dye dispersed differently (i.e., area changes) according to the plant shape, but the same amount of dye is retained. Comparatively, Hurd et al. (1996) showed that blade morphology (i.e., undulate versus smooth) affected the flow patterns, with the undulations generating recirculating eddies, and the smooth blades acting like plates. However, despite differences in flow patterns, nitrogen uptake was similar between the two different blade morphologies. This supports the previous statement demonstrating that that freshwater macrophytes of different morphologies have different ways of interacting with the flow, while retaining the same amount of fluid.

In addition to plant morphology, the angle of the plant in the flow is important as an increase in the angle of deflection results in a decrease in the drag forces acting on the macrophyte (Dawson and Robinson, 1984). Consequently, plants living in faster moving water have leaves with low branching angles, which produce a more streamlined surface. In contrast plants living in slower moving water have leaves that stick out more into the flow presenting a rough surface which, increases the drag coefficient, but results in the

production of small vortices behind the leaves that increase the supply of carbon dioxide and nutrients, thereby increasing the rate of photosynthesis (Ennos, 1999; Sand-Jensen and Pedersen, 1999; Schutten and Davy, 2000). Moreover, it is well documented that smooth, flexible stems are best able to reduce drag (Armstrong, 1989; Johnson, 2001), especially when the angle of deflection is greater than 30°, the plant is more streamlined and the pressure drop around the stem is reduced. When deflected almost horizontally (as seen with *Ceratophyllum* and *Vallisneria*) the leaf can block vertical exchange flow (Nepf and Koch, 1999). This could deprive the leaves higher up in a canopy of nutrient-enriched water if the flow was prevented from travelling vertically. However, if the flow is not blocked, secondary flow may promote direct transport between the sediments and the water column and thus lessen diffusive boundary layer limitations on nutrient and inorganic carbon exchange (Nepf and Koch, 1999).

Furthermore, the rate of change in the angle of deflection with change in velocity increased with increasing complexity in architecture (i.e., *Vallisneria* < *Elodea* < *Ceratophyllum*). This is likely because *Vallisneria*'s architecture is already deflected from the vertical, *Elodea* is relatively rigid with whorls of leaves, and *Ceratophyllum* is relatively flexible with highly dissected leaves exposed to the flow. It is also interesting to note that *Ceratophyllum,* which was the most compliant plant retained the least dye and *Vallisneria*, the plant whose compliance changed the least, retained the most dye (Figure 3.19). This relates back to the argument that the size of the recirculation zone is dependent on the size, shape, and orientation of the leaf (Schwinge et al., 2002). There were however, no significant differences among the different plant morphologies and the rate of change in the frequency of oscillations with velocity. Oscillations are due to

phase differences between lift and the shedding frequency of vortices, and are not found for circular cylinders (Norberg, 2003). These plant movements are important because they cause a dampening of the flow which in turn causes a dissipation of mechanical energy, which increases the effectiveness of energy transfer (Bruchert et al., 2003). Additionally, oscillations can noticeably change the formation of vortex shedding patterns even with cylinders (Williamson, 1996), potentially increasing local mixing. Local mixing can also be increased because the waving of plants (i.e., monami) has been shown to cause in increase in the vertical transport of momentum into the canopy (Ackerman and Okubo, 2003; Ghisalberti and Nepf, 2002).

Finally, the technique of isokinetic dye injection appears to be valid in that differences in upstream flows were not detected. Changes present in the relative downstream position of the empty test section were due to the expansion of the dye plume, which increased with distance from the source (i.e., dye injector; Mercier and Jaluria, 1999; Macdonald et al., 2002; Hara and Kato, 2004).

Implications of the Macrophyte-Flow Interaction

The significance of these findings relate to issues of macrophyte productivity (e.g., photosynthesis and nutrient uptake), sediment capture, and the evolutionary question about form and function relationships, that has previously been examined in seaweeds (Norton et al., 1982). Light is the limiting factor in determining the maximum depth at which plants occur in a given body of water (Riemer, 1993), and since it is known that both low (Hurd and Stevens, 1997; Schutten and Davy, 2000) and high (Koch, 1993) flows affect photon capture, macrophytes must adapt to maximize photosynthesis, and thus primary productivity. At low flow, a thick diffusive boundary

layer occurs which, leads to a decrease in the amount of carbon availability, and thus a reduction in photosynthesis (Koch, 1993;1994). At high flow, photosynthesis can be limited by the washing away of extracellular enzymes that catalyze the reaction between bicarbonate and carbon dioxide (Koch, 1994), and by breakage of the photosynthetically active parts of the plant (Koch, 1993; Stewart and Carpenter, 2003). The question of form and function relationships relates to the structural similarities of the plants on fluid dynamics. For example, linear-bladed morphologies are better suited to higher flows because they are better able to comply to the flow (Gutierrez and Fernandez, 1992) and thus are damaged at higher velocities than branched morphologies (Sheath and Hambrook, 1988). Conversely, morphologies with small scale roughness are able to induce turbulence at lower velocities thus enhancing local mixing and preventing the depletion of nutrients. For example, undulate margins have been shown to take up labeled carbon at a faster rate than smooth blades at the same velocity (Armstrong, 1989). This is congruent with the current study whereby *Vallisneria* interacted the least with the flow because of its high angle of deflection, *Ceratophyllum* broke the flow up into smaller turbulence structures, and *Elodea* affected the flow in a fashion between these two extremes. Thus, the interaction between macrophyte morphology and fluid dynamics has implications for the productivity of the individual plant and the ecosystem.

Quantitative similarities in the concentration of dye among plant morphologies may result from different flow patterns that maximize contact of flow with the leaves, and as such provide light and nutrients to the leaf surface. But, as mentioned above, a morphology that increases nutrient uptake may not be the same morphology that increases photosynthesis, as high levels of dissection may cause self-shading (Norton et

al., 1982). As well, it has been documented that linear-bladed seaweeds have higher rates of photosynthesis than branched morphologies (Irwin and Davenport, 2002). This suggests that *Vallisneria* should have better photosynthetic abilities than the whorled and dissected morphologies, and *Ceratophyllum* should have better nutrient uptake than the linear-bladed and whorled morphologies.

Leaf development in aquatic macrophytes is a dynamic process which, emphasizes the close relationship between environment and leaf structure (Rascio, 2002). One classic example of this is found in a number of seaweeds where high drag morphologies (e.g., rugosity and undulation) are found in low energy environments and low drag morphologies (e.g., smooth, straight blades) are found in high energy environments (Ackerman and Okubo, 1993; Hurd and Stevens, 1997). Consequently, species with high phenotypic plasticity may adopt a variety of morphologies to meet environmental conditions without being developmentally committed to those conditions should they change (Taylor and Hay, 1984). For example, in order to increase photosynthetic ability, plants generally increase the size of the leaf surfaces thus increasing the number of chloroplasts in contact with the environment (Rascio, 2002; Ronzhina et al., 2004). Specifically, *Elodea* reduces the thickness of its leaves, *Ceratophyllum* has a highly dissected morphology and, *Vallisneria* has few layers of photosynthetic cells, due to the presence of inner aerenchyma lacunae, which can be involved in supplying carbon dioxide (Rascio, 2002). Another plant feature that increases photosynthesis is the ability of the plant to oscillate with the flow, thus causing the fluid to become stirred (Koehl and Alberte, 1988). For example, algae with undulate blades have been shown to oscillate with greater amplitude, but smooth blades oscillate

with greater frequency (Koehl and Alberte, 1988). The greater amplitude would increase local mixing, whereas the greater frequency would mean that less surface area is being exposed to the flow, thus decreasing the drag forces.

The flexibility of the plant stem can also cause changes in flow patterns (e.g., canopies of flexible plants tend to have a logarithmic velocity profile whereas canopies of more rigid plants do not have a logarithmic velocity profile), as was demonstrated in canopies of *Myriophyllum* and *Hydrilla* (Shi and Hughes, 2002). It has also been shown that morphology can affect the flow within the canopy. The flow within a canopy of whorled and dissected leafed morphologies was reduced considerably more than the flow in a linear-bladed leafed canopy, demonstrating that there was less interaction between the flow and the linear-bladed morphology (Sand-Jensen and Mebus, 1996; Champion and Tanner, 2000). This corresponds with the results seen in the angle of deflection data, where the linear-bladed morphology (*Vallisneria*) changed the least with increasing velocity. As such, it is likely that *Vallisneria* is better suited to higher flow environments because it is less affected by the flow, whereas *Ceratophyllum* may be better suited to slower flow environments because of its high level of interaction with the flow. It appears that there is a strong relationship between plant morphology and fluid dynamics that may have influenced the convergent evolution of these morphologies.

At the larger scale, an improved understanding of flow effects would aid in efforts to restore streams and rivers, and maintain water quality as aquatic macrophytes act as ecosystem engineers. This is especially important as many streams have been degraded as the result of anthropogenic processes including: channelization, removal of riparian vegetation, irrigation, pollutant discharges, and stormwater runoff (Poff et al., 1997).

Restoration efforts often focus on improving physical habitat within the channel, replanting streamside forests, and building stormwater retention structures. One of the goals of these restoration practices is to create flow conditions that improve the "health" of streams, as such it is important to link the physical aspects of the flow and the biological aspects of the plant (Hart and Finelli, 1999), since freshwater macrophytes act as ecosystem engineers in aquatic systems (Wright et al., 2004). It should be noted that the range of velocities examined here are typical of within canopy conditions. If higher velocities were obtainable, transport limitations (i.e., diffusional stress) would become negligible, and there would be more compliance observed in the plants, less retention of fluid, and ultimately dislodgment and loss of plant biomass.

Literature cited

Ackerly, D.D., S.A. Dudley, S.E. Sultan, J. Schmitt, J.S. Coleman, C.R. Linder, D.R. Sandquist, M.A. Gerber, A.S. Evans, T.E. Dawson, and M.J. Lechowicz. 2000. The evolution of plant ecophysiological traits: recent advances and future directions. *BioScience.* 50(11):979-995.

Ackerman, J.D., and T.M. Hoover. 2001. Measurement of local bed shear stress in streams using a Preston-static tube. *Limnology and Oceanography.* 46(8): 2080-2087.

Ackerman, J.D., and A. Okubo. 1993. Reduced mixing in a marine macrophyte canopy. *Functional Ecology.* 7:305-309.

Anderson, S.M., and A.C. Charters. 1982. A fluid dynamics study of seawater flow through *Gelidium rudifrons. Limnology and Oceanography.* 37(3):399-412.

Armstrong, S.L. 1989. The behaviour in flow of the morphologically variable seaweed *Hedophyllum sessile* (C.Ag.) Setchell. *Hydrobiologia.* 183:115-122.

Borchardt, M.A. 1994. Effects of flowing water on nitrogen- and phosphorus-limited photosynthesis and optimum N:P ratios by *Spirogyra fluviatilis* (Charophyceae). *Journal of Phycology.* 30:418-430.

Bruchert, F., O. Speck, and H-C. Spatz. 2003. Oscillations of plants' stems and their damping: theory and experimentation. *Philosophical Transactions of the Royal Society of London Series B-Biological Sciences.* 358:1487-1492.

Carollo, F.G., V. Ferro, and D. Termini. 2002. Flow velocity measurements in vegetated channels. *Journal of Hydraulic Engineering.* 128(7):664-673.

Champion, P.D., and C.C. Tanner. 2000. Seasonality of macrophytes and interaction with flow in a New Zealand lowland stream. *Hydrobiologia.* 441:1-12.

Cheer, A.Y.L, and M.A.R. Koehl. 1987. Paddles and rakes: fluid flow through bristled appendages of small organisms. *Journal of Theoretical Biology.* 129:17-39

Cook, C.D.K., B.J. Gut, E.M. Rix, J. Schneller, M. Seitz. 1974. *Water plants of the world: a manual for the identification of the genera of freshwater macrophytes.* Dr. W. Junk b.v., publishers. The Hague.

Coutanceau, M., and J. Defaye. 1991. Circular cylinder wake configurations: A flow visulization survey. *Applied Mechanics Reviews.* 44(6):255-305.

Dawson, F.H. 1988. Water flow and vegetation of running waters. e.d Symoens, JJ *Vegetation of inland waters.* Kluwer academic publishers group. Pp.283-309.

Dawson, F.H., and W.N. Robinson. 1984. Submerged macrophytes and the hydraulic roughness of a lowland chalkstream. *Verhandlungen der Internationalen Vereinigung fur Limnologie.* 22(3):1944-1948.

Dodds, W.K., and B.J.F. Biggs. 2002. Water velocity attenuation by stream periphyton and macrophytes in relation to growth form and architecture. *Journal of the North American Benthological Society.* 21(1): 2-15.

Dorken, M.E., and S.C.H. Barrett. 2004. Phenotypic plasticity of vegetative and reproductive traits in monoecious and dioecious populations in *Sagittaria latifolia* (Alismataceae): a clonal aquatic plant. *Journal of Ecology.* 92: 32-44.

Elliott, A.H. 2000. Settling of fine sediment in a channel with emergent vegetation. *Journal of Hydraulic Engineering.* 126(8):570-577.

Ennos, A.R. 1999. The aerodynamics and hydrodynamics of plants. *The Journal of Experimental Biology.* 202:3281-3284.

French, T.D., and P.A. Chambers. 1996. Habitat partitioning in riverine macrophyte communities. *Freshwater Biology.* 36:509-520.

Ghisalberti, M., and H.M. Nepf. 2002. Mixing layers and coherent structures in vegetated aquatic flows. *Journal of Geophysical Research.* 107(C2): 3.1-3.11.

Givnish, T.J., 2002. Ecological constraints on the evolution of plasticity in plants. *Evolutionary Ecology.* 16:213-242.

Goliber, T.E., and L.J. Feldman. 1990. Developmental analysis of leaf plasticity in the heterophyllous aquatic plant *Hippuris vulgaris. American Journal of Botany.* 77(3):399-412.

Gutierrez, L.M., and C. Fernandez. 1992. Water motion and morphology in *Chondrus crispus* (Rhodothyta). *Journal of Phycology.* 28:156-162.

Hara, T., and S. Kato. 2004. Numerical simulation of thermal plumes in free space using the standard κ–ε model. *Fire Safety Journal.* 39:105-129.

Hart, D.D., and C.M. Finelli. 1999. Physical-biological coupling in streams: The pervasive effects of flow on benthic organisms. *Annual Review of Ecology and Systematics.* 30:363-395.

Hurd, C.L., P.J. Harrison, and L.D. Druehl. 1996. Effect of seawater velocity in inorganic nitrogen uptake by morphologically distinct forms of *Macrocystis intgrifolia* from wave-sheltered and exposed sites. *Marine Biology.* 126:205-214.

Hurd, C.L. and C.L. Stevens. 1997. Flow visualization around single- and multiple-linear-bladed seaweeds with various morphologies. *Journal of Phycology.* 33:360-367.

Hurd, C.L, C.L Stevens, B.E. Laval, G.A. Lawrence, and P.J. Harrison. 1997. Visualization of seawater flow around morphologically distinct forms of the giant kelp *Macrocystis integrifolia* from wave-sheltered and exposed sites. *Limnology and Oceanography.* 42(1):156-163.

Irwin, S., and J. Davenport. 2002. Hyperoxic boundary layers inhabitated by the epiphytic meiophauna of *Fucus serratus. Marine Ecology Progress Series.* 244:73-79.

Järvelä, J. 2002. Flow resistance of flexible and stiff vegetation: a flume study with natural plants. *Journal of Hydrology.* 269:44-54.

Johnson, A.S. 2001. Drag, drafting, and mechanical interactions in canopies of the red alga *Chondrus crispus. Biological Bulletin.* 201:126-135.

Jumars, P.A., J.E. Eckman, and E. Koch. 2001. *Macroscopic animals and plants in benthic flows.* In. The benthic boundary layer: Transport processes and biogeochemistry. B.P. Boudreau ed. Oxford University Press. Pp. 320-347.

Kiya, M., O. Mochizuki, and H. Ishikawa. 2000. Challenging issues in separated and complex turbulent flows. *Proceedings of the 10th International Conference on Lazer Techniques.* 1-13.

Koch, E.W. 1993. The effect of water flow on photosynthetic processes of the alga *Ulva lactuca* L. *Hydrobiologia.* 260/261:457-462.

Koch, E.W. 1994. Hydrodynamics, diffusion-boundary layers and photosynthesis of the seagrass *Thalassia testudinum* and *Cymodocea nodosa. Marine Biology.* 119:767-776.

Koehl, M.A.R. 1996. When does morphology matter? *Annual Review of Ecology and Systematics.* 27:501-542.

Koehl, M.A.R., and R.S. Alberte. 1988. Flow, flapping, and photosynthesis of *Nereocystis luetkeana*: a functional comparison of undulate and flat blade morphologies. *Marine Biology.* 99:435-444.

Kundu, P.K. 1990. *Fluid Mechanics.* Academic Press, San Diego, Toronto. 638 p.

Leonard, L.A., and M.E. Luther. 1995. Flow hydrodynamics in tidal marsh canopies. *Limnology and Oceanography.* 40(8):1474-1484.

Losee, R.F., and R.G. Wetzel. 1993. Littoral flow rates within and around submersed macrophyte communities. *Freshwater Ecology.* 29:7-17.

Macdonald, R.W., R.K. Strom, and P.R. Slawson. 2002. Water flume study of the enhancement of buoyant rise in pairs of merging plumes. *Atmospheric Environment.* 36:4603-4615.

Mercier, G.P., and Y. Jaluria. 1999. Fire-induced flow of smoke and hot gases in open vertical enclosures. *Experimental Thermal and Fluid Science.* 19:77-84.

Nepf, H.M. 1999. Drag, turbulence, and diffusion in flow through emergent vegetation. *Water Resources Research.* 35(2):479-489.

Nepf, H.M., and E.W. Koch. 1999. Vertical secondary flows in submersed plant-like arrays. *Limnology and Oceanography.* 44(4):1072-1080.

Norberg, C. 2003. Fluctuating lift on a circular cylinder: review and new measurements. *Journal of Fluids and Structures.* 17:57-96.

Norton, T.A., A.C. Mathieson, and M. Neushul. 1982. A review of some aspects of form and function in seaweeds. *Botanica Marina.* XXV: 501-510.

Nowell, A.R.M., and P.A. Jumars. 1984. Flow environments of aquatic benthos. *Annual Review of Ecology and Systematics.* 15:303-328

Palmer, M.R., H.M. Nepf, T.J.R. Pettersson, and J.D. Ackerman. 2004. Observations of particle capture on a cylindrical collector: implications for particle accumulation and removal in aquatic systems. *Limnology and Oceanography.* 49(1):76-85.

Poff, N.L., J.D. Allan, M.B. Bain, J.R. Kar, K.L. Prestgaard, B.D. Ritcher, R.E. Sparks, and J.C. Stromberg. 1997. The natural flow regime. *Bioscience.* 47(11):769-782.

Rascio, N. 2002. The underwater life of secondary aquatic plants: Some problems and solutions. *Critical Reviews in Plant Sciences.* 21(4):401-427.

Riemer, D.N. 1993. *Introduction to Freshwater Vegetation.* Krieger Publishing Company, Malabar, Florida.

Ronzhina, D.A., G.F. Nekrasova, and V.I. P'yankov. 2004. Comparative characterization of the pigment complex in emergent, floating, and submerged leaves of hydrophytes. *Russian Journal of Plant Physiology.* 51(1):21-27.

Sand-Jensen, K., and J.R. Mebus. 1996. Fine-scale patterns of water velocity within macrophyte patches in streams. *Oikos.* 76:169-180.

Sand-Jensen, K., and O. Pedersen. 1999. Velocity gradients and turbulence around macrophyte stand in streams. *Freshwater Biology.* 42:315-328.

Santamaria, L. 2002. Why are most aquatic plants widely distributed? Dispersal, clonal growth and small-scale heterogeneity in a stressful environment. *Acta Oecologica.* 23:137-154.

Santamaria, L., J. Figuerola, J.J. Pilon, M. Mjelde, A.J. Green, T. De Boer, R.A. King, and R.J. Gornall. 2003. Plant performance across latitude: the role of plasticity and local adaptation in an aquatic plant. *Ecology.* 84(9):2454-2461.

Schlichting, C.D. 1986. The evolution of phenotypic plasticity in plants. *Annual Review of Ecology and Systematics.* 17:667-693.

Schutten, J., and A.J. Davy. 2000. Predicting the hydraulic forces on submerged macrophytes from current velocity, biomass and morphology. *Oecologia.* 123:445-452.

Schwinge, J., D.E., Wiley, and D.F. Fletcher. 2002. Simulation of the flow around spacer filaments between narrow channel walls. 1. Hydrodynamics. *Industrial and Engineering Chemistry Research.* 41:2977-2987.

Sheath, R.G., and J.A. Hambrook. 1988. Mechanical adaptations to flow in freshwater red algae. *Journal of Phycology.* 24:107-111.

Shi, Z. and J.M.R. Hughes. 2002. Laboratory flume studies of microflow enviroments of aquatic plants. *Hydrological Processes.* 16:3279-3289.

Stevens, C.L., and C.L. Hurd. 1997. Boundary-layers around linear-bladed aqutic macrophytes. *Hydrobiologia.* 346:119-128.

Taylor, P.R., and M.E. Hay. 1984. Functional morphology of intertidal seaweeds: adaptive significance of aggregate vs. solitary forms. *Marine Ecology Progress Series.* 18:295-302.

Vogel, S. 1987. Flow-assisted mantle cavity refilling in jetting squid. *Biological Bulletin.* 172:61-68.

Vogel, S. 1994. *Life in Moving Fluids the Physical Biology of Flow 2nd ed.* Princeton University Press, Princeton, N.J. 467 p.

Wiegleb, G. 1984. A study of habitat conditions of the macrophytic vegetation in selected river systems in western lower saxony (Federal Republic of Germany). *Aquatic Botany.* 18:313-352.

Williamson, C.H.K. 1996. Vortex dynamics in the cylinder wake. *Annual Review of Fluid Mechanics.* 28:477-539.

Wright, J.P., W.S.C. Gurney, and C.G. Jones. 2004. Patch dynamics in a landscape modifies by ecosystem engineers. *Oikos.* 105:336-348.

Wuest, A., and A. Lorke. 2003. Small scale hydrodynamics in lakes. *Annual review of fluid mechanics.* 35:373-412.

Box 3.1: Matlab commands for the image analysis.

1) Import file
   I=imread('c:\julianne\photoshop\elodea\4inc6ta.png');
2) Edit image
   I=rgb2gray(I);
      Convert to gray scale
   I=imadjust(I,[0 0.2],[0 1]);
      Adjusts the intensity of the image.
   Pixval
      Gives pixel value at mouse click.
   I=imsubtract(I,69);
      Subtracts background value (use value given by above command)
3) Crop image
   I=imcrop(I);
      Use mouse to select area based on lines drawn on the flume
   I=imresize(I,[600 900],'bicubic');
      To make image larger and thus easier to see; the matrix dimensions change depending on domain.
4) Extract pixel values
   [n x]=imhist(I,100);
      Groups the pixel values into 100 different bins
   n
      Gives the number of pixels in each bin

Table 3.1: Shear velocity (u_*) determined for each of the velocities used for the experiments.

U (cms^{-1})	**u_* (cms^{-1})**
1.3	0.12
2.0	0.24
5.0	0.42
8.4	0.33
11.0	0.35

Table 3.2: Pump settings for isokinetic release of dye at each water velocity.

Water Velocity ($cms^{-1} \pm$ St.dev)	**Pump Speed**	**Increment**	**Internal Tubing Diameter**
1.3 ± 0.1	Slow	0	3/32" = 0.21 cm
2.0 ± 0.5	Slow	3	3/32" = 0.21 cm
5.0 ± 0.3	Fast	10	3/32" = 0.21 cm
8.4 ± 0.5	Slow	2	3/16" = 0.42 cm
11.0 ± 0.9	Slow	6	3/16" = 0.42 cm

Table 3.3: ANCOVA results for the area of dye coverage and the concentration of dye for (a) the empty test section, (b) the circular cylinder, (c) *Vallisneria*, (d) *Elodea*, and (e) *Ceratophyllum*. (Area = area of dye coverage; Conc. = concentration of dye; velocity = average flume velocites; side/top = side and top perspectives; before/after = upstream and downstream domain). Grey values are significant.

(a)

Univariate Results for Each DV (Empty Test Section)
Sigma-restricted parameterization
Effective hypothesis decomposition

Effect	Degr. of Freedom	area SS	area MS	area F	area p	conc. SS	conc. MS	conc. F	conc. p
Intercept	1	15.89635	15.89635	20.60062	0.000392	5.986195	5.986195	80.56224	0.000000
velocity	1	0.02138	0.02138	0.02771	0.870021	1.988960	1.988960	26.76743	0.000113
side/top	1	2.68113	2.68113	3.47456	0.082011	0.000279	0.000279	0.00375	0.951949
before/after	1	31.75762	31.75762	41.15577	0.000012	0.536225	0.536225	7.21652	0.016915
side/top*before/after	1	3.63022	3.63022	4.70453	0.046566	0.028648	0.028648	0.38554	0.543972
Error	15	11.57467	0.77164			1.114578	0.074305		
Total	19	49.66502				3.668690			

(b)

Univariate Results for Each DV (Cylinder)
Sigma-restricted parameterization
Effective hypothesis decomposition

Effect	Degr. of Freedom	area SS	area MS	area F	area p	conc. SS	conc. MS	conc. F	conc. p
Intercept	1	22.059	22.0598	22.2123	0.00027	1.97869	1.97869	95.6720	0.00000
velocity	1	5.436	5.4365	5.4741	0.03354	0.43785	0.43785	21.1706	0.00034
side/top	1	0.434	0.4345	0.4375	0.51833	0.01650	0.01650	0.7979	0.38580
before/after	1	95.683	95.6839	96.3455	0.00000	0.03349	0.03349	1.6196	0.22251
side/top*before/after	1	0.329	0.3294	0.3317	0.57318	0.00042	0.00042	0.0207	0.88752
Error	15	14.897	0.9931			0.31023	0.02068		
Total	19	116.781				0.79851			

(c)

Univariate Results for Each DV (*Vallisneria*)
Sigma-restricted parameterization
Effective hypothesis decomposition

Effect	Degr. of Freedom	area SS	area MS	area F	area p	conc. SS	conc. MS	conc. F	conc. p
Intercept	1	25.68525	25.68525	60.8871	0.000001	2.074531	2.074531	37.30564	0.000020
velocity	1	2.07688	2.07688	4.9233	0.042343	0.199396	0.199396	3.58567	0.077732
side/top	1	0.36396	0.36396	0.8628	0.367672	0.002246	0.002246	0.04038	0.843438
before/after	1	81.81758	81.81758	193.9494	0.000000	0.012980	0.012980	0.23342	0.635978
side/top*before/after	1	0.45547	0.45547	1.0797	0.315228	0.003279	0.003279	0.05897	0.811423
Error	15	6.32775	0.42185			0.834136	0.055609		
Total	19	91.04164				1.052036			

(d)

Univariate Results for Each DV (*Elodea*)
Sigma-restricted parameterization
Effective hypothesis decomposition

Effect	Degr. of Freedom	area SS	area MS	area F	area p	conc. SS	conc. MS	conc. F	conc. p
Intercept	1	40.6380	40.63798	111.6627	0.000000	2.949523	2.949523	120.1269	0.000000
velocity	1	0.1589	0.15888	0.4366	0.518806	0.649332	0.649332	26.4457	0.000120
side/top	1	0.4885	0.48855	1.3424	0.264725	0.029748	0.029748	1.2116	0.288375
before/after	1	92.4244	92.42442	253.9585	0.000000	0.028255	0.028255	1.1508	0.300344
side/top*before/after	1	1.7768	1.77681	4.8822	0.043100	0.078995	0.078995	3.2173	0.093045
Error	15	5.4590	0.36394			0.368301	0.024553		
Total	19	100.3077				1.154631			

(e)

Univariate Results for Each DV (*Ceratophyllum*)
Sigma-restricted parameterization
Effective hypothesis decomposition

Effect	Degr. of Freedom	area SS	area MS	area F	area p	conc. SS	conc. MS	conc. F	conc. p
Intercept	1	43.71454	43.71454	109.4433	0.000000	3.492296	3.492296	32.72128	0.000041
velocity	1	1.35136	1.35136	3.3833	0.085738	0.446894	0.446894	4.18720	0.058675
side/top	1	1.69315	1.69315	4.2390	0.057310	0.152006	0.152006	1.42423	0.251243
before/after	1	65.79465	65.79465	164.7228	0.000000	0.005253	0.005253	0.04921	0.827427
side/top*before/after	1	1.87377	1.87377	4.6912	0.046839	0.033108	0.033108	0.31021	0.585767
Error	15	5.99140	0.39943			1.600929	0.106729		
Total	19	76.70433				2.238190			

Table 3.4: Post hoc comparisons for the area of dye coverage (Table 3) in the different domains surrounding different test subjects: (a) empty test section, (b) circular cylinder, (c) *Vallisneria*, (d) *Elodea*, and (e) *Ceratophyllum*. Significant results indicated in bold.

(a) **Empty flume**	**side; upstream**	**top; upstream**	**side; downstream**	**top; downstream**
side; upstream				
top; upstream	0.81			
side; downstream	**< 0.001**	**< 0.001**		
top; downstream	**< 0.001**	**0.002**	**0.003**	

(b) **Cylinder**	**side; upstream**	**top; upstream**	**side; downstream**	**top; downstream**
side; upstream				
top; upstream	0.94			
side; downstream	**< 0.001**	**< 0.001**		
top; downstream	**< 0.001**	**< 0.001**	0.28	

(c) ***Vallisneria***	**side; upstream**	**top; upstream**	**side; downstream**	**top; downstream**
side; upstream				
top; upstream	0.95			
side; downstream	**< 0.001**	**< 0.001**		
top; downstream	**< 0.001**	**< 0.001**	0.26	

(d) ***Elodea***	**side; upstream**	**top; upstream**	**side; downstream**	**top; downstream**
side; upstream				
top; upstream	0.58			
side; downstream	**< 0.001**	**< 0.001**		
top; downstream	**< 0.001**	**< 0.001**	0.078	

(e) ***Ceratophyllum***	**side; upstream**	**top; upstream**	**side; downstream**	**top; downstream**
side; upstream				
top; upstream	0.95			
side; downstream	**< 0.001**	**< 0.001**		
top; downstream	**< 0.001**	**< 0.001**	**0.021**	

Table 3.5: Post hoc comparisons for the concentration of dye (Table 3) in the different domains surrounding different test subjects: (a) empty test section, (b) circular cylinder, (c) *Vallisneria*, (d) *Elodea*, and (e) *Ceratophyllum*. Significant results indicated in bold.

(a) **Empty flume**	**side; upstream**	**top; upstream**	**side; downstream**	**top; downstream**
side; upstream				
top; upstream	0.59			
side; downstream	**0.011**	**0.042**		
top; downstream	**0.034**	0.11	0.66	

(b) **Cylinder**	**side; upstream**	**top; upstream**	**side; downstream**	**top; downstream**
side; upstream				
top; upstream	0.76			
side; downstream	0.56	0.37		
top; downstream	0.88	0.67	0.64	

(c) ***Vallisneria***	**side; upstream**	**top; upstream**	**side; downstream**	**top; downstream**
side; upstream				
top; upstream	0.76			
side; downstream	0.62	0.84		
top; downstream	0.64	0.87	0.97	

(d) ***Elodea***	**side; upstream**	**top; upstream**	**side; downstream**	**top; downstream**
side; upstream				
top; upstream	0.76			
side; downstream	0.75	0.99		
top; downstream	0.33	0.20	0.20	

(e) ***Ceratophyllum***	**side; upstream**	**top; upstream**	**side; downstream**	**top; downstream**
side; upstream				
top; upstream	0.55			
side; downstream	0.46	0.19		
top; downstream	0.36	0.75	0.10	

Table 3.6: ANCOVA results for (a) the area covered in dye and (b) the concentration of dye in that area for the different domains. (Velocity = covariate; Plant = empty test section, circular cylinder, *Vallisneria, Elodea,* and *Ceratophyllum*; Side/Top = perspectives; and Before/After = upstream and downstream).

(a)	Univariate Results for Each DV (Spreadsheet8) Sigma-restricted parameterization Effective hypothesis decomposition				
Effect	Degr. of Freedom	area SS	area MS	area F	area p
Intercept	1	142.9880	142.9880	220.1792	0.000000
velocity	1	1.9909	1.9909	3.0657	0.083840
plant	4	14.7433	3.6858	5.6756	0.000456
side/top	1	2.7284	2.7284	4.2013	0.043711
before/after	1	355.9598	355.9598	548.1224	0.000000
plant*side/top	4	2.9329	0.7332	1.1291	0.348892
plant*before/after	4	11.5184	2.8796	4.4341	0.002764
side/top*before/after	1	4.0612	4.0612	6.2537	0.014463
plant*side/top*before/after	4	4.0045	1.0011	1.5416	0.198277
Error	79	51.3039	0.6494		
Total	99	449.2434			

(b)	Univariate Results for Each DV (Spreadsheet8) Sigma-restricted parameterization Effective hypothesis decomposition			
Effect	concentration SS	concentration MS	concentration F	concentration p
Intercept	15.77032	15.77032	261.6230	0.000000
velocity	3.18859	3.18859	52.8973	0.000000
plant	0.44452	0.11113	1.8436	0.128760
side/top	0.11398	0.11398	1.8909	0.172993
before/after	0.11516	0.11516	1.9104	0.170817
plant*side/top	0.08680	0.02170	0.3600	0.836338
plant*before/after	0.50106	0.12526	2.0781	0.091504
side/top*before/after	0.01323	0.01323	0.2195	0.640741
plant*side/top*before/after	0.13123	0.03281	0.5443	0.703693
Error	4.76202	0.06028		
Total	9.35658			

Table 3.7: Post hoc comparisons between the subjects for the area covered in dye (Table 6) in the different domains; (a) side upstream, (b) top upstream, (c) side downstream, and (d) top downstream. Significant results indicated in bold.

(a)	Cylinder	*Vallisneria*	*Elodea*	*Ceratophyllum*	Empty flume
Cylinder					
Vallisneria	0.98				
Elodea	0.85	0.83			
Ceratophyllum	0.91	0.89	0.94		
Empty flume	0.75	0.73	0.89	0.83	

(b)	Cylinder	*Vallisneria*	*Elodea*	*Ceratophyllum*	Empty flume
Cylinder					
Vallisneria	0.97				
Elodea	0.66	0.68			
Ceratophyllum	0.98	0.99	0.67		
Empty flume	0.99	0.96	0.65	0.97	

(c)	Cylinder	*Vallisneria*	*Elodea*	*Ceratophyllum*	Empty flume
Cylinder					
Vallisneria	0.090				
Elodea	0.74	**0.043**			
Ceratophyllum	0.38	0.41	0.23		
Empty flume	**0.007**	0.28	**0.002**	0.059	

(d)	Cylinder	*Vallisneria*	*Elodea*	*Ceratophyllum*	Empty flume
Cylinder					
Vallisneria	0.63				
Elodea	0.72	0.39			
Ceratophyllum	**0.036**	**0.010**	0.080		
Empty flume	**< 0.001**	**< 0.001**	**< 0.001**	**0.009**	

Table 3.8: Post hoc comparisons between the subjects for the concentration of dye in the plume (Table 6) in the different domains; (a) side upstream, (b) top upstream, (c) side downstream, and (d) top downstream. Significant results indicated in bold.

(a)	Cylinder	*Vallisneria*	*Elodea*	*Ceratophyllum*	Empty flume
Cylinder					
Vallisneria	0.90				
Elodea	0.77	0.86			
Ceratophyllum	0.38	0.46	0.57		
Empty flume	0.73	0.64	0.52	0.22	

(b)	Cylinder	*Vallisneria*	*Elodea*	*Ceratophyllum*	Empty flume
Cylinder					
Vallisneria	0.91				
Elodea	0.75	0.66			
Ceratophyllum	0.25	0.30	0.14		
Empty flume	0.90	0.81	0.84	0.20	

(c)	Cylinder	*Vallisneria*	*Elodea*	*Ceratophyllum*	Empty flume
Cylinder					
Vallisneria	0.23				
Elodea	0.58	0.52			
Ceratophyllum	0.47	0.64	0.87		
Empty flume	**0.005**	0.11	**0.025**	**0.038**	

(d)	Cylinder	*Vallisneria*	*Elodea*	*Ceratophyllum*	Empty flume
Cylinder					
Vallisneria	0.46				
Elodea	0.15	0.49			
Ceratophyllum	0.055	0.23	0.61		
Empty flume	0.052	0.23	0.60	0.99	

Table 3.9: ANCOVA results for velocity in the (a) streamwise component (u) and (b) vertical component (w) for the test subjects. (Velocity = different test velocities (covariate); Plant = empty test section, circular cylinder, *Vallisneria, Elodea*, and *Ceratophyllum*; and Before/After = upstream and downstream).

(a)

Univariate Results for Each DV (streamwise velocity (u))
Sigma-restricted parameterization
Effective hypothesis decomposition

Effect	Degr. of Freedom	vel (x) SS	vel (x) MS	vel (x) F	vel (x) p
Intercept	1	72.107	72.107	84.873	0.000000
velocity	1	3819.222	3819.222	4495.343	0.000000
plant	4	2.998	0.750	0.882	0.474875
before/after	1	4.424	4.424	5.207	0.023220
plant*before/after	4	3.877	0.969	1.141	0.337392
Error	289	245.533	0.850		
Total	299	4079.899			

(b)

Univariate Results for Each DV (vertical velocity (w))
Sigma-restricted parameterization
Effective hypothesis decomposition

Effect	vel (z) SS	vel (z) MS	vel (z) F	vel (z) p
Intercept	0.07739	0.077394	1.51060	0.220048
velocity	0.30981	0.309814	6.04708	0.014515
plant	1.00565	0.251412	4.90716	0.000766
before/after	1.28823	1.288225	25.14408	0.000001
plant*before/after	1.03662	0.259155	5.05828	0.000593
Error	14.80655	0.051234		
Total	18.85226			

Table 3.10: Post hoc comparisons for velocity (Table 8a,b) in the (a) streamwise component (u), and (b) vertical component (w) for the different test subjects. (Cell No.:1 = upstream of the cylinder; 2 = downstream of the cylinder; 3 = upstream of *Elodea*; 4 = downstream of *Elodea*; 5 = upstream of *Ceratophyllum*; 6 = downstream of *Ceratophyllum*; 7 = upstream of *Vallisneria*; 8 = downstream of *Vallisneria*; 9 = upstream in the empty test section; and 10 = downstream in the empty test section).

(a)

LSD test; variable vel (x) (streamwise velocity (u))
Probabilities for Post Hoc Tests
Error: Between MS = .84960, df = 289.00

Cell No	plant	before/after	{1} 6.1293	{2} 6.0660	{3} 6.5593	{4} 5.9762	{5} 6.3313	{6} 6.1044	{7} 6.4380	{8} 5.8553	{9} 6.4047	{10} 6.4584
1	1	1		0.81789	0.20241	0.57785	0.54886	0.92789	0.35985	0.31957	0.41399	0.23205
2	1	2	0.81789		0.07366	0.64442	0.33509	0.84330	0.17689	0.27921	0.21881	0.04434
3	2	1	0.20241	0.07366		0.03469	0.49868	0.09895	0.71873	0.01092	0.64619	0.71379
4	2	2	0.57785	0.64442	0.03469		0.19731	0.50987	0.09396	0.53435	0.12007	0.01364
5	5	1	0.54886	0.33509	0.49868	0.19731		0.40969	0.75153	0.08432	0.82767	0.64403
6	5	2	0.92789	0.84330	0.09895	0.50987	0.40969		0.22582	0.20088	0.27553	0.06952
7	8	1	0.35985	0.17689	0.71873	0.09396	0.75153	0.22582		0.03483	0.92117	0.94074
8	8	2	0.31957	0.27921	0.01092	0.53435	0.08432	0.20088	0.03483		0.04654	0.00210
9	9	1	0.41399	0.21881	0.64619	0.12007	0.82767	0.27553	0.92117	0.04654		0.84498
10	9	2	0.23205	0.04434	0.71379	0.01364	0.64403	0.06952	0.94074	0.00210	0.84498	

(b)

LSD test; variable vel (z) (vertical velocity (w))
Probabilities for Post Hoc Tests
Error: Between MS = .05123, df = 289.00

Cell No	plant	before/after	{1} -.0053	{2} -.3220	{3} 19333	{4} -.1218	{5} -.0587	{6} -.1176	{7} -.0273	{8} -.0871	{9} -.1140	{10} -.1202
1	1	1		0.00000	0.01686	0.08550	0.51925	0.09740	0.79029	0.22657	0.18963	0.08974
2	1	2	0.00000		0.00000	0.00003	0.00011	0.00002	0.00001	0.00000	0.00225	0.00003
3	2	1	0.01686	0.00000		0.00000	0.00250	0.00000	0.00801	0.00004	0.00024	0.00000
4	2	2	0.08550	0.00003	0.00000		0.35046	0.92955	0.16273	0.46813	0.90832	0.97401
5	5	1	0.51925	0.00011	0.00250	0.35046		0.38358	0.70486	0.67370	0.50372	0.36245
6	5	2	0.09740	0.00002	0.00000	0.92955	0.38358		0.18229	0.52397	0.95801	0.95547
7	8	1	0.79029	0.00001	0.00801	0.16273	0.70488	0.18229		0.37645	0.29524	0.16974
8	8	2	0.22657	0.00000	0.00004	0.46813	0.67370	0.52397	0.37645		0.69059	0.48831
9	9	1	0.18963	0.00225	0.00024	0.90832	0.50372	0.95801	0.29524	0.69059		0.92660
10	9	2	0.08974	0.00003	0.00000	0.97401	0.36245	0.95547	0.16974	0.48831	0.92660	

Table 3.11: ANCOVA results (a) and post hoc comparison (b) for examining the angle of deflection and the different test subjects. (Velocity = covariate; and Plant = circular cylinder, *Vallisneria, Elodea*, and *Ceratophyllum*). Significant differences indicated in bold.

(a)	Univariate Results for Each DV (angle) Sigma-restricted parameterization Effective hypothesis decomposition				
Effect	Degr. of Freedom	angle SS	angle MS	angle F	angle p
Intercept	1	3906.17	3906.167	36.64167	0.000008
velocity	1	1761.57	1761.575	16.52439	0.000660
plant	3	11849.58	3949.859	37.05153	0.000000
Error	19	2025.49	106.604		
Total	23	15636.64			

(b)	**Cylinder**	***Vallisneria***	***Elodea***	***Ceratophyllum***
Cylinder				
Vallisneria	**< 0.001**			
Elodea	**0.008**	**< 0.001**		
Ceratophyllum	**< 0.001**	**0.023**	**< 0.001**	

Table 3.12: ANCOVA results (a) and post hoc comparisions (b) for the frequency of oscillations between the different test subjects. (Velocity = covariate; and Plant = circular cylinder, *Vallisneria, Elodea*, and *Ceratophyllum*). Significant differences indicated in bold.

(a)	Univariate Results for Each DV (oscillations) Sigma-restricted parameterization Effective hypothesis decomposition			
Effect	Degr. of Freedom	oscillations per second SS	oscillations per second MS	oscillations per second F
Intercept	1	0.030908	0.030908	1.27783
velocity	1	0.721379	0.721379	29.82397
plant	3	0.532280	0.177427	7.33535
Error	19	0.459570	0.024188	
Total	23	1.713229		

(b)	**Cylinder**	***Vallisneria***	***Elodea***	***Ceratophyllum***
Cylinder				
Vallisneria	**< 0.001**			
Elodea	**0.001**	0.73		
Ceratophyllum	**0.002**	0.61	0.87	

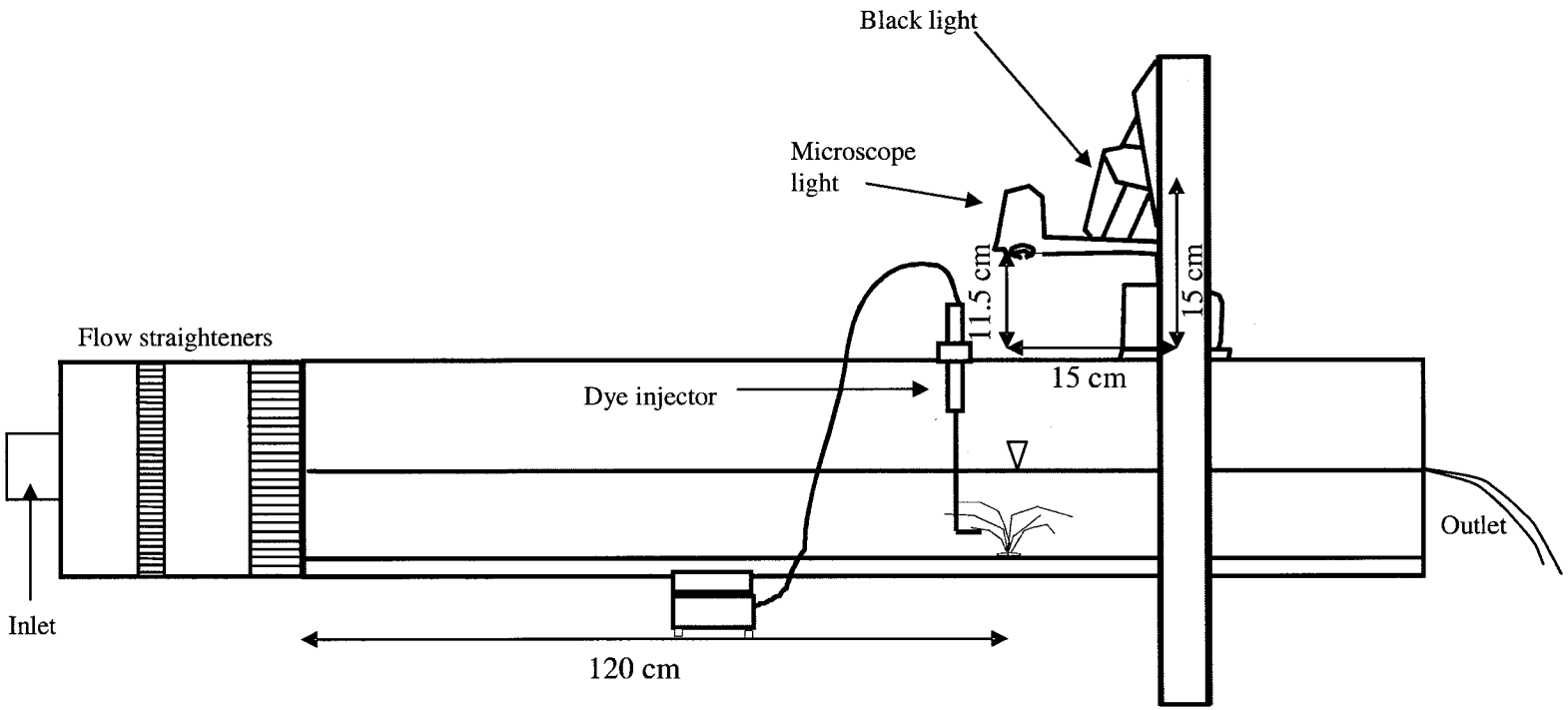

Figure 3.1: Lighting and dye injector set up for the photos (flume dimensions: 19.2 cm (width) x 24.7 cm (height) x 170 cm (length) with water depth ranging from 9.7-13.3 cm from the lowest (1.27 cms^{-1}) to the highest (11.0 cms^{-1}) test velocities)

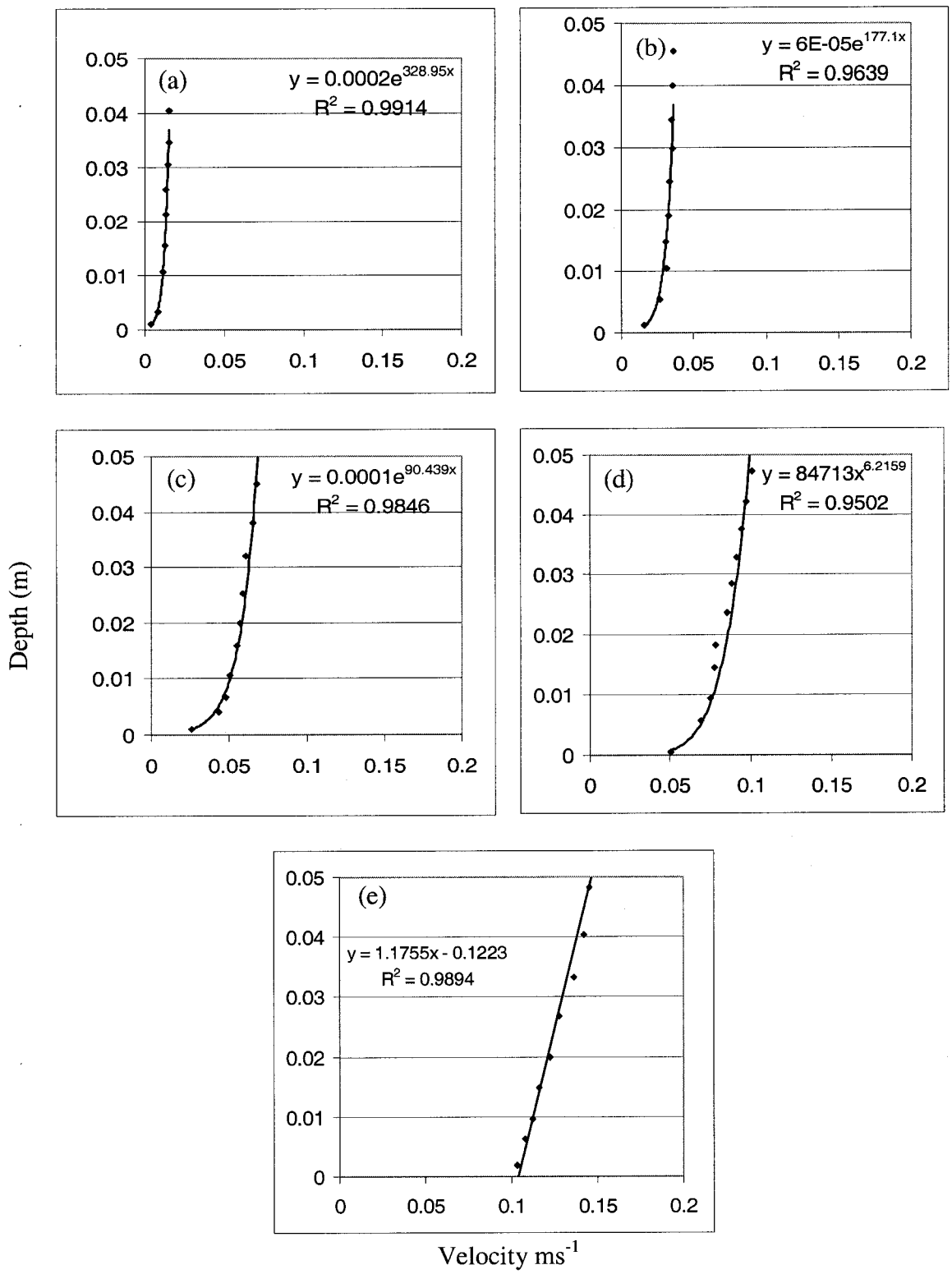

Figure 3.2: Velocity profiles in the empty test section at: (a) 0.013 ms^{-1}, (b) 0.020 ms^{-1}, (c) 0.050 ms^{-1}, (d) 0.084 ms^{-1}, and (e) 0.11 ms^{-1}. Each point represents the mean of 120 s of data samples taken at 25 Hz using an acoustic doppler velicometer (ADV).

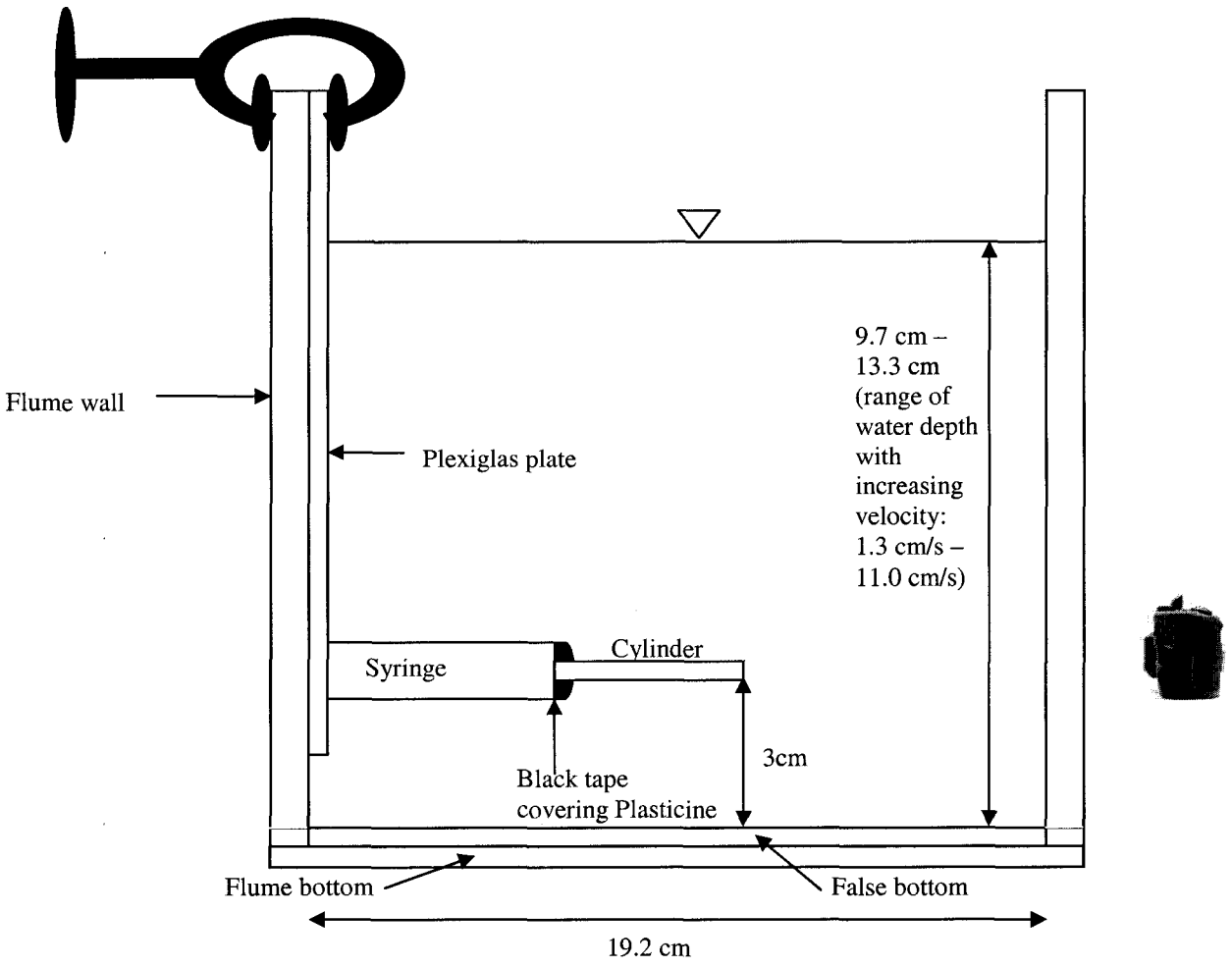

Figure 3.3: Diagram of the positioning device attached to the side of the flume with the cylinder in place for the top perspective.

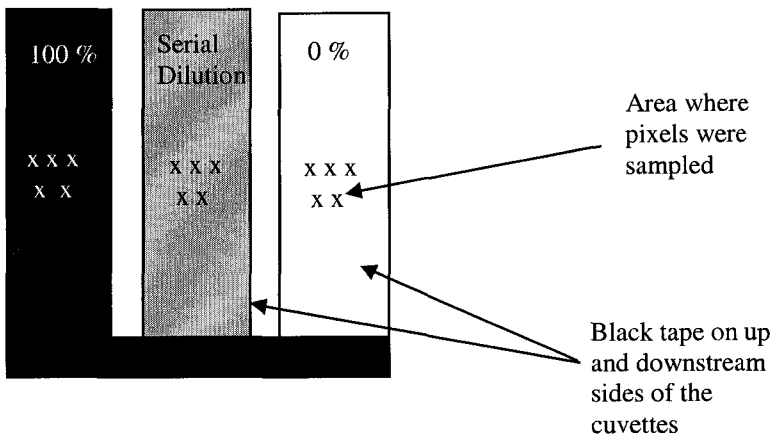

Figure 3.4: Cuvette set up for creating the concentration curve.

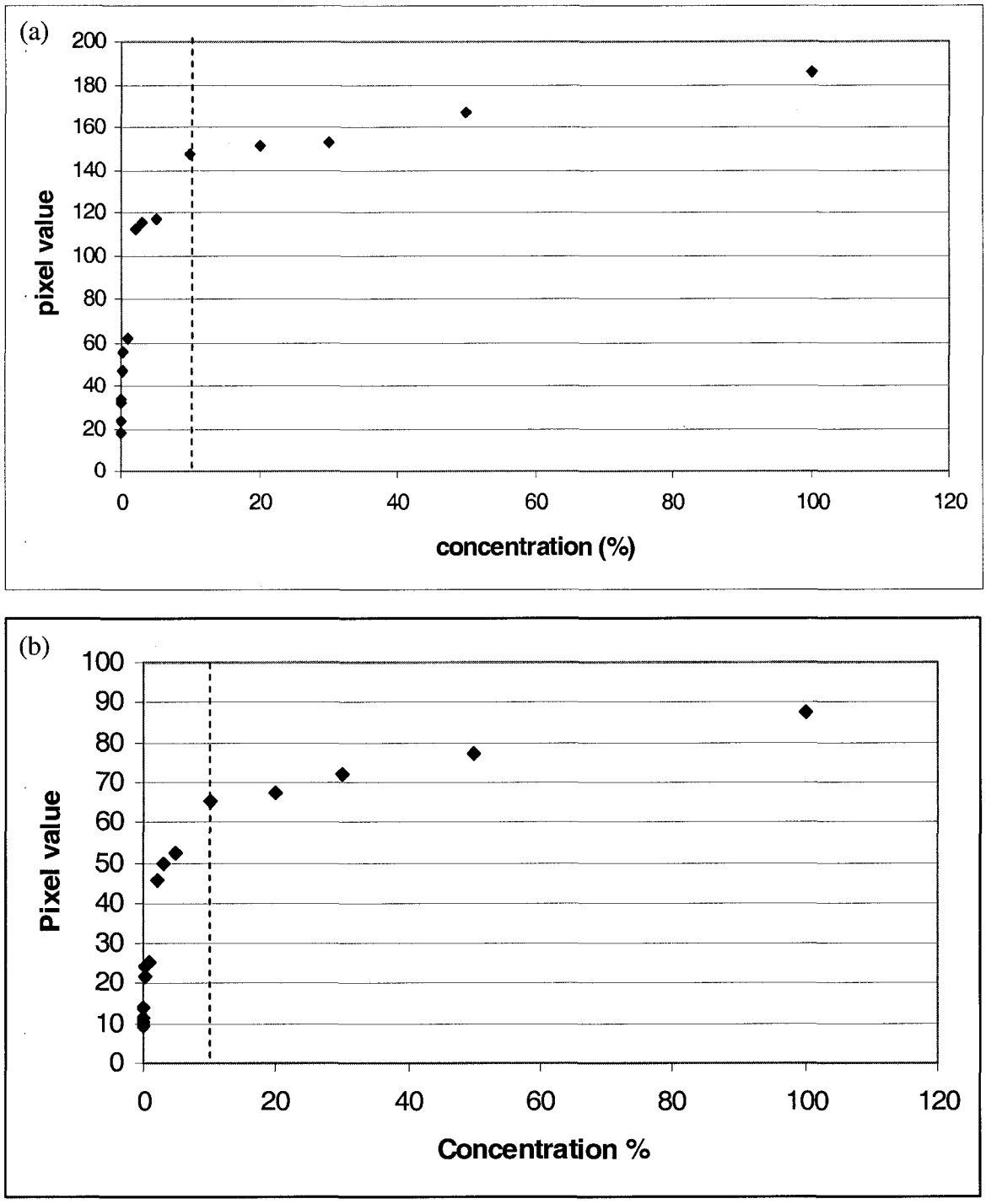

Figure 3.5: Original concentration curve (pixel value (i.e., intensity) vs. dye concentration) for the (a) side and (b) top perspectives. The dotted line is at the 10% concentration point, where the graph was divided into a linear and non-linear components.

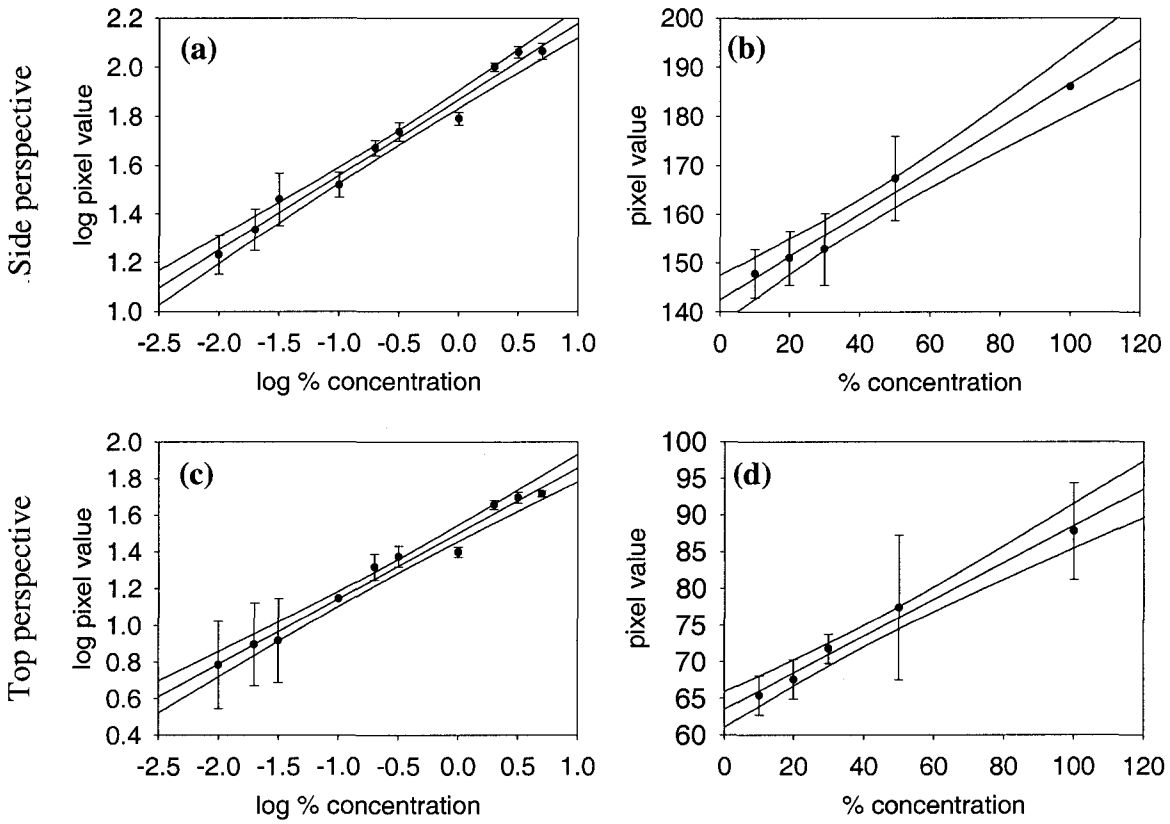

Figure 3.6: Pixel intensity vs. dye concentration curves. (a) log (pixel value) versus log (dye concentration) in the side perspective for 0.01-5% dye, (log pixel value = (0.30 ± 0.02) log %concentration + (1.86 ± 0.02); $r^2 = 0.98$; $p = 0.001$). (b) pixel value versus dye concentration in the side perspective for 10-100% dye (pixel value = (0.44 ± 0.03) %concentration + (143 ± 2); $r^2 = 0.98$; $p < 0.001$). (c) log (pixel value) versus log (dye concentration) in the top perspective for 0.01-5% dye, (log pixel value = (0.36 ± 0.02) log %concentration + (1.50 ± 0.02); $r^2 = 0.98$; $p < 0.001$). (d) pixel value versus dye concentration in the top perspective for 10-100% dye (pixel value = (0.25 ± 0.02) %concentration + (63.5 ± 0.9); $r^2 = 0.99$; $p < 0.001$).

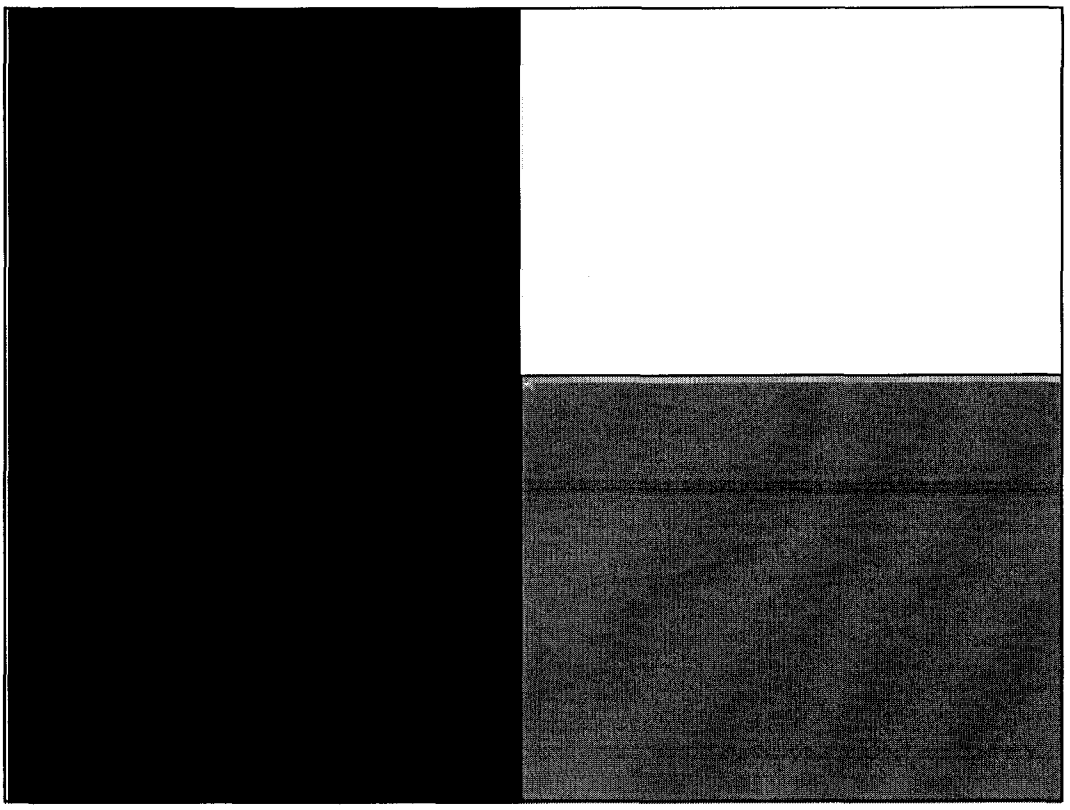

Figure 3.7: Mock photo used to test image analysis method in MATLAB.

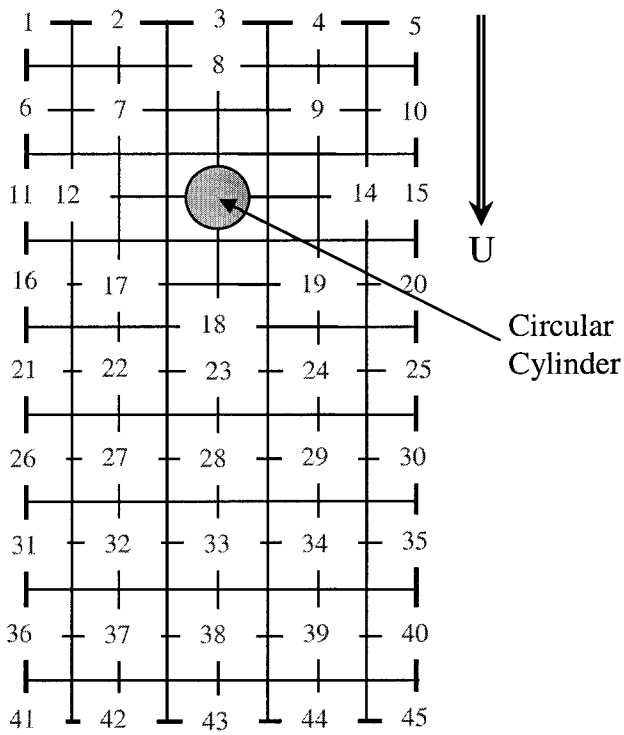

Figure 3.8: Grid used to take ADV measurements in the test section (120 cm downstream of the flow straighteners). The grid was drawn on the top of the flume wall in the downstream direction, and on a sliding piece of plexiglass in the cross stream direction. The centre of the probe was aligned with the centre of both lines.

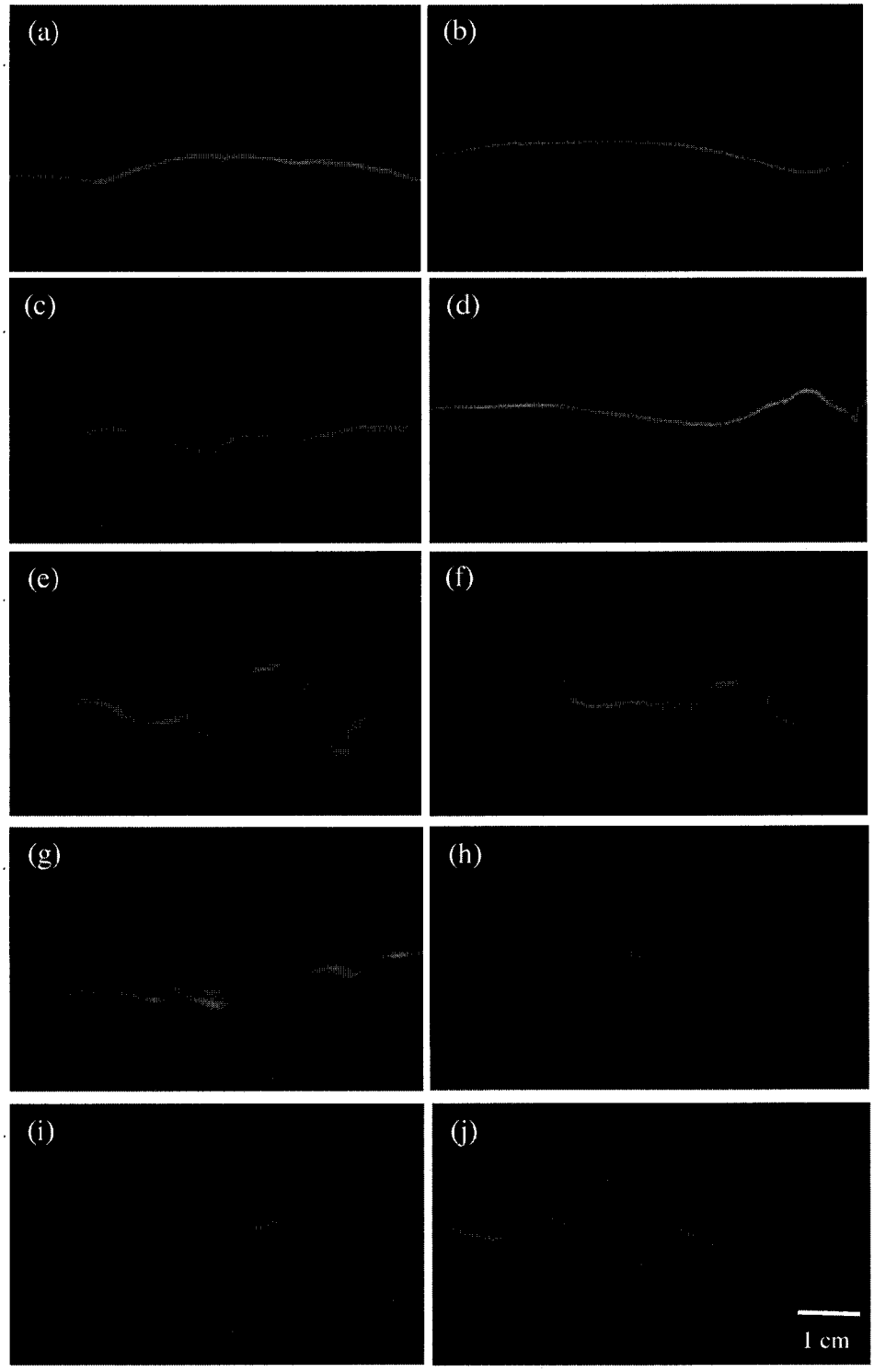

Figure 3.9: Flow visualization in the empty test section using fluoroscein dye in the side (left) and the top (right) perspectives. Velocities increase from top to bottom panels [(a) and (b) are 1.3 cms^{-1}, (c) and (d) are 2.0 cms^{-1}, (e) and (f) are 5.0 cms^{-1}, (g) and (h) are 8.4 cms^{-1}, and (i) and (j) are 11.0 cms^{-1}]. Flow is from left to right. Top and side photos were taken sequentually.

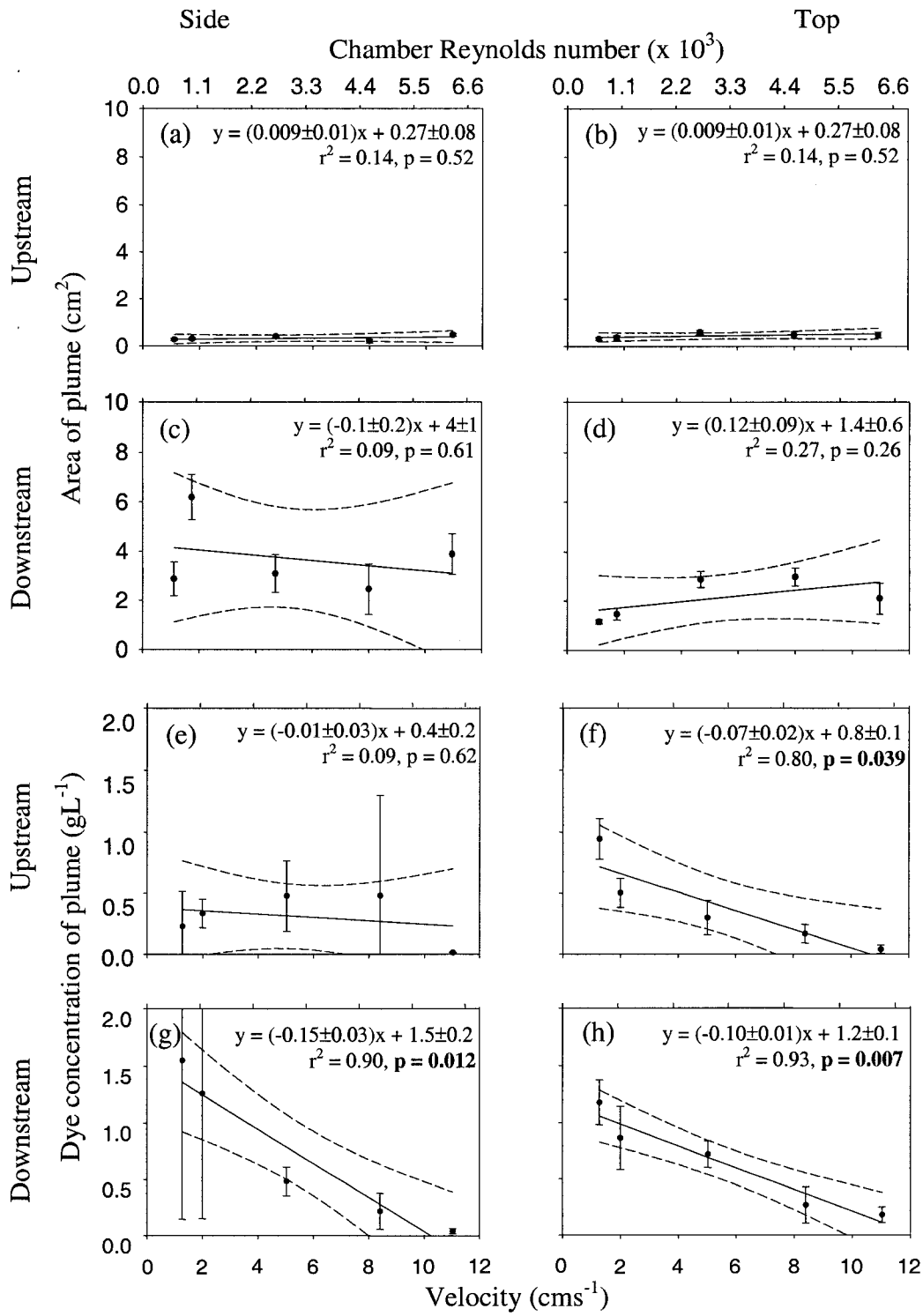

Figure 3.10: Regression of area of dye coverage (a-d) and concentration of dye (e-h) versus velocity or Reynolds number (based on the hydraulic diameter) in the different domains for the empty test section: (a) and (e) upstream in the side perspective, (b) and (f) upstream in the top perspective, (c) and (g) downstream in the side perspective, and (d) and (h) downstream in the top perspective. Solid line is the regression and dotted lines are the 95% confidence limits of the mean.

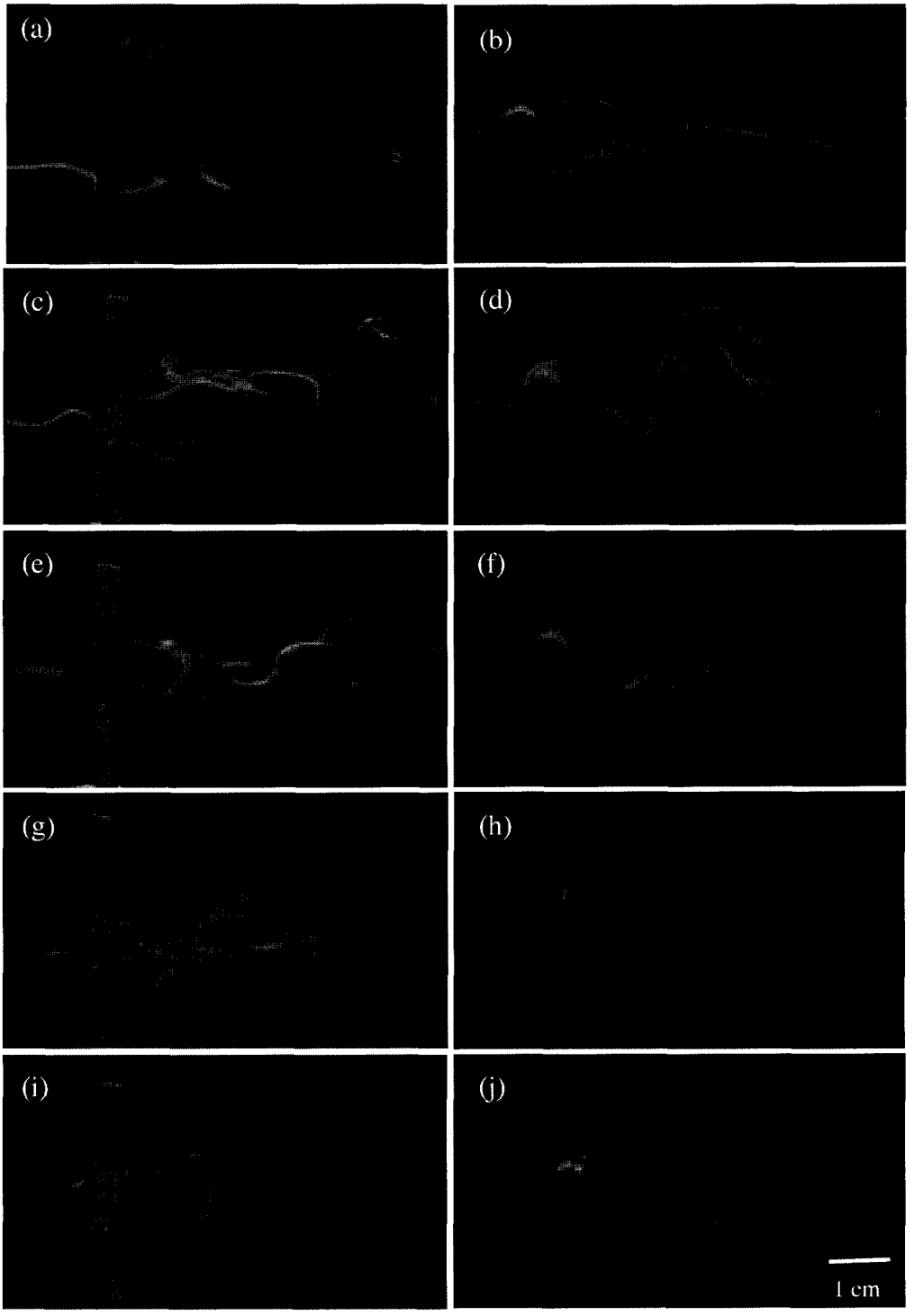

Figure 3.11: Flow visualization around a 0.7 cm diameter circular cylinder using fluoroscein dye in the side (left) and the top (right) perspectives. Velocities increase from top to bottom panels [(a) and (b) are 1.3 cms^{-1}, (c) and (d) are 2.0 cms^{-1}, (e) and (f) are 5.0 cms^{-1}, (g) and (h) are 8.4 cms^{-1}, and (i) and (j) are 11.0 cms^{-1}]. Flow is from left to right. Top and side photos were taken sequentually.

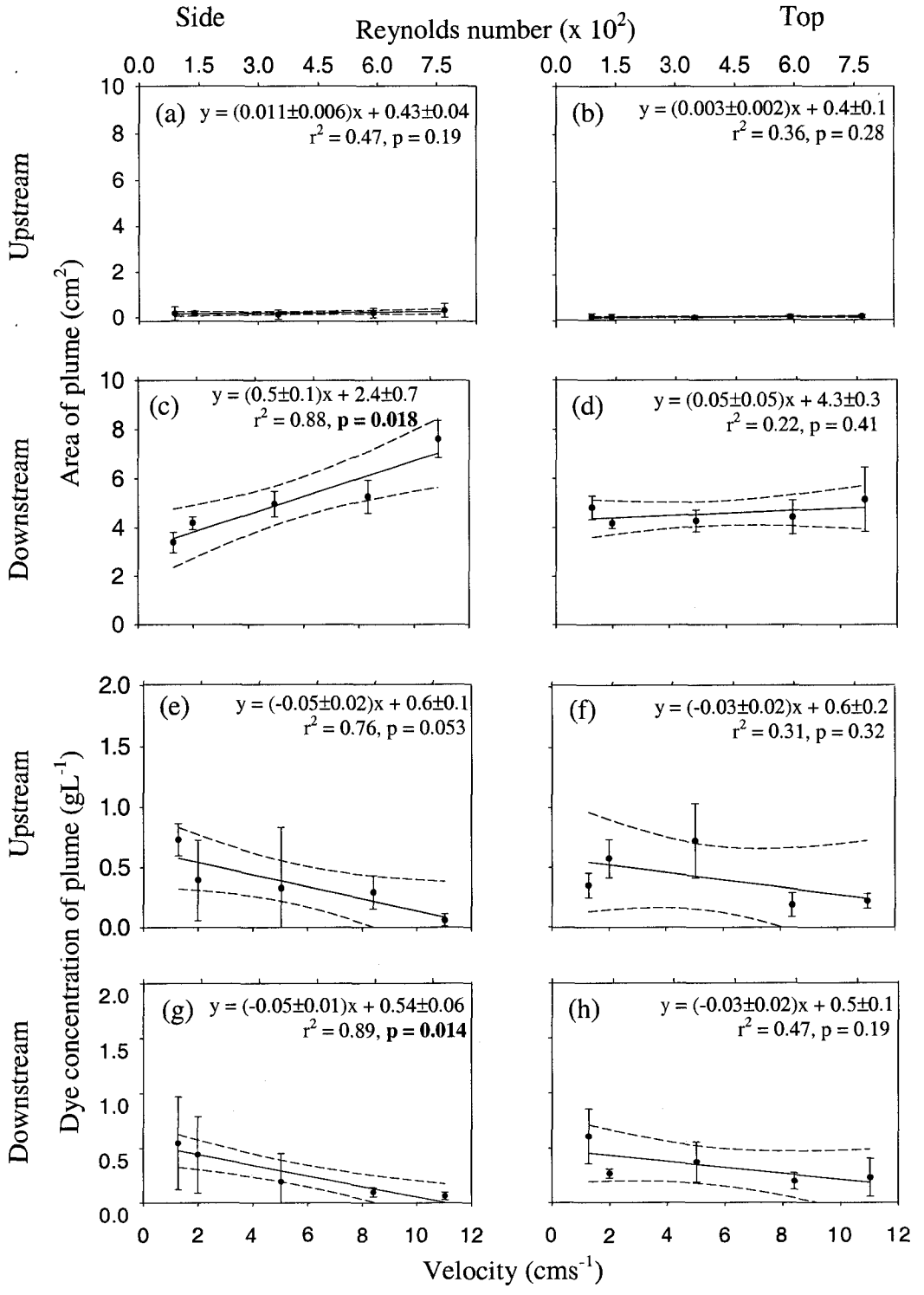

Figure 3.12: Regression of area of dye coverage (a-d) and concentration of dye (e-h) versus velocity or Reynolds number (based on the diameter) in the different domains for the circular cylinder: (a) and (e) upstream in the side perspective, (b) and (f) upstream in the top perspective, (c) and (g) downstream in the side perspective, and (d) and (h) downstream in the top perspective. Solid line is the regression and dotted lines are the 95% confidence limits of the mean.

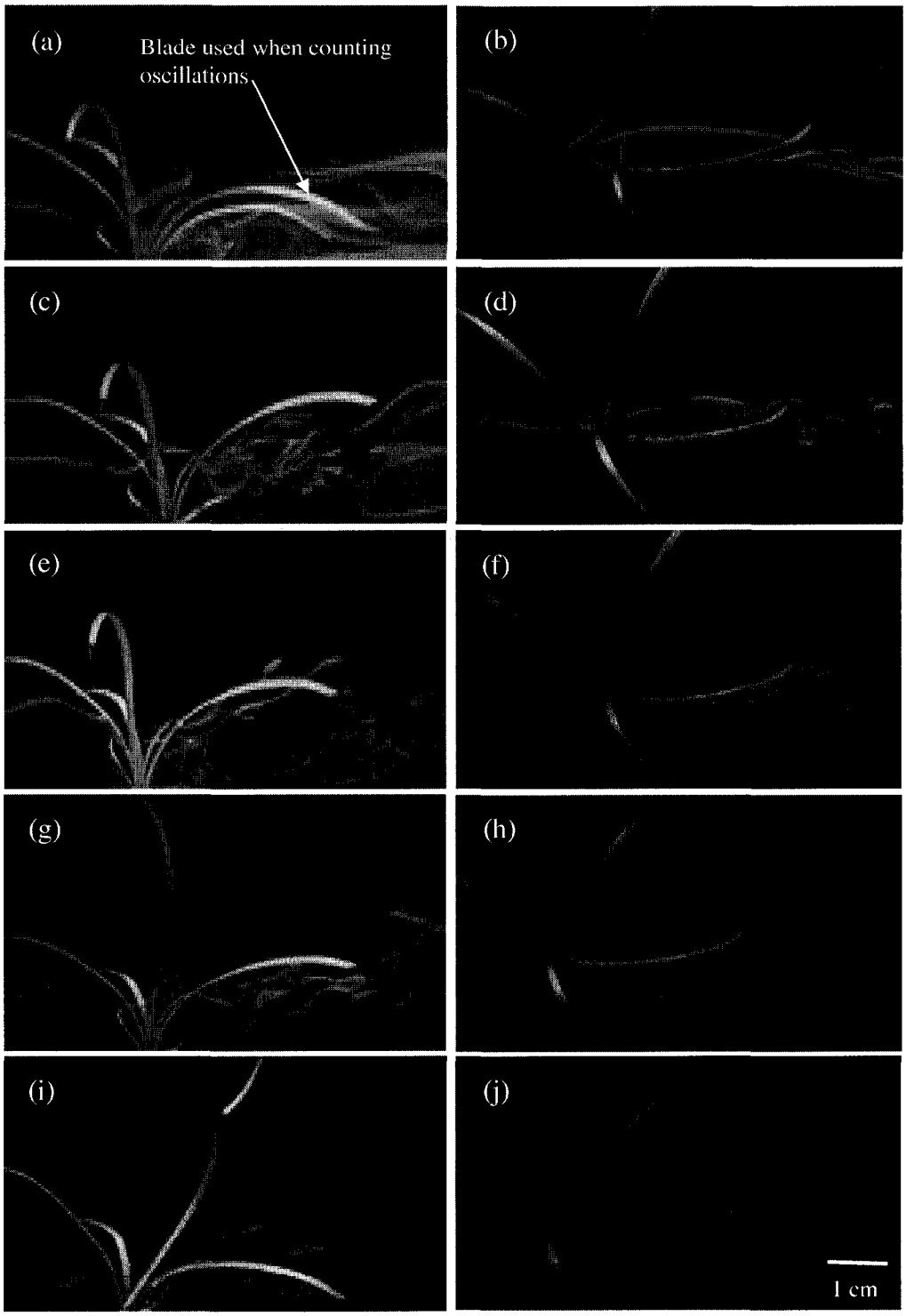

Figure 3.13: Flow visualization around *Vallisneria americana* using fluoroscein dye in the side (left) and the top (right) perspectives. Velocities increase from top to bottom panels [(a) and (b) are 1.3 cms^{-1}, (c) and (d) are 2.0 cms^{-1}, (e) and (f) are 5.0 cms^{-1}, (g) and (h) are 8.4 cms^{-1}, and (i) and (j) are 11.0 cms^{-1}]. Flow is from left to right. Top and side photos were taken sequentually.

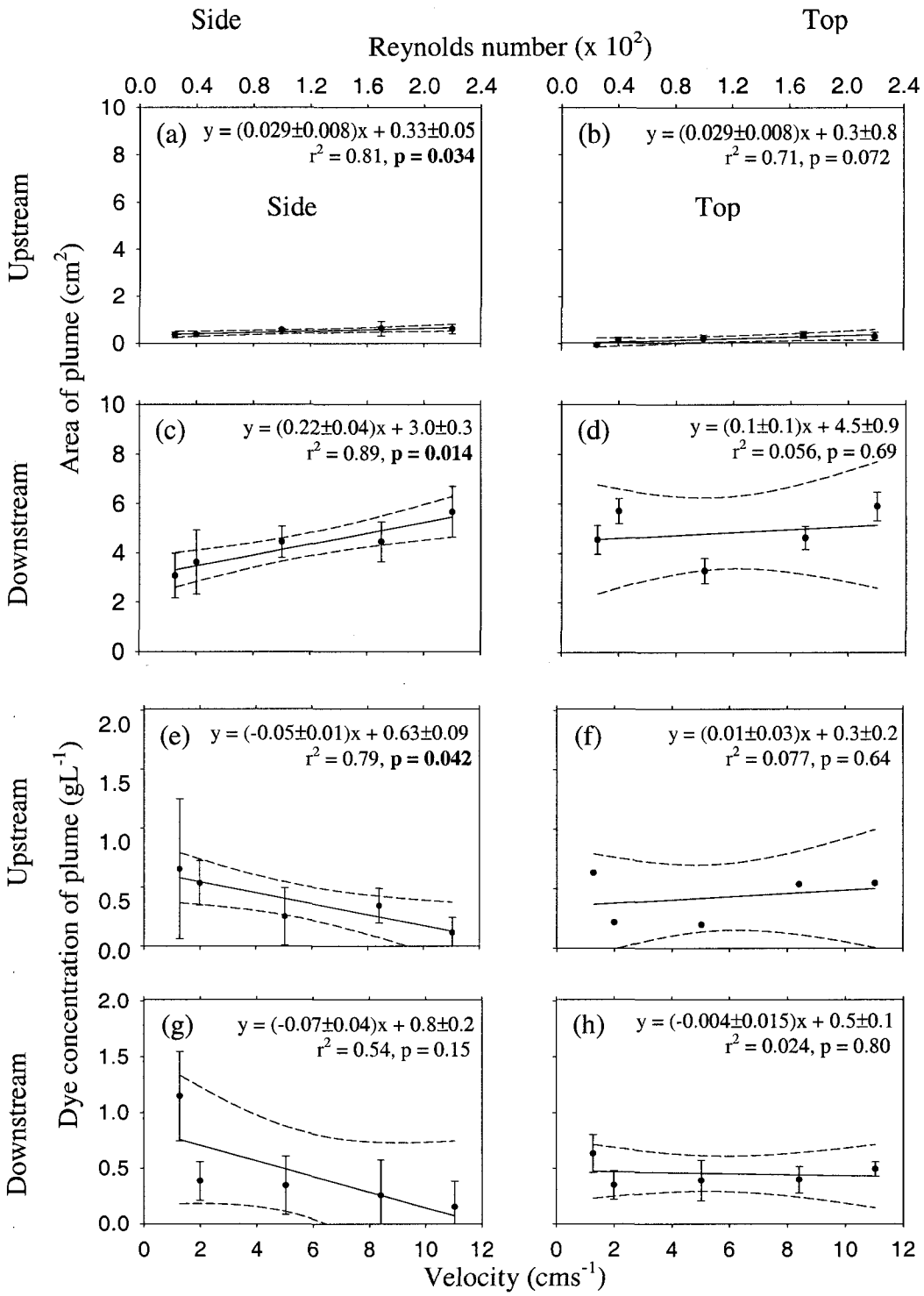

Figure 3.14: Regression of area of dye coverage (a-d) and concentration of dye (e-h) versus velocity or stem Reynolds number (based on the plant diameter) in the different domains for *Vallisneria americana*: (a) and (e) upstream in the side perspective, (b) and (f) upstream in the top perspective, (c) and (g) downstream in the side perspective, and (d) and (h) downstream in the top perspective. Solid line is the regression and dotted lines are the 95% confidence limits of the mean.

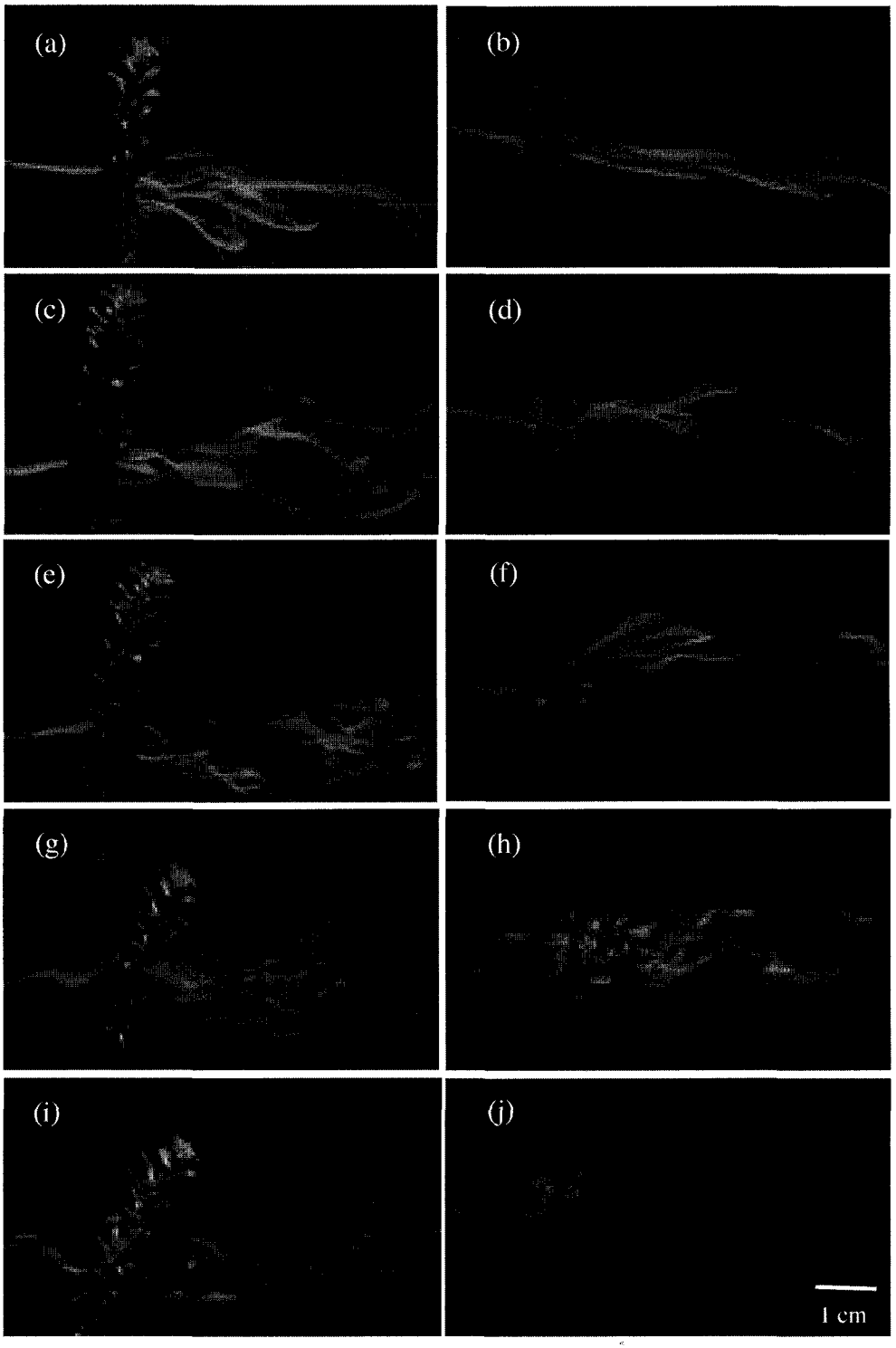

Figure 3.15: Flow visualization around *Elodea canadensis* using fluoroscein dye in the side (left) and the top (right) perspectives. Velocities increase from top to bottom panels [(a) and (b) are 1.3 cms^{-1}, (c) and (d) are 2.0 cms^{-1}, (e) and (f) are 5.0 cms^{-1}, (g) and (h) are 8.4 cms^{-1}, and (i) and (j) are 11.0 cms^{-1}]. Flow is from left to right. Top and side photos were taken sequentually.

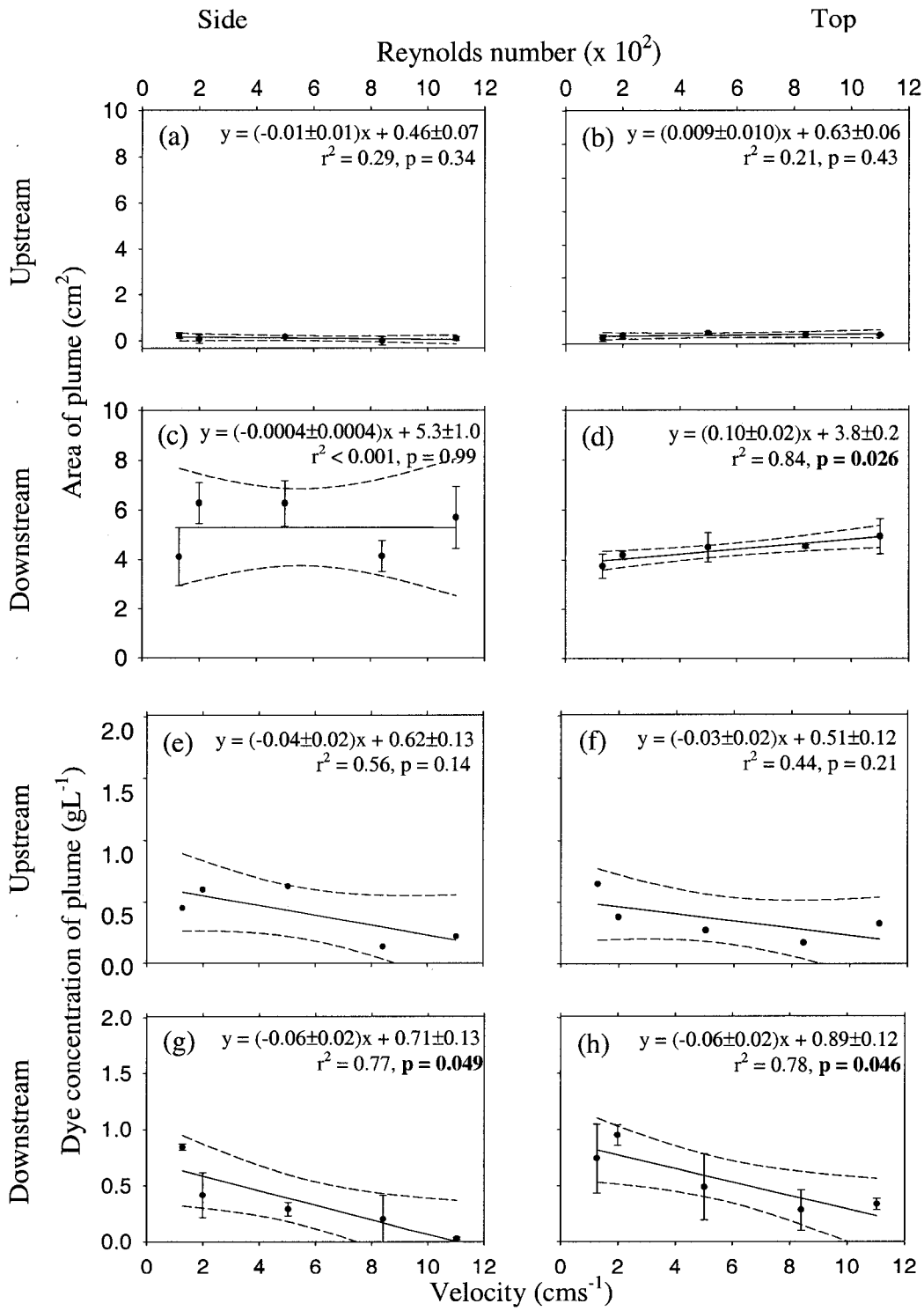

Figure 3.16: Regression of area of dye coverage (a-d) and concentration of dye (e-h) versus velocity or stem Reynolds number (based on the plant diameter) in the different domains for *Elodea canadensis*: (a) and (e) upstream in the side perspective, (b) and (f) upstream in the top perspective, (c) and (g) downstream in the side perspective, and (d) and (h) downstream in the top perspective. Solid line is the regression and dotted lines are the 95% confidence limits of the mean.

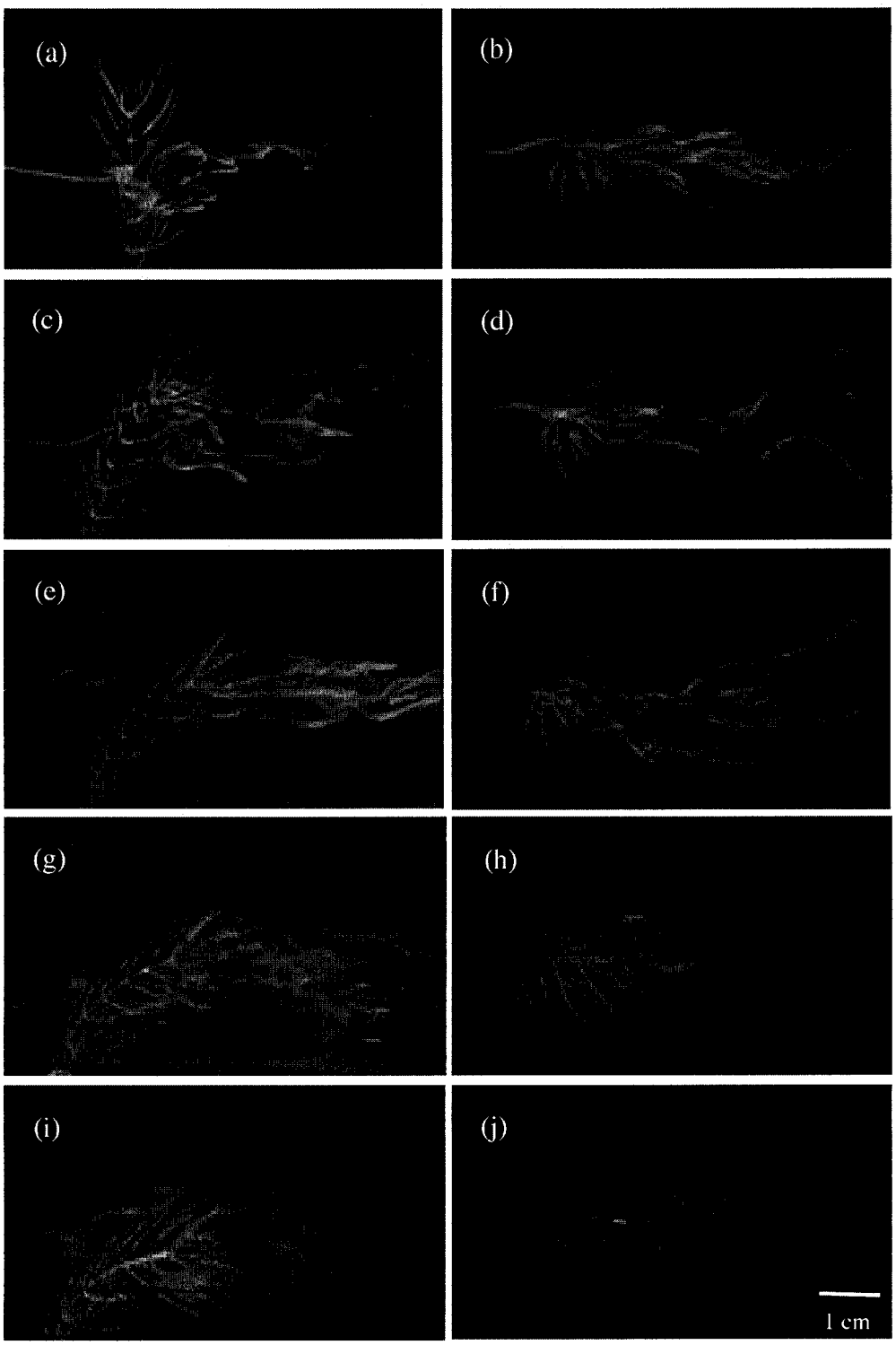

Figure 3.17: Flow visualization around *Ceratophyllum demersum* using fluoroscein dye in the side (left) and the top (right) perspectives. Velocities increase from top to bottom panels [(a) and (b) are 1.3 cms^{-1}, (c) and (d) are 2.0 cms^{-1}, (e) and (f) are 5.0 cms^{-1}, (g) and (h) are 8.4 cms^{-1}, and (i) and (j) are 11.0 cms^{-1}]. Flow is from left to right. Top and side photos were taken sequentually.

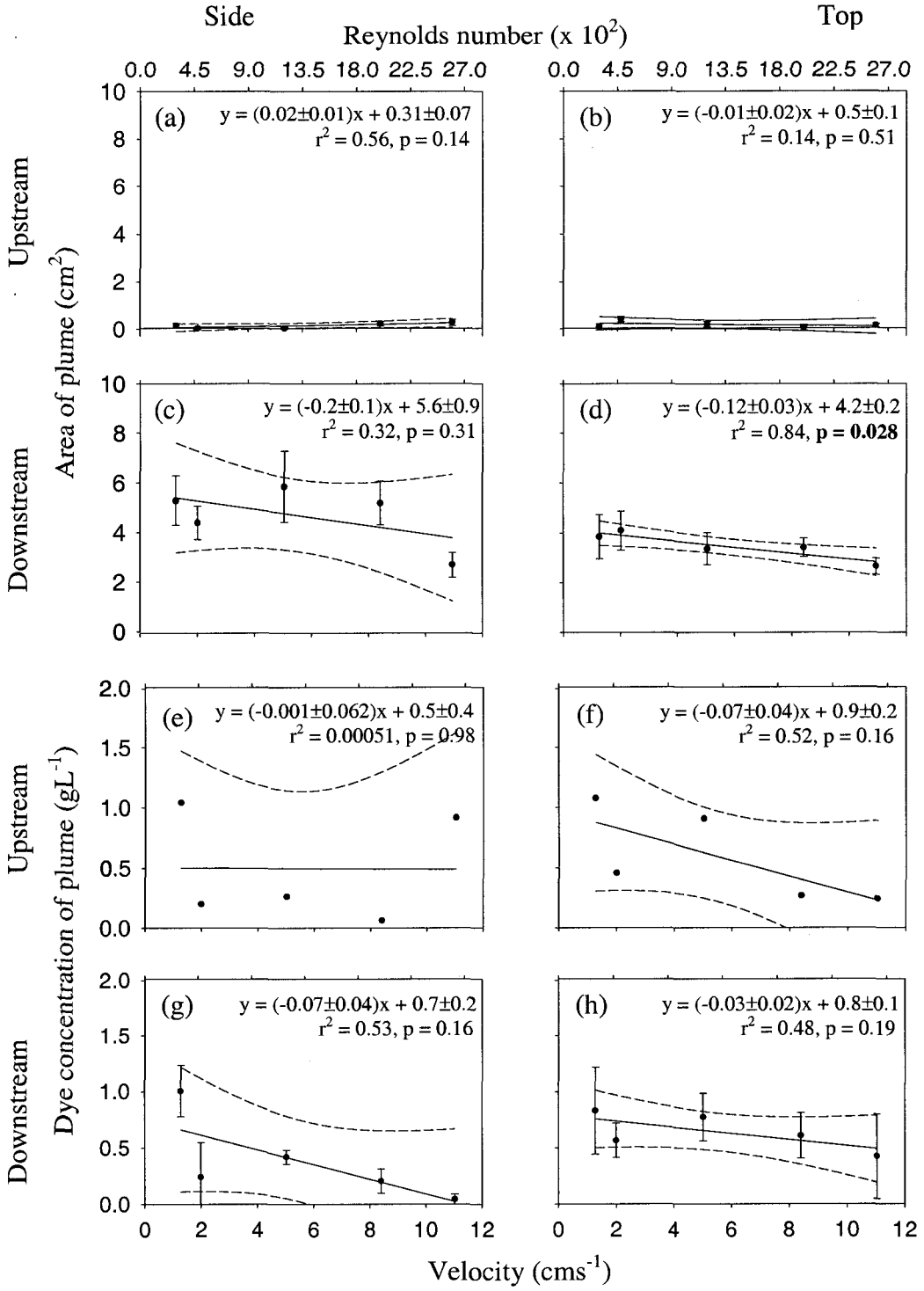

Figure 3.18: Regression of area of dye coverage (a-d) and concentration of dye (e-h) versus velocity or stem Reynolds number (based on the diameter) in the different domains for *Ceratophyllum demersum*: (a) and (e) upstream in the side perspective, (b) and (f) upstream in the top perspective, (c) and (g) downstream in the side perspective, and (d) and (h) downstream in the top perspective. Solid line is the regression and dotted lines are the 95% confidence limits of the mean.

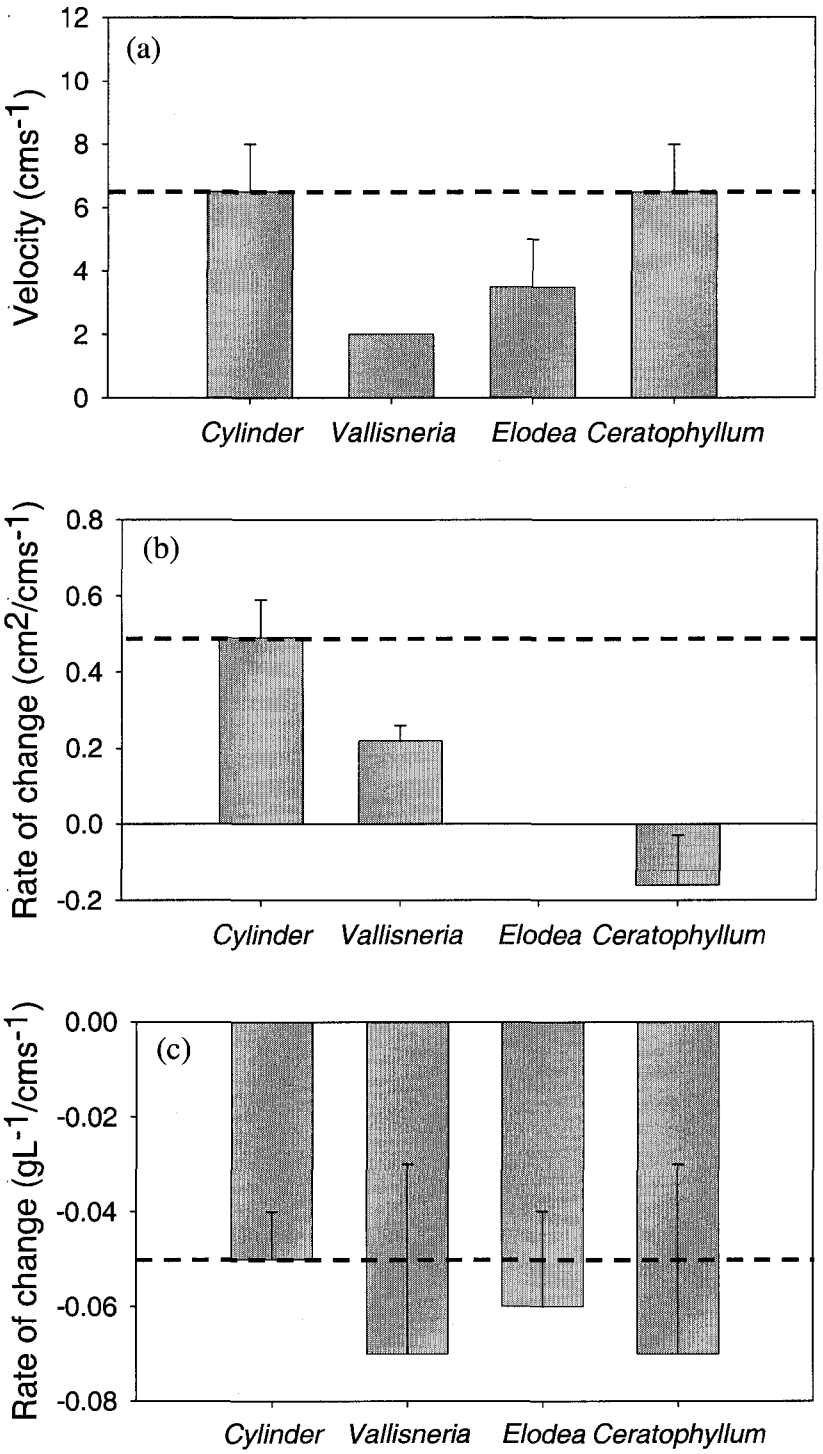

Figure 3.19: Comparison of the fluid dynamic conditions around plants and a physical model (a) The velocity at which the transition from laminar to turbulent occurs for the different plants; (b) Rate of change in the area of dye coverage with increasing velocity for the different test subjects; and (c) The rate of change in the concentration of dye with increasing velocity for the different test subjects. The dotted line represents the average result for the physical model (circular cylinder).

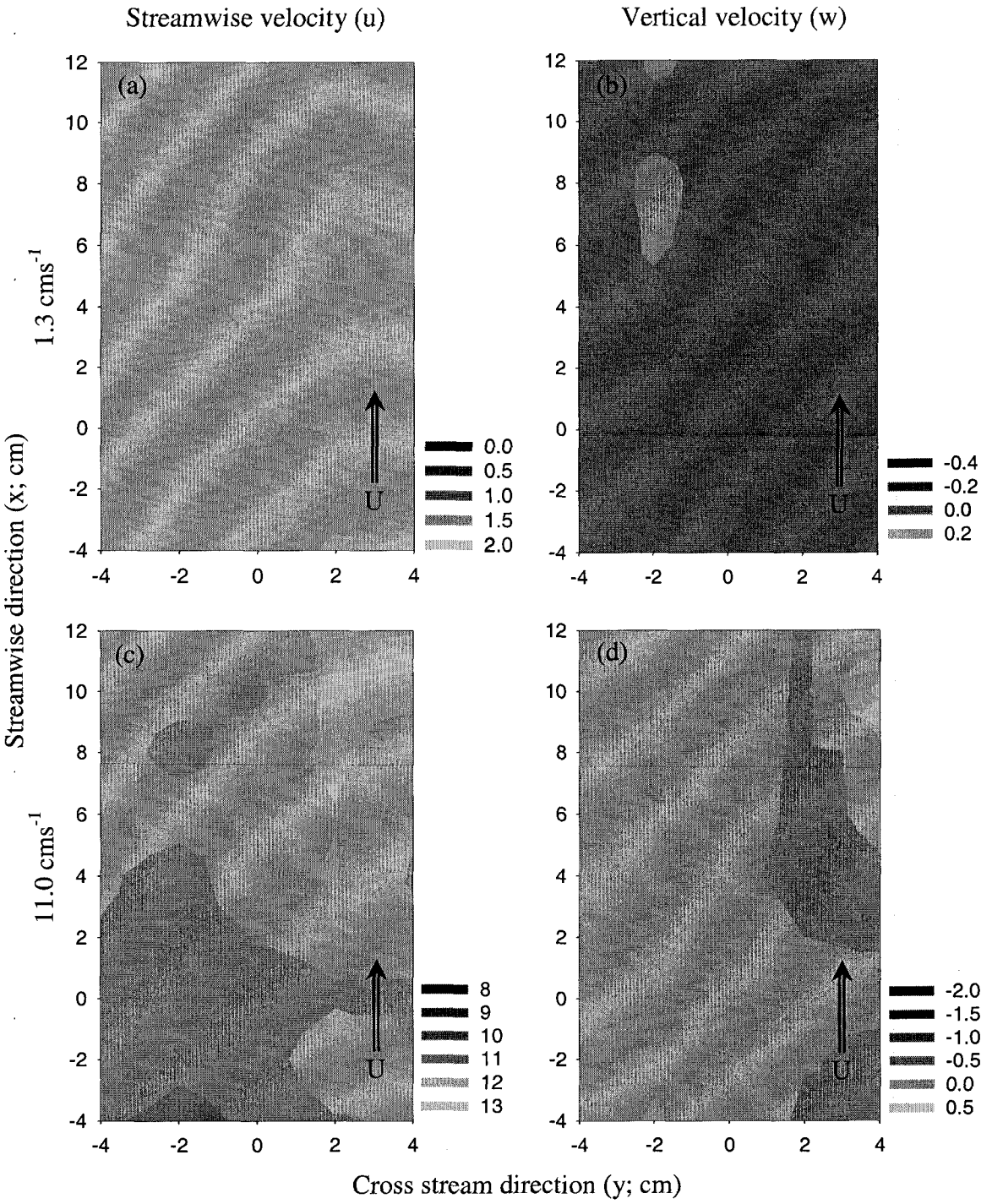

Figure 3.20: Contours of the velocity field measured 3 cm from the flume bottom in a 2 cm x 2 cm grid in an empty flume. Each point of the contours was the mean of 120 s of data samples at 25 Hz. (a) streamwise velocity (u) at 1.3 cms^{-1}, (b) vertical velocity (w) at 1.3 cms^{-1}, (c) streamwise velocity (u) at 11.0 cms^{-1}, and (d) vertical velocity (w) at 11.0 cms^{-1}. Scale bars in cms^{-1}.

Streamwise velocity (u) Vertical velocity (w)

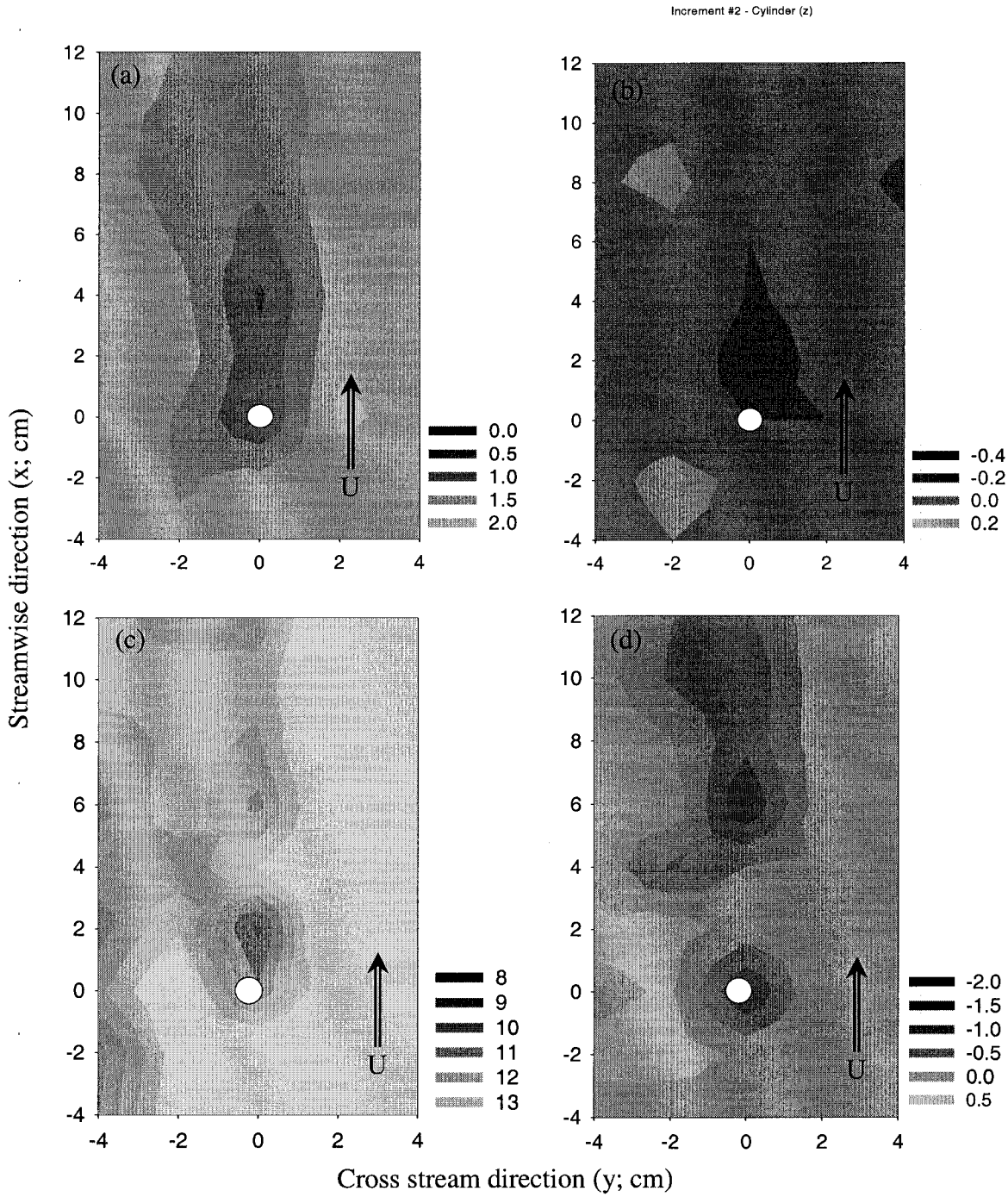

Figure 3.21: Contours of the velocity field measured 3 cm from the flume bottom in a 2 cm x 2 cm grid (3 cm in the vicinity of the cylinder) around a circular cylinder. Each point of the contours was the mean of 120 s of data samples at 25 Hz. (a) streamwise velocity (u) at 1.3 cms^{-1}, (b) vertical velocity (w) at 1.3 cms^{-1}, (c) streamwise velocity (u) at 11.0 cms^{-1}, and (d) vertical velocity (w) at 11.0 cms^{-1}. Scale bars in cms^{-1}.

Streamwise velocity (u) Vertical velocity (w)

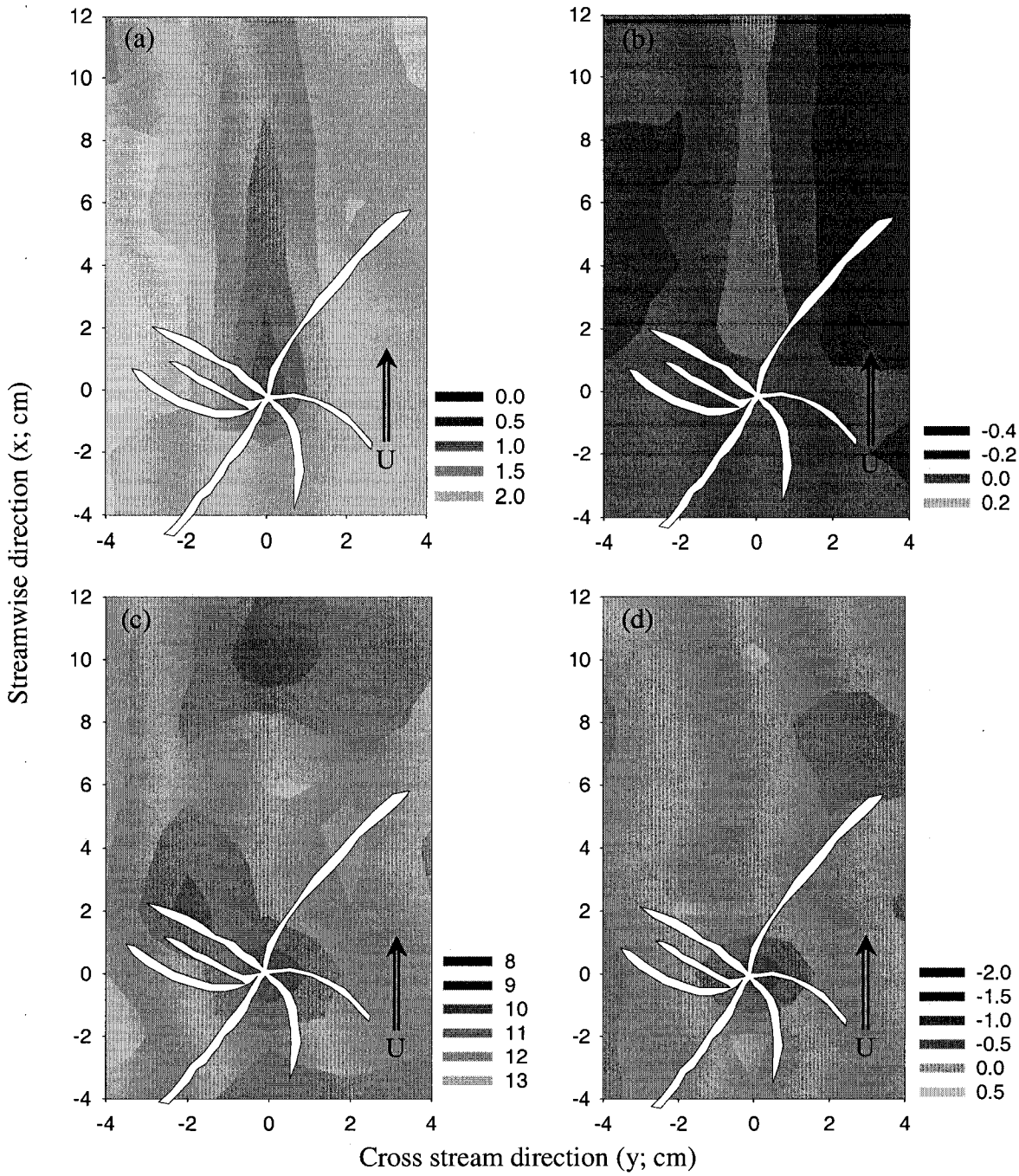

Figure 3.22: Contours of the velocity field measured 3 cm from the flume bottom in a 2 cm x 2 cm grid (3 cm in the vicinity of the plant) around *Vallisneria americana*. Each point of the contours was the mean of 120 s of data samples at 25 Hz. (a) streamwise velocity (u) at 1.3 cms^{-1}, (b) vertical velocity (w) at 1.3 cms^{-1}, (c) streamwise velocity (u) at 11.0 cms^{-1}, and (d) vertical velocity (w) at 11.0 cms^{-1}. Scale bars in cms^{-1}.

Streamwise velocity (u) Vertical velocity (w)

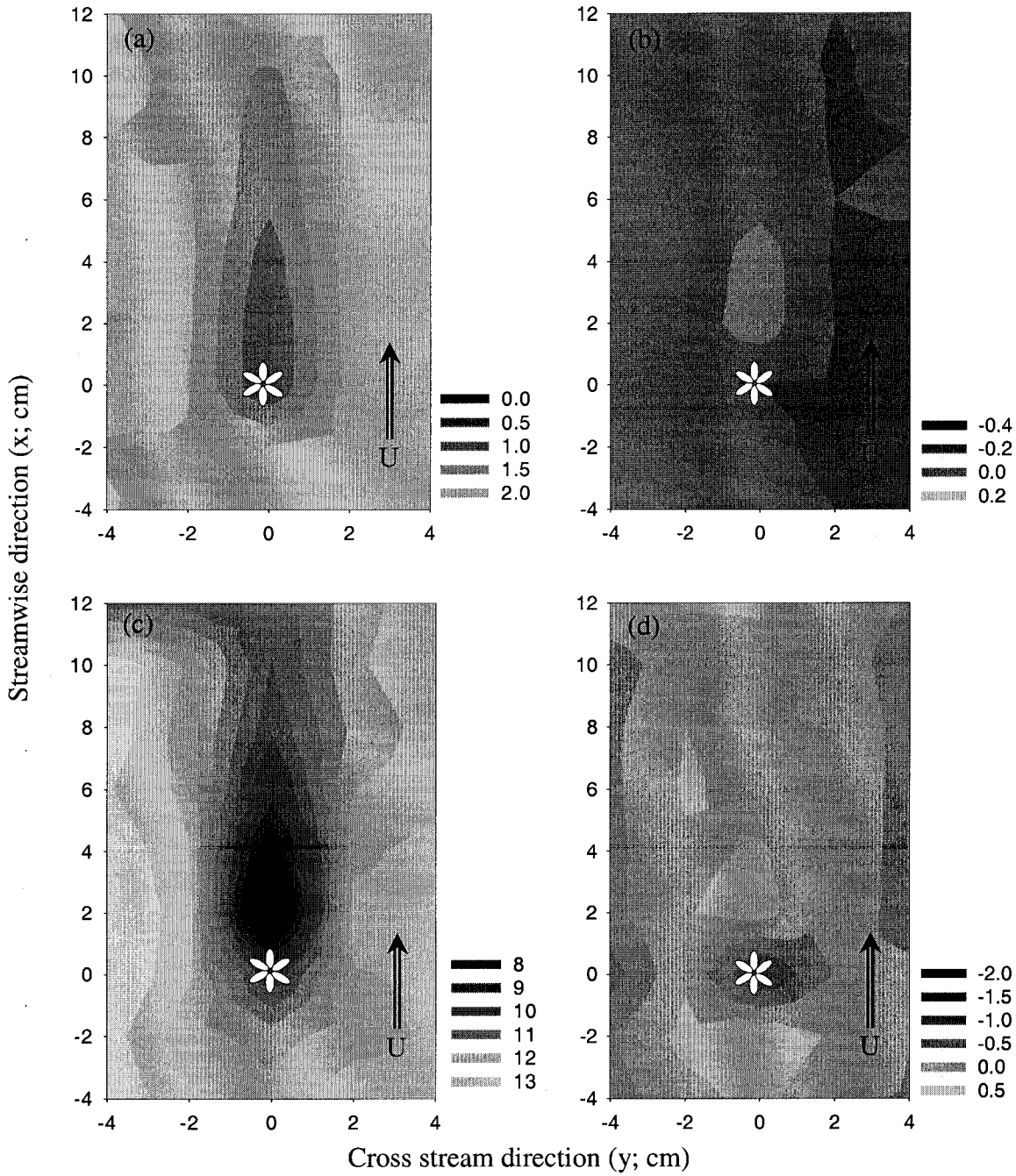

Figure 3.23: Contours of the velocity field measured 3 cm from the flume bottom in a 2 cm x 2 cm grid (3 cm in the vicinity of the plant) around *Elodea canadensis*. Each point of the contours was the mean of 120 s of data samples at 25 Hz. (a) streamwise velocity (u) at 1.3 cms^{-1}, (b) vertical velocity (w) at 1.3 cms^{-1}, (c) streamwise velocity (u) at 11.0 cms^{-1}, and (d) vertical velocity (w) at 11.0 cms^{-1}. Scale bars in cms^{-1}.

Streamwise velocity (u) Vertical velocity (w)

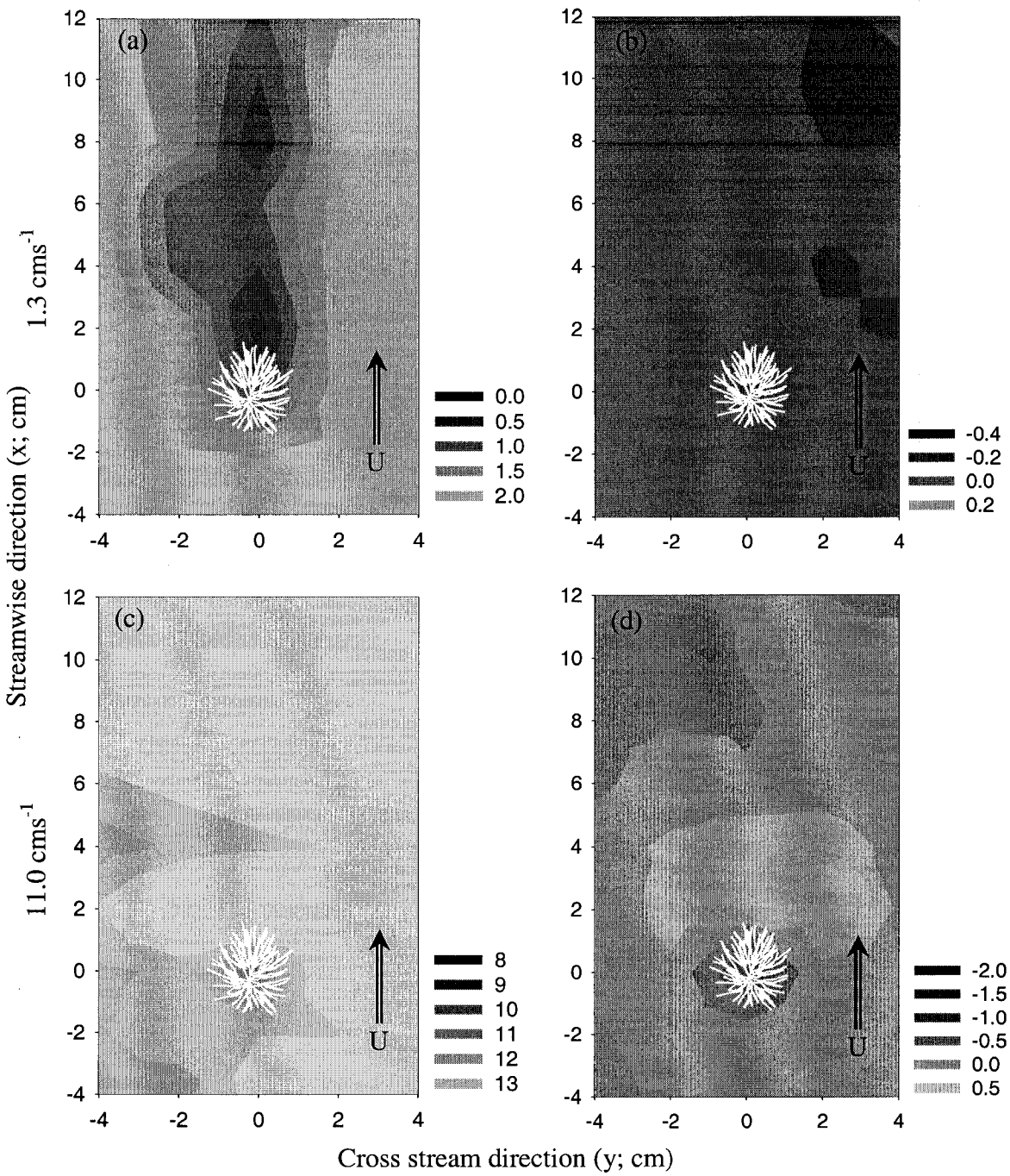

Figure 3.24: Contours of the velocity field measured 3 cm from the flume bottom in a 2 cm x 2 cm grid (3 cm in the vicinity of the plant) around *Ceratophyllum demersum*. Each point of the contours was the mean of 120 s of data samples at 25 Hz. (a) streamwise velocity (u) at 1.3 cms^{-1}, (b) vertical velocity (w) at 1.3 cms^{-1}, (c) streamwise velocity (u) at 11.0 cms^{-1}, and (d) vertical velocity (w) at 11.0 cms^{-1}. Scale bars in cms^{-1}.

Deflection Oscillation

Cylinder

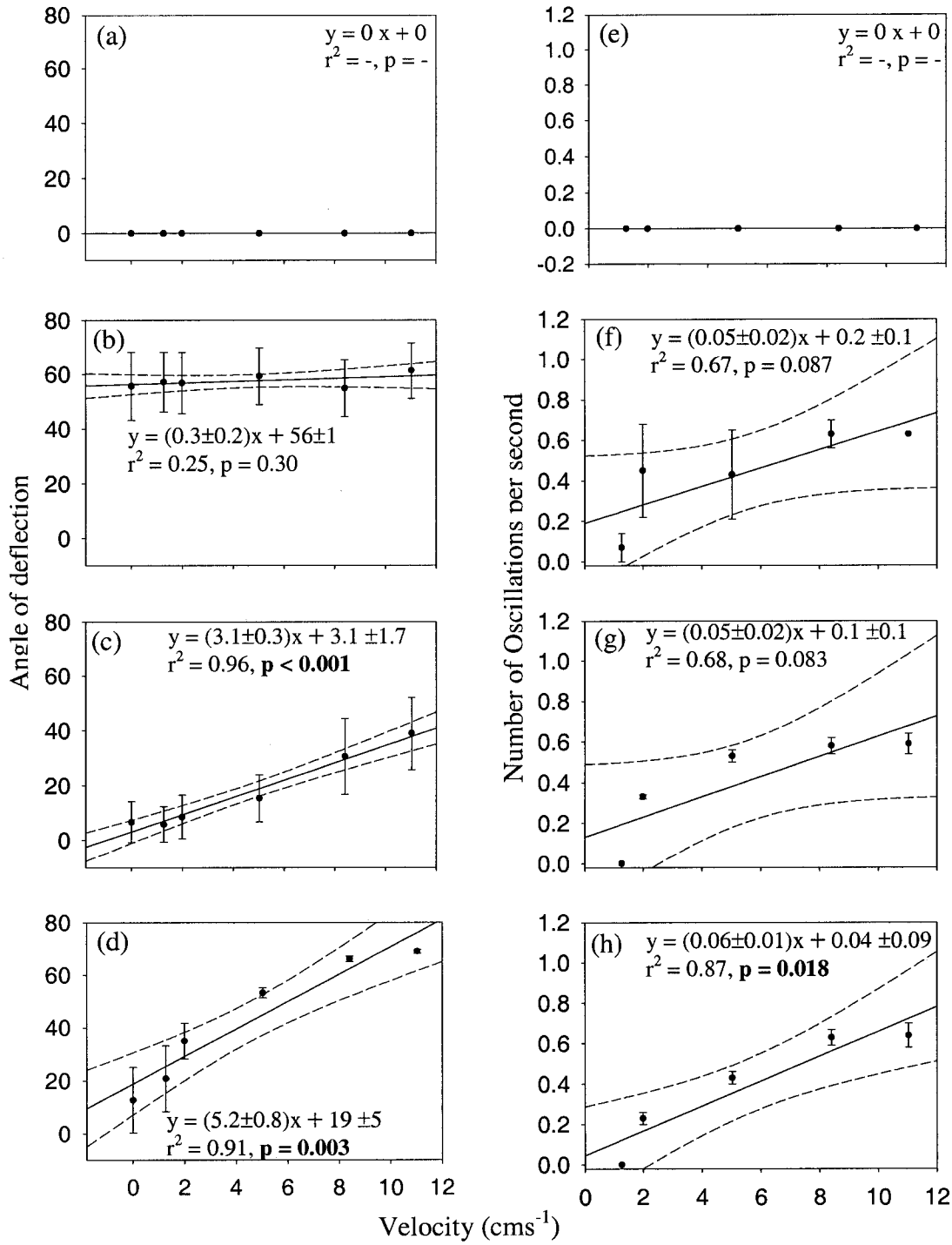

Figure 3.25: Regressions for the angle of deflection for (a) the circular cylinder and the different plant species (b) *Vallisneria,* (c) *Elodea,* and (d) *Ceratophyllum.* Regressions for the number of oscillations per second with increasing velocity for (e) the circular cylinder and the different plant species (f) *Vallisneria,* (g) *Elodea,* and (h) *Ceratophyllum.* Solid line is the regression and dotted lines are the 95% confidence limits of the mean.

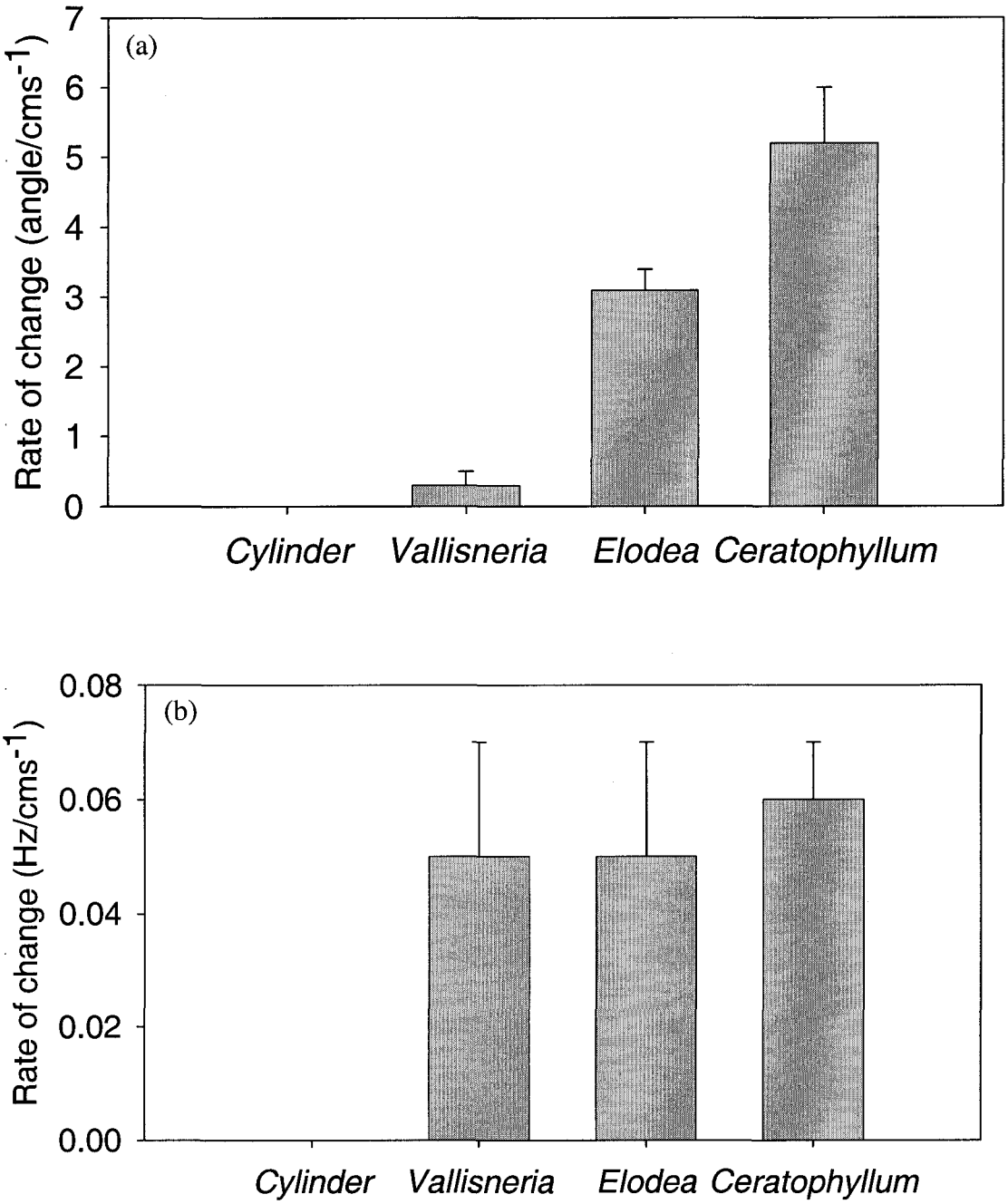

Figure 3.26: (a) Rate of change in the angle of deflection with change in velocity for the different test subjects; and (b) the rate of change in the number of oscillations per second with change in velocity for the different test subjects. The cylinder is always at zero because it was rigid and as such remained stationary.

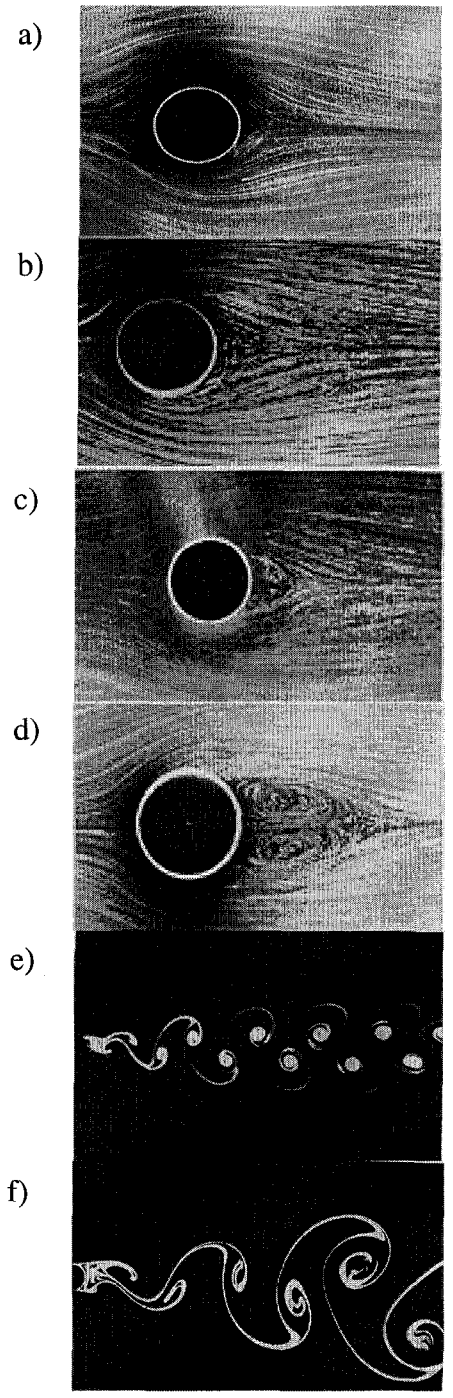

Figure 3.27: The transition to turbulent flow of a fluid as it passes a circular cylinder seen in cross section at different Reynolds numbers: (a) 1, (b) 10, (c) 13, (d) 26, (e)105, and (f) 150.
(From: http://nmm.media.mit.edu/student/95/aries/mas864/obstacles.html)

The Effect of Internodal Spacing on Downstream Flow Patterns and Compliance in *Elodea canadensis* and *Ceratophyllum demersum*

Abstract:

Aquatic macrophytes experience both diffusive and mechanical stresses, and as such, must contend with different constraints. Specifically, at low velocities, plants must overcome boundary layer limitations in order to increase exchange rates and hence nutrient uptake, whereas at high velocities they must reduce drag to minimize tissue damage or dislodgement. Given these constraints and the plasticity in macrophyte morphology, the experimentally manipulated internodal spacing and compliance (deflection of the plant from the vertical) of a whorled leaf macrophyte, *Elodea canadensis*, and a whorled macrophyte with highly dissected leaves, *Ceratophyllum demersum*, were examined in a flow chamber at velocities from ~1 – 11 cms^{-1}. Fluoroscein dye was used to visualize the flow patterns and a digital camera was used to record the images. Increasing the internodal spacing in *Elodea* affected the downstream flow patterns by reducing the plant-flow interaction (e.g., less fluid came in contact with the plant surface as compared to the other plants) but not the degree of compliance exhibited by the plant. Conversely, in *Ceratophyllum,* the downstream flow patterns did not change significantly with increased internodal spacing, but the compliance increased considerably. These results suggest that *Elodea* may be better suited to faster flow environments because it would experience less of a plant-flow interaction, which would minimize hydrodynamic drag. Conversely, *Ceratophyllum* may be better suited to slower flow environments because of the high plant-flow interaction, which would induce small scale mixing close to the leaf surface, thus enhancing mass transfer. It appears that fluid

dynamics have a determining role in the plastic response of macrophyte morphology, and thus the evolution of plant form and function.

Introduction:

Freshwater macrophytes are phenotypically plastic in that they are able to change their morphology and physiology in response to environmental conditions (Idestam-Almquist and Kautsky, 1995; Santamaria et al., 2003). This allows macrophytes to grow in a wider range of environments than would be possible for a single morphotype (DeWitt et al., 1998). Macrophytes are also able to change their morphology in response to water motion and thus to colonize different hydrodynamic environments (Sculthorpe, 1967; Stewart and Carpenter, 2003). For example, at slower velocities entire leaf forms in macroalgae tend to be shorter and thicker as opposed to longer and more slender in faster velocities (Norton et al., 1982; Guitierrez and Fernandez, 1992) so that it would seem logical to expect the same in freshwater macrophytes. Dissected morphologies however, show the opposite trend whereby internodal leaf segments are slender in slow flow environments and shorter and firmer in faster moving water (Sculthorpe, 1967). Macrophytes have also been known to increase their internodal spacing in response to low light levels (Cronin and Lodge, 2003), and to living in wave-sheltered sites (Idestam-Almquist and Kautsky, 1995). It would seem important, therefore, to determine whether a change in plant architecture such as internodal spacing effects the local fluid dynamic conditions, and thus the diffusional and mechanical stress acting on submerged freshwater plants.

Gas exchange and light capture are essential to the productivity of plants. One way that plants enhance uptake, is through heterophylly (different leaf morphologies on

the same plant, or in the same species, depending on environment), which is a prime example of the functional explanation of plant architecture (e.g., *Properpinaca palusturis*; Sculthorpe, 1967; Wells and Pigluicci, 2000). As a comparison, macroalgae increase the surface area:volume in order to maximize light capture, and to increase the flux of nutrients available to the plant (Hurd, 2000). Another way to increase nutrient flux to the plant is through the possession of fine-scale roughness elements (such as fine hairs, toothed edges, bullate surfaces etc.), which generate turbulent flow at the plant surface at low velocities (Abelson et al., 1993; Hurd, 2000). One of the principle ways in which this occurs is through vortex generation as the fluid passes by an object (Kundu, 1990; See chapter 3). This type of turbulence generation would also be important to freshwater macrophytes as a means of increasing local mixing that would deliver nutrients through inertial processes as opposed to diffusion (Okubo et al., 2002). It is reasonable to postulate that internodal spacing in freshwater macrophytes may be important in the generation of vortices in that it would affect the presentation of whorls of leaves to the mainstream flow.

Macrophytes must also be able to withstand the potential of mechanical damage present in a flowing system due to fluid dynamic forces (e.g., lift, drag, shear stress, acceleration forces; Vogel, 1994; Okubo et al., 2002). Flexibility can increase in the ability of macrophytes to become compliant under flowing conditions, and thus decrease the magnitude of hydrodynamic forces experienced (Sand-Jensen, 2003). Plants that grow in energetic environments tend to be small in stature and limited in lateral spread, whereas plants that grow in predictable habitats tend to be higher in stature and extensive in lateral spread (Barrat-Segretain, 2001). In contrast, giant kelps are both long and

flexible, and this morphology may reduce the drag experienced by these algae (Denny et al., 1997). It has also been found that macroalgae with fewer branches are better able to withstand the mechanical stresses of higher velocities than highly branched macroalgae (Sheath and Hambrook, 1988). Schutten and Davy (2000) confirmed this result in freshwater plants, where plants with less surface area were found to experience lower drag. Clearly the ability of a plant to reduce the risk of damage is central to its survival and, it would be useful to determine how freshwater macrophytes respond to increasing flow conditions (i.e., remain stiff, comply, or break). As indicated above, internodal spacing is an important morphological feature that appears to confer benefits at both low and high velocities. It would be instructive to investigate how this feature affects the fluid dynamics surrounding freshwater macrophytes with whorled leaves. It is expected that an increased internodal spacing would generate less turbulence and less compliance by the plant. The following chapter examines the null hypothesis that internodal spacing has no effect on the flow or compliance of whorled-leafed macrophytes with entire and highly dissected leaves (i.e., *Elodea canadensis* and *Ceratophyllum demersum*, respectively).

Materials and Methods:

In order to examine the null hypotheses, photographs and short videos were taken of Fluoroscein dye moving: (1) in an empty test section; (2) past a circular cylinder (0.7 cm diameter); (3) past *Elodea canadensis* (referred to as *Elodea* in this report); (4) past *Elodea* with the leaf whorl at every second node removed; (5) past *Elodea* with the leaf whorl at every second and third node removed; (6) past *Ceratophyllum demersum* (referred to as *Ceratophyllum* in this report); (7) past *Ceratophyllum* with the leaf whorl

at every second node removed; and (8) past *Ceratophyllum* with the leaf whorl at every second and third node removed (all plant segments in 5 cm lengths: Figures 4.1, 4.3, 4.5, 4.7, 4.9, 4.12, 4.15). All specimens of *Elodea* were collected from Tabor Lake, Prince George, B.C., and all specimens of *Ceratophyllum* were purchased from Ward Scientific Supply (Rochester, NY, USA). The whorls were removed where they attached to the stem by pulling them off with tweezers. A sample size of three was used for each intact and manipulated segment of each plant.

The experimental protocols and procedures were the same as those used in Chapter 3. The plants were examined in a recirculating flow chamber (see Chapter 3; Figure 3.1) operated at velocities ranging from about 1-11 cms^{-1}, similar to the velocities used by Nepf and Koch (1999), and Leonard and Luther (1995). Fluoroscein dye was injected isokinetically upstream of the plant and excited by a black light. A white light was also used to ensure that the plants were visible and could be recorded as photographs and video clips by the digital camera (Nikon CoolPix995; Melville, NY, USA). A pixel intensity versus dye concentration curve was used in the image analysis undertaken in MATLAB version 6.5 (Mathworks, Natick, Massachusetts). The area of dye coverage and the concentration of dye were determined for an upstream and downstream domain with respect to the plant in both the side and top perspective. The angle of deflection (angle from the vertical), the frequency of oscillations, and the angle of the leaves of *Ceratophyllum* from the stem were also measured from the video recordings.

Statistical Analysis

Effect of Velocity on Dye Coverage and Concentration

The average and standard deviation of the area of dye coverage and/or the concentration of dye in that area, were computed from the three images taken at each velocity. The area or concentration was then regressed on the test velocity and whorl Reynolds number based on the diameter of the subject (i.e., $\mathrm{Re} = \frac{ul}{\upsilon}$, where l is the diameter of the stem plus the leaves, u is the velocity, and υ is the kinematic velocity; Vogel, 1994). The null hypothesis examined was that the slope of the regression is equal to zero, in other words there is no trend in area of dye coverage or concentration of dye with increasing velocity.

Effect of Internodal Spacing on the Rate of Oscillation

Analyses of covariance (ANCOVAs) were conducted using the frequency of oscillations as the dependent variable. The different plants were the categorical factors, and velocity was the continuous predictor (the covariate). A Fisher LSD test was used for Post Hoc comparisons. This statistical test was chosen to test whether there is a difference between slopes for the different regressions.

Effect of Velocity and Node Position on the Leaf Angles of *Ceratophyllum*

The dissected nature of the leaves of *Ceratophyllum* provided the opportunity to examine the response of leaf segments on the upstream and downstream side of the plant. The leaves were defined as moving closer to the stem when they moved towards the stem in the same direction as the flow in the chamber. ANCOVAs were conducted using angle of the *Ceratophyllum* leaf segment from the stem as the dependent variable. The node position on the stem was the categorical factor, and velocity was the continuous predictor

(the covariate). A Fisher LSD test was used for Post Hoc comparisons between leaf angles of the different nodes.

Results:

It was established in Chapter 3 that the upstream flow patterns were not significantly different in any perspective or morphology because the dye was injected isokinetically. Consequently, only the downstream flow patterns are examined here.

Cylinder

The flow patterns downstream of the circular cylinder have been discussed in the previous chapter, but are included here for comparative purposes. Laminar flow was observed at the slower velocities, as indicated by the loops of dye ("stickiness"), and the large area of recirculation downstream of the cylinder. The transition from laminar to turbulent flow occurred between 5.0 cms^{-1} and 8.4 cms^{-1} (i.e., Re ~ 350-590). At the faster velocities, the flow was turbulent, with fewer loops of dye and a smaller recirculation zone. This is best seen in the top perspective where the dye streaklines revealed a classic attached eddy at 1.3 cms^{-1} (Re ~ 90; Figure 4.1b), a von Karman vortex street at 2 cms^{-1} (Re ~ 140; Figure 4.1d), and more turbulent structures (eddies) at higher velocities (Figure 4.1f,h,j).

There was a significant increase in the dye coverage downstream in the side perspective with velocity (i.e., 0.5 cm^2/cms^{-1}; $p = 0.018$; Figure 4.2c), and a positive trend in the top perspective ($p = 0.41$; Figure 4.2d). Additionally, the dye concentration tended to decrease with velocity in the up and downstream domains, and this was significant in the case of the downstream side perspective ($p = 0.014$; Figure 4.2g).

Elodea

The pattern of flow around *Elodea* was reported in Chapter 3 but it is repeated here for comparative purposes. The downstream dye streaklines were attached to the individual whorls in filamentous loops, and recirculation was present at the lower velocities (Figure 4.3a-d). The transition from laminar to turbulent occurred at ~ 5.0 cms^{-1} (Re ~ 500), as indicated by the onset of eddies downstream of the plant (Figure 4.3e,f). Von Karman vortices were shed at 8.4 cms^{-1} (Re ~ 840; Figure 4.3h) and more turbulence (widely spaced eddies, and less stickiness and recirculation) was evident at 11.0 cms^{-1} (Re ~ 1100; Figure 4.3i-j).

There was a significant increase in the area of dye coverage with velocity downstream in the top perspective ($p = 0.026$) of ~ 0.10 cm^2/cms^{-1} (Figure 4.4d). Additionally, the dye concentration tended to decrease with velocity in the up and downstream domains, and this was significant in the case of the downstream side ($p = 0.049$) and top perspectives ($p = 0.046$; Figure 4.4g,h).

Elodea with the Leaf Whorl at Every Second Node Removed

The dye streaklines downstream of *Elodea* with the whorls at every second node removed showed a large amount of "stickiness" to the whorls at the lower velocities (Figure 4.5a-f). The transition from laminar to turbulent occurred between 5.0 cms^{-1} and 8.4 cms^{-1} (Re ~ 500-840; Figure 4.5e-h). At the higher velocities, turbulence was indicated by the closely spaced eddies, and the reduced amount of stickiness and recirculation as compared to the slower velocities (4.5g-j). There was also some compliance (bending into the flow) with increasing velocity.

There was a significant increase in the area of dye coverage with velocity downstream in the side perspective ($p = 0.015$), which was on the order of ~ 0.2

cm^2/cms^{-1} (Figure 4.6c), although this trend was not significant in the top perspective. Additionally, the dye concentration tended to decrease with velocity in the upstream and downstream domains, and this was significant in the case of the downstream top perspective ($p = 0.016$; Figure 4.6g,h).

Elodea with the Leaf Whorls at Every Second and Third Node Removed

The dye streaklines downstream of *Elodea* with the whorls at every second and third node removed were laminar, as indicated by the loops in the dye attached to the individual whorls, at the lower velocities (Figure 4.7a,b). The transition from laminar to turbulent flow occurred between 5.0 cms^{-1} and 8.4 cms^{-1} (Re ~ 500-840) as indicated by the dye streakline becoming increasingly wavy (Figure 4.7c-h). The onset of eddies denotes that the flow was turbulent at the higher velocities (Figure 4.7g-j). There was little compliance, or bending into the flow with increasing velocity.

There were no significant trends in the area of dye coverage with velocity downstream of the plant, and the trend in the side perspective was positive, but was negative in the top perspective (Figure 4.8c,d). The dye concentration however, decreased significantly with velocity in the downstream side ($p = 0.035$) and top ($p = 0.007$) perspectives at –0.07 and –0.05 gL^{-1}/cms^{-1}, respectively (Figure 4.8g,h).

Ceratophyllum

The flow patterns downstream of *Ceratophyllum* were discussed in Chapter 3, and are presented here for comparative purposes. The dye streaklines downstream of *Ceratophyllum* "stuck" to the individual leaf segments at 1.3 cms^{-1} (Re ~ 300), and there was considerable recirculation behind the plant (Figure 4.9a,b). The transition of the dye from smooth laminar to eddies occurred between 5.0 and 8.4 cms^{-1} (Re ~ 1200-2000;

Figure 4.9c-f). Closely spaced eddies, and the reduced amount of stickiness and recirculation, indicated turbulent flow at the higher velocities (Figure 4.9g-j).

There was a significant decrease in the area of dye coverage with velocity downstream in the top perspective ($p = 0.028$), with a rate on the order of -0.1 cm^2/cms^{-1} (Figure 4.10d). There was also a tendency for the dye concentration to decrease with velocity in the up and downstream domains, although no cases were significant (Figure 4.10e-h).

An examination of the effect of velocity on leaf angle on the upstream side of the stem revealed that all leaves moved closer to the stem with increasing velocity (~ -1°/cms^{-1}), although this was only significant for the bottom most ($p = 0.006$) and the third leaf up from the bottom ($p = 0.02$; Figure 4.11a,c). On the downstream side of the stem, the bottom three leaves moved significantly closer to the stem with increasing velocity (~ -1°/cms^{-1}), but moving up the stem the trend was similar for the next two leaves, but not significant, and the leaf at the apex moved away from the stem, though the trend was not significant (Figure 4.11a-f).

Ceratophyllum with the Leaf Whorls at Every Second Node Removed

The dye streaklines downstream of *Ceratophyllum* with the whorls at every second node removed were laminar, as denoted by smooth dye streaklines and the large amount of "stickiness" on the individual leaf segments at the lower velocities. At the lower velocities, there was also recirculation behind the plant (Figure 4.12a-f). The transition from laminar to turbulent flow occurred between 5.0 cms^{-1} and 8.4 cms^{-1} (Re ~ 1200-2000) as indicated by the dye streakline changing from smooth to more chaotic in structure (Figure 4.12e-h). At the higher velocities, turbulence was indicated by the

closely spaced eddies, and less stickiness and recirculation (Figure 4.12g-j). There was also a high amount of compliance of the plant into the flow with increasing velocity.

There was a positive but not significant trend in the area of dye coverage with velocity downstream of the plant in the top perspective (Figure 4.13d). There was however, a significant decrease in dye concentration of $-0.07\ gL^{-1}/cms^{-1}$ ($p = 0.039$) in the side and $-0.031\ gL^{-1}/cms^{-1}$ ($p = 0.007$) in the top perspective (Figure 4.13g,h).

The leaf at the base of the plant on the upstream side tended to move away from the stem with increasing velocity, but this was not significant. Conversely, the next leaf showed a non-significant trend to move closer to the stem, and the top three leaves moved significantly closer to the stem with increasing velocity (i.e., -1.6 to $-3.2\ °/cms^{-1}$; Figure 4.14a-e). On the downstream side of the stem, the leaf at the base of the plant tended to move towards the stem, the next leaf moved significantly away from the stem at a rate of ~ $0.5\ °/cms^{-1}$. The third and fourth leaves from the bottom of the plant moved towards the stem with increasing velocity, but the leaf at the apex of the plant moved significantly away from the stem with increasing velocity (Figure 4.14a-e).

Ceratophyllum with the Leaf Whorls at Every Second and Third Node Removed

At the slower velocities, laminar flow was indicated by the filamentous dye loops attached to the individual leaf segments, and the recirculation behind *Ceratophyllum* with the whorls at every second and third node removed (Figure 4.15a-f). The dye streakline downstream became increasingly complex with increasing velocity and the transition occurred between $5.0\ cms^{-1}$ and $8.4\ cms^{-1}$ (Re ~ 1200-2000; Figure 4.15e-h). At the higher velocities, turbulence was indicated by the closely spaced eddies, and a reduced

amount of stickiness and recirculation (Figure 4.15g-j). This manipulated segment of *Ceratophyllum* showed a high amount of compliance with velocity, similar to above.

There was no significant trend in the area of dye coverage downstream in the side perspective although there was a tendency for an increase with velocity (Figure 4.16c,d). There was also a tendency for the dye concentration to decrease with velocity in both the side and top perspectives (Figure 4.16g,h).

The leaf at the base of the plant tended to move closer to the stem as did the second and third leaves up the stem, and the leaf at the apex did so significantly ($p = 0.031, 0.026, <0.001$, respectively). The rate of change in compliance towards the stem increased as the leaves approached the apex of the plant (-1.3 to -2.0 $°/cms^{-1}$; Figure 4.17a-d). On the downstream side of the stem, the bottom three leaves tended to move away from the stem, whereas the leaf at the apex tended to move closer to the stem with increasing velocity (Figure 4.17a-d).

Effect of Manipulating Internodal Spacing

Area of Dye Coverage

An ANCOVA was undertaken on all of the plant types to determine whether there were significant differences among their responses to velocity. There was a significant effect of velocity on area of dye coverage ($p = 0.023$; Table 4.1a), plant type (i.e., species and internodal spaces; $p < 0.001$), side versus top perspective ($p = 0.036$), and upstream versus downstream domain ($p < 0.001$). There were also significant interactions between the plant and the upstream versus downstream domain ($p = 0.001$), as well as between the side versus top perspective and the upstream versus downstream domain ($p = 0.002$).

Upon closer inspection however, ANCOVAs conducted on each plant species and manipulation revealed that in terms of area of dye coverage, there was a significant effect of velocity for the cylinder ($p < 0.001$; Table 4.2a), but not for *Elodea* ($p = 0.52$; Table 4.2b), or *Elodea* with the whorl at every second node removed ($p = 0.08$; Table 4.2c), or for *Elodea* with the whorls at every second and third node removed ($p = 0.78$; Table 4.2d). There were significant differences between the upstream and downstream domains for all plants, but no significant effect of side versus top perspectives for any of the manipulations (Table 4.2). Pairwise comparisons in the side perspective downstream revealed significant differences in the area of dye coverage between the cylinder and *Elodea* with the whorls at every second and third node removed ($p = 0.001$), the cylinder and the empty test section ($p = 0.003$), *Elodea* and *Elodea* with the whorls at every second and third node removed ($p < 0.001$), *Elodea* and the empty test section ($p = 0.001$), and between *Elodea* with the whorls at every second node removed and *Elodea* with the whorls at every second and third node removed ($p = 0.039$: Table 4.3c). In the top perspective, significant differences occurred between the subjects and the empty test section ($p < 0.001$), but not among any of the subjects (Table 4.3d).

ANCOVAs were conducted on *Ceratophyllum* and its manipulated stems. This analysis demonstrated that there was only a marginal effect of velocity on the area of dye coverage for *Ceratophyllum* ($p = 0.08$; Table 4.4b), and no effect for *Ceratophyllum* with the whorl at every second node ($p = 0.39$; Table 4.4c) and every second and third node removed ($p = 0.11$; Table 4.4d). There was however, a significant upstream versus downstream effect, but no significant effect of side versus top perspective for either of the plants (Table 4.4). Pairwise comparisons showed that the area of dye coverage in the

side perspective was significantly different between *Ceratophyllum* with the whorls at every second node removed and the cylinder ($p = 0.006$), the cylinder and the empty test section ($p = 0.003$), and between *Ceratophyllum* and the empty test section ($p = 0.042$: Table 4.5c). In the top perspective, significant differences in area of dye coverage occurred between the subjects and the empty test section, the cylinder and *Ceratophyllum* ($p = 0.023$), and between the cylinder and *Ceratophyllum* with the whorls at every second node removed ($p = 0.007$; 4.5d).

Concentration of Dye

An ANCOVA was conducted on the concentration of dye for all of the subjects, which revealed a significant effect of velocity ($p < 0.001$; Table 4.1b), plant type ($p = 0.39$), side versus top perspective ($p = 0.007$), and upstream versus downstream domain ($p < 0.001$). Separate ANCOVAs conducted for *Elodea* and its manipulated internodes showed that there was a significant effect of velocity on the concentration of dye for all of the plants (Table 4.2). However, there were no significant effects of upstream versus downstream domain, or side versus top perspective for any of the plants (Table 4.2). Pairwise comparisons showed that in the side perspective, downstream of the *Elodea* manipulations, significant differences occurred between the subjects and the empty test section (Table 4.6c), but not among any of the subjects. In the top perspective, the only significant difference occurred between the cylinder and the empty test section ($p = 0.029$; Table 4.6d).

ANCOVAs conducted on the concentration of dye for the different *Ceratophyllum* internodal manipulations showed that velocity had a significant effect on *Ceratophyllum* with the whorl from every second node removed ($p = 0.003$; Table 4.4c)

and *Ceratophyllum* with the whorls from every second and third node removed ($p < 0.001$; Table 4.2d), but only marginal significance for unmanipulated section of *Ceratophyllum* ($p = 0.059$; Table 4.4b). The same pattern occurred in the upstream versus downstream position, but no significant effects were noted between the side and top perspectives (Table 4.4). In the side perspective, downstream of the *Ceratophyllum* manipulations, significant differences in concentration were found between the cylinder and *Ceratophyllum* ($p = 0.040$), the cylinder and the empty test section ($p = 0.002$), and between *Ceratophyllum* and the empty test section ($p = 0.020$: Table 4.7c). In the top perspective downstream, significant differences were found between the cylinder and *Ceratophyllum* ($p = 0.031$), Ceratophyllum with the whorls at every second and third node removed ($p = 0.004$), and the empty test section ($p = 0.029$; Table 4.7d).

Angle of Leaf from the Stem

An ANCOVA of the leaf angle results for the different manipulations of *Ceratophyllum* revealed a significant effect of manipulation on leaf angle ($p = 0.005$: Table 4.8a). However, there were only significant differences between the leaves on the upstream side of the stem of *Ceratophyllum*, and the leaves in the upstream and downstream position on the manipulated segments of *Ceratophyllum* (Table 4.8b). In terms of the rate of change in the leaf angle, the apical leaf in the approaching flow moved towards the stem at a faster rate than the leaves lower down on the stem for all three plant segments (Figure 4.18a). Only unmanipulated *Ceratophyllum* showed a trend in the downstream direction, whereby the apical leaf moved away from the stem, and the other leaves moved towards the stem at a faster rate the closer they were to the base of the plant (Figure 4.18b). Neither of the *Ceratophyllum* manipulations showed a trend in

the rate of change in leaf and angle from the stem with increasing velocity. The same analyses were not conducted for *Elodea* due to the relatively short and stiff structure of the leaves, which were not observed to change in angle of deflection upon viewing the video clips.

Angle of Deflection

The angle of deflection for the different species and their associated manipulations increased significantly with increasing velocity ($p < 0.003$; Table 4.19a-g). The rate ranged from 2-3 °/cms^{-1} for *Elodea* and 4-5 °/cms^{-1} for *Ceratophyllum.* As such, the ANCOVA showed that there was a significant effect of velocity ($p < 0.001$), as well as for plant type ($p < 0.001$; Table 4.9a). More specifically, post hoc tests showed that there were significant differences between the cylinder and *Elodea,* and the three *Ceratophyllum* manipulations. Differences also occurred: between *Elodea* and *Elodea* with the whorls at every second node removed and *Ceratophyllum*; between *Elodea* with the whorls at every second and third node removed and the three *Ceratophyllum* manipulations; *Elodea* with the whorls at every second and third node removed and *Ceratophyllum* and *Ceratophyllum* with the whorls at every second and third node removed; and between unmanipulated *Ceratophyllum* and the two *Ceratophyllum* manipulations (Table 4.9b).

Oscillations

The frequency of oscillations increased with velocity for both plant species and their associated manipulations (Figure 4.20a-g). This was significant for *Elodea* with the whorls at every second node removed ($p = 0.031$), *Ceratophyllum* ($p = 0.018$), *Ceratophyllum* with the leaves at every second node removed ($p = 0.006$), and

Ceratophyllum with the leaves at every second and third node removed ($p = 0.048$). The ANCOVA showed that velocity ($p < 0.001$) and plant type ($p = 0.002$; Table 4.10a) had a significant effect on the frequency of oscillation. However, pairwise comparisons revealed that all of the significant pairwise differences occurred between the cylinder (which did not oscillate) and the test subjects (Table 4.10b).

Comparison of Plant Types

The transition from laminar to turbulent flow, occurred at a velocity equal to or greater than the physical model for all plants with the exception of unmanipulated *Elodea* (Figure 4.21a). The transition for the cylinder, *Elodea* with the leaves from every second node removed, and *Ceratophyllum* occurred between 5 and 8.4 cms^{-1}, for *Elodea* between 2 and 5 cms^{-1}, at ~ 8.4 cms^{-1} for *Elodea* with the leaves from every second and third node removed, and between 8.4 and 11 cms^{-1} for *Ceratophyllum* with the leaves from every second, and every second and third node removed. It should be noted that the use of Re did not change the pattern of observation reported here. Specifically the Re for the cylinder ranged from 90-770, from 130-1100 for *Elodea* and its manipulations, and from 300-2600 for *Ceratophyllum* and its manipulations. Collectively, this would indicate that the manipulations reduced the level of local mixing.

A direct comparison of the rate of change in the area of dye coverage with increasing velocity revealed that the rate was slower for all of the plants than for the physical model (Figure 4.21b). The rate of change for the circular cylinder increased significantly on the order of ~ 0.5 cm^2/cms^{-1}, as it did for *Elodea* with the whorl at every second node removed although at a slower rate on the order of ~ 0.2 cm^2/cms^{-1}. There was a positive, although non-significant trend seen in *Elodea* with the whorls at every

second and third node removed (~ 0.08 cm^2/cms^{-1}), and in *Ceratophyllum* with the whorls at every second and third node removed (~ 0.2 cm^2/cms^{-1}). Non-significant negative trends in the area of dye coverage with increasing velocity were seen in *Elodea* (~ -0.0004 cm^2/cms^{-1}), *Ceratophyllum* (~ -0.2 cm^2/cms^{-1}), and *Ceratophyllum* with the whorl at every second node removed (~ -0.01 cm^2/cms^{-1}).

A direct comparison of the rate of change in concentration of dye with velocity showed that the rate of change for the plants was less than the rate for the physical model (Table 4.21c). The rate for the circular cylinder decreased significantly, at ~ -0.05 gL^{-1}/cms^{-1}, as did *Elodea* (~ -0.06 gL^{-1}/cms^{-1}), *Elodea* with the whorls at every second and third node removed (~ -0.07 gL^{-1}/cms^{-1}), and *Ceratophyllum* with the whorl at every second node removed (~ -0.07 gL^{-1}/cms^{-1}). The rates for *Elodea* with the whorl at every second node removed (~ -0.06 gL^{-1}/cms^{-1}), *Ceratophyllum* (~ -0.07 gL^{-1}/cms^{-1}), and *Ceratophyllum* with the whorls at every second and third node removed (~ -0.08 gL^{-1}/cms^{-1}), also decreased though non-significantly.

The rate of change in the angle of deflection with increasing velocity was lower for the *Elodea* series than for the *Ceratophyllum* series of manipulations (Figure 4.22a). *Elodea* and *Elodea* with the whorl at every second node removed showed an increase on the order of ~ 3.1 $°/cms^{-1}$, whereas *Elodea* with the whorls at every second and third node removed showed a much slower rate of change at ~ 1.9 $°/cms^{-1}$. The rate of change for *Ceratophyllum* (~ 5.2 $°/cms^{-1}$), *Ceratophyllum* with the whorl at every second node removed (~ 4.4 $°/cms^{-1}$), and *Ceratophyllum* with the whorls at every second and third node removed (~ 5.2 $°/cms^{-1}$) were similar. The rate of change in the frequency of

oscillations with increasing velocity was similar for all plants although the *Elodea* manipulations oscillated at lower rates (i.e., 0.05 vs. 0.07 Hz/cms^{-1}; Figure 4.22b).

Discussion:

The response of flow to internodal spacing was different between the entire-whorled (*Elodea*) and dissected-whorled (*Ceratophyllum*) morphologies. For *Elodea* the plant-flow interaction decreased with increased spacing, reducing the opportunity for dye attachment (Schwinge et al., 2002), and thus exchange between the fluid and the leaf surface. For *Ceratophyllum* and the associated manipulations, the plant-flow interaction was greater because the angle of the leaf from the stem did not differ significantly among the different manipulations. Resultantly, there was always a highly dissected, mesh-like obstruction maintaining similar downstream flow patterns (i.e., small scale eddies) (Nowell and Jumars, 1984; Sand-Jensen and Pedersen, 1999). This would enhance the local mixing and contact of the fluid with the leaf surface, a feature that suggests this morphology may be better suited to slower flows.

Despite differences in dye patterns, the concentration of dye decreased at a slower rate for the plants than for the cylinder. This suggests that although plants, and different manipulations thereof, have different ways of affecting the flow, they still retained more fluid than a physical model. This would provide more opportunity for nutrient uptake. A similar trend was demonstrated in macroalgae by Hurd et al. (1996) where different blade morphologies produced different flow patterns, but the uptake of nitrogen remained similar between the two morphologies. It is not known whether other nutrients would behave the same manner. It seems reasonable to expect that a variation in the morphology of a freshwater plant species (i.e., internodal spacing) and the resultant fluid

dynamic patterns identified above may influence nutrient uptake. This is an issue that should to be examined experimentally in freshwater macrophytes.

The compliance of *Elodea* and *Ceratophyllum* increased with velocity which would increase the interception efficiency of both direct and diffuse light but could lead to canopy shading (Niinemets and Fleck, 2002). In addition, there was a trend for the individual leaves of the *Ceratophyllum* to fold in closer to the stem as velocity increased, which would decrease drag, but also photosynthesis due to self-shading. Subsequently, at slower velocities where diffusion is limiting, the leaves protrude more into the flow, thus presenting more surface area for photon capture and increasing the efficiency of light use by the plant (Gutschick, 1999; Niinemets and Fleck, 2002). Leaf shape, the length of internodes, and the pattern of leaf arrangement are all important in defining the total amount of direct light a shoot can receive (Niklas, 1992). This is especially true for aquatic macrophytes because water attenuates the intensity of sunlight and preferentially absorbs the red wavelengths of light, so that submerged aquatic plants experience significantly lower light intensities shifted in favour of blue wavelengths (Niklas, 1997).

These results demonstrate that an increasing internodal spacing has different implications for different plant morphologies. For example, *Elodea* may be better suited to faster flow because the plant-flow interaction decreased with increased internodal spacing. Conversely, *Ceratophyllum* would probably be better suited to slower flow conditions because the highly dissected morphology ensures greater plant-flow interaction. Additionally, the high level of compliance would increase the amount of surface area exposed for photon capture as well as reduce drag, as mentioned above.

It is important to recognize that the plants in this study were grown in a low flow environment prior to the experiments. Had they been taken from high flow areas, there may have been morphological differences such as shorter internodal spaces (Idestam-Almquist and Kautsky, 1995) and more robustness in their structure (Schutten and Davey, 2000). This however, should have minimal effects on the results of the experiment because the plant segments were experimentally manipulated to alter the internodal spacing, and since the experiments were conducted at the lower end of the velocity range, breakage was not an issue, although there may have be a decrease in the degree of compliance.

Often, while plants acclimate to increase productivity, they increase the chance of mechanical damage (Ennos, 1999). For example, a natural response of aquatic macrophytes to increase photosynthesis is to grow closer to the light source (i.e., away from the bottom), thus increasing mechanical stress by exposing the plant to higher velocities (Ennos, 1999; Strand and Weisner, 2001). A strategy of minimizing mechanical stress in aquatic systems is for plants to become more compliant with the flow (streamlined) in order to reduce the hydrodynamic drag (Schulthorpe, 1967). However, in order to inhabit faster moving environments, the length of the leaf must be small since drag is a function of surface area (Vogel, 1994). Hence, in order to reduce drag, plants must either become compliant to the flow, or reduce the size of individual surfaces facing the flow. Therefore, an increase in internodal spacing would be beneficial to plants that grow higher in the water column in relatively low flow environments because the reduction in leaf area would decrease drag. This is important because the plants need to remain erect in the water column in order to maximize light

interception. An increase in internodal spacing would not be beneficial at higher velocities because the plants would either be deflected downwards (i.e., increased compliance) and/or not be robust enough to withstand high drag forces.

Internodal spacing is a form of phenotypic plasticity that can link certain plant characteristics to environmental conditions (Santamaria et al., 2003; Idestam-Almquist and Kautsky, 1995). For example, plants growing in wave-protected sites tend to be longer, with longer internodes as well as more shoots with longer branches, as compared to those in the wave-exposed sites (Idestam-Almquist and Kautsky, 1995). This pattern also applies to marine invertebrates where intersetal spacing increases with decreasing velocity (Sebens et al., 1997; Marchinko and Palmer, 2003). It would appear that this form of phenotypic plasticity (i.e., internodal spacing and compliance) is important for aquatic macrophytes.

The null hypothesis that internodal spacing has no effect on the flow patterns generated by the plants and their compliance under different velocities was rejected. Internodal spacing has been found to affect surface area to volume ratios (Denny, 1993; Hurd and Stevens, 1997; Gutschick, 1999) and the degree of compliance (Sculthorpe, 1967; Sand-Jensen, 2003; Speck, 2003). The surface area:volume ratio is important for diffusion, local mixing, and drag. For example, the aerial form of the heterophyllous plant, *Properpinaca palustris,* has leaves with toothed margins that are smaller, broader, thicker and fewer in number than those on submerged streams, which are highly dissected (Schulthorpe, 1967; Wells and Pigluicci, 2000). This high level of dissection is thought to increase the surface area:volume ratio, but the small leaf segments would also work to trip boundary layers (i.e., change them from laminar to turbulent) (Gutschick, 1999), thus

increasing the delivery of gases to the leaf surface. In addition to plants altering their morphology in response to environmental conditions, plants can also change their local conditions, as was shown by Koehl and Alberte (1988), who found that the flapping of macroalgae increased photosynthesis, whereas the clumping together of fronds decreased photosynthesis due to self shading. This demonstrates that the macrophyte-flow interaction is a complicated one in that water motion has an effect on plant morphology, and this interaction can affect productivity. In other words, fluid dynamics have had a determining role in the plasticity of freshwater macrophytes because of the plant-flow interaction, which matches plant morphology to environmental condition. In this case, increased internodal spacing allowed the plant to remain higher in the water column in a relatively low energy environment because of a lower plant-flow interaction.

Literature Cited

Abelson, A., T. Miloh, and Y. Loya. 1993. Flow patterns induced by substrata and body morphologies of benthic organisms, and their roles in determining availability of food particles. *Limnology and Oceanography.* 38(6):1116-1124.

Barrat-Segretain, M-H. 2001. Biomass allocation in three macrophyte species in relation to the disturbance level of their habitat. *Freshwater Biology.* 46:935-945.

Cronin, G., and D.M. Lodge. 2003. Effects of light and nutrient availability on the growth, allocation, carbon/nitrogen balance, phenolic chemistry, and resistance to herbivory of two freshwater macrophytes. *Oecologia.* 137:32-41.

Denny, M.W. 1993. *Air and Water The Biology and Physics of Life's Media.* Princeton Univeristy Press, U.S.A. 341 pp.

Denny, M.W., B.P Gaylord, and E.A. Cowen. 1997. Flow and Flexibility II. The roles of size and shape in determining wave forces on the bull kelp *Nereocystis luetkeana. The Journal of Experimental Biology.* 200:3165-3183.

DeWitt, T.J., A. Sih, and D.S. Wilson. 1998. Costs and limits of phenotypic plasticity. *TREE* 13(2):77-81.

Ennos, A.R. 1999. The aerodynamics and hydrodynamics of plants. *The Journal of Experimental Biology.* 202:3281-3284.

Gutierrez, L.M., and C. Fernandez. 1992. Water motion and morphology in *Chondrus crispus* (Rhodothyta). *Journal of Phycology.* 28:156-162.

Gutschick, V.P. 1999. Research reviews: Biotic and abiotic consequences of differences in leaf structure. *New Phytologist.* 143(1):3-18.

Hurd, C.L. 2000. Water motion, marine macroalgal physiology, and production. *Journal of Phycology.* 36:453-472.

Hurd, C.L., P.J. Harrison, and L.D. Druehl. 1996. Effect of seawater velocity in inorganic nitrogen uptake by morphologcially distinct forms of macrocystis intgrifolia from wave-sheltered and exposed sites. *Marine Biology.* 126:205-214.

Hurd, C.L. and C.L. Stevens. 1997. Flow visualization around single- and multiple-bladed seaweeds with various morphologies. *Journal of Phycology.* 33:360-367.

Idestam-Almquist, J., and L. Kautsky. 1995. Plastic responses in morphology of *Potamogeton pectinatus* L. to sediment and above-sediment conditions at two sites in the northern Baltic proper. *Aquatic Botany.* 52:205-216.

Koehl, M.A.R., and R.S. Alberte. 1988. Flow, flapping, and photosynthesis of Nereocystis luetkeana: a functional comparison of undulate and flat blade morphologies. *Marine Biology*. 99:435-444.

Kundu, P.K. 1990. *Fluid Mechanics.* Academic Press, San Diego, Toronto. 638 p.

Marchinko, K.B., and A.R. Palmer. 2003. Feeding in flow extremes: dependence of cirrus form on wave-exposure in four barnacle species. *Zoology.* 106:127-141.

Nepf, H.M., and E.W. Koch. 1999. Vertical secondary flows in submersed plant-like arrays. *Limnology and Oceanography.* 44(4):1072-1080.

Niinemets, U., and S. Fleck. 2002. Petiole mechanics, leaf inclination, morphology, and investment in support in relation to light availablility in the canopy of *Liriodendron tulipifera. Oecologia.* 132:21-33.

Niklas, K.J. 1992. *Plant Biomechanics An Engineering Approach to Plant Form and Function.* The University of Chicago Press, Chicago, 607 pp.

Niklas, K.J. 1997. *The Evolutionary Biology of Plants.* The University of Chicago Press, Chicago, 449 pp.

Norton, T.A., A.C. Mathieson, and M. Neushul. 1982. A review of some aspects of form and function in seaweeds. *Botanica Marina.* XXV: 501-510.

Nowell, A.R.M., and P.A. Jumars. 1984. Flow environments of aquatic benthos. *Annual Review of Ecology and Systematics.* 15:303-328

Okubo, A., J.D. Ackerman, and D.P. Swaney. 2002. Passive Diffusion in Ecosystems. Pp. 31-106 in A. Okubo and S Levin (eds.) *Diffusion and Ecological Problems: New Perspectives, 2nd ed.* Springer Verlag. 467 pp.

Sand-Jensen, K. 2003. Drag and reconfiguration of freshwater macrophytes. *Freshwater Biology.* 48:271-283.

Sand-Jensen, K., and O. Pedersen. 1999. Velocity gradients and turbulence around macrophyte stand in streams. *Freshwater Biology.* 42:315-328.

Santamaria, L. 2002. Why are most aquatic plants widely distributed? Dispersal, clonal growth and small-scale heterogeneity in a stressful environment. *Acta Oecologica.* 23:137-154.

Santamaria, L., J. Figuerola, J.J. Pilon, M. Mjelde, A.J. Green, T. De Boer, R.A. King, and R.J. Gornall. 2003. Plant performace across latitude: the role of plasticity and local adapatation in an aquatic plant. *Ecology.* 84(9):2454-2461.

Schutten, J., and A.J. Davy. 2000. Predicting the hydraulic forces on submerged macrophytes from current velocity, biomass and morphology. *Oecologia.* 123:445-452.

Sculthorpe, C.D. 1967. *The Biology of Aquatic Vascular Plants.* Edward Arnold, London (Reprinted 1985 Koeltz Scientific, Konigstein), 610 pp.

Sebens, K.P., J. Witting, and B. Helmuth. 1997. Effects of water flow and branch spacing on particle capture by the reef coral *Madracis mirabilis* (Duchassaing and Michelotti). *Journal of Experimental Marine Biology and Ecology.* 211:1-28.

Sheath, R.G., and J.A. Hambrook. 1988. Mechanical adaptations to flow in freshwater red algae. *Journal of Phycology.* 24:107-111.

Speck, O. 2003. Field measurements of wind speed and reconfigureation in *Arundo donax* (Poaceae) with estimates of drag forces. *American Journal of Botany.* 90(8):1353-1256.

Stewart, H.L., and R.C. Carpenter. 2003. The effects of morphology and water flow on photosynthesis of marine macroalgae. *Ecology.* 84(11):2999-3012.

Strand, J.A., and S.E.B. Weisner. 2001. Morphological plastic responses to water depth and wave exposure in an aquatic plant (Myrophyllum spicatum). *Journal of Ecology.* 89:166-175.

Schwinge, J., D.E., Wiley, and D.F. Fletcher. 2002. Simulation of the flow around spacer filaments between narrow channel walls. 1. Hydrodynamics. *Industrial and Engineering Chemistry Research.* 41:2977-2987.

Vogel, S. 1994. *Life in Moving Fluids The Physical Biology of Flow.* Princeton University Press, Princeton, N.J. 467 pp.

Wells, C.L., and M. Pigliucci. 2000. Adaptive phenotypic plasticity: the case of heterophylly in aquatic plants. *Perspectives in Plant Ecology, Evolution and Systematics.* 3(1):1-18.

Table 4.1: ANCOVA results for (a) the area covered in dye and (b) the concentration of dye in that area for the different domains for all of the test subjects combined. (Velocity = average flume velocity; Plant = empty test section, circular cylinder, *Elodea, Elodea* with the leaves at every second node removed, *Elodea* with the leaves at every second and third node removed, *Ceratophyllum*, *Ceratophyllum* with the leaves at every second node removed, and *Ceratophyllum* with the leaves at every second and third node removed; Area = area of dye coverage; Conc. = concentration of dye; side/top = side and top perspectives; before/after = upstream and downstream domain). Grey values are significant.

(a)	Univariate Results for Each DV (ancova_spreadsheet_ch2) Sigma-restricted parameterization Effective hypothesis decomposition				
Effect	Degr. of Freedom	area SS	area MS	area F	area p
Intercept	1	213.8189	213.8189	380.6048	0.000000
velocity	1	2.9844	2.9844	5.3124	0.022797
plant	7	18.0545	2.5792	4.5911	0.000133
side/top	1	2.5104	2.5104	4.4687	0.036478
before/after	1	526.8370	526.8370	937.7872	0.000000
plant*side/top	7	3.5427	0.5061	0.9009	0.508095
plant*before/after	7	13.6716	1.9531	3.4766	0.001927
side/top*before/after	1	5.3689	5.3689	9.5567	0.002449
plant*side/top*before/after	7	3.6078	0.5154	0.9174	0.495361
Error	127	71.3470	0.5618		
Total	159	647.9242			

(b)	Univariate Results for Each DV (ancova_spreadsheet_ch2) Sigma-restricted parameterization Effective hypothesis decomposition			
Effect	conc. SS	conc. MS	conc. F	conc. p
Intercept	25.73763	25.73763	537.2375	0.000000
velocity	5.30758	5.30758	110.7884	0.000000
plant	0.73668	0.10524	2.1967	0.038698
side/top	0.36289	0.36289	7.5749	0.006786
before/after	0.57799	0.57799	12.0648	0.000703
plant*side/top	0.11445	0.01635	0.3413	0.933496
plant*before/after	0.62744	0.08963	1.8710	0.079586
side/top*before/after	0.07847	0.07847	1.6380	0.202932
plant*side/top*before/after	0.21367	0.03052	0.6372	0.724427
Error	6.08424	0.04791		
Total	14.10342			

Table 4.2: ANCOVA results for the area of dye coverage and the concentration of dye for (a) the circular cylinder, (b) *Elodea*, (c) *Elodea* with the leaves at every second node removed, and (d) *Elodea* with the leaves at every second and third node removed.

(a)

Univariate Results for Each DV (Cylinder)
Sigma-restricted parameterization
Effective hypothesis decomposition

Effect	Degr. of Freedom	area SS	area MS	area F	area p	conc. SS	conc. MS	conc. F	conc. p
Intercept	1	22.0598	22.05984	22.21238	0.000278	1.978697	1.978697	95.67204	0.000000
velocity	1	5.4365	5.43651	5.47411	0.033544	0.437853	0.437853	21.17066	0.000346
side/top	1	0.4346	0.43455	0.43756	0.518336	0.016504	0.016504	0.79797	0.385807
before/after	1	95.6839	95.68394	96.34554	0.000000	0.033497	0.033497	1.61964	0.222516
side/top*before/after	1	0.3294	0.32944	0.33172	0.573188	0.000428	0.000428	0.02070	0.887524
Error	15	14.8970	0.99313			0.310231	0.020682		
Total	19	116.7814				0.798514			

(b)

Univariate Results for Each DV (*Elodea*)
Sigma-restricted parameterization
Effective hypothesis decomposition

Effect	Degr. of Freedom	area SS	area MS	area F	area p	conc. SS	conc. MS	conc. F	conc. p
Intercept	1	40.6380	40.63798	111.6627	0.000000	2.949523	2.949523	120.1269	0.000000
velocity	1	0.1589	0.15888	0.4366	0.518806	0.649332	0.649332	26.4457	0.000120
side/top	1	0.4885	0.48855	1.3424	0.264725	0.029748	0.029748	1.2116	0.288375
before/after	1	92.4244	92.42442	253.9585	0.000000	0.028255	0.028255	1.1508	0.300344
side/top*before/after	1	1.7768	1.77681	4.8822	0.043100	0.078995	0.078995	3.2173	0.093045
Error	15	5.4590	0.36394			0.368301	0.024553		
Total	19	100.3077				1.154631			

(c)

Univariate Results for Each DV (*Elodea* 2nd)
Sigma-restricted parameterization
Effective hypothesis decomposition

Effect	Degr. of Freedom	area SS	area MS	area F	area p	conc. SS	conc. MS	conc. F	conc. p
Intercept	1	27.41857	27.41857	108.3929	0.000000	1.351336	1.351336	41.09747	0.000016
velocity	1	0.91044	0.91044	3.5992	0.078628	0.174365	0.174365	5.30288	0.037153
side/top	1	0.07360	0.07360	0.2910	0.598076	0.116977	0.116977	3.55756	0.080193
before/after	1	83.12936	83.12936	328.6323	0.000000	0.108770	0.108770	3.30796	0.090396
side/top*before/after	1	0.14255	0.14255	0.5635	0.465267	0.102537	0.102537	3.11839	0.099202
Error	14	3.54138	0.25296			0.460337	0.032881		
Total	18	89.33794				0.999678			

(d)

Univariate Results for Each DV (*Elodea* 3rd)
Sigma-restricted parameterization
Effective hypothesis decomposition

Effect	Degr. of Freedom	area SS	area MS	area F	area p	conc. SS	conc. MS	conc. F	conc. p
Intercept	1	28.67930	28.67930	108.2845	0.000000	3.083176	3.083176	96.75612	0.000000
velocity	1	0.02018	0.02018	0.0762	0.786266	0.732808	0.732808	22.99695	0.000236
side/top	1	0.38676	0.38676	1.4603	0.245589	0.129212	0.129212	4.05494	0.062343
before/after	1	56.47179	56.47179	213.2207	0.000000	0.049666	0.049666	1.55861	0.231004
side/top*before/after	1	0.08260	0.08260	0.3119	0.584784	0.000477	0.000477	0.01498	0.904222
Error	15	3.97277	0.26485			0.477982	0.031865		
Total	19	60.93410				1.390145			

Table 4.3: Post hoc comparisons between *Elodea* and its associated manipulations for the area covered in dye in the (a) side perspective upstream, (b) in the top perspective upstream, (c) in the side perspective downstream, and (d) in the top perspective downstream. Significant results indicated in bold. (*Elodea* 2^{nd} = *Elodea* with every second node removed; *Elodea* 3^{rd} = *Elodea* with every second and third node removed)

(a)

	Cylinder	*Elodea*	*Elodea* 2^{nd}	*Elodea* 3^{rd}	Empty flume
Cylinder					
Elodea	0.84				
Elodea 2^{nd}	0.94	0.9			
Elodea 3^{rd}	0.76	0.91	0.81		
Empty flume	0.73	0.88	0.79	0.97	

(b)	Cylinder	*Elodea*	*Elodea* 2^{nd}	*Elodea* 3^{rd}	Empty flume
Cylinder					
Elodea	0.63				
Elodea 2^{nd}	0.91	0.71			
Elodea 3^{rd}	0.93	0.70	0.98		
Empty flume	0.99	0.62	0.90	0.92	

(c)	Cylinder	*Elodea*	*Elodea* 2^{nd}	*Elodea* 3^{rd}	Empty flume
Cylinder					
Elodea	0.72				
Elodea 2^{nd}	0.24	0.13			
Elodea 3^{rd}	**0.001**	**< 0.001**	**0.039**		
Empty flume	**0.003**	**0.001**	0.071	0.8	

(d)	Cylinder	*Elodea*	*Elodea* 2^{nd}	*Elodea* 3^{rd}	Empty flume
Cylinder					
Elodea	0.69				
Elodea 2^{nd}	0.96	0.73			
Elodea 3^{rd}	0.22	0.40	0.24		
Empty flume	**< 0.001**	**< 0.001**	**< 0.001**	**< 0.001**	

Table 4.4: ANCOVA results for the area of dye coverage and the concentration of dye for (a) the circular cylinder, (b) *Ceratophyllum*, (c) *Ceratophyllum* with the leaves at every second node removed, and (d) *Ceratophyllum* with the leaves at every second and third node removed.

(a)

Univariate Results for Each DV (Cylinder)
Sigma-restricted parameterization
Effective hypothesis decomposition

Effect	Degr. of Freedom	area SS	area MS	area F	area p	conc. SS	conc. MS	conc. F	conc. p
Intercept	1	22.0598	22.05984	22.21238	0.000278	1.978697	1.978697	95.67204	0.000000
velocity	1	5.4365	5.43651	5.47411	0.033544	0.437853	0.437853	21.17066	0.000346
side/top	1	0.4346	0.43455	0.43756	0.518336	0.016504	0.016504	0.79797	0.385807
before/after	1	95.6839	95.68394	96.34554	0.000000	0.033497	0.033497	1.61964	0.222516
side/top*before/after	1	0.3294	0.32944	0.33172	0.573188	0.000428	0.000428	0.02070	0.887524
Error	15	14.8970	0.99313			0.310231	0.020682		
Total	19	116.7814				0.798514			

(b)

Univariate Results for Each DV (*Ceratophyllum*)
Sigma-restricted parameterization
Effective hypothesis decomposition

Effect	Degr. of Freedom	area SS	area MS	area F	area p	conc. SS	conc. MS	conc. F	conc. p
Intercept	1	43.71454	43.71454	109.4433	0.000000	3.492296	3.492296	32.72128	0.000041
velocity	1	1.35136	1.35136	3.3833	0.085738	0.446894	0.446894	4.18720	0.058675
side/top	1	1.69315	1.69315	4.2390	0.057310	0.152006	0.152006	1.42423	0.251243
before/after	1	65.79465	65.79465	164.7228	0.000000	0.005253	0.005253	0.04921	0.827427
side/top*before/after	1	1.87377	1.87377	4.6912	0.046839	0.033108	0.033108	0.31021	0.585767
Error	15	5.99140	0.39943			1.600929	0.106729		
Total	19	76.70433				2.238190			

(c)

Univariate Results for Each DV (*Ceratophyllum* 2nd)
Sigma-restricted parameterization
Effective hypothesis decomposition

Effect	Degr. of Freedom	area SS	area MS	area F	area p	conc. SS	conc. MS	conc. F	conc. p
Intercept	1	20.26384	20.26384	65.0744	0.000001	2.454023	2.454023	104.3530	0.000000
velocity	1	0.24563	0.24563	0.7888	0.388484	0.291062	0.291062	12.3769	0.003106
side/top	1	0.25525	0.25525	0.8197	0.379584	0.061093	0.061093	2.5979	0.127844
before/after	1	49.58870	49.58870	159.2470	0.000000	0.148957	0.148957	6.3341	0.023707
side/top*before/after	1	0.46875	0.46875	1.5053	0.238762	0.001925	0.001925	0.0819	0.778716
Error	15	4.67092	0.31139			0.352748	0.023517		
Total	19	55.22925				0.855785			

(d)

Univariate Results for Each DV (*Ceratophyllum* 3rd)
Sigma-restricted parameterization
Effective hypothesis decomposition

Effect	Degr. of Freedom	area SS	area MS	area F	area p	conc. SS	conc. MS	conc. F	conc. p
Intercept	1	21.88786	21.88786	28.40197	0.000084	4.919771	4.919771	106.5441	0.000000
velocity	1	2.13744	2.13744	2.77357	0.116574	1.097093	1.097093	23.7590	0.000202
side/top	1	0.11254	0.11254	0.14603	0.707719	0.013358	0.013358	0.2893	0.598574
before/after	1	65.82507	65.82507	85.41545	0.000000	0.227015	0.227015	4.9163	0.042470
side/top*before/after	1	0.80929	0.80929	1.05014	0.321717	0.085267	0.085267	1.8466	0.194266
Error	15	11.55969	0.77065			0.692639	0.046176		
Total	19	80.44402				2.115372			

Table 4.5: Post hoc comparisons between *Ceratophyllum* and its associated manipulations for the area covered in dye in the (a) side perspective upstream, (b) in the top perspective upstream, (c) in the side perspective downstream, and (d) in the top perspective downstream. Significant results indicated in bold. (*Ceratophyllum* 2^{nd} = *Ceratophyllum* with every second node removed; *Ceratophyllum* 3^{rd} = *Ceratophyllum* with every second and third node removed)

(a)	Cylinder	*Ceratophyllum*	*Ceratophyllum* 2^{nd}	*Ceratophyllum* 3^{rd}	Empty flume
Cylinder					
Ceratophyllum	0.91				
Ceratophyllum 2^{nd}	0.78	0.87			
Ceratophyllum 3^{rd}	0.88	0.98	0.89		
Empty flume	0.73	0.82	0.95	0.84	

(b)	Cylinder	*Ceratophyllum*	*Ceratophyllum* 2^{nd}	*Ceratophyllum* 3^{rd}	Empty flume
Cylinder					
Ceratophyllum	0.98				
Ceratophyllum 2^{nd}	0.97	0.95			
Ceratophyllum 3^{rd}	0.64	0.66	0.62		
Empty flume	0.99	0.97	0.98	0.63	

(c)	Cylinder	*Ceratophyllum*	*Ceratophyllum* 2^{nd}	*Ceratophyllum* 3^{rd}	Empty flume
Cylinder					
Ceratophyllum	0.35				
Ceratophyllum 2^{nd}	**0.006**	0.07			
Ceratophyllum 3^{rd}	0.16	0.64	0.18		
Empty flume	**0.003**	**0.042**	0.82	0.11	

(d)	Cylinder	*Ceratophyllum*	*Ceratophyllum* 2^{nd}	*Ceratophyllum* 3^{rd}	Empty flume
Cylinder					
Ceratophyllum	**0.023**				
Ceratophyllum 2^{nd}	**0.007**	0.67			
Ceratophyllum 3^{rd}	0.16	0.38	0.19		
Empty flume	**< 0.001**	**0.005**	**0.015**	**< 0.001**	

Table 4.6: Post hoc comparisons between *Elodea* and its associated manipulations for the concentration of dye in the (a) side perspective upstream, (b) in the top perspective upstream, (c) in the side perspective downstream, and (d) in the top perspective downstream. Significant results indicated in bold.

(a)	Cylinder	*Elodea*	*Elodea* 2nd	*Elodea* 3rd	Empty flume
Cylinder					
Elodea	0.74				
Elodea 2nd	0.54	0.34			
Elodea 3rd	0.58	0.38	0.95		
Empty flume	0.70	0.47	0.82	0.87	

(b)	Cylinder	*Elodea*	*Elodea* 2nd	*Elodea* 3rd	Empty flume
Cylinder					
Elodea	0.72				
Elodea 2nd	0.37	0.59			
Elodea 3rd	0.74	0.49	0.22		
Empty flume	0.89	0.82	0.45	0.64	

(c)	Cylinder	*Elodea*	*Elodea* 2nd	*Elodea* 3rd	Empty flume
Cylinder					
Elodea	0.53				
Elodea 2nd	0.56	0.96			
Elodea 3rd	0.37	0.79	0.75		
Empty flume	**0.002**	**0.012**	**0.011**	**0.024**	

(d)	Cylinder	*Elodea*	*Elodea* 2nd	*Elodea* 3rd	Empty flume
Cylinder					
Elodea	0.11				
Elodea 2nd	0.075	0.85			
Elodea 3rd	0.13	0.91	0.77		
Empty flume	**0.029**	0.56	0.69	0.49	

Table 4.7: Post hoc comparisons between *Ceratophyllum* and its associated manipulations for the concentration of dye in the (a) side perspective upstream, (b) in the top perspective upstream, (c) in the side perspective downstream, and (d) in the top perspective downstream. Significant results indicated in bold.

(a)	Cylinder	*Ceratophyllum*	*Ceratophyllum* 2nd	*Ceratophyllum* 3rd	Empty flume
Cylinder					
Ceratophyllum	0.33				
Ceratophyllum 2nd	0.65	0.15			
Ceratophyllum 3rd	0.42	0.87	0.20		
Empty flume	0.70	0.17	0.95	0.23	

(b)	Cylinder	*Ceratophyllum*	*Ceratophyllum* 2nd	*Ceratophyllum* 3rd	Empty flume
Cylinder					
Ceratophyllum	0.19				
Ceratophyllum 2nd	0.89	0.24			
Ceratophyllum 3rd	0.92	0.16	0.81		
Empty flume	0.89	0.15	0.79	0.97	

(c)	Cylinder	*Ceratophyllum*	*Ceratophyllum* 2nd	*Ceratophyllum* 3rd	Empty flume
Cylinder					
Ceratophyllum	0.42				
Ceratophyllum 2nd	0.11	0.44			
Ceratophyllum 3rd	**0.040**	0.21	0.63		
Empty flume	**0.002**	**0.020**	0.11	0.27	

(d)	Cylinder	*Ceratophyllum*	*Ceratophyllum* 2nd	*Ceratophyllum* 3rd	Empty flume
Cylinder					
Ceratophyllum	**0.031**				
Ceratophyllum 2nd	0.080	0.68			
Ceratophyllum 3rd	**0.004**	0.47	0.26		
Empty flume	**0.029**	0.98	0.66	0.48	

Table 4.8: (a) ANCOVA and (b) post hoc comparisons for the angle of the *Ceratophyllum* leaves (and the manipulations thereof) from the stem in the up and downstream position. Significant results indicated in bold.

(a)	Univariate Results for Each DV (leaf angle) Sigma-restricted parameterization Effective hypothesis decomposition				
Effect	Degr. of Freedom	angle SS	angle MS	angle F	angle p
Intercept	1	167470.3	167470.3	845.3146	0.000000
velocity	1	1556.2	1556.2	7.8551	0.005646
plant	2	2149.5	1074.8	5.4250	0.005187
front/back	1	436.3	436.3	2.2022	0.139636
plant***front/back**	2	1281.1	640.6	3.2333	0.041823
Error	173	34274.0	198.1		
Total	179	39944.6			

(b)	*Cerato* Up	*Cerato* Down	*Cerato* 2nd Up	*Cerato* 2nd Down	*Cerato* 3rd Up	*Cerato* 3rd Down
Cerato Up						
Cerato Down	**0.0019**					
Cerato 2nd Up	**0.0049**	0.93				
Cerato 2nd Down	**0.0051**	0.86	0.94			
Cerato 3rd Up	**<0.001**	0.33	0.31	0.27		
Cerato 3rd Down	**<0.001**	0.43	0.40	0.36	0.86	

Table 4.9: (a) ANCOVA and (b) post hoc comparisons for the angle of deflection between *Elodea* and *Ceratophyllum* and there associated manipulations. Significant results indicated in bold.

(a)	Univariate Results for Each DV (plant angle) Sigma-restricted parameterization Effective hypothesis decomposition				
Effect	Degr. of Freedom	Angle SS	Angle MS	Angle F	Angle p
Intercept	1	81.18	81.181	1.11304	0.298862
Velocity	1	7072.33	7072.327	96.96575	0.000000
Plant	6	7655.67	1275.944	17.49395	0.000000
Error	34	2479.84	72.936		
Total	41	17207.83			

(b)	Cylinder	*Elodea*	*Elodea* 2nd	*Elodea* 3rd	*Cerato*	*Cerato 2nd*	*Cerato 3rd*
Cylinder							
Elodea	**0.0018**						
Elodea 2nd	0.53	**0.0097**					
Elodea 3rd	0.048	0.19	0.16				
Cerato	**<0.001**	**<0.001**	**<0.001**	**<0.001**			
Cerato 2nd	**<0.001**	0.70	**0.003**	0.098	**<0.001**		
Cerato 3rd	**<0.001**	0.10	**<0.001**	**0.0053**	**0.0031**	0.21	

Table 4.10: (a) ANCOVA and (b) post hoc comparisons for the frequency of oscillations for *Elodea, Ceratophyllum*, and there associated manipulations. Significant results indicated in bold.

(a)	Univariate Results for Each DV (oscillations) Sigma-restricted parameterization Effective hypothesis decomposition				
Effect	Degr. of Freedom	oscillations per second SS	oscillations per second MS	oscillations per second F	oscillations per second p
Intercept	1	0.007968	0.007968	0.39643	0.534231
Velocity	1	1.155310	1.155310	57.47910	0.000000
Plant	6	0.577107	0.096185	4.78538	0.001923
Error	27	0.542690	0.020100		
Total	34	2.275107			

(b)	Cylinder	*Elodea*	*Elodea* 2nd	*Elodea* 3rd	*Cerato*	*Cerato* 2nd	*Cerato* 3rd
Cylinder							
Elodea	**<0.001**						
Elodea 2nd	**0.005**	0.14					
Elodea 3rd	**<0.001**	0.61	0.32				
Cerato	**<0.001**	0.83	0.20	0.76			
Cerato 2nd	**0.001**	0.31	0.63	0.60	0.42		
Cerato 3rd	**<0.001**	0.59	0.34	0.97	0.74	0.63	

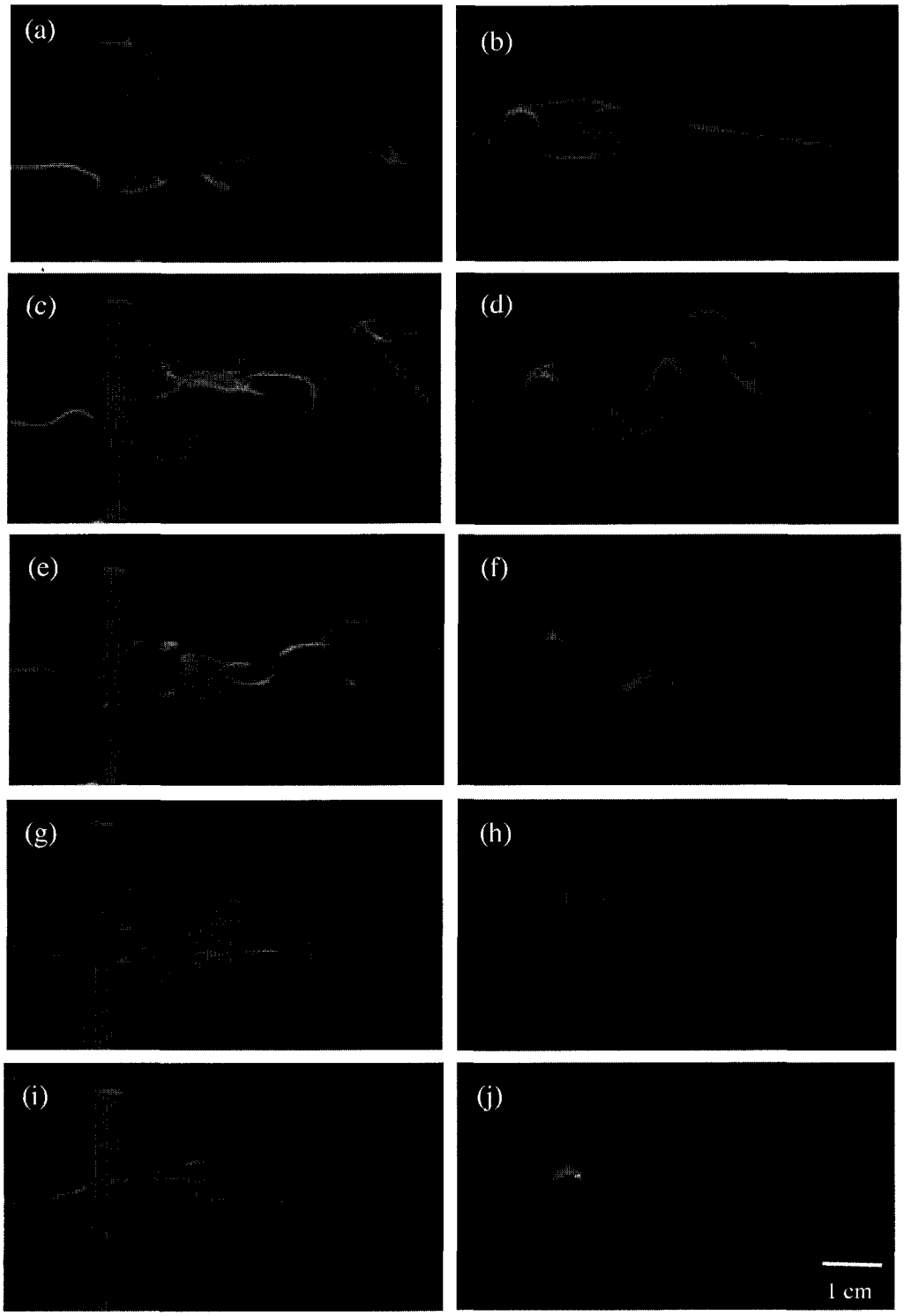

Figure 4.1: Flow visualization around a 0.7 cm diameter circular cylinder using fluoroscein dye in the side (left) and the top (right) perspectives. Velocities increase from top to bottom panels [(a) and (b) are 1.3 cms^{-1}, (c) and (d) are 2.0 cms^{-1}, (e) and (f) are 5.0 cms^{-1}, (g) and (h) are 8.4 cms^{-1}, and (i) and (j) are 11.0 cms^{-1}]. Flow is from left to right. Top and side photos were taken sequentially.

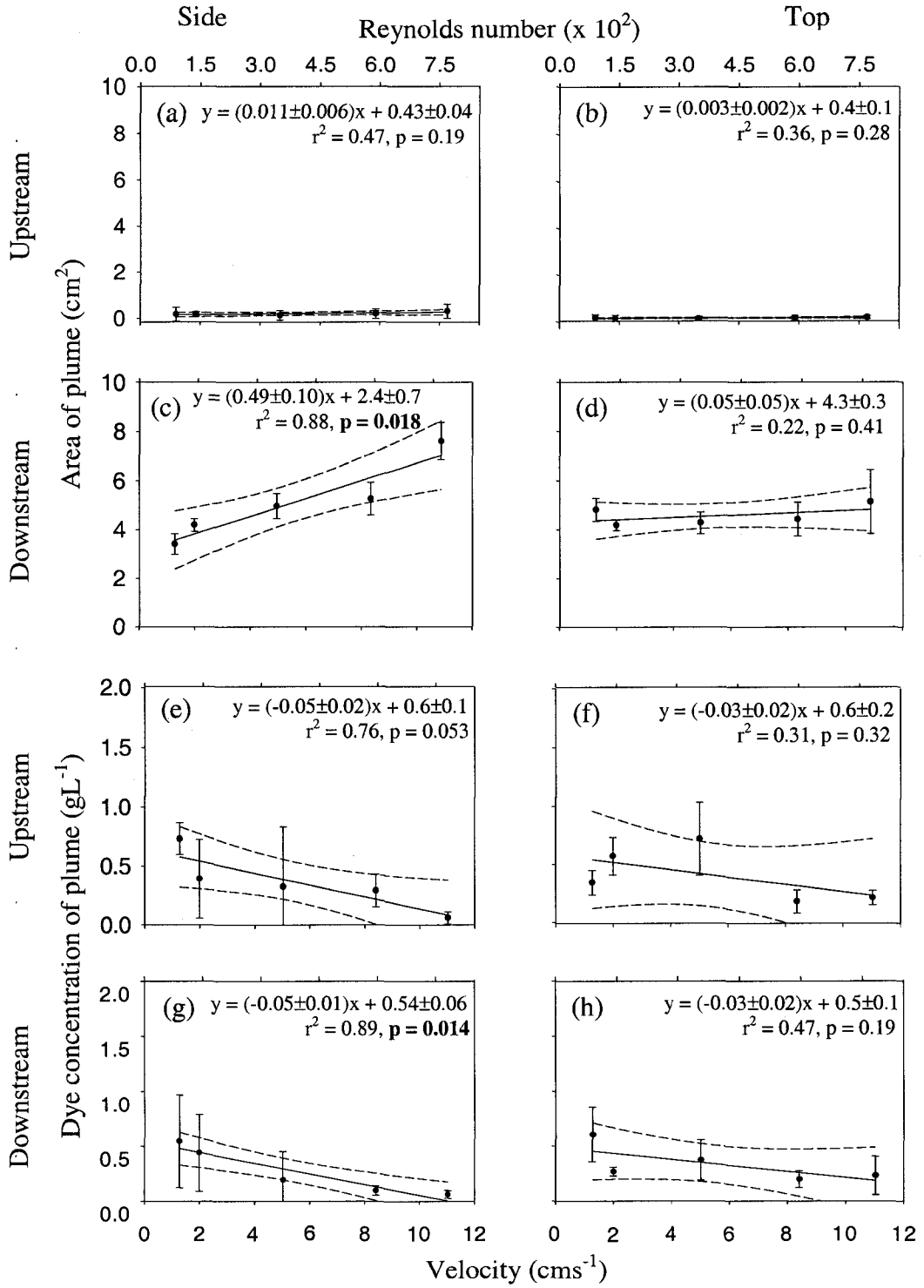

Figure 4.2: Regression of area of dye coverage (a-d) and concentration of dye (e-h) versus velocity or Reynolds number (based on the diameter) in the different domains for the circular cylinder: (a) and (e) upstream in the side perspective, (b) and (f) upstream in the top perspective, (c) and (g) downstream in the side perspective, and (d) and (h) downstream in the top perspective. Solid line is the regression and dotted lines are the 95% confidence limits of the mean.

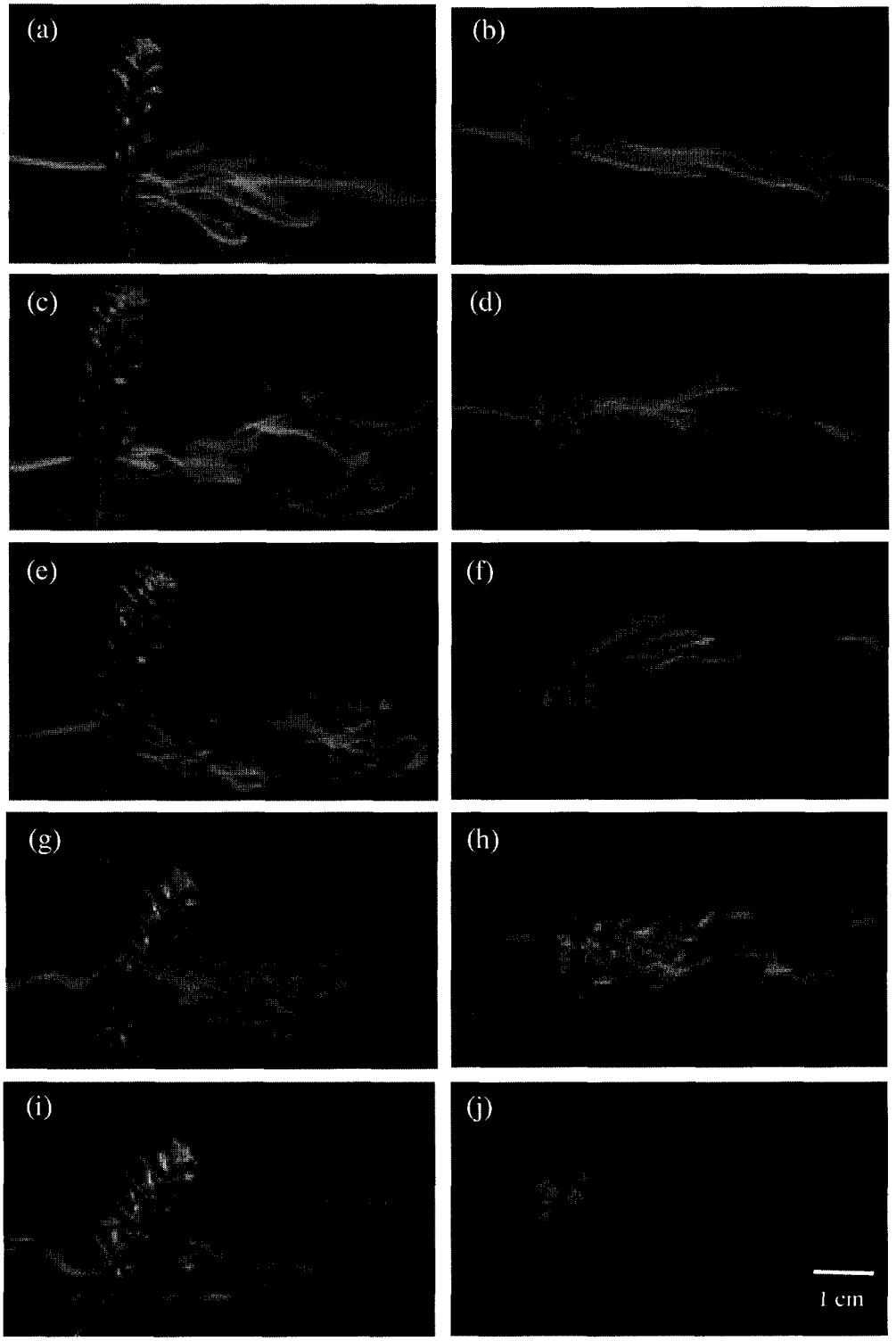

Figure 4.3: Flow visualization around *Elodea canadensis* using fluoroscein dye in the side (left) and the top (right) perspectives. Velocities increase from top to bottom panels [(a) and (b) are 1.3 cms^{-1}, (c) and (d) are 2.0 cms^{-1}, (e) and (f) are 5.0 cms^{-1}, (g) and (h) are 8.4 cms^{-1}, and (i) and (j) are 11.0 cms^{-1}]. Flow is from left to right. Top and side photos were taken sequentially.

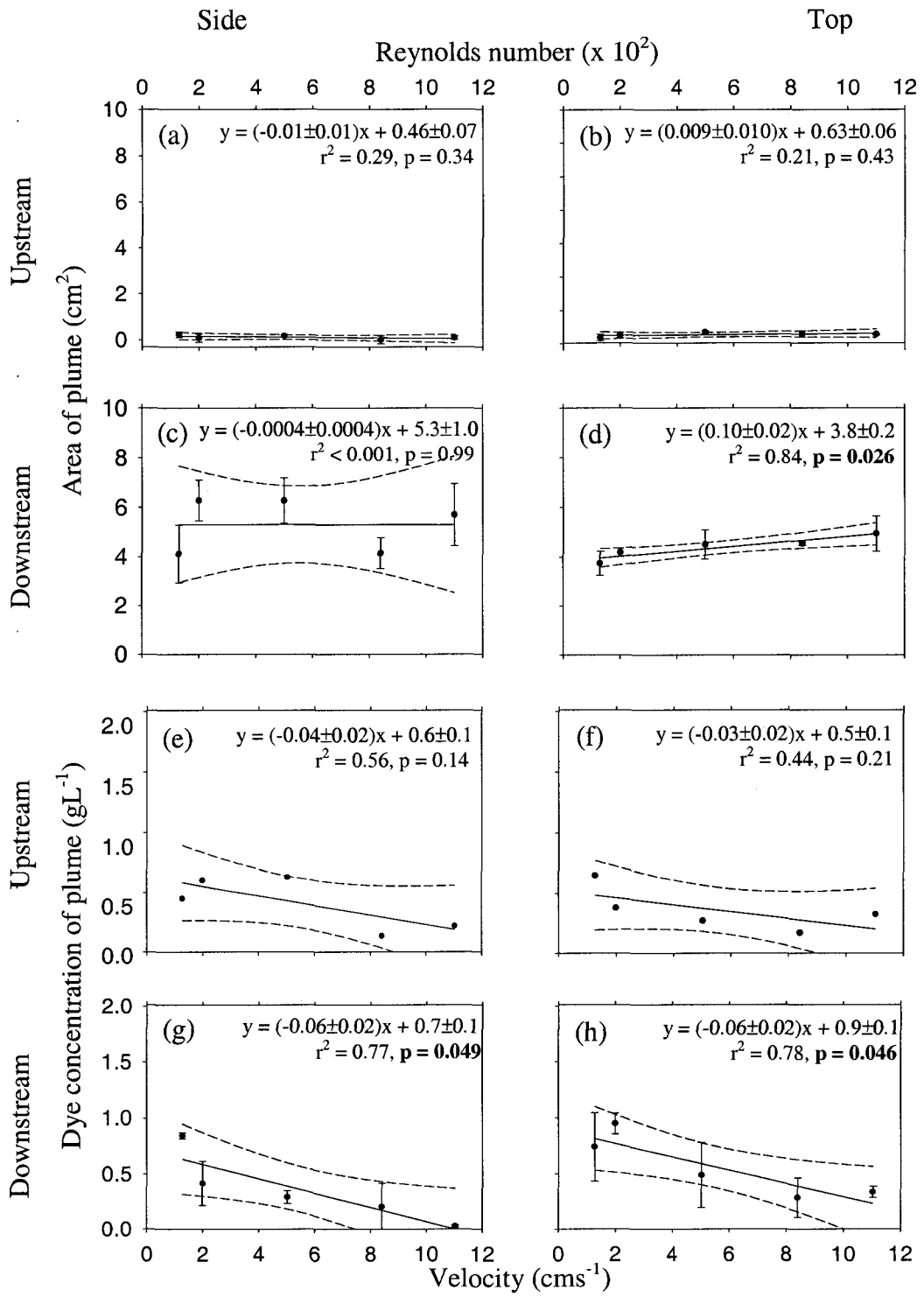

Figure 4.4: Regression of area of dye coverage (a-d) and concentration of dye (e-h) versus velocity or stem Reynolds number (based on the plant diameter) in the different domains for *Elodea canadensis*: (a) and (e) upstream in the side perspective, (b) and (f) upstream in the top perspective, (c) and (g) downstream in the side perspective, and (d) and (h) downstream in the top perspective. Solid line is the regression and dotted lines are the 95% confidence limits of the mean.

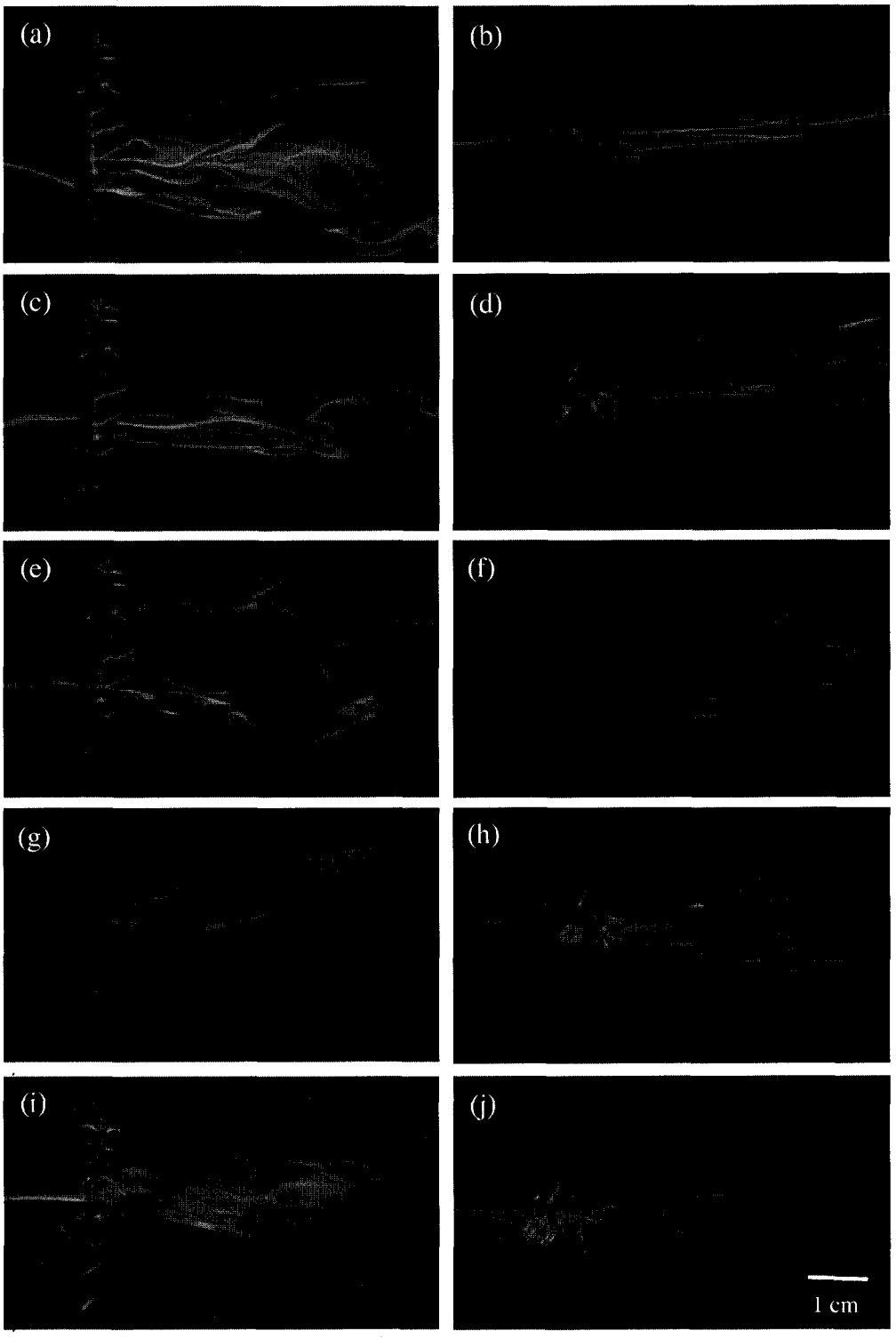

Figure 4.5: Flow visualization around *Elodea* with the whorl at every second node removed using fluoroscein dye in the side (left) and the top (right) perspectives. Velocities increase from top to bottom panels [(a) and (b) are 1.3 cms^{-1}, (c) and (d) are 2.0 cms^{-1}, (e) and (f) are 5.0 cms^{-1}, (g) and (h) are 8.4 cms^{-1}, and (i) and (j) are 11.0 cms^{-1}]. Flow is from left to right. Top and side photos we re taken sequentially.

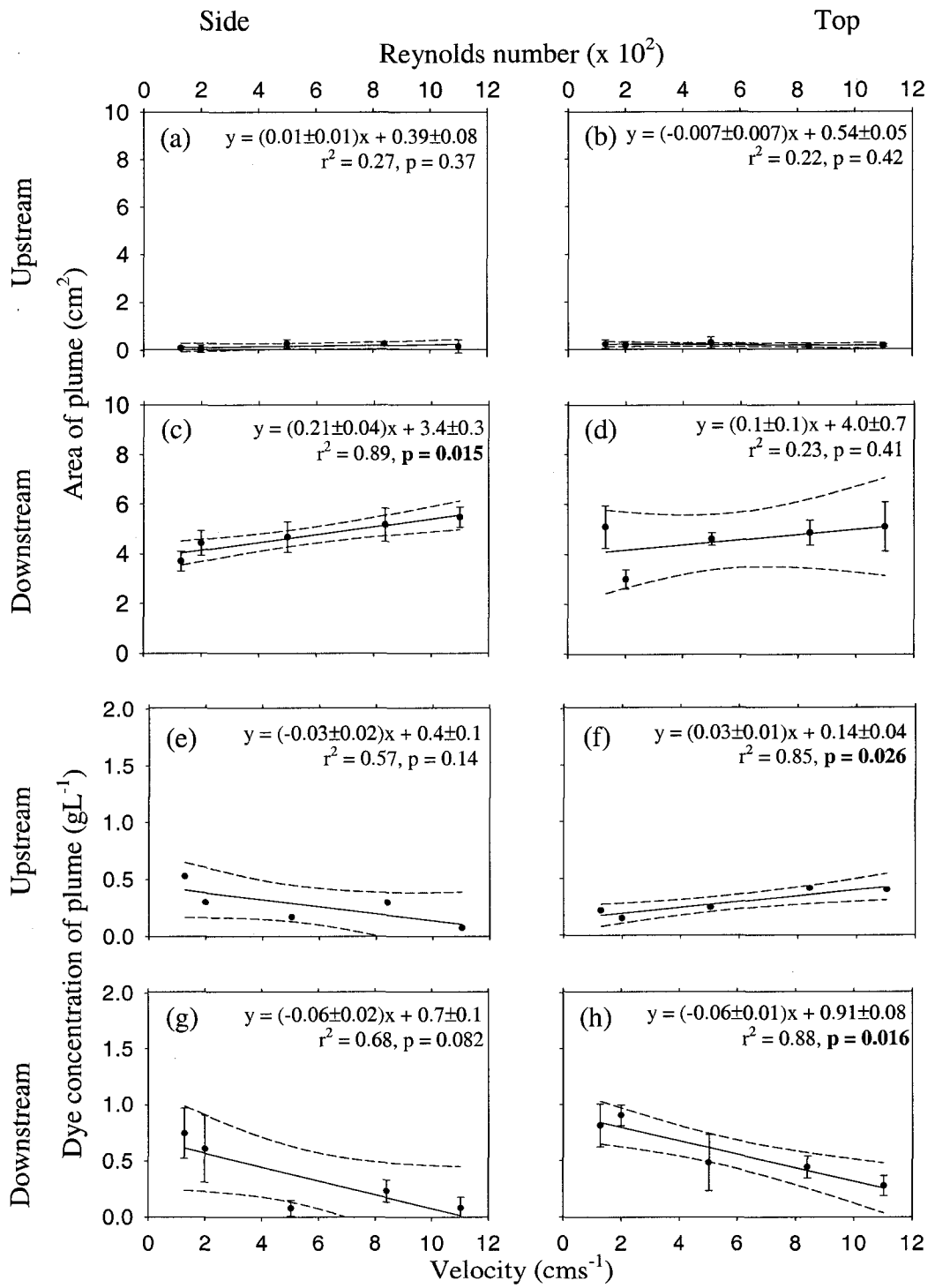

Figure 4.6: Regression of area of dye coverage (a-d) and concentration of dye (e-h) versus velocity or stem Reynolds number (based on the plant diameter) in the different domains for *Elodea canadensis* with every second node removed: (a) and (e) upstream in the side perspective, (b) and (f) upstream in the top perspective, (c) and (g) downstream in the side perspective, and (d) and (h) downstream in the top perspective. Solid line is the regression and dotted lines are the 95% confidence limits of the mean.

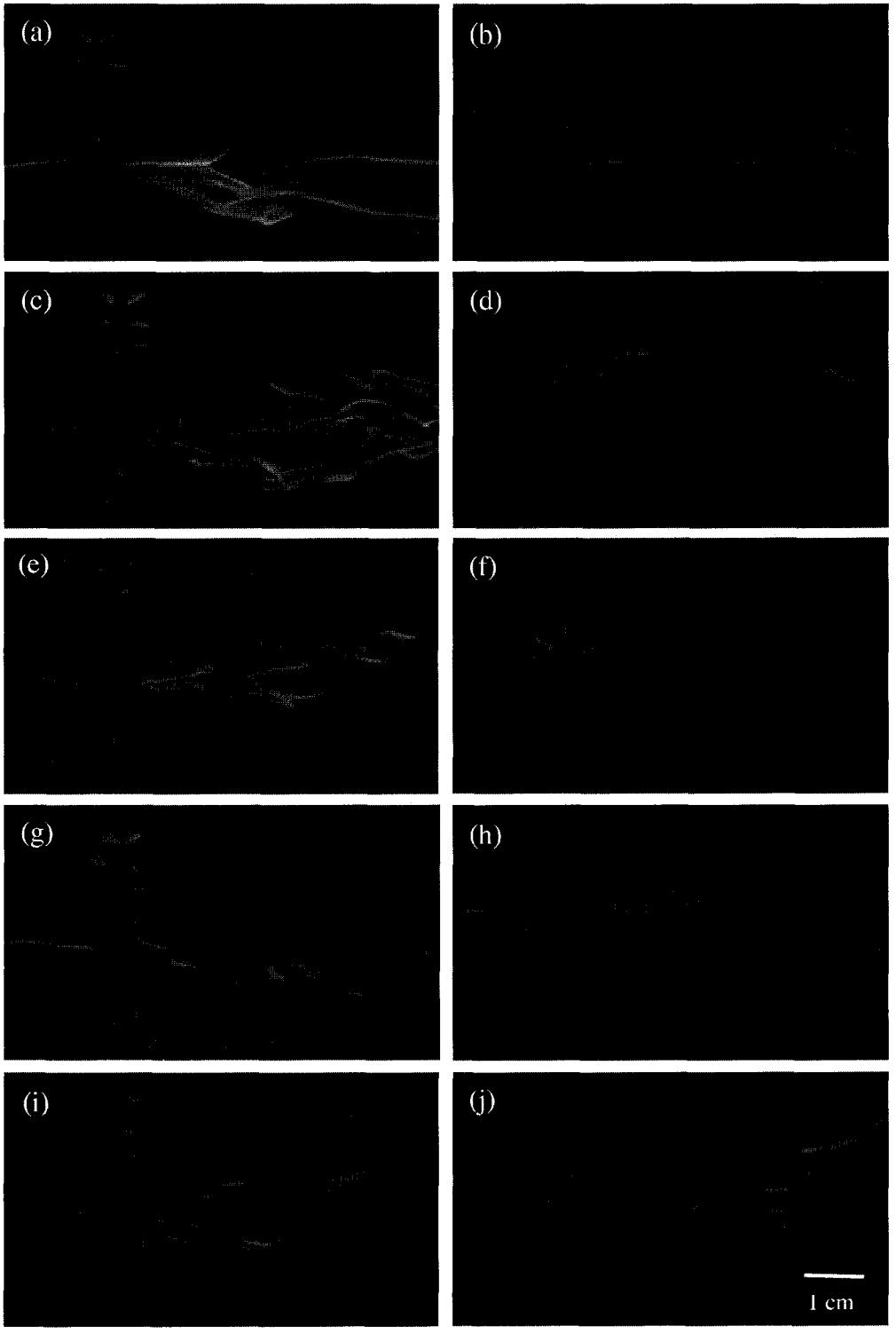

Figure 4.7: Flow visualization around *Elodea* with the whorls at every second and third node removed using fluoroscein dye in the side (left) and the top (right) perspectives. Velocities increase from top to bottom panels [(a) and (b) are 1.3 cms^{-1}, (c) and (d) are 2.0 cms^{-1}, (e) and (f) are 5.0 cms^{-1}, (g) and (h) are 8.4 cms^{-1}, and (i) and (j) are 11.0 cms^{-1}]. Flow is from left to right. Top and side photos were taken sequentially.

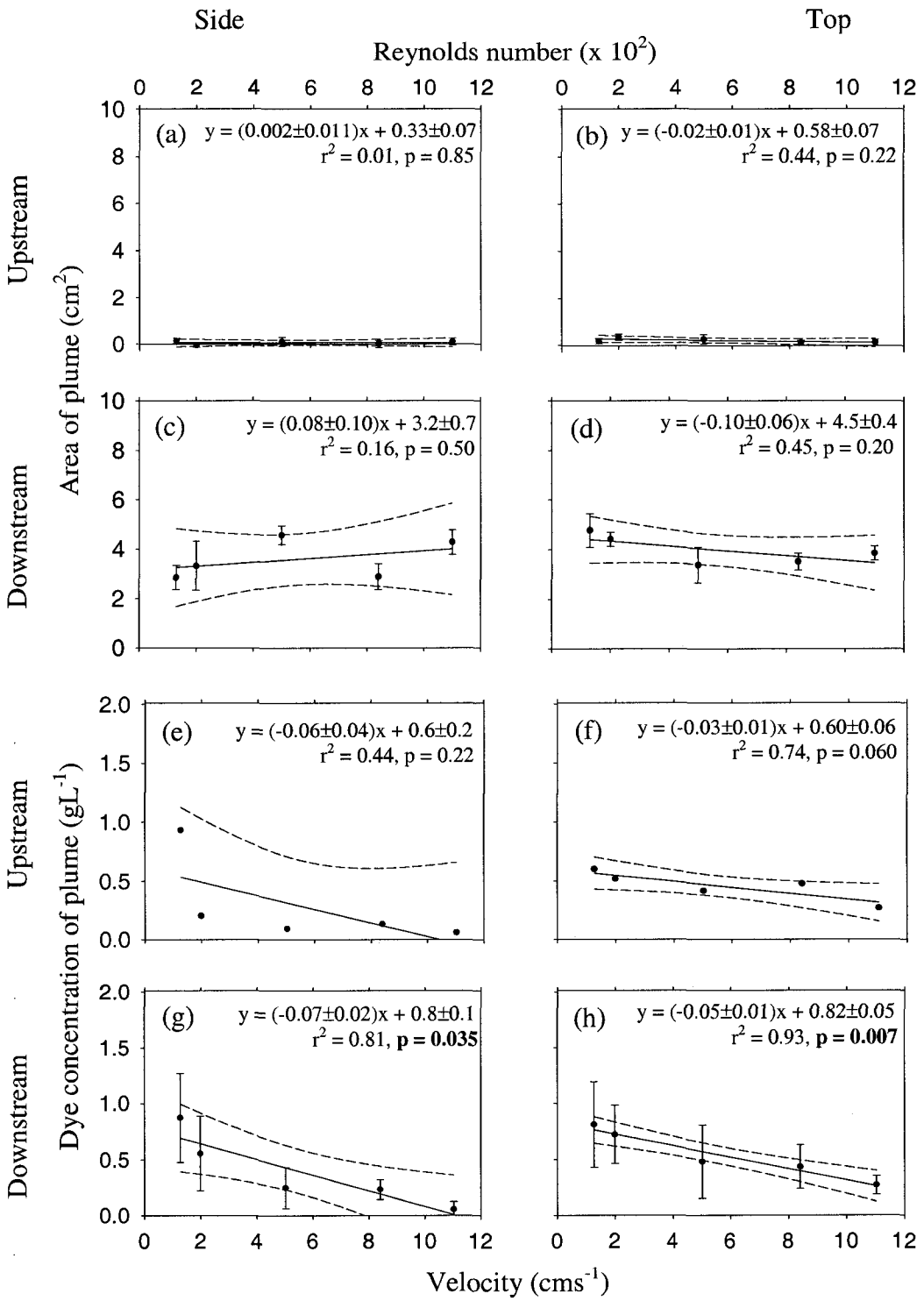

Figure 4.8: Regression of area of dye coverage (a-d) and concentration of dye (e-h) versus velocity or stem Reynolds number (based on the plant diameter) in the different domains for *Elodea canadensis* with every second and third node removed: (a) and (e) upstream in the side perspective, (b) and (f) upstream in the top perspective, (c) and (g) downstream in the side perspective, and (d) and (h) downstream in the top perspective. Solid line is the regression and dotted lines are the 95% confidence limits of the mean.

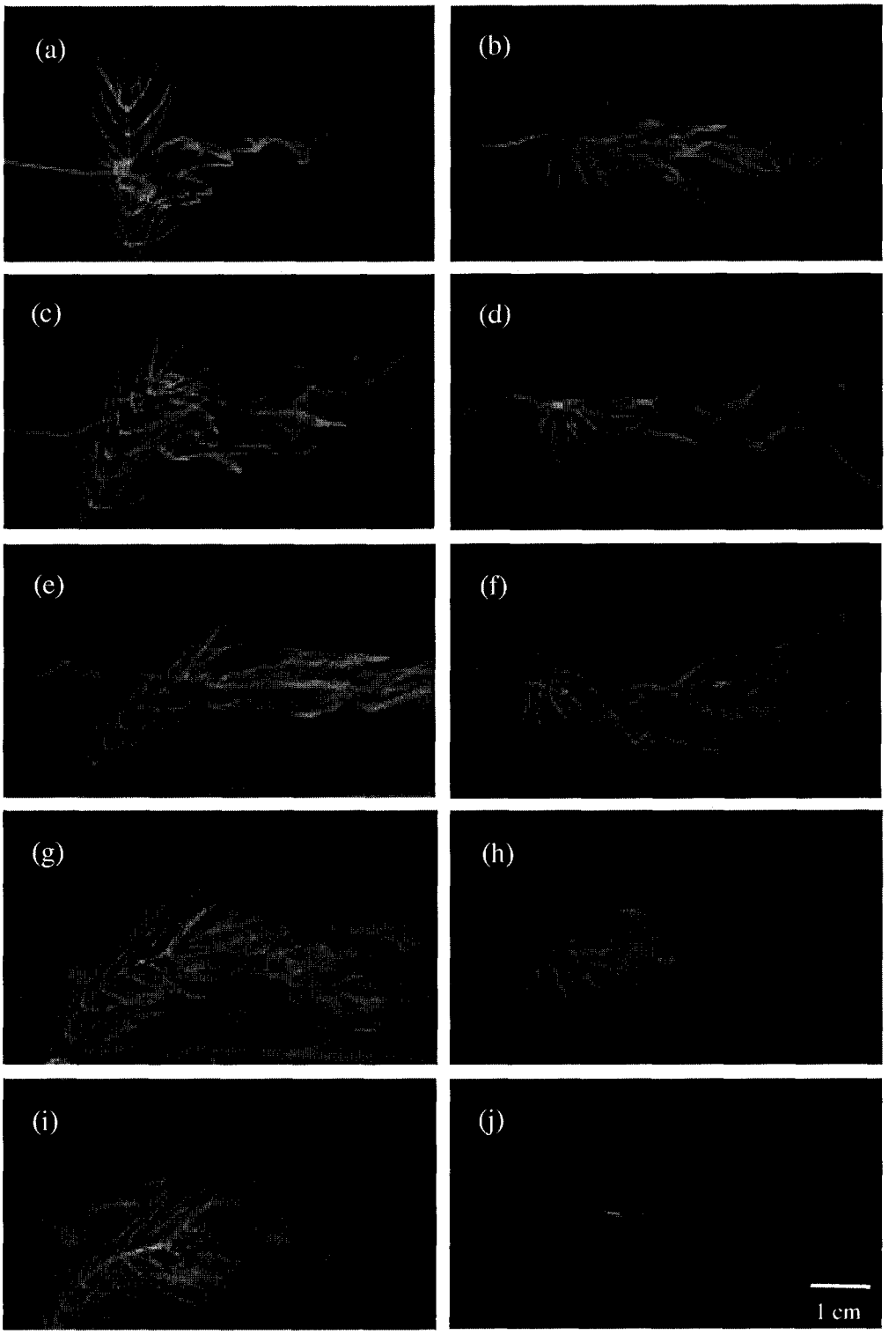

Figure 4.9: Flow visualization around *Ceratophyllum demersum* using fluoroscein dye in the side (left) and the top (right) perspectives. Velocities increase from top to bottom panels [(a) and (b) are 1.3 cms^{-1}, (c) and (d) are 2.0 cms^{-1}, (e) and (f) are 5.0 cms^{-1}, (g) and (h) are 8.4 cms^{-1}, and (i) and (j) are 11.0 cms^{-1}]. Flow is from left to right. Top and side photos were taken sequentially.

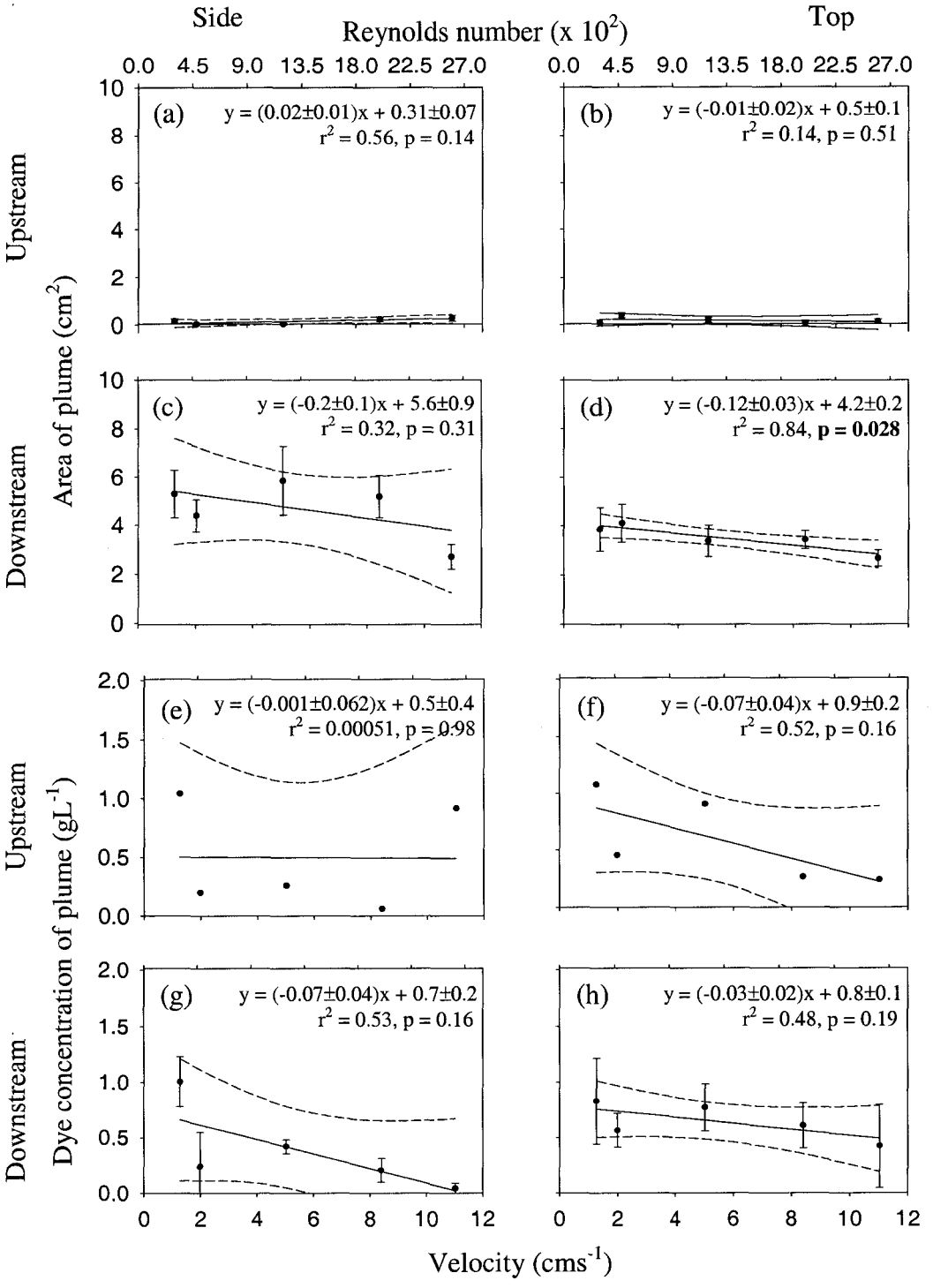

Figure 4.10: Regression of area of dye coverage (a-d) and concentration of dye (e-h) versus velocity or stem Reynolds number (based on the diameter) in the different domains for *Ceratophyllum demersum*: (a) and (e) upstream in the side perspective, (b) and (f) upstream in the top perspective, (c) and (g) downstream in the side perspective, and (d) and (h) downstream in the top perspective. Solid line is the regression and dotted lines are the 95% confidence limits of the mean.

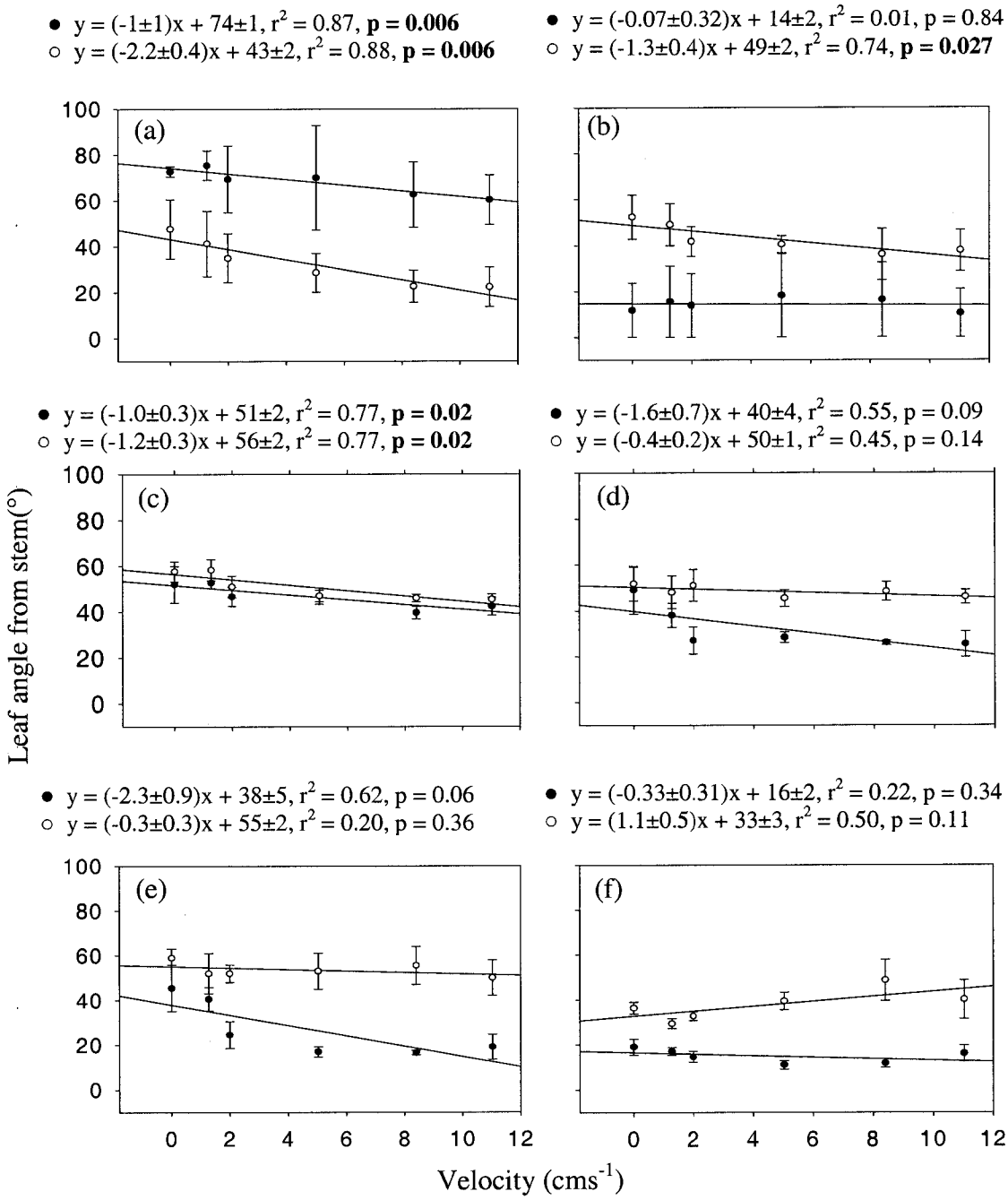

Figure 4.11: Regression analysis for the leaf angle from the stem of *Ceratophyllum* in the upstream (i.e., faces the oncoming flow; •) and downstream (i.e., in the wake of the flow; ○) position from the plant stem (a) is the bottom most leaf, (b) is the second leaf from the bottom, (c) is the third leaf from the bottom, (d) is the fourth leaf from the bottom, (e) is the fifth leaf from the bottom, and (f) is the top most leaf (apex).

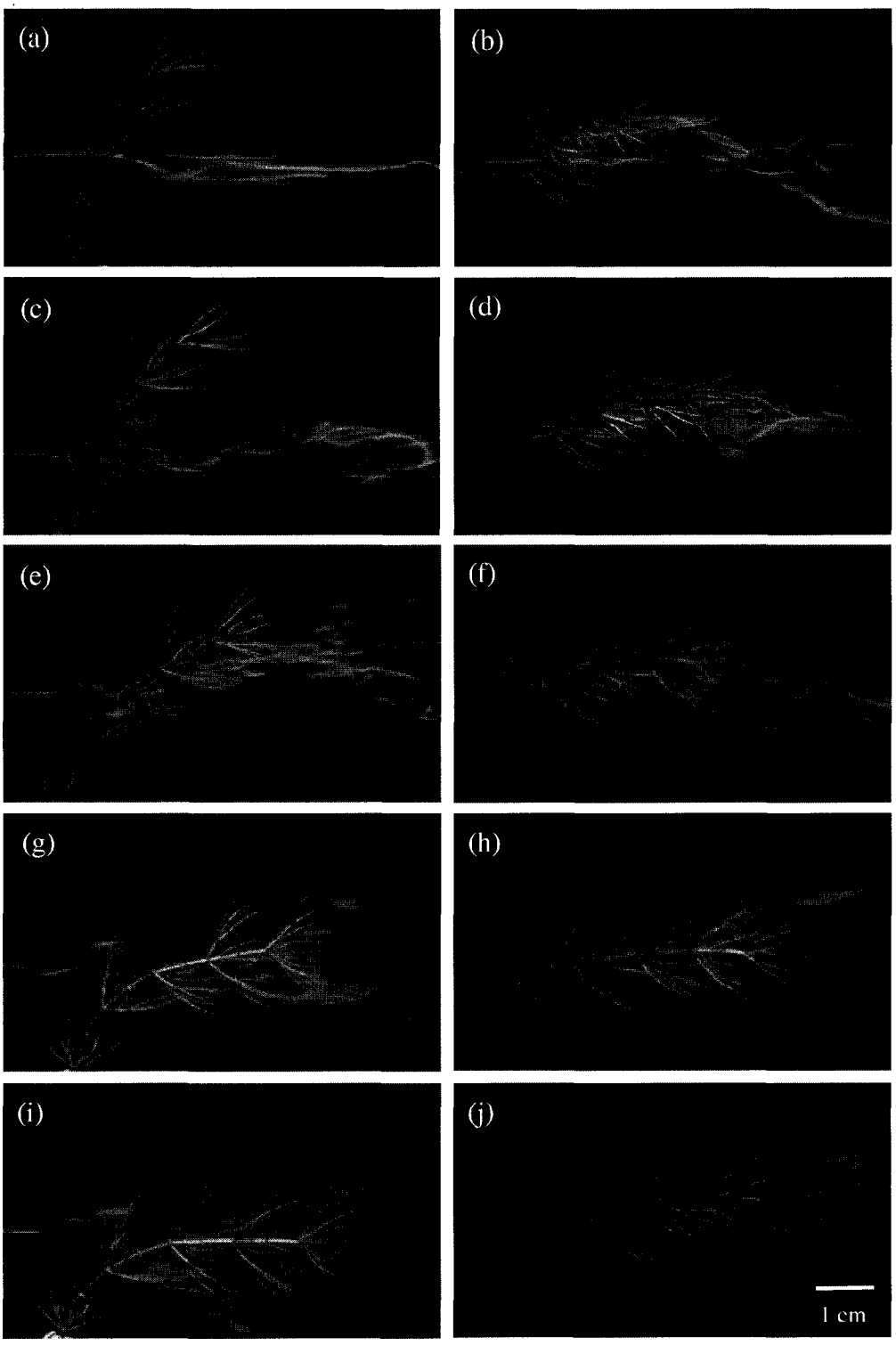

Figure 4.12: Flow visualization around *Ceratophyllum* with the whorl at every second node removed using fluoroscein dye in the side (left) and the top (right) perspectives. Velocities increase from top to bottom panels [(a) and (b) are 1.3 cms^{-1}, (c) and (d) are 2.0 cms^{-1}, (e) and (f) are 5.0 cms^{-1}, (g) and (h) are 8.4 cms^{-1}, and (i) and (j) are 11.0 cms^{-1}]. Flow is from left to right. Top and side photos were taken sequentially.

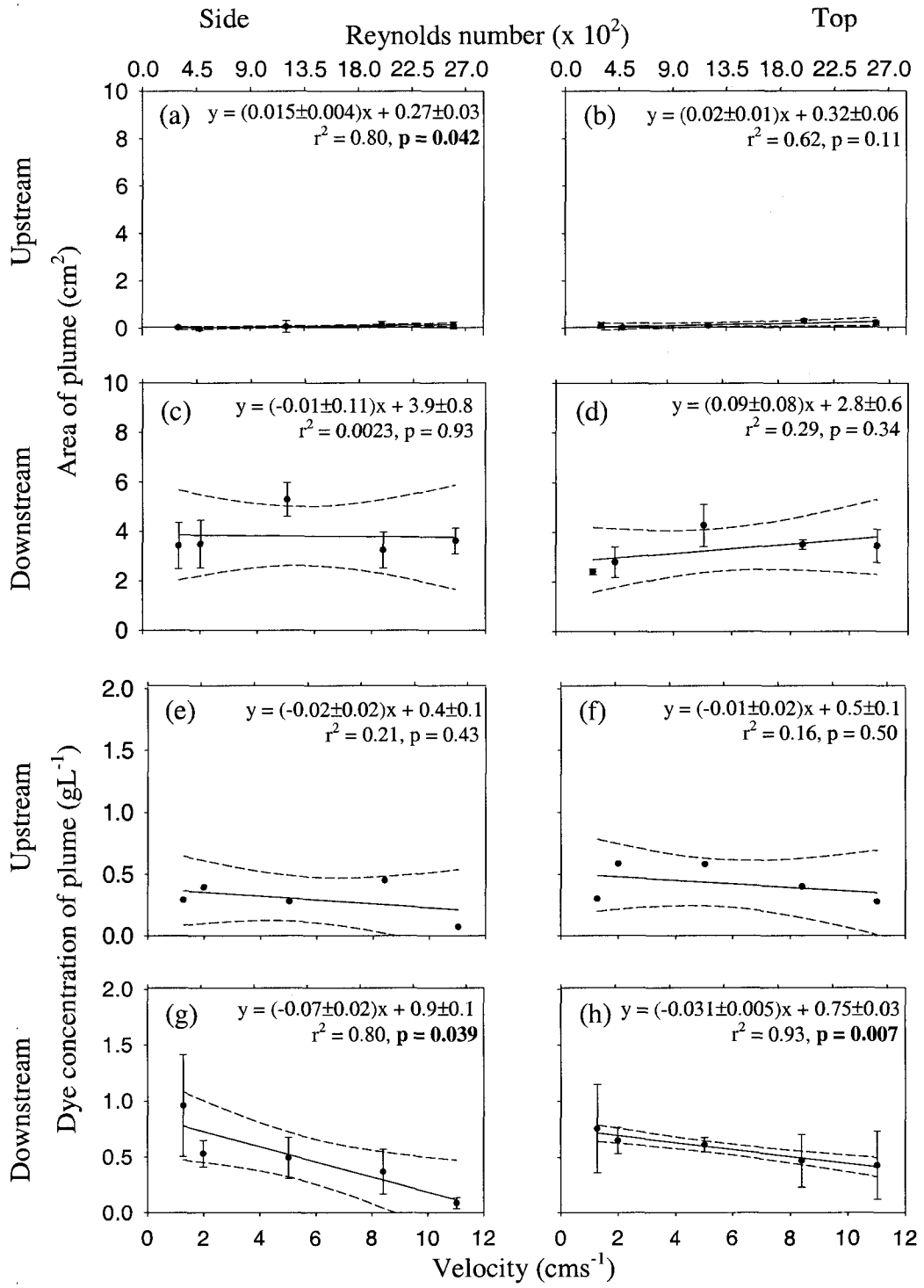

Figure 4.13: Regression of area of dye coverage (a-d) and concentration of dye (e-h) versus velocity or stem Reynolds number (based on the diameter) in the different domains for *Ceratophyllum demersum* with every second node removed: (a) and (e) upstream in the side perspective, (b) and (f) upstream in the top perspective, (c) and (g) downstream in the side perspective, and (d) and (h) downstream in the top perspective. Solid line is the regression and dotted lines are the 95% confidence limits of the mean.

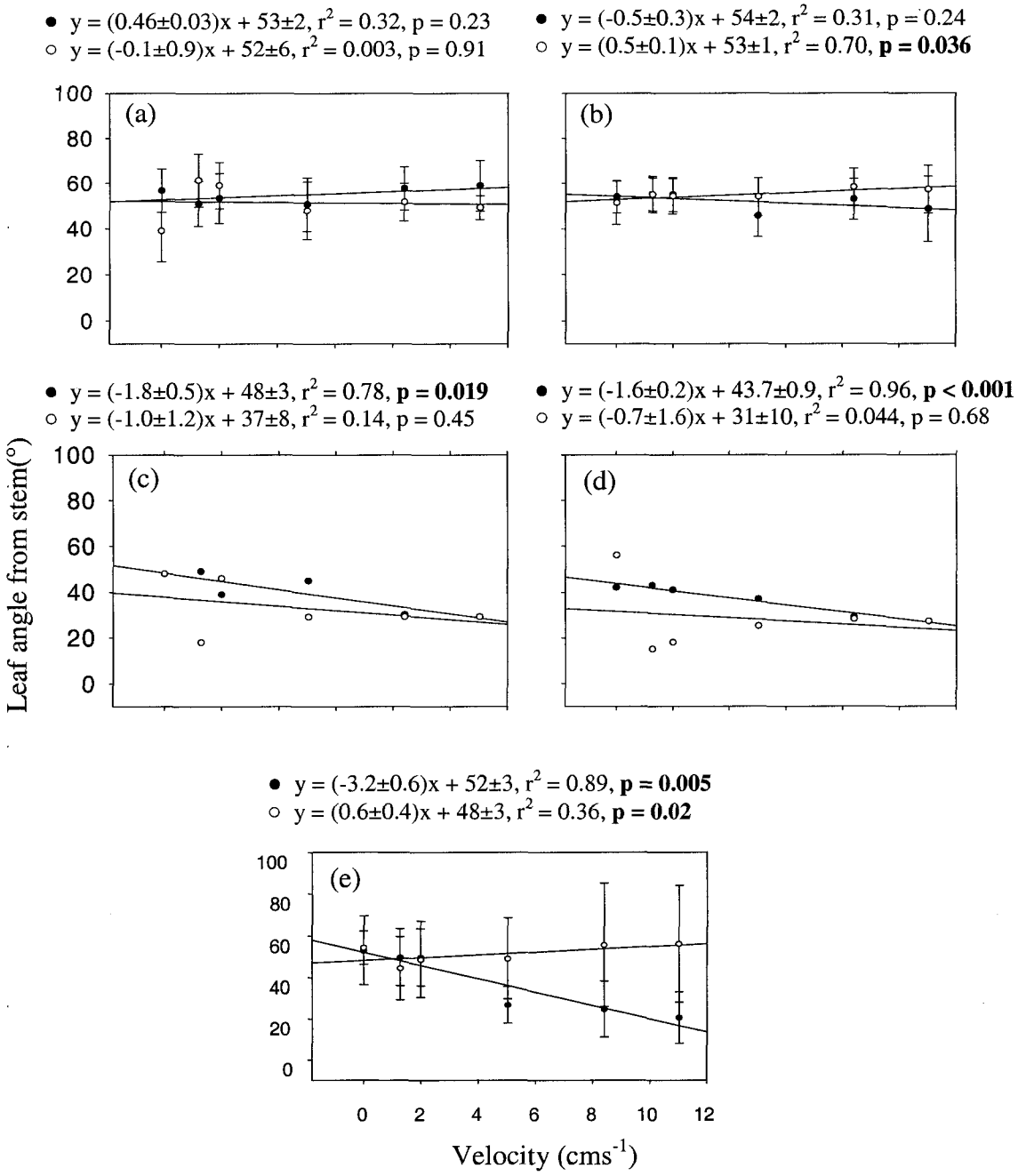

Figure 4.14: Regression analysis for the leaf angle from the stem of the *Ceratophyllum* with every second node removed in the upstream (i.e., faces the oncoming flow; •) and downstream (i.e., in the wake of the flow; ○) position from the plant stem (a) is the bottom most leaf, (b) is the second leaf from the bottom, (c) is the third leaf from the bottom, (d) is the fourth leaf from the bottom, and (e) is the top most leaf (apex).

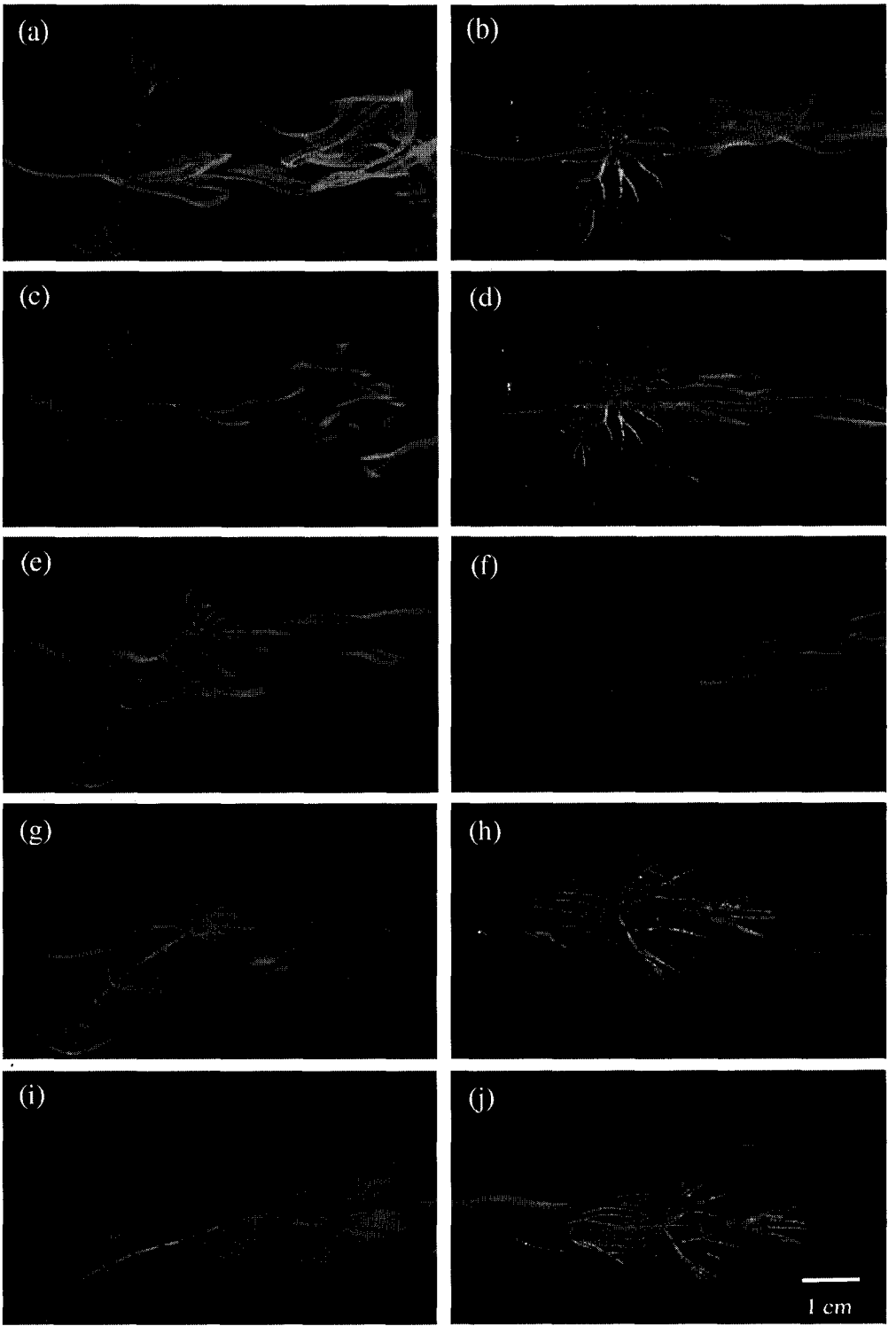

Figure 4.15: Flow visualization around *Ceratophyllum* with the whorl at every second and third node removed using fluoroscein dye in the side (left) and the top (right) perspectives. Velocities increase from top to bottom panels [(a) and (b) are 1.3 cms^{-1}, (c) and (d) are 2.0 cms^{-1}, (e) and (f) are 5.0 cms^{-1}, (g) and (h) are 8.4 cms^{-1}, and (i) and (j) are 11.0 cms^{-1}]. Flow is from left to right. Top and side photos were taken sequentially.

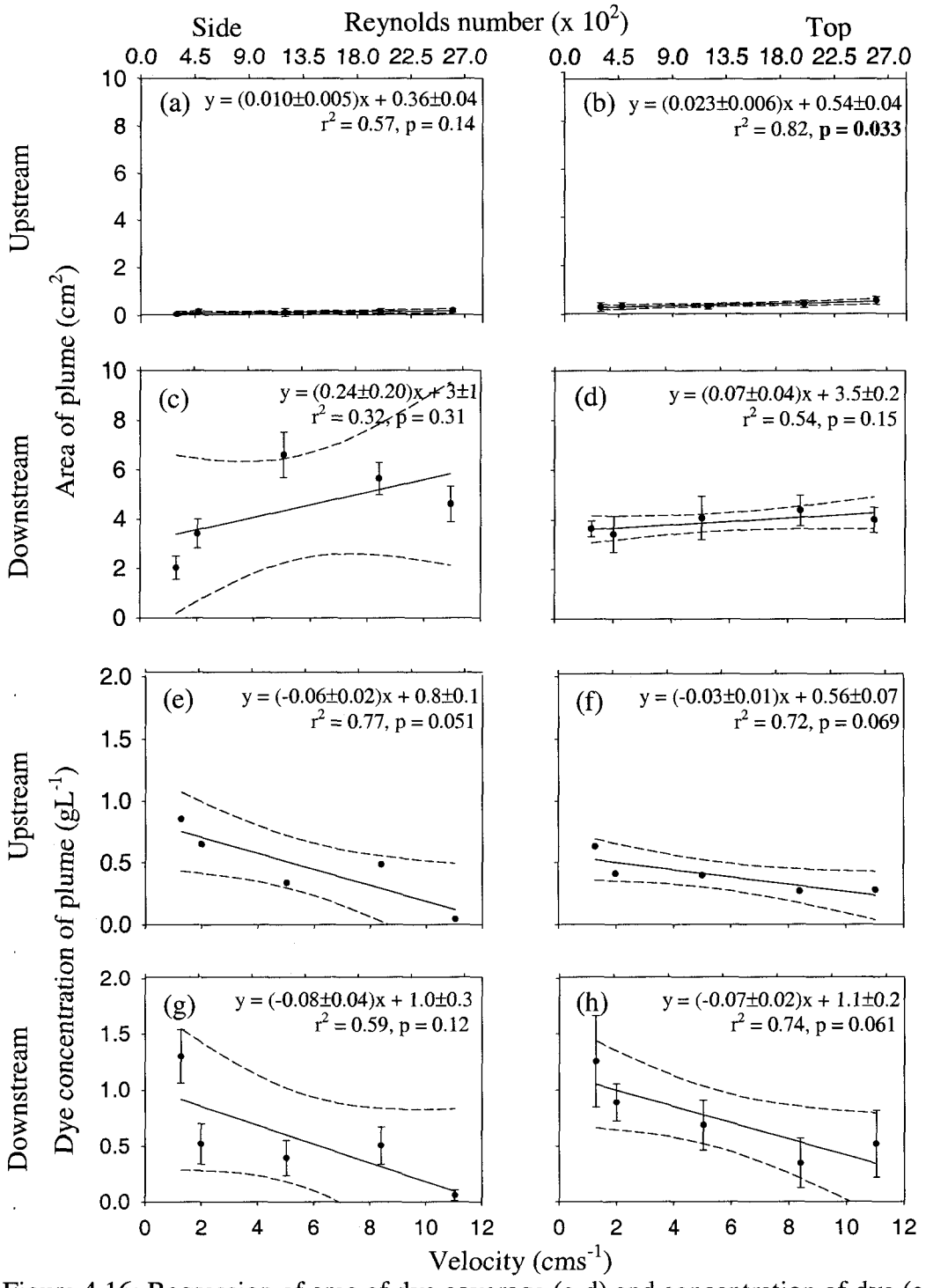

Figure 4.16: Regression of area of dye coverage (a-d) and concentration of dye (e-h) versus velocity or stem Reynolds number (based on the diameter) in the different domains for *Ceratophyllum demersum* with every second and third node removed: (a) and (e) upstream in the side perspective, (b) and (f) upstream in the top perspective, (c) and (g) downstream in the side perspective, and (d) and (h) downstream in the top perspective. Solid line is the regression and dotted lines are the 95% confidence limits of the mean.

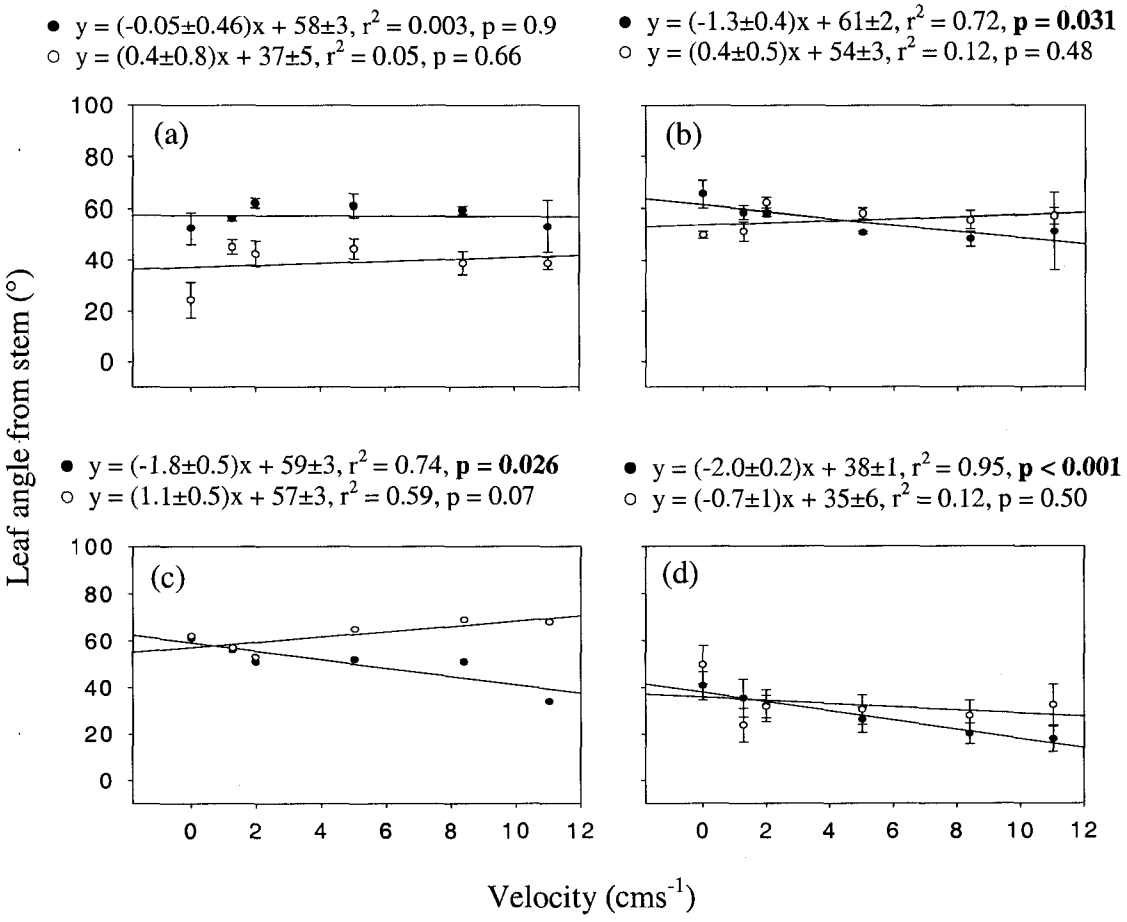

Figure 4.17: Regression analysis for the leaf angle from the stem of the *Ceratophyllum* with every second and third node removed in the upstream (i.e., faces the oncoming flow; •) and downstream (i.e., in the wake of the flow; ○) position from the plant stem (a) is the bottom most leaf, (b) is the second leaf from the bottom, (c) is the third leaf from the bottom, and (d) is the top most leaf (apex).

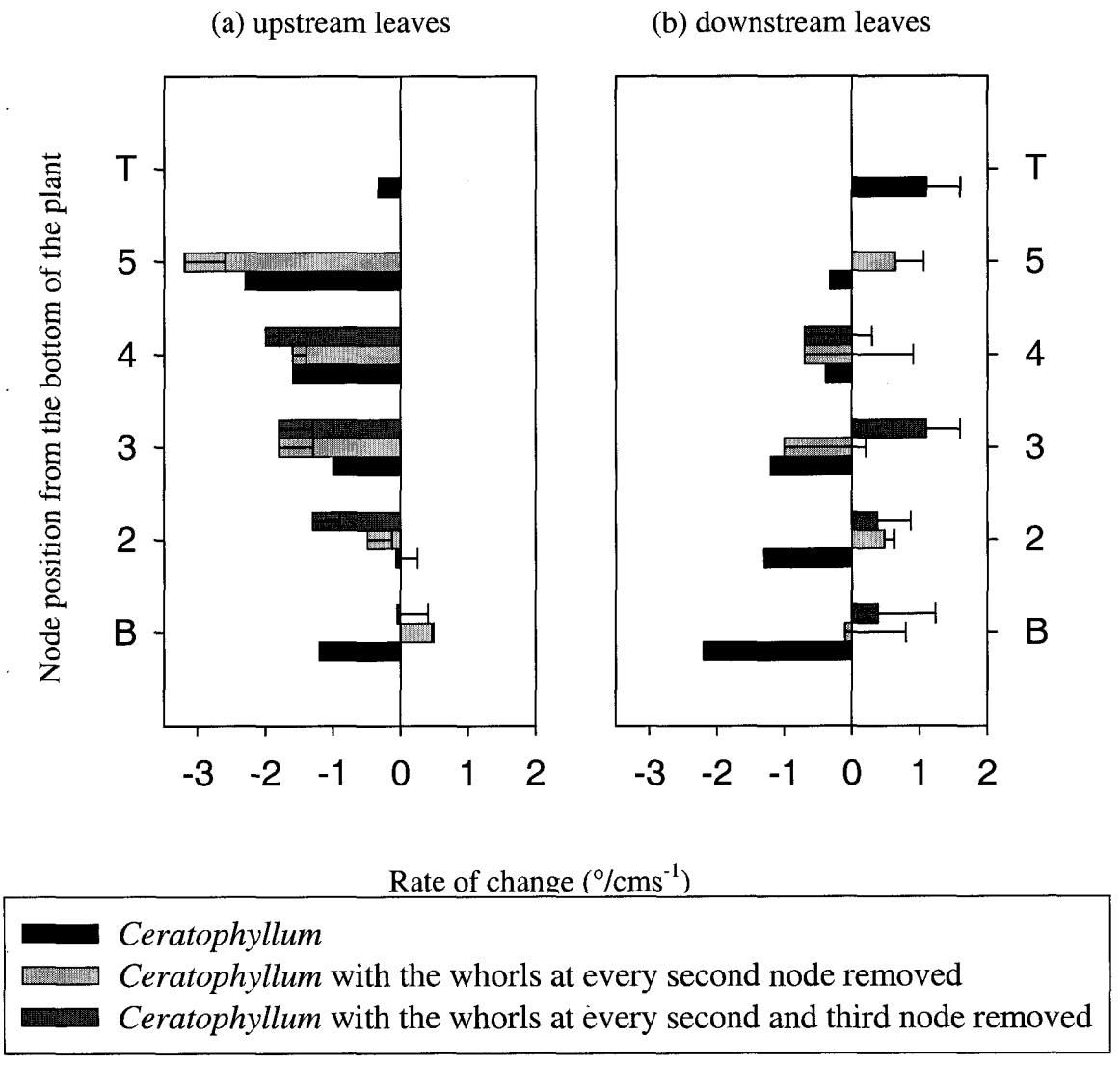

Figure 4.18: The rate of change in the angle of the leaf from the stem with change in velocity for *Ceratophyllum* and its associated manipulations for the leaves (a) facing the approaching flow (i.e., on the upstream side of the plant) and (b) in the downstream flow (i.e., on the downstream side of the plant).

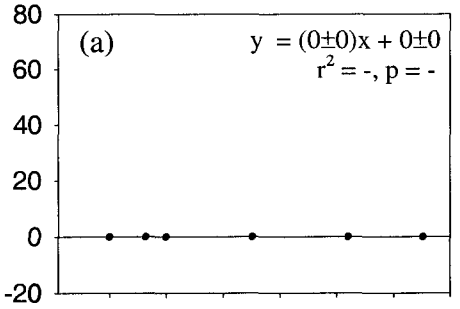

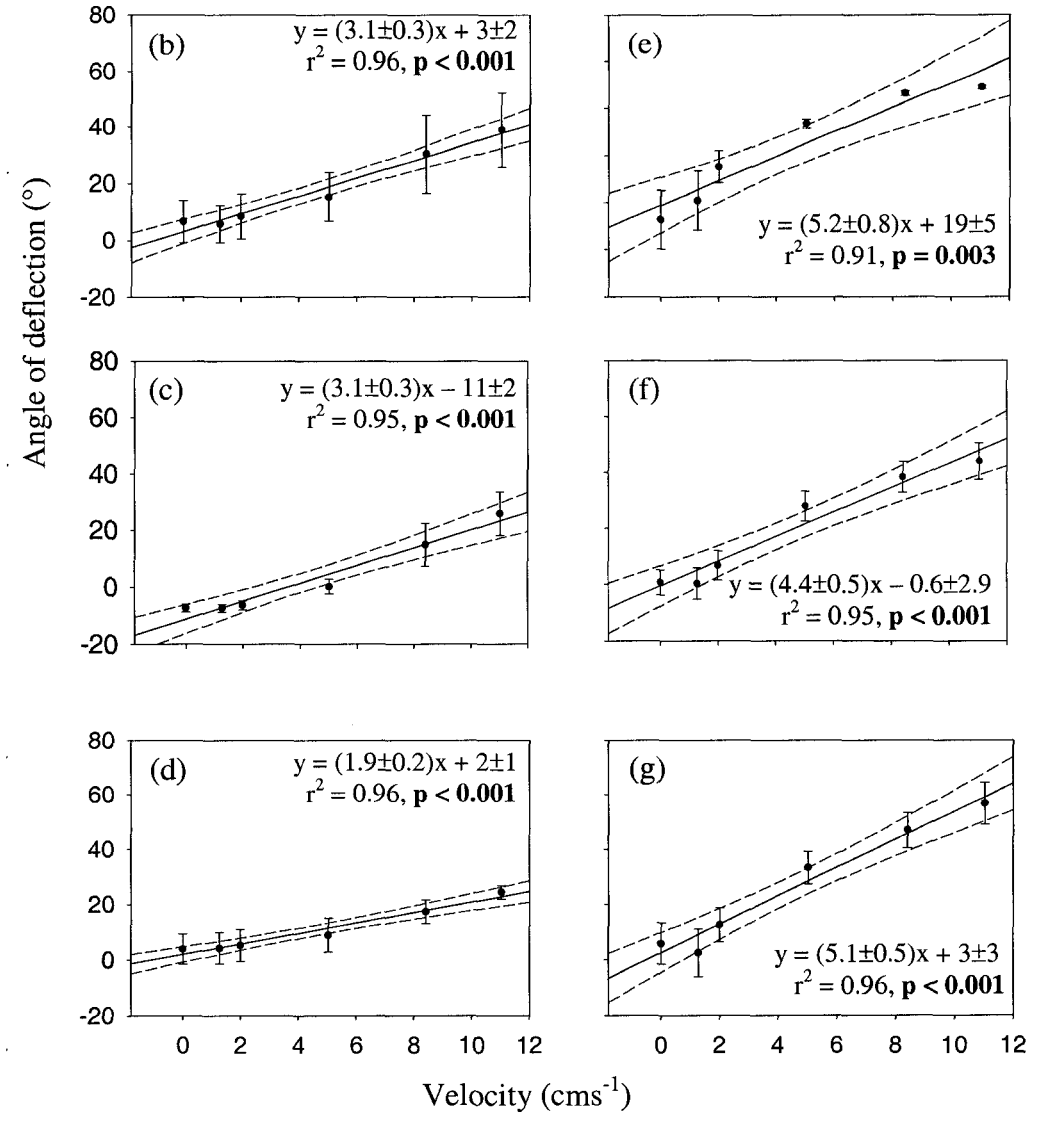

Figure 4.19: Regression results for the angle of deflection versus velocity for (a) the circular cylinder, (b) *Elodea*, (c) *Elodea* with every second node removed, (d) *Elodea* with every second and third node removed, (e) *Ceratophyllum*, (f) *Ceratophyllum* with every second node removed, and (g) *Ceratophyllum* with every second and third node removed. Solid line is the regression and dotted lines are the 95% confidence limits of the mean.

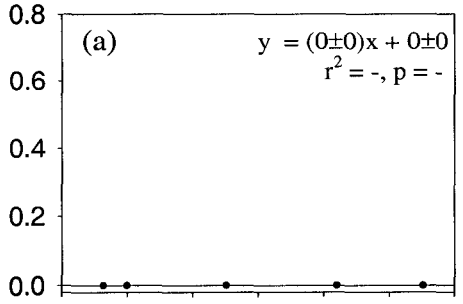

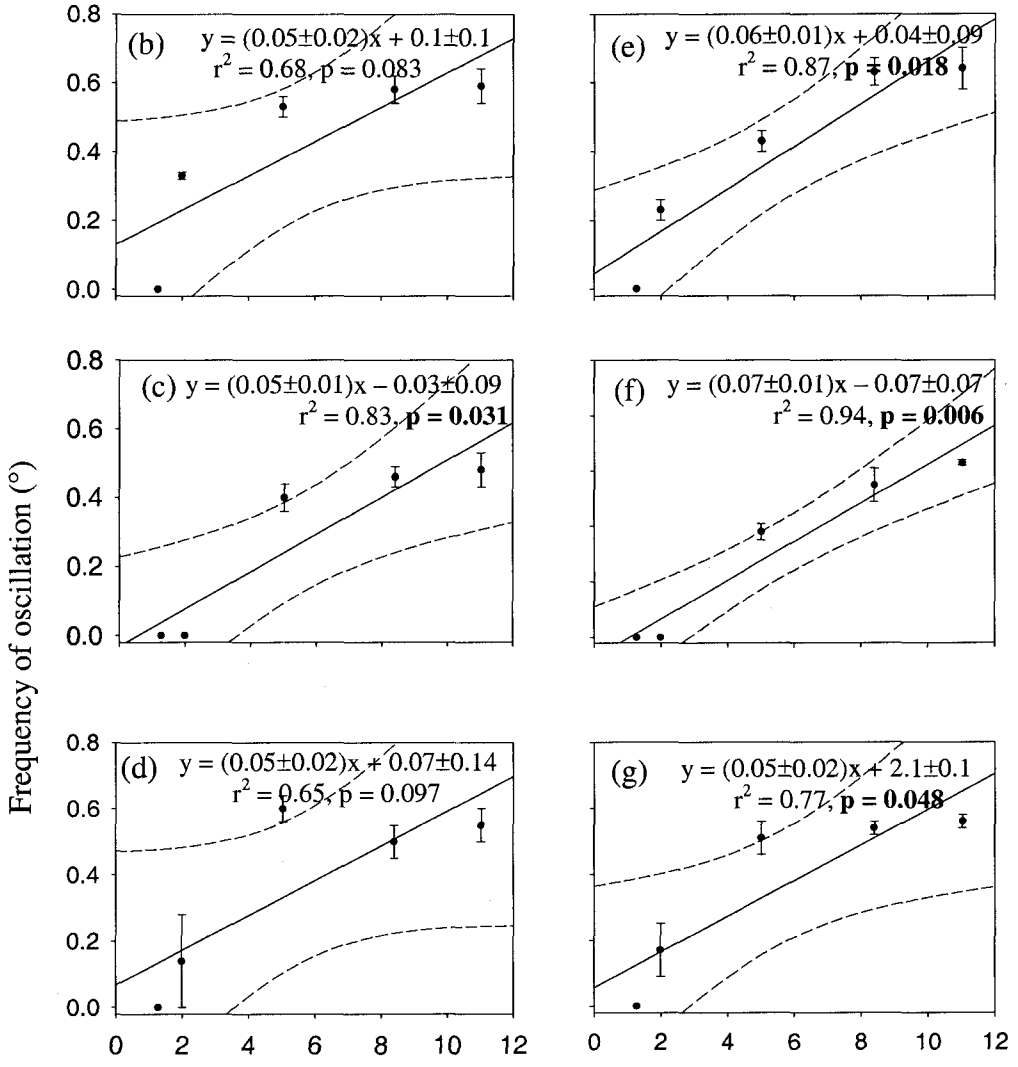

Figure 4.20: Regression results for the frequency of oscillation with increasing velocity for (a) the circular cylinder, (b) *Elodea*, (c) *Elodea* with every second node removed, (d) *Elodea* with every second and third node removed, (e) *Ceratophyllum*, (f) *Ceratophyllum* with every second node removed, and (g) *Ceratophyllum* with every second and third node removed. Solid line is the regression and dotted lines are the 95% confidence limits of the mean.

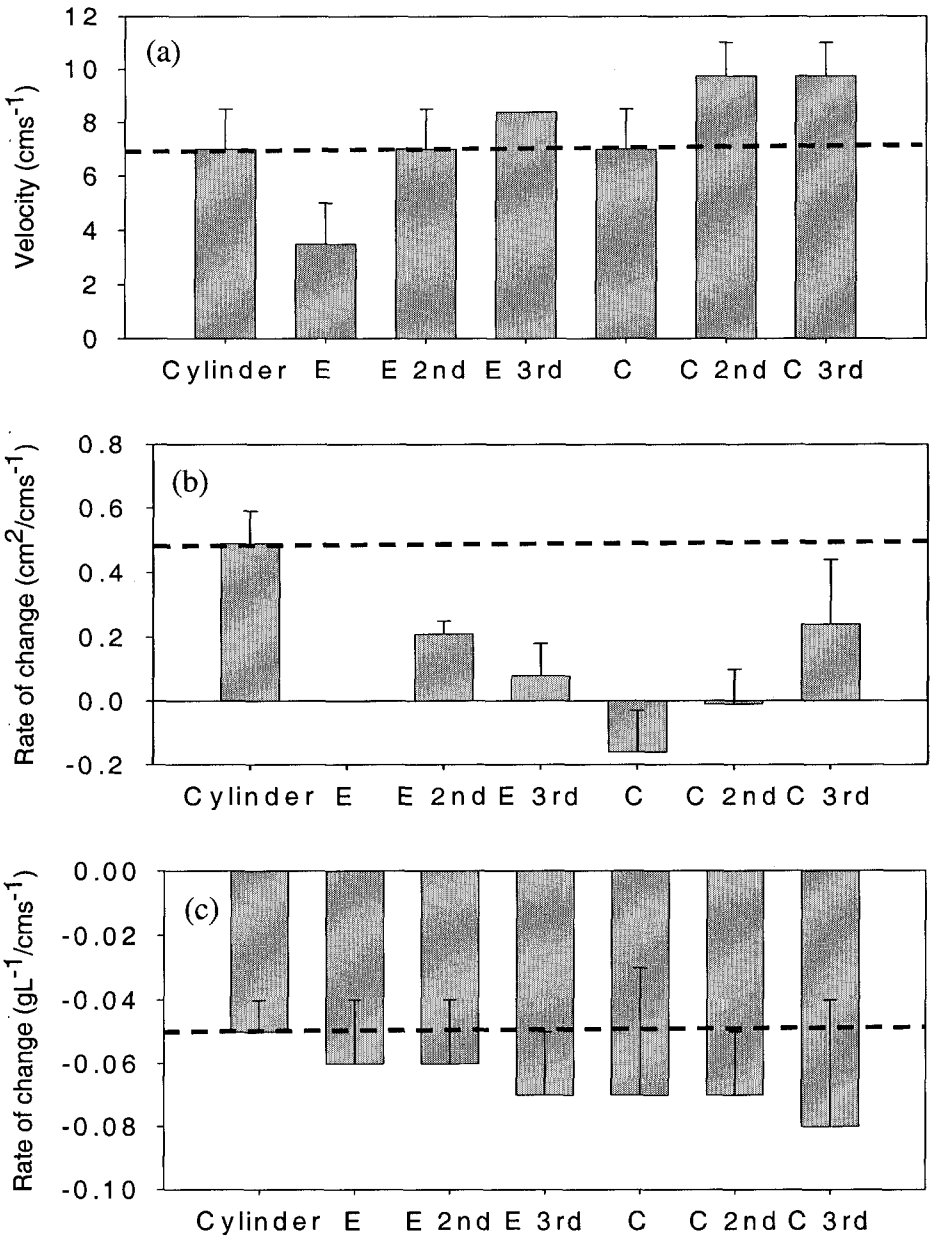

Figure 4.21: Comparison of the fluid dynamic conditions around plants and a physical model (a) The velocity at which the transition from laminar to turbulent occurs for the different plants; (b) Rate of change in the area of dye coverage with change in velocity for the different test subjects; and (c) The rate of change in the concentration of dye with change in velocity for the different test subjects. The dotted line shows the comparison with respect to the physical model. (E = *Elodea*; E 2^{nd} = *Elodea* with the whorl at every second node removed; E 3^{rd} = *Elodea* with the whorls at every second and third node removed; C = *Ceratophyllum;* C 2^{nd} = *Ceratophyllum* with the whorl at every second node removed; and C 3^{rd} = *Ceratophyllum* with the whorl at every second and third node removed)

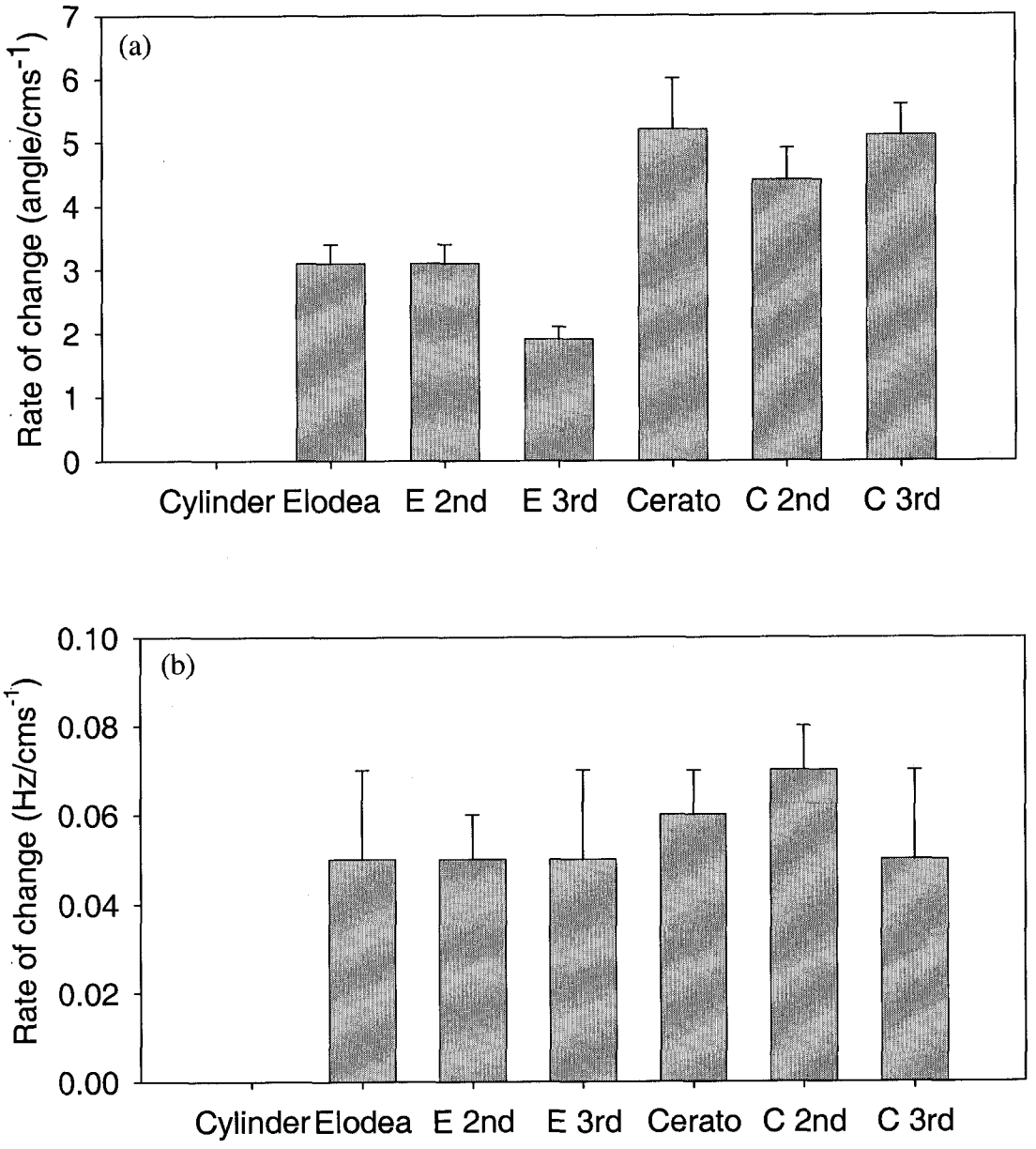

Figure 4.22: (a) Rate of change in the angle of deflection with change in velocity for the different test subjects; and (b) the rate of change in the number of oscillations per second with change in velocity for the different test subjects. The cylinder is always at zero because it was rigid and as such remained stationary.

Chapter 5: Conclusion to Thesis

Aquatic plants are important constituents of freshwater systems because they act as ecosystem engineers, in that they alter the physical environment, which leads to a wide range of other changes (Wright et al., 2004). Of these physical factors, the flow environment has the potential to limit macrophyte productivity at both low and high velocities. At low velocity, the potential for diffusional stress is high due to the existence of a thick boundary layer (Hurd et al., 1997; Schutten and Davy, 2000), whereas at high velocities, the potential for damage or breakage is dominant due to the increase in drag forces acting on the plant (Sand-Jensen, 2003). Macrophytes can be plastic in their morphology, exhibiting heterophylly and foliar plasticity with changing environmental conditions. It is reasonable to suggest that fluid dynamics may have played a determining role in plant architecture.

This thesis investigated the interactions between a number of characteristically shaped freshwater macrophytes and their flow environment. A review of the existing data on plant-flow interactions was presented in Chapter 2. Chapter 3 examined the interaction of linear-bladed, whorled and dissected leaf plants with flow by examining flow patterns qualitatively and quantitatively. Chapter 4 examined the effect of the plastic trait of internodal spacing on macrophyte-flow interaction in whorled and dissected leafed macrophytes using the same methodology to macrophytes that were manipulated experimentally.

Experiments revealed that the linear-bladed species *Vallisneria,* and the whorled species *Elodea,* affected the flow similar to a circular cylinder (used as a physical model). Conversely, the whorled dissected leafed species, *Ceratophyllum* acted more like a mesh,

in that it broke the flow up into smaller eddies. In all cases the transition from laminar to turbulent flow occurred at slower velocities for plants than the cylinder indicating an increase in local mixing. This would be beneficial to the plants as it would replenish the nutrients near the leaf surface, and thus promote the flux of nutrients and dissolved gases across the boundary layer to the leaf surface (Anderson and Charters, 1982; Hurd et al., 1996), thereby increasing productivity (Borchardt, 1994). Another important difference between the different plant morphologies and the circular cylinder was that both the rate of change in area and concentration of the dye were slower for plants than for the cylinder. This indicates that plants retain fluid for a longer time than a cylinder, perhaps providing more opportunity for uptake. In terms of plant compliance, the rate of change in angle of deflection was smallest for *Vallisneria* (linear-bladed) and greatest for *Ceratophyllum* (dissected), indicating that *Vallisneria* interacts less with the flow.

In terms of the effects of manipulated internodal spacing on the flow (Chapter 4), the transition from laminar to turbulent flow occurred at faster velocities for plants with increased internodal spacing than for the cylinder. This suggests a decrease in local mixing, which indicates that increased internodal spacing is a response to slower flows, rather than to other factors (e.g., nutrient flux; Idestam-Almquist and Kautsky, 1995). However, plants with increased internodal spacing are generally exposed to higher flow conditions because they exist higher in the water column, generally to increase light interception (Ennos, 1999; Santamaria, 2002; Cronin and Lodge, 2003). The rate of change in area of dye coverage decreased at a slower rate for the plants than for the cylinder, as did the rate of change in the concentration of dye, reiterating the observation that plants retain more fluid than a physical model. Whereas this indicates an increase in

the opportunity for nutrient uptake by the plants, it should be noted that the fluid is not as well mixed as the fluid around intact plants and is retained for a longer period of time. *Elodea* with the whorl at every second and third node removed, interacted the least of the plants of this species with the flow, demonstrating that internodal spacing does have an effect on the downstream fluid patterns. All of the *Ceratophyllum* plants exhibited a high plant-flow interaction, but the unmanipulated plant was the most compliant, demonstrating that internodal spacing has an effect on how the plants responded to the flow.

This thesis showed that freshwater macrophytes of different morphologies have different ways of interacting with the flow, while retaining the same amount of fluid. *Vallisneria* may be better suited to faster flow environments because it had the least flow interaction shown by the angle of deflection in the flow compared to the whorled and dissected morphologies. This would indicate that drag forces would be less for this linear-bladed architecture (Sheath and Hambrook, 1988; Gutierrez and Fernandez, 1992; Schutten and Davy, 2000). This is consistent with observations that smooth bladed morphologies in macroalgae are found in faster flow environments than other morphologies (Ackerman and Okubo, 1993; Hurd and Stevens, 1997). Conversely, it is expected that *Ceratophyllum* would be better suited to slower flow environments because it had the greatest flow interaction that led to the creation of small scale mixing, which would enhance nutrient flux (Anderson and Charters, 1982; Nowell and Jumars, 1984; Gutschick, 1999) and thus productivity. It is likely that *Elodea* is best suited to a flow environment between these two extremes because, at low flows the plant-flow interaction generated a large area of recirculation and many filamentous loops of attached dye

whereas at higher flows it deflected in the flow and generated vortices. In terms of phenotypic plasticity, increased internodal spacing was found to decrease the plant-flow interaction in *Elodea*, as is evident in the reduced recirculation of dye, and in *Ceratophyllum,* as evident from a decrease in the degree of compliance. An increase in internodal spacing would be beneficial in relatively low flow environments because there would be less drag on the plants. This is important because the plants with this plastic response are taller and therefore extend higher in the water column to increase light interception. Conversely, this mechanism would not function in relatively high flow environments because the plants would be deflected downwards (i.e., increased compliance) and/or not be robust enough to withstand high drag forces. Consequently, the plant-flow interaction can be linked to the productivity of freshwater macrophytes as demonstrated by the different responses to flow discussed above. These different responses observed throughout this study suggest that the fluid dynamic environment influences the plasticity of plant architecture, and the evolution of leaf morphology in general.

Literature Cited

Ackerman, J.D., and A. Okubo. 1993. Reduced mixing in a marine macrophyte canopy. *Functional Ecology.* 7:305-309.

Anderson, S.M., and A.C. Charters. 1982. A fluid dynamics study of seawater flow through *Gelidium rudifrons. Limnology and Oceanography.* 37(3):399-412.

Borchardt, M.A. 1994. Effects of flowing water on nitrogen- and phosphorus-limited photosynthesis and optimum N:P ratios by *Spirogyra fluviatilis* (Charophyceae). *Journal of Phycology.* 30:418-430.

Cronin, G., and D.M. Lodge. 2003. Effects of light and nutrient availability on the growth, allocation, carbon/nitrogen balance, phenolic chemistry, and resistance to herbivory of two freshwater macrophytes. *Oecologia.* 137:32-41.

Ennos, A.R. 1999. The aerodynamics and hydrodynamics of plants. *The Journal of Experimental Biology.* 202:3281-3284.

Gutierrez, L.M., and C. Fernandez. 1992. Water motion and morphology in *Chondrus crispus* (Rhodothyta). *Journal of Phycology.* 28:156-162.

Gutschick, V.P. 1999. Research reviews: Biotic and abiotic consequences of differences in leaf structure. *New Phytologist.* 143(1):3-18.

Henry, H.A.L., and S.C. Thomas. 2002. Interactive effects of lateral shade and wind on stem allometry, biomass allocation, and mechanical stability in *Abutilon theophrasti* (Malvaceae). *American Journal of Botany.* 89(10):1609-1615.

Hurd, C.L., P.J. Harrison, and L.D. Druehl. 1996. Effect of seawater velocity in inorganic nitrogen uptake by morphologcially distinct forms of macrocystis intgrifolia from wave-sheltered and exposed sites. *Marine Biology.* 126:205-214.

Hurd, C.L. and C.L. Stevens. 1997. Flow visualization around single- and multiple-bladed seaweeds with various morphologies. *Journal of Phycology.* 33:360-367.

Hurd, C.L, C.L Stevens, B.E. Laval, G.A. Lawrence, and P.J. Harrison. 1997. Visualization of seawater flow around morphologically distinct forms of the giant kelp macrocystis integrifolia from wave-sheltered and exposed sites. *Limnology and Oceanography.* 42(1):156-163.

Idestam-Almquist, J., and L. Kautsky. 1995. Plastic responses in morphology of *Potamogeton pectinatus* L. to sediment and above-sediment conditions at two sites in the northern Baltic proper. *Aquatic Botany.* 52:205-216.

Nepf, H.M. 1999. Drag, turbulence, and diffusion in flow through emergent vegetation. *Water Resources Research.* 35(2):479-489.

Nowell, A.R.M., and P.A. Jumars. 1984. Flow environments of aquatic benthos. *Annual Review of Ecology and Systematics.* 15:303-328

Sand-Jensen, K. 2003. Drag and reconfiguration of freshwater macrophytes. *Freshwater Biology.* 48:271-283.

Santamaria, L. 2002. Why are most aquatic plants widely distributed? Dispersal, clonal growth and small-scale heterogeneity in a stressful environment. *Acta Oecologica.* 23:137-154.

Schutten, J., and A.J. Davy. 2000. Predicting the hydraulic forces on submerged macrophytes from current velocity, biomass and morphology. *Oecologia.* 123:445-452.

Sculthorpe, C.D. 1967. *The Biology of Aquatic Vascular Plants.* Edward Arnold, London (Reprinted 1985 Koeltz Scientific, Konigstein), 610 pp.

Sheath, R.G., and J.A. Hambrook. 1988. Mechanical adaptations to flow in freshwater red algae. *Journal of Phycology.* 24:107-111.

Speck, O. 2003. Field measurements of wind speed and reconfiguration in *Arundo donax* (Poaceae) with estimates of drag forces. *American Journal of Botany.* 90(8):1353-1256.

Vogel, S. 1994. *Life in Moving Fluids The Physical Biology of Flow.* Princeton University Press, Princeton, N.J. 467 pp.

Wright, J.P., W.S.C. Gurney, and C.G. Jones. 2004. Patch dynamics in a landscape modifies by ecosystem engineers. *Oikos.* 105:336-348.